

**Cell-specific phytohormone responses mapped by the
COLORFUL-biosensors during plant-microbe interactions**

Dissertation

for the award of the degree

"Doctor rerum naturalium"

(Dr.rer.nat.)

of the Georg-August-Universität Göttingen

within the doctoral program biology

of the Georg-August University School of Science (GAUSS)

submitted by

Mohamed El-Sayed Ali El-Sayed

from Egypt

Göttingen, 2020

Thesis Committee

1. Supervisor: Prof. Dr. Volker Lipka

Plant Cell Biology, Albrecht-von-Haller-Institute for Plant Sciences

2. Supervisor: PD Dr. Thomas Teichmann

Plant Cell Biology, Albrecht-von-Haller-Institute for Plant Sciences

3. Supervisor: Dr. Hassan Ghareeb

Plant Cell Biology, Albrecht-von-Haller-Institute for Plant Sciences

Members of the Examination Board

Reviewer: Prof. Dr. Volker Lipka

Plant Cell Biology,
Albrecht-von-Haller-Institute for Plant Sciences

Second reviewer: PD Dr. Thomas Teichmann

Plant Cell Biology,
Albrecht-von-Haller-Institute for Plant Sciences

Further Members of the Examination Board

Prof. Dr. Ivo Feußner

Plant Biochemistry,
Albrecht-von-Haller-Institute for Plant Sciences

Prof. Dr. Andrea Polle

Forest Botany and Tree Physiology
Faculty of Forest Science and Ecology

PD Dr. Marcel Wiermer

Plant Cell Biology,
Albrecht-von-Haller-Institute for Plant Sciences

PD Dr. Till Ischebeck

Plant Biochemistry,
Albrecht-von-Haller-Institute for Plant Sciences

Date of the oral examination: 15.04.2020

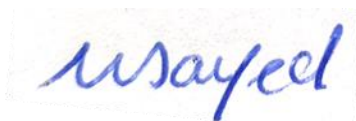
Promovierenden-Erklärung der Georg-August-Universität Göttingen

Ich gebe folgende Erklärung ab:

1. Die Gelegenheit zum vorliegenden Promotionsvorhaben ist mir nicht kommerziell vermittelt worden. Insbesondere habe ich keine Organisation eingeschaltet, die gegen Entgelt Betreuerinnen und Betreuer für die Anfertigung von Dissertationen sucht oder die mir obliegenden Pflichten hinsichtlich der Prüfungsleistungen für mich ganz oder teilweise erledigt.
2. Hilfe Dritter wurde bis jetzt und wird auch künftig nur in wissenschaftlich vertretbarem und prüfungsrechtlich zulässigem Ausmaß in Anspruch genommen. Insbesondere werden alle Teile der Dissertation selbst angefertigt; unzulässige fremde Hilfe habe ich dazu weder unentgeltlich noch entgeltlich entgegengenommen und werde dies auch zukünftig so halten.
3. Die Ordnung zur Sicherung der guten wissenschaftlichen Praxis an der Universität Göttingen wird von mir beachtet.
4. Eine entsprechende Promotion wurde an keiner anderen Hochschule im In- oder Ausland beantragt; die eingereichte Dissertation oder Teile von ihr wurden/werden nicht für ein anderes Promotionsvorhaben verwendet.

Mir ist bekannt, dass unrichtige Angaben die Zulassung zur Promotion ausschließen bzw. später zum Verfahrensabbruch oder zur Rücknahme des erlangten Grades führen können.

Mohamed El-Sayed



Göttingen, den 20.02.2020

*I dedicate my PhD dissertation to my family, my lovely wife **Mrs. Shireen Ibrahim** who never gave up on me, my children **Malek** and **Hamza** without whom this dissertation would have been completed at least five years earlier😊, as well as my parents **Mr. El-Sayed Ali** and **Mrs. Amal Foad**.*

SUMMARY

Plants are concurrently challenged by various invaders that can severely affect their development and productivity. Salicylic acid (SA), jasmonic acid (JA) and ethylene (ET)-dependent defense pathways are generally regarded as the major defense-related phytohormones. However, accumulating evidence suggests that abscisic acid (ABA) also functions as a modulator of plant innate immunity. Moreover, it is well established that pathogen attack modifies hormone-homeostasis in the host leading to activation or suppression of immune responses. However, the spatio-temporal cellular activities of SA, JA, ET and ABA in defense have so far not been fully understood.

To enable quantitative measurement of SA, JA, ET and ABA signaling outputs at the single-cell level, a set of multi-modular hormone-signaling reporters termed “COLORFUL-SA, -JA, -JA/ET and -ABA, respectively, were developed. These COLORFUL-reporters, together with a software-supported high-throughput imaging protocol for output quantification, were used to resolve the spatio-temporal dynamics of respective hormonal signaling activities in Arabidopsis leaves. Functional characterization was performed using exogenous hormone treatments and mutant analyses which confirmed specificity, sensitivity and rapid responsiveness of these COLORFUL-biosensors. Distinct cell and tissue type-specific signaling patterns, which are consistent with previously described spatial roles of these hormones in Arabidopsis were observed. Moreover, the COLORFUL-reporter lines were utilized to resolve the kinetics of hormone signaling and hormone crosstalk in Arabidopsis at interaction sites with the biotrophic oomycete *Hyaloperonospora arabidopsidis* Noco2 and Emwa1 strains, which represent virulent and avirulent isolates, respectively. Thus, this study pioneered the spatial dissection of plant immune responses at the initial site of invasion and allowed mapping of the respective hormone signaling activities at an unprecedented single-cell resolution.

In the conducted comparative plant-microbe interaction studies, the virulent and avirulent oomycete isolates exhibited remarkably different invasion dynamics, which correlated with spatiotemporally distinct hormone signatures. At cellular resolution, these hormone-specific reporter signatures demarcate pathogen entry and progression and highlight initiation, transduction and local containment of immune signals. The avirulent isolate Emwa1 significantly triggered SA responses in the cells that are in direct contact with the invaded cells (adjacent cells), suggesting that these may contribute to effector-triggered immunity (ETI) mediated by the Col-0 RPP4 resistance gene. Moreover, during incompatible interactions with Emwa1, a drastic suppression of JA and JA/ET signaling was observed in the adjacent cells, whereas a pronounced activation of the JA/ET

signaling pathway was observed in the adjacent cells during compatible interactions with Noco2. Thus, in compatible interactions, JA/ET-dependent signaling may play a role in antagonizing the SA response-associated with ETI in the adjacent cells. Furthermore, ABA signaling was activated in invaded cells during both compatible and incompatible interactions and showed a similar activation pattern to the SA responses triggered in Noco2-haustoriated cells.

In order to test whether other unrelated biotrophic pathogens activate a similar pattern of ABA and SA responses, the ascomycete fungal pathogen *Golovinomyces orontii* was used. Interestingly, a cross-kingdom-conserved induction of a cellularly confined activation of ABA- but not of SA-signaling was observed at Arabidopsis interaction sites. Mutant analyses supported the hypothesis that ABA functions as an important and common susceptibility factor for both biotrophic pathogens. To further corroborate this hypothesis, the ABA biosynthesis mutants *aba1-101* and *aba2-1* were challenged with Noco2 and *Golovinomyces orontii* which showed significantly lower spore counts relative to the wildtype Col-0. To further investigate the cell-specific contribution of ABA signalosome components to susceptibility, the sporulation of Noco2 and *Golovinomyces orontii* was tested on different ABA signaling mutants. The enhanced disease resistance of the double loss-of-function mutants of the positive ABA regulators SnRK2D and SnRK2I suggested a functional role of these kinases on ABA-dependent susceptibility. Individual and double mutants of *SnRK2D* and *SnRK2I* were crossed with COLORFUL-ABA to test the correlation of the enhanced disease resistance in the *snrk2d snrk2i* double mutant to ABA signaling activities. The significant reduction in ABA signaling activity in these lines provided additional proof that SnRK2D and SnRK2I are redundantly involved in upregulation of the ABA signaling cascade by virulent biotrophic pathogens.

In addition, two recent studies were performed in our lab to characterize the sporulation of the aforementioned pathogens on different Arabidopsis Type 2C protein phosphatase (PP2C) loss-of-function mutants. PP2Cs are negative regulators of the ABA signaling cascade. The PP2CA knockout mutant *pp2ca-1* showed enhanced disease resistance to Noco2 and *Golovinomyces orontii* in contrast to the *ahg3-1* missense mutant of the same gene and wildtype Col-0 (Lübbers 2018; Schliekmann 2017). These two mutants were crossed with the COLORFUL-SA and COLORFUL-ABA to evaluate their contribution to the regulation of SA and ABA signaling cascades. Notably, *pp2ca-1* exhibits significantly induced ABA and SA signaling activities during interaction with *H. arabidopsidis* Noco2 relative to Arabidopsis wildtype and *ahg3-1*. These results may be explained by a physical interaction between PP2CA and SA as recently reported by Manohar et al. (2017) for the PP2C proteins PP2C-D4/PP2C6, ABI1 and ABI2. In the future, the COLORFUL reporter system developed and established in this study will allow further disentanglement of the complexities of basal and R-gene mediated resistance during different plant-microbe interactions in more detail and at cellular resolution.

TABLE OF CONTENTS

SUMMARY	I
TABLE OF CONTENTS	III
LIST OF ABBREVIATIONS	X
1. INTRODUCTION	1
1.1. Plant development-adaptation balance is a globally important issue for food security.....	1
1.2. Plants activate immune responses for adaptation to biotic stress.....	1
1.3. Pathogens utilize different strategies to invade the host plant.....	4
1.4. Pathogen lifestyles are associated with the viability of host tissues.....	4
1.5. Model pathosystems unravel the complexity of the plant immune system.....	5
1.6. Hormone signaling orchestrates the plant immune responses.....	8
1.6.1. Absciscic acid is a decisive factor in plant development and adaptation to stress.....	9
1.6.1.1. Absciscic acid biosynthesis takes place in two cellular compartments.....	9
1.6.1.2. Absciscic acid accumulation stimulates the expression of ABA-responsive genes in cytosol and nucleus.....	10
1.6.1.3. Absciscic acid modulates plant immunity in response to different pathogens	12
1.6.2. Pathogen-dependent activation of SA biosynthesis and signaling cascades promotes resistance against biotrophic and hemibiotrophic pathogens	13
1.6.2.1. ICS1 is a major player of pathogen-induced SA production	13
1.6.2.2. NPR1 orchestrates a nucleocytoplasmic regulation of SA signaling.....	14
1.6.2.3. Upregulation of salicylic acid accumulation and signaling promotes plant resistance during different biotrophic interactions	17

1.6.3. Jasmonate biosynthesis and signaling promote resistance against necrotrophs.....	18
1.6.3.1. Jasmonate biosynthesis occurs sequentially in multi-cellular compartments	18
1.6.3.2. Jasmonate signaling is activated via two different JA-dependent transcriptional networks	19
1.6.3.3. Jasmonic acid shows a dual contribution to defense responses against several necrotrophs	21
1.6.4. Ethylene modulates high complexity <i>in planta</i> aspects.....	22
1.6.4.1. Members of multigene families regulate ethylene biosynthesis.....	22
1.6.4.2. Both ethylene and jasmonic acid up-regulate the expression of <i>PDF1-2</i>	22
1.6.4.3. Ethylene promotes resistance against necrotrophs and susceptibility against biotrophs.....	24
1.7. Hormone crosstalk in plant immunity equips plants with a powerful adaptive capacity.	25
1.7.1. JA-ET synergistic crosstalk	25
1.7.2. JA-JA/ET antagonistic crosstalk	26
1.7.3. SA-JA/ET antagonistic crosstalk.....	26
1.7.4. ABA-SA crosstalk.....	27
1.7.5. ABA-JA/ET crosstalk.....	28
1.8. Hormone sensing	29
1.8.1. Limitations of classical hormone detection and quantification assays	29
1.8.2. Assays using biologically active fluorescently labeled hormones.....	29
1.8.3. FRET based reporters	30
1.8.4. Degrons based reporters.....	30
1.8.5. Hormone-inducible promoter-based reporters	31
1.8.5.1. Native promoter-based reporters.....	31
1.8.5.2. Synthetic promoter-based reporters	33
1.9. Tools for normalization of reporter activity	34
1.10. Objectives.....	34
2. MATERIALS AND METHODS	36
2.1. Materials	36

2.1.1.	Arabidopsis plant materials	36
2.1.2.	Crosses of COLORFUL-biosensor lines with different mutants	38
2.1.3.	Chemicals	38
2.1.4.	Buffers and solutions	39
2.1.5.	Oligonucleotides	40
2.1.6.	Nucleic acid modifying enzymes	41
2.1.7.	Pathogens	42
2.1.8.	Devices	42
2.2.	Methods.....	44
2.2.1.	Growth conditions and cultivation of <i>A. thaliana</i>	44
2.2.1.1.	Seed production	44
2.2.1.2.	Infection experiments	44
2.2.1.3.	Hormone treatment experiments.....	45
2.2.2.	Cultivation of the oomycete <i>H. arabidopsidis</i>	45
2.2.3.	Cultivation of the fungus <i>G. orontii</i>	45
2.2.4.	Functional characterization of COLORFUL-biosensors	46
2.2.4.1.	The responsiveness of the COLORFUL-biosensors to exogenous hormone applications .	46
2.2.4.2.	Selection of COLORFUL-biosensor lines	47
2.2.4.3.	ABA treatment experiments	47
2.2.4.4.	Time course experiments	47
2.2.4.5.	Tissue-specific distribution of COLORFUL-ABA reporter activity and dependency of reporter activity on ABA biosynthesis	48
2.2.5.	ABA, SA, JA, and JA/ET marker gene expression analyses in response to hormone treatment	48
2.2.5.1.	Sample collection	48
2.2.5.2.	RNA extraction from plant materials.....	48
2.2.5.3.	Determination of the RNA integrity and concentration.....	49
2.2.5.4.	DNase treatment of total RNA samples.....	49
2.2.5.5.	Reverse transcription of the total RNA	49
2.2.5.6.	Quantitative Real Time Polymerase Chain Reaction (qRT-PCR).....	50
2.2.6.	Pathogen-associated disease phenotype of ABA biosynthetic and signaling mutants.....	52

2.2.7. Plant-microbe interaction experiments to map pathogen-mediated hormone signaling.....	53
2.2.7.1. <i>H. arabidopsidis</i> -Noco2 and -Emwa1 infection experiments	53
2.2.7.2. <i>G. orontii</i> infection experiments	53
2.2.7.3. Visualization of pathogens during microscopy	54
2.2.7.4. Evaluation of growth dynamics of Emwa1 and Noco2.....	54
2.2.8. Confocal Laser Scanning Microscopy	55
2.2.9. Cellular fluorescence quantification.....	56
2.2.10. Image analysis.....	57
2.2.11. Statistical analysis	58

3. RESULTS..... 59

3.1. COLORFUL-biosensors reveal hormone signaling outputs at single-cell resolution...59

3.1.1. <i>PP2CA</i> expression shows the highest correlation with the exogenous ABA treatment and incubation time in comparison to other ABA tested marker genes	59
3.1.2. COLORFUL-ABA harbours three distinct fluorescent protein-based reporter cassettes and a BASTA-resistance selection marker.....	62
3.1.3. COLORFUL-SPOTTER allows comparative large-scale quantitative data analyses on single-cell level	64
3.1.4. COLORFUL-reporters show consistent quantitative readouts for the reporter activity in different transgenic lines.....	66
3.1.5. Nuclear targeted COLORFUL-modules exhibit cell-type specific activities	66
3.1.6. The COLORFUL-reporter activity correlates with hormone dose and treatment incubation time	68
3.1.6.1. COLORFUL-ABA reporter reveals a rapid responsiveness, high specificity and accuracy to minor changes in ABA levels.....	68
3.1.6.2. Transcriptional analyses reflect positive correlations of SA, JA and JA/ET reporter activities with exogenous hormone applications	70
3.1.7. COLORFUL-biosensors explore distinct tissue-specific signaling outputs	72
3.1.7.1. ABA reporter activity correlates with the well-known ABA differential pattern in all investigated Arabidopsis tissues	72
3.1.7.2. <i>aba1-101</i> mutant analyses display a global reduction in ABA signaling activities in Arabidopsis	75
3.1.7.3. SA, JA, and JA/ET reporters disclose reporter activities in different Arabidopsis tissues...	79

3.2. COLORFUL-reporters enable the investigation of different hormone signaling cascades crosstalk.....	80
3.3. The virulent and the avirulent isolates of the oomycete <i>H. arabidopsidis</i> exhibit distinct invasion dynamics	82
3.4. <i>Arabidopsis-H. arabidopsidis</i> interaction sites show spatio-temporally distinct ABA, SA, JA, and JA/ET signaling outputs	86
3.4.1. Both virulent and avirulent oomycete isolates trigger local ABA responses in the haustoriated cells.....	88
3.4.2. Emwa1 and Noco2 differentially regulate SA signaling in two distinct domains	90
3.4.3. Compatible and incompatible <i>H. arabidopsidis</i> interactions with Col-0 exhibit distinct cell type-specific JA responses	92
3.4.4. In contrast to virulent isolate, Emwa1 does not trigger JA/ET signaling in the adjacent cell zone	95
3.5. <i>G. orontii</i> shows a conserved spatial pattern of pathogen-activated ABA but not SA signaling at their interaction sites with <i>A. thaliana</i>.....	99
3.6. ABA mediates susceptibility to Noco2 and <i>G. orontii</i>.....	102
3.7. Pathogen-induced ABA signaling is dependent on ABA biosynthesis.....	104
3.8. The ABA core regulatory components SnRK2D, SnRK2I, and PP2CA mediate the pathogen-induced ABA and SA responses	107
3.8.1. SnRK2D and SnRK2I display negative impacts on the plant immune responses	107
3.8.2. PP2CA negatively regulates immune responses	110
3.8.2.1. <i>pp2ca-1</i> exhibits significantly induced ABA signaling activities in comparison to the wildtype	111
3.8.2.2. SA signaling is highly activated at <i>pp2ca1-H. arabidopsidis</i> interactions sites relative to the wildtype and the missense mutant <i>ahg3-1</i>	114
4. DISCUSSION	117
4.1. COLORFUL reporters facilitate robust live-cell readouts of hormone signaling output	117
4.1.1. The reference and the membrane marker modules allowed live-cell imaging and monitoring of tissue integrity.....	117

4.1.2.	The reporter module activities are controlled by promoters of highly responsive and well-known marker genes	118
4.1.2.1.	ABA treatment induced a higher <i>PP2CA</i> transcript level in comparison to other investigated ABA responsive genes	118
4.1.2.2.	COLORFUL-biosensors displayed hormone dosage- and incubation time-dependent activities on a transcriptional level	119
4.1.2.2.1.	VENUS reporter signal activation displays high sensitivity of the employed promoters to minor changes in hormone signaling	120
4.1.2.2.2.	COLORFUL-ABA exhibits a high dependency of the reporter signal on endogenous hormone levels	121
4.1.2.2.3.	Hormone treatment progressively induces <i>PP2CA</i> , <i>PR1</i> , <i>VSP2</i> and <i>PDF1-2a</i> transcript levels	121
4.2.	COLORFUL-ABA explore distinct cell-type specific hormone sensitivities and signaling outputs	122
4.3.	COLORFUL-biosensors map long-distance ABA signaling in different Arabidopsis tissues.....	123
4.4.	Hormone treatment induces differential organ-specific SA-, JA-, and JA/ET-reporter activities.....	125
4.5.	GFP-LTI6b and mKATE2-N7 modules allow visualization of the invasion process and are used as markers for cell viability	125
4.6.	Arabidopsis-<i>H. arabidopsidis</i> interactions display spatio-temporally distinct ABA, SA, JA and JA/ET signaling outputs.....	127
4.6.1.	Emwa1 and Noco2 trigger unsynchronized predominant ABA signaling outputs locally confined to the invaded cells	128
4.6.2.	The virulent and avirulent isolates of <i>H. arabidopsidis</i> differentially induce SA signaling in two distinct domains	129
4.6.3.	JA/ET signaling is activated to neutralize the activity of the SA pathway and to enhance biotrophy	130
4.7.	COLORFUL-biosensors are effective and suitable systems to address hormone crosstalk	130
4.8.	COLORFUL-reporters show a pathogen type dependent hormone crosstalk	132

4.9. ABA functions as an essential common susceptibility factor at Arabidopsis biotrophic interaction sites.....	134
4.10. SnRK2D, SnRK2I, and AHG-3 are key regulatory components for pathogen-mediated ABA and SA signaling outputs.....	135
4.10.1. The <i>SnRK2D</i> and <i>SnRK2I</i> loss-of-function double mutant exhibits reduced susceptibility and ABA signaling activities	136
4.10.2. The <i>AHG-3/PP2CA</i> knockout mutant shows enhanced resistance as well as ABA and SA signaling responses.....	137
5. REFERENCES	136
6. Supplemental material.....	162
ACKNOWLEDGEMENTS	163
CURRICULUM VITAE	165

LIST OF ABBREVIATIONS

Abbreviation	Description
%	Percent
°C	Degree Celcius
μ	Micro
μm	Micro meter
μM	Micro molar
1 ^{ry}	Primary
2 nd	Secondary
A.	<i>Agrobacterium</i>
A./At	<i>Arabidopsis/ Arabidopsis thaliana</i>
ABA	Abscisic acid
ACC	1-aminocyclopropane-1-carboxylic acid
Avr	<i>Avirulence</i>
B.	<i>Botrytis</i>
bp	Base pair(s)
BR	Brassinosteroid
CaMV35S	Cauliflower Mosaic Virus 35S RNA
cDNA	Complementary DNA
CK	Cytokinin
CLSM	Confocal laser scanning microscopy
cm	Centimetres
Col-0	Columbia
DAMP	Damage-associated molecular pattern
dH ₂ O	Deionised water
DNA	Deoxyribonucleic acid
DNase	Deoxyribonuclease
dNTP	Desoxynucleotid triphosphate
dpi	Day(s) post inoculation
e.g.	Exempli gratia, for example
EF-Tu	ELONGATION FACTOR THERMO UNSTABLE
Emwa1	<i>H. arabidopsidis</i> isolate Emwa1
ER	Endoplasmatic reticulum
ET	Ethylene
et al.	et alii; and others
ETI	Effector-triggered immunity
ETS	Effector-triggered susceptibility
F.	<i>Fusarium</i>
FB28	Fluorescent Brightener 28
flg22	Flagellin
FLS2	FLAGELLINSENSING2
FRET	Förster resonance energy transfer
g	Gram
G.	<i>Golovinomyces</i>
GA	Gibberellin

Abbreviation	Description
GFP	Green fluorescent protein
GOI	Gene of interest
<i>GUS</i>	<i>β</i> -glucuronidase
<i>H.</i>	<i>Hyaloperonospora</i>
hpi	Hour post inoculation
HR	Hypersensitive response-related cell death
i.e.	id est, that is
ICS	Iso chorismate synthase
JA	Jasmonic acid
JAZ	JASMONATE ZIM DOMAIN
L	Liter
log	Decadic logarithm
<i>LUC</i>	Luciferase-coding sequence
M	Molar
MAMP	Microbe-associated molecular patterns
MAPK/ MPK	Mitogen activated protein kinase
MeJA	Methyl jasmonate
min	Minute(s)
ml	Millilitres
mM	Millimolar
mm	Millimeter
mRNA	Messenger ribonucleic acid
MS	Murashige and Skoog medium
NLS	Nuclear localization signal
Noco2	<i>Hyaloperonospora arabidopsidis</i> isolate Noco2
<i>P.</i>	<i>Pseudomonas</i>
PAMP	Pathogen-associated molecular patterns
PAL	PHENYLALANINE AMMONIA LYASE
PCR	Polymerase chain reaction
PDF1-2	PLANT DEFENSIN1.2
pH	Negative decimal logarithm of the H ⁺ concentration
PP2C	TYPE 2C PROTEIN PHOSPHATASE
PR1	PATHOGENESIS-RELATED GENE1
PRR	Membrane-localized pattern recognition receptor
<i>Pst</i>	<i>Pseudomonas syringae</i> pv. Tomato
PTI	PAMP-triggered immunity
pv.	Pathovar
PYL	PYRABACTIN LIKE
PYR1	PYRABACTIN RESISTANCE 1
qRT-PCR	Quantitative real-time polymerase chain reaction
R	Resistance
RCAR	REGULATORY COMPONENT OF ABA RECEPTOR
rev	Reverse
RNA	Ribonucleic acid
ROS	Reactive oxygen species
rpm	Rounds per minute
RT-PCR	Reverse transcription polymerase chain reaction
SA	Salicylic acid
sec	Second(s)

Abbreviation	Description
SL	Strigolactone
SnRK2s	SNF1-RELATED PROTEIN KINASE 2
TAE	Tris-acetate-EDTA
T-DNA	Transfer DNA
Tris	Tris-(hydroxymethyl)-aminomethane
<i>UBQ10</i>	<i>POLYUBIQUITIN 10</i>
<i>UBQ5</i>	<i>POLYUBIQUITIN 5</i>
V	Volt
v/v	Volume per volume
VSP2	VEGETATIVE STORAGE PROTEIN 2
w/v	Weight per volume
YFP	Yellow fluorescent protein

1. INTRODUCTION

1.1. Plant development-adaptation balance is a globally important issue for food security

During their life cycle, plants are concurrently challenged by various abiotic and biotic stresses that can severely affect their development and productivity. To counter this, plants have evolved mechanisms to maintain the balance between developmental processes and adaptation to diverse abiotic and biotic stresses. Plants in nature have to compete with a plethora of microorganisms such as bacteria, fungi, and oomycetes, as well as viruses, nematodes, insects, and even other parasitic plants. Nevertheless, only a minority of these species interacting with plants are considered parasitic. The impact of plant diseases on food security has become an issue of global importance, which has sparked an increased effort to improve approaches for crop protection.

1.2. Plants activate immune responses for adaptation to biotic stress

Myriads of potential invaders are frequently trying to colonize plants. However, plants have evolved highly sophisticated sequential, antagonistic, and synergistic immune responses to resist a broad range of potentially harmful invaders (Pieterse et al. 2012). Basic and applied plant research has put a focus on exploring the two-tier plant innate immune system that allows plants to efficiently identify invaders and to trigger specific signaling cascades that help to prevent host colonization (Hacquard et al. 2017). Plants do not have particular cells that detect and neutralize pathogens. Therefore, each attacked plant cell must have the capacity to activate defense responses at the expense of normal cellular processes, e.g., growth and development.

Upon pathogen recognition, local defense activities are immediately stimulated by the perception of invader signatures (Adie et al. 2007). Plants possess the ability to recognize a wide range of non-self-pathogen/microbe-associated molecular patterns

1. INTRODUCTION

(P/MAMPs) such as flagellin, chitin, glycoproteins, and lipopolysaccharides (Hogenhout & Bos 2011) by cognate membrane-localized pattern recognition receptors (PRRs) (Jones & Dangl 2006; Pieterse et al. 2012). Similar to P/MAMPs, PRRs are also involved in recognition of invasion-associated self-signals, termed damage-associated molecular patterns (DAMPs), which are released from plant cell walls during infection (Wu & Baldwin 2010).

FLAGELLINSENSING2 (*AtFLS2*), a well-known PRR, is a member of the receptor-like kinase (RLK) family and can bind the peptide flg22 of bacterial flagellin (Zipfel 2014). Another thoroughly characterized PRR is the EF-TU RECEPTOR (*AtEFR*), which perceives a peptide derived from the bacterial translation elongation factor-Tu (EF-Tu) (Schoonbeek et al. 2015). PRRs act as radars to recognize PAMPs, and induce a basal resistance response, so-called PAMP-triggered immunity (PTI), which is the first layer of defense (Boller & He 2009).

The PTI activates sufficient defense responses to resist nonpathogenic microbes, and is responsible for basal resistance levels against adapted pathogens (Henry et al. 2013). Consequently, PRR-deficient mutants show altered disease phenotypes compared with the wildtype plants during infection. For example, leaves of *fls2* plants display enhanced susceptibility to virulent bacterial strains of *Pseudomonas syringae* (Zipfel et al. 2004), since the FLS2 protein controls stomatal closure which is essential to limit bacterial entry through foliar guard cells (Melotto et al. 2006). Moreover, *efr* mutants show enhanced susceptibility to *Agrobacterium tumefaciens* (Zipfel et al. 2006). The lysin motif (LysM)-containing chitin elicitor receptor kinase 1 (CERK1), the lysin motif receptor kinase 5 (LYK5), and LYK4 are essential for the perception of the fungal cell wall MAMP chitin in Arabidopsis. CERK1 and LYK5 interact together during chitin perception, *cerk1* as well as *lyk4 lyk5-2* double mutant exhibit a complete loss of chitin response and exhibit higher susceptibility to different pathogens (Coa et al. 2014; Erwig et al. 2017; Gimenez-Ibanez et al. 2009; Miya et al. 2007; Wan et al. 2008; Zhang & Zhou 2010;). These examples show the importance and the contribution of basal defense responses in plant disease resistance.

Consequently, adapted pathogens develop repertoires of virulence mechanisms to either cope with or suppress PTI. To do so, pathogens secrete effector molecules into

1. INTRODUCTION

the plant cells to dampen the basal defense responses (Cui et al. 2015; Dou & Zhou 2012) leading to effector-triggered susceptibility (ETS) (Nishimura & Dangl 2010). These effector molecules may be small secreted proteins, small RNAs (sRNA) or secondary metabolites (Rodriguez-Moreno et al. 2018).

In a co-evolutionary arms race, plants develop a second type of pathogen recognition in addition to PTI, which directly or indirectly targets these effectors. Plant cells recruit nucleotide-binding/leucine-rich-repeat (NLR) receptors to recognize effector molecules (Cui et al. 2015), resulting in effector-triggered immunity (ETI) or *Resistance* (R)-gene mediated resistance, which is based on cytoplasmic resistance proteins (R proteins) (Katagiri & Tsuda 2010; Kim et al. 2002). NLRs are multi-domain proteins with a conserved modular structure consisting of a variable N terminal domain, a central nucleotide-binding (NB) domain, and a C-terminal leucine-rich repeat (LRR) domain (Cesari 2018). Moreover, NLRs fall broadly into two major subgroups that have distinct N-terminal domains. NLRs with a Toll-Interleukin1 Receptor (TIR) domain or coiled-coil (CC) domain are referred to as TNLs or CNLs, respectively (Bonardi et al. 2012).

PTI and ETI are always associated with the activation of a diverse array of immune responses, such as the production of reactive oxygen species (ROS), cellular Ca^{2+} influx spikes, activation of mitogen-activated protein kinases (MAPKs), hormone signaling, and transcriptional reprogramming (Tsuda & Somssich 2015). The activation of these responses contributes to locally and systemically triggered immunity (Katagiri & Tsuda 2010). PTI is associated with relatively low amplitudes of immune responses, whereas ETI provokes vigorous immune responses typically associated with hypersensitive response-related cell death (HR) (Hatsugai et al. 2017). All plant cells possess the capacity to activate HR machinery in order to initiate programmed cell death at biotrophic interaction sites (Feechan et al. 2015) to restrict the proliferation of biotrophic pathogens. HR is also associated with different plant growth and developmental processes (Huysmans et al. 2017), as well as with responses to environmental cues such as mechanical damage or abiotic stress (Love et al. 2008). Cell death requires the initiation of specific genes to activate the cell death machinery. Therefore, it is not surprising that invading pathogens develop tactics to hijack cell death regulators (Dickman & Fluhr 2013).

1.3. Pathogens utilize different strategies to invade the host plant

Based on their nature and size, pathogens have different methods for invading plants. Plant viruses infiltrate into host cells via wounds or by utilizing insect vectors (Park et al. 2018). Bacteria gain entry to the apoplast from the leaf's surface via natural openings such as hydathodes and stomata, or wounds (Huang 1986). Some larger sized fungi and oomycetes have the capacity to form invasion structures, the so-called appressoria, which they utilize to adhere tightly to the plant's surface and exert physical forces to penetrate the cell wall and secrete effectors from the penetration pores. Once these pathogens gain entry to the host cell, they develop a root-like feeding structure, the so-called haustorium, to improve nutrient uptake from host cells.

1.4. Pathogen lifestyles are associated with the viability of host tissues

Depending on the strategies used to acquire nutrients from their hosts, plant pathogens have different lifestyles categorized into two main types, *i.e.*, necrotrophic and biotrophic pathogens (Glazebrook 2005). Necrotrophic pathogens feed on the contents of dead host cells and destroy the host by utilizing phytotoxins and cell wall-degrading enzymes (Wen 2013). One example of this is the necrotrophic fungus *Botrytis cinerea*, which can severely colonize and destroy a huge number of dicotyledonous plant species and a few monocotyledonous plants. Its targets include various plants cultivated for human consumption, for example, protein, fiber and oil producing crops as well as horticultural crops such as chickpeas, lettuce, broccoli, beans, grapes, strawberries, and raspberries (Fournier & Giraud 2008; Valette-Collet et al. 2003; Williamson et al. 2007;).

In contrast to necrotrophs, biotrophic pathogens colonize host cells and acquire nutrients from intact host tissues; thus, they need to keep their hosts alive (Xin et al. 2016). The haustorium enables nutrient uptake across the extracellular matrix between the haustorial membrane and the host cell plasma membrane (PM) (Fawke et al. 2015; Presti & Kahmann 2017). For instance, the oomycete species *Hyaloperonospora arabidopsidis* has long been recognized for inducing downy mildew on a wide range of Brassicaceae species, such as garlic mustard, horseradish, cruciferous vegetables, Shepherd's purse, Cheiranthus spp., Cucurbits, treacle mustard, sweet alyssum and

1. INTRODUCTION

radish (Choi et al. 2018; Mehta et al. 2018; Mohammed et al. 2019). Another well-known filamentous pathogen with worldwide distribution is the biotrophic *ascomycete* fungus *Golovinomyces orontii* which causes powdery mildew symptoms on a broad range of economically important plants, such as sugar beet, bell pepper, watermelon, melon, cucumber, giant pumpkin, tomato, potato, tobacco, pea, and eggplant (Braun et al. 2019; Micali et al. 2011; Vági et al. 2007).

In addition, some pathogens have developed a specific combination of both lifestyles and are therefore called hemibiotrophs (Pieterse et al. 2012). They initially act as biotrophs, and later switch to a necrotrophic phase. Here, the prototypical bacterial plant pathogen *P. syringae* is widely distributed and serves as a model organism. Isolates of this species show a high degree of host-plant specificity (Morris et al. 2008) and are able to infect more than 200 plant species including economically important plants, such as bean, tomato, soybean, broccoli, cucumber, and tobacco (Zembek et al. 2018; Xin et al. 2018).

1.5. Model pathosystems unravel the complexity of the plant immune system

Numerous pathogens of different lifestyles cause devastating economic losses. Accordingly, many model plant-pathosystems have been investigated to elucidate the fundamental aspects of plant-pathogen interactions to help improve the strategies for plant security. For instance, the *H. arabidopsidis*-*Arabidopsis* pathosystem has been very helpful in uncovering the association between biotrophic oomycetes and their host plants, emphasizing the natural coevolution that has taken place between host and pathogen (Holub 2008). The species *H. arabidopsidis* contains virulent and avirulent isolates for the same *Arabidopsis* genotype allowing comparative study of compatible and incompatible interactions within the same plant-pathosystem (Coates & Beynon 2010). Virulent *H. arabidopsidis* isolates germinate on the host leaf surface, invade cell boundaries separating neighbouring epidermal pavement cells, propagate and establish haustoria in epidermal pavement as well as underneath mesophyll cells (Coates & Beynon 2010).

1. INTRODUCTION

PRR-mediated perception of oomycete PAMPs activates PTI (Fabro et al. 2011). Effector-mediated suppression of PTI during compatible interactions facilitates further pathogen proliferation, colonization of the whole leaf, and completion of the pathogen life cycle (Figure 1a, upper panel) (Caillaud et al. 2013; Deb et al. 2018). In marked contrast, avirulent *H. arabidopsidis* isolates produce effectors which stimulate ETI associated with a locally contained HR restricting pathogen growth to the initially attacked cells (Figure 1a, lower panel) (Van der Biezen et al. 2002; Wang et al. 2011).

Another well-known model pathogen is the powdery mildew fungus *G. orontii*. The biotroph *G. orontii* epiphytically colonizes the leaf surface, via germinating spores that form an appressorium to facilitate cell wall penetration, followed by development of a haustorium for effector secretion and nutrient uptake. *G. orontii* also suppresses PTI via the secretion of effectors to facilitate further pathogen proliferation, colonization of only the host epidermal cell layer, and completion of the pathogen life cycle (Figure 1b) (Kuhn et al. 2016).

1. INTRODUCTION

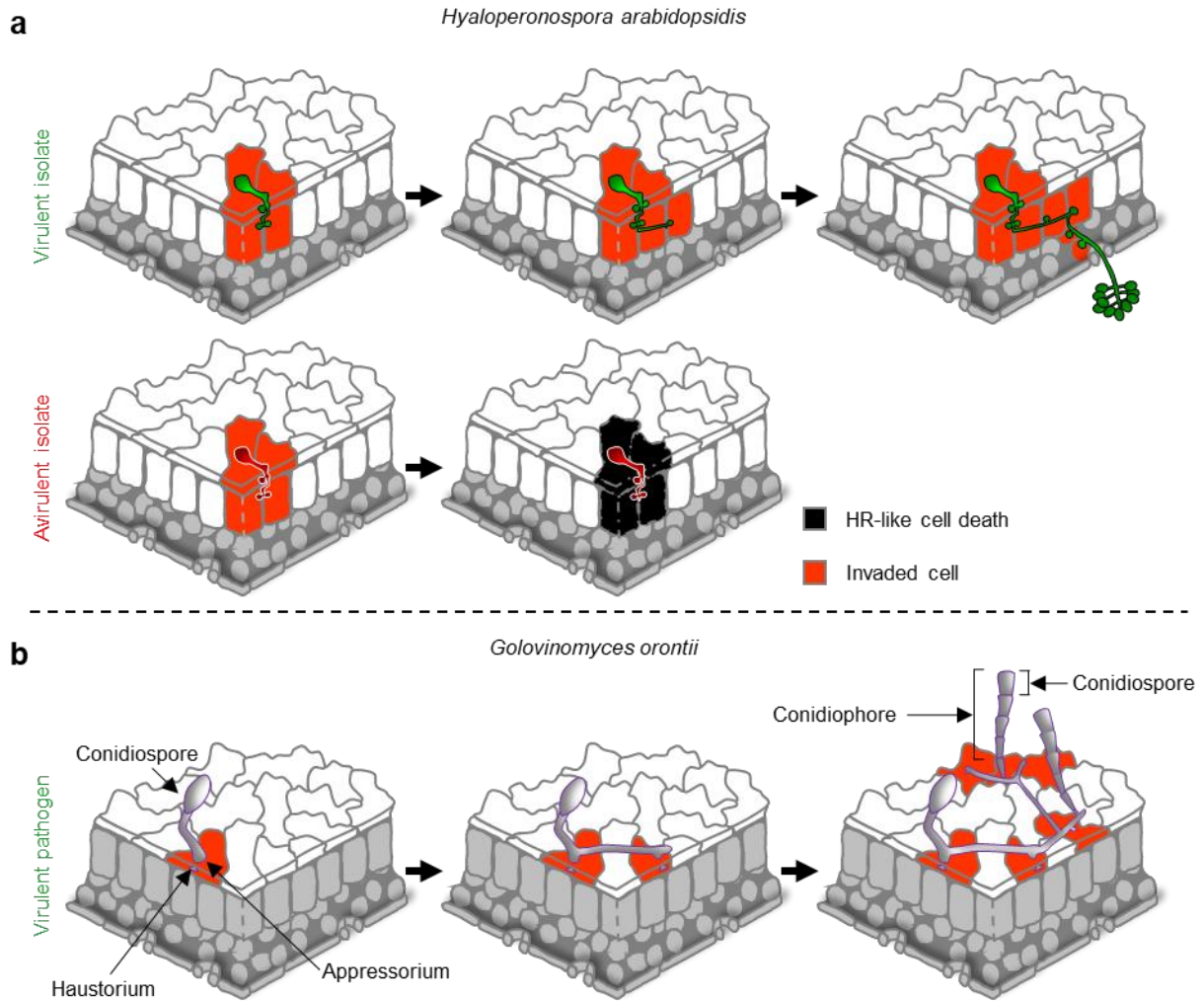


Figure 1: Virulent biotrophic pathogens disable the immune responses to endophytically or epiphytically colonize *Arabidopsis* leaves. (a) The virulent and avirulent isolates of the oomycete *H. arabidopsidis* grow endophytically, infiltrate the host leaf surface, invade cell boundaries separating neighbouring pavement cells, propagate and establish haustoria for effector secretion and nutrients uptake from the pavement and the underneath mesophyll cells. *Arabidopsis* recognizes their PAMPs and activates PTI. (a, upper panel) In the compatible interactions, the virulent isolate suppresses PTI via the secretion of effectors, thus facilitating further pathogen proliferation, colonization of the whole leaf, and completion of the pathogen life cycle. (a, lower panel) In the incompatible interaction, plant recognition of the effectors secreted by the avirulent isolate stimulates ETI to eventually activate the hypersensitive response-like cell death machinery to restrict pathogen growth to the initially attacked cells. (b) The powdery mildew fungus *G. orontii* grows epiphytically. To colonize the leaf surface, the invading spores form an appressorium to facilitate pavement cell wall penetration and develop haustorium. *G. orontii* suppresses the induced PTI via the secretion of effector molecules, thus allowing further pathogen proliferation, colonization of only the host epidermal cell layer, and completion of the pathogen life cycle.

1.6. Hormone signaling orchestrates the plant immune responses

In order to defeat intruders, plants use hormone biosynthesis, signaling, and crosstalk to modulate and fine-tune the battery of plant defense responses to efficiently fight back the pathogen and to simultaneously minimize potential growth and development penalties. Hormones are natural compounds that regulate plant growth and development, as well as plant responses to various biotic and abiotic stresses (Manohar et al. 2017; Robert-Seilaniantz et al. 2011). The phytohormones discovered so far are: salicylic acid (SA), jasmonic acid (JA), ethylene (ET), abscisic acid (ABA), cytokinins (CKs), auxins, gibberellins (GAs), brassinosteroids (BRs), and strigolactones (SL) (Asami & Nakagawa 2018; Pieterse et al. 2009). Signaling pathways mediated by plant hormones interact antagonistically or synergistically. With respect to plant pathogen interactions, this crosstalk adds another layer of regulation and complexity in order to allow adequate defense responses to different pathogens (Jaillais & Chory 2010; Mundy et al. 2006; Pieterse et al. 2012).

Microbes interfere with plant hormone biosynthesis and signaling to enhance virulence underpinning the importance of hormone signaling and crosstalk in orchestrating the expression of pathogenesis-related genes (Li et al. 2019a). Particularly, crosstalk between SA, JA and ET-dependent defense pathways, have been proposed to be the central regulatory hormone backbone of plant immunity (Shigenaga & Argueso 2016). Additionally, there are accumulating pieces of evidence which suggest that ABA, GAs, auxins, CKs, and BRs are mediators of different immune responses *in planta* (Denancé et al. 2013; Lievens et al. 2017; Naseem et al. 2014). In this investigation, the main focus will be on mapping signaling patterns of SA, JA, and ET, as well as ABA during plant-microbe interactions. Therefore, the next section will address biosynthesis, signaling, crosstalk, and the roles of ABA, SA, JA, and ET in defense responses.

1.6.1. Absciscic acid is a decisive factor in plant development and adaptation to stress

ABA is a fundamental regulator in numerous aspects of plant growth and developmental processes such as seed germination, maturation, dormancy, seedling establishment, cell growth, and stomatal closure. Moreover, ABA modulates the adaptation to various abiotic stresses such as drought, high temperature, and high salinity (Lee and Luan, 2012; Raghavendra et al. 2010). For instance, in water stress conditions, ABA accumulates in order to promote stomatal movement to protect the vegetative tissues from dehydration or excessive hydration (Umezawa et al. 2010). Therefore, because of the vital roles of ABA in plant adaptation to stress and the potential economic importance of this hormone, it has been intensively studied to understand its biosynthesis, perception, and signal transduction (Xiong & Zhu 2003).

1.6.1.1. Absciscic acid biosynthesis takes place in two cellular compartments

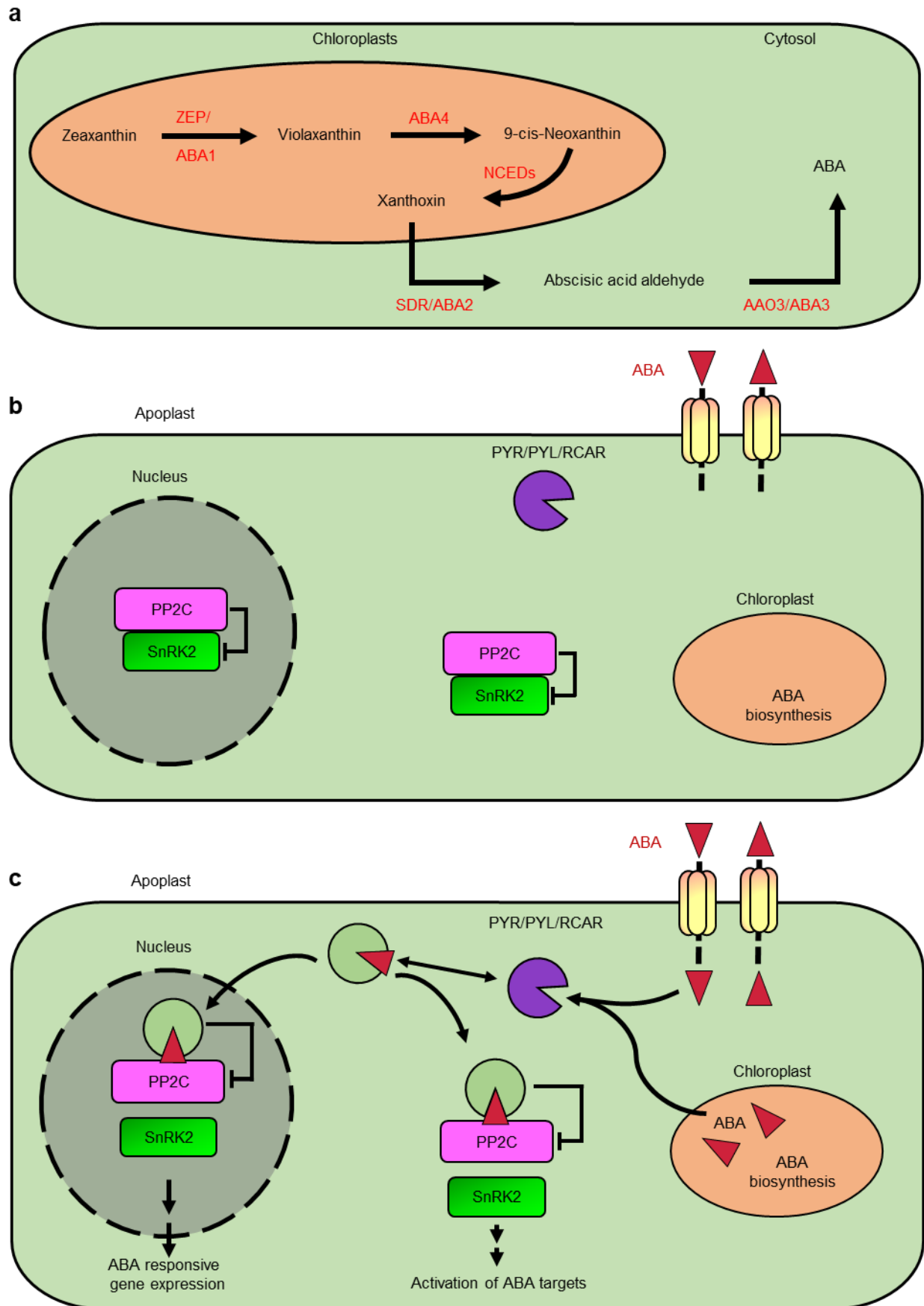
ABA biosynthesis is initiated in plastids by the conversion of zeaxanthin to violaxanthin in a process catalyzed by ZEAXANTHIN EPOXIDASE (ZEP) which is also known as LOW EXPRESSION OF OSMOTIC STRESS-RESPONSIVE GENES 6 (LOS6) and ABA1 (Finkelstein 2013; Finkelstein & Rock 2002; Xiong et al. 2002). Next, ABA4 catalyzes the reaction of violaxanthin to 9-*cis*-neoxanthin that will be turned into xanthoxin in a process catalyzed by 9-*cis*-EPOXYCAROTENOID DIOXYGENASE (NCED). Xanthoxin translocates to the cytosol (Nambara & Marion-Poll 2005), where it will be modified into absciscic acid aldehyde by the short-chain alcohol dehydrogenase/reductase (ABA2/SDR) (González-Guzmán et al. 2002). Eventually, the absciscic aldehyde will be oxidized to ABA by the ABSCISIC ALDEHYDE OXIDASE (AAO)/ABA3 (Dong et al. 2015; Mehrotra et al. 2014; Sah et al. 2016) (Figure 2a).

1.6.1.2. Absciscic acid accumulation stimulates the expression of ABA-responsive genes in cytosol and nucleus

The major breakthrough in dissecting ABA signaling was achieved by the discovery of the ABA receptors PYRABACTIN RESISTANCE 1 (PYR1) (Park et al. 2009), PYRABACTIN LIKE (PYL) and REGULATORY COMPONENT OF ABA RECEPTOR (RCAR) (Ma et al. 2009), as well as the exploration of the interaction between the ABA receptors and different members of the clade A TYPE 2C PROTEIN PHOSPHATASEs (PP2Cs) (Nishimura et al. 2010; Santiago et al. 2009). Moreover, SNF1-RELATED PROTEIN KINASEs 2 (SnRK2s) act as positive regulators of the ABA signaling cascade (Fujii et al. 2011; Fujita et al. 2009; Maszkowska et al. 2019; Umezawa et al. 2010). These kinases phosphorylate and activate the downstream targets of ABA signaling, such as ion channels that mediate stomatal closure and transcription factors for the synthesis of proteins and molecules required for adaptation to various environmental cues (Hauser et al. 2011).

At basal ABA levels, PP2Cs bind and deactivate SnRK2s (Raghavendra et al. 2010) by de-phosphorylation. SnRK2s auto-phosphorylation is required for the activation of the expression of ABA-responsive genes (Yang et al. 2017; Kulik et al. 2011). Therefore, PP2Cs are negative regulators of ABA signaling (Figure 2b). Upon ABA accumulation under stress conditions, the intracellular PYR/PYL/RCAR receptors will perceive ABA, forming an ABA-receptor complex (Gonzalez-Guzman et al. 2012; Zhang et al. 2015). The ABA-receptor complex binds and inactivates PP2Cs resulting in the activation of SnRK2s, which phosphorylate the ABA transcription factors in both the nucleus and cytosol (Xie et al. 2018) (Figure 2c).

1. INTRODUCTION



1. INTRODUCTION

Figure 2: Absciscic acid biosynthesis and signaling cascade in Arabidopsis. (a) ABA biosynthesis is initiated in plastids by the conversion of zeaxanthin to violaxanthin in a process catalyzed by zeaxanthin epoxidase (ZEP/ABA1). Next, ABA4 catalyzes the violaxanthin conversion to 9-cis-neoxanthin that will be turned into xanthoxin by 9-cis-EPOXYCAROTENOID DIOXYGENASE (NCED). Xanthoxin translocates to the cytosol, where it will be modified into abscisic acid aldehyde by the short-chain alcohol dehydrogenase/reductase (SDR/ABA2). Eventually, the abscisic aldehyde will be oxidized to ABA by the abscisic aldehyde oxidase (AAO/ABA3). (b,c) ABA signaling cascade, (b) At basal ABA levels, members of TYPE 2C PROTEIN PHOSPHATASE (PP2Cs) bind and deactivate SNF1-RELATED PROTEIN KINASE 2 (SnRK2s). SnRK2s auto-phosphorylation is required to activate the expression of ABA-responsive genes. (c) Upon ABA accumulation under stress conditions, the intracellular ABA receptors, PYRABACTIN RESISTANCE 1 (PYR1), PYRABACTIN LIKE (PYL) and REGULATORY COMPONENT OF ABA RECEPTOR (RCAR) perceive ABA, forming ABA-receptor complex. The ABA-receptor complex binds and inactivates PP2Cs resulting in the activation of SnRK2s, which phosphorylate the ABA transcription factors in both the nucleus and cytosol. Figure is adapted from Fujii et al. (2011), Umezawa et al. (2010), Maszkowska et al. (2019), Xie et al. (2018), and Zhang et al. (2015).

1.6.1.3. Absciscic acid modulates plant immunity in response to different pathogens

In addition to its well-known roles in development and abiotic stress, there is a growing body of evidence suggesting that ABA also plays a multifaceted function in defense responses after infection with pathogens (Ton et al. 2009). ABA simulates either resistance or susceptibility to distinct pathogens depending on the pathogen lifestyle (Manohar et al. 2017). ABA is proved to compromise defense responses to several pathogens, such as *B. cinerea* (Sivakumaran et al. 2016), *Ralstonia solanacearum* (Zhou et al. 2008), *Plectosphaerella cucumerina* (Sánchez-Vallet et al. 2012), and *Magnaporthe oryzae* (Ulferts et al. 2015). Moreover, some pathogens can hijack the ABA signaling pathway via the secretion of specific effectors to promote susceptibility, such as *P. syringae* (De Torres-Zabala et al. 2009; De Torres-Zabala et al. 2007; Lievens et al. 2017; Mohr & Cahill 2003). Spoel & Dong (2008) revealed that ABA triggers pathogen invasion through the suppression of callose and lignin depositions that are fundamental for the physical strengthening of the cell wall in order to hinder pathogen invasion. In contrast, ABA has been shown to mediate resistance against the necrotrophic fungus *Alternaria brassicicola* in Arabidopsis (García-Andrade et al. 2011) and the brown spot fungal pathogen in rice (De Vleeschauwer et al. 2010).

Moreover, ABA-dependent antiviral responses such as callose deposition at plasmodesmata and RNA silencing are triggered in plants challenged with viruses (Alazem & Lin 2017).

1.6.2. Pathogen-dependent activation of SA biosynthesis and signaling cascades promotes resistance against biotrophic and hemibiotrophic pathogens

SA grabbed the attention of a large number of researchers because of its critical functions in the plant cell. SA mediates local and systemic defense responses towards biotrophic and hemibiotrophic pathogens, contributes to abiotic stress adaptation, and plays an important role in numerous developmental processes in the plant (Manohar et al. 2017; Rivas-San Vicente & Plasencia 2011). Moreover, SA interferes directly and indirectly with several physiological processes mediated by other hormones via the antagonistic and synergistic crosstalk (Vlot et al. 2009).

1.6.2.1. ICS1 is a major player of pathogen-induced SA production

SA is produced via a series of enzymatic reactions in Arabidopsis by two distinct metabolic pathways, the PHENYLALANINE AMMONIA LYASE (PAL) pathway, and the isochorismate (IC) pathway. Both pathways are initiated in chloroplast from the precursor chorismate (Figure 3a). In the PAL pathway, about 10 % of pathogen-induced SA is produced from chorismate by the PAL enzyme (Rekhter et al. 2019). In the cytoplasm, the PAL pathway converts the chorismate-derived L-phenylalanine into cinnamic acid, which is transformed into SA in a process catalyzed by BENZOIC ACID-2-HYDROXYLASE (BA2H). In the IC pathway, ISOCHORISMATE SYNTHASE1 (ICS1), which is encoded by *SA INDUCTION-DEFICIENT 2/ENHANCED DISEASE SUSCEPTIBILITY16 (SID2/EDS16)* (Gina et al. 2011) is responsible for the production of 90 % of pathogen-induced SA (Garcion et al. 2008). The chloroplast envelope localized multidrug and toxin extrusion (MATE) family transporter protein EDS5 is required for transportation of isochorismate from the chloroplast into the cytosol (Rekhter et al. 2019; Serrano et al. 2013). However, the conversion of isochorismate to SA in SA-producing bacteria is catalyzed by ISOCHORISMATE PYRUVATE LYASE

1. INTRODUCTION

(IPL) (Strawn et al. 2007; Verberne et al. 2000; Wildermuth et al. 2001). From genomic analyses, no IPL homolog has been recognized in Arabidopsis (Klessig et al. 2018). Moreover, *ics1*, *eds5*, and the GH3 acyl adenylase-avrPphB SUSCEPTIBLE3 (PBS3) deficient mutant *bs3* showed reduced SA production in pathogen challenged plants (Jagadeeswaran et al. 2007; Lee et al. 2007; Nobuta et al. 2007; Rekhter et al. 2019). Additionally, Rekhter et al. (2019) performed CLSM experiments to recognize the subcellular localization of ICS1 and PBS3, and they elucidated a spatial separation of the plastid localized isochorismate and the cytosol localized PBS3 proteins. Therefore, they concluded that the plastid localized EDS5 exports the isochorismate into the cytosol to be transformed into SA in a process catalyzed by PBS3 (Figure 2a). Similarly, Torrens-Spence et al. (2019) highlighted the importance of PBS3 in SA biosynthesis in plants. However, they showed that PBS3 catalyzes the conversion of isochorismate into isochorismoyl-glutamate. Next, the enhanced *Pseudomonas* susceptibility1 (EPS1)/Isochorismoyl-glutamate A pyruvoyl-glutamate lyase (IPGL), a BAHD acyltransferase-family protein converts isochorismoyl-glutamate into SA. Consequently, these two recently published investigations closed a significant knowledge gap in plant SA biosynthesis.

1.6.2.2. NPR1 orchestrates a nucleocytoplasmic regulation of SA signaling

High throughput screens have been carried out to identify SA receptors and regulators of signal transduction (Manohar et al. 2017). As a result, a large number of SA binding proteins (SABPs) were identified, which display a wide range of affinities for SA (Klessig et al. 2016). Wu et al. (2012) proposed that *NON-EXPRESSER OF PR1* (*NPR1*), functions as a nucleocytoplasmic master transcriptional co-regulator of SA-dependent genes. Fu et al. (2012) and Wu et al. (2012) reported that the two paralogs of NPR1, NPR3 and NPR4 have very similar domain structures as NPR1, and they considered NPR3 and NPR4 as SA receptors. NPR3 and NPR4 function as E3 ligase adaptors and control the SA cascade via SA-dependent ubiquitination of NPR1 and they show differential binding affinities for SA and also for NPR1 (Becker et al. 2019; Ding et al. 2018; Mou et al. 2003).

At lower SA levels (Figure 3b), the oligomeric NPR1 senses fluctuations in the cellular redox status triggered by changes in SA content, and a physical interaction between

1. INTRODUCTION

NPR4 and NPR1 occurs, which leads to the degradation of NPR1 (Wu et al. 2012). However, under conditions of high SA concentration (Figure 3c), the intermolecular disulfide bonds in NPR1 are reduced, shifting the status of NPR1 from the oligomeric to the monomeric form in a process catalyzed in the cytosol by thioredoxins (TRX- h5/-h3) (Caarls et al. 2015). Subsequently monomeric NPR1 translocates into the nucleus to activate the expression of SA responsive genes. Interestingly, NPR1 physically interacts with different affinities, and recruits several members of the TGA family of basic leucine zipper protein (bZIP) transcription factors, which includes 10 members, TGA1-TGA10 with an overrepresentation of the TGA2, TGA5, and TGA6 in promoting the pathogen-mediated expression of the SA responsive *PATHOGENESIS-RELATED GENE1 (PR1)* via the association with its *as-1-like* promoter element (Becker et al. 2019; Ding et al. 2018). Moreover, NPR3 interacts with NPR1 promoting its degradation (Fu et al. 2012), a process which is proposed to be involved in mediating programmed cell death in which NPR1 acts as a negative regulator (Caarls et al. 2015).

1. INTRODUCTION

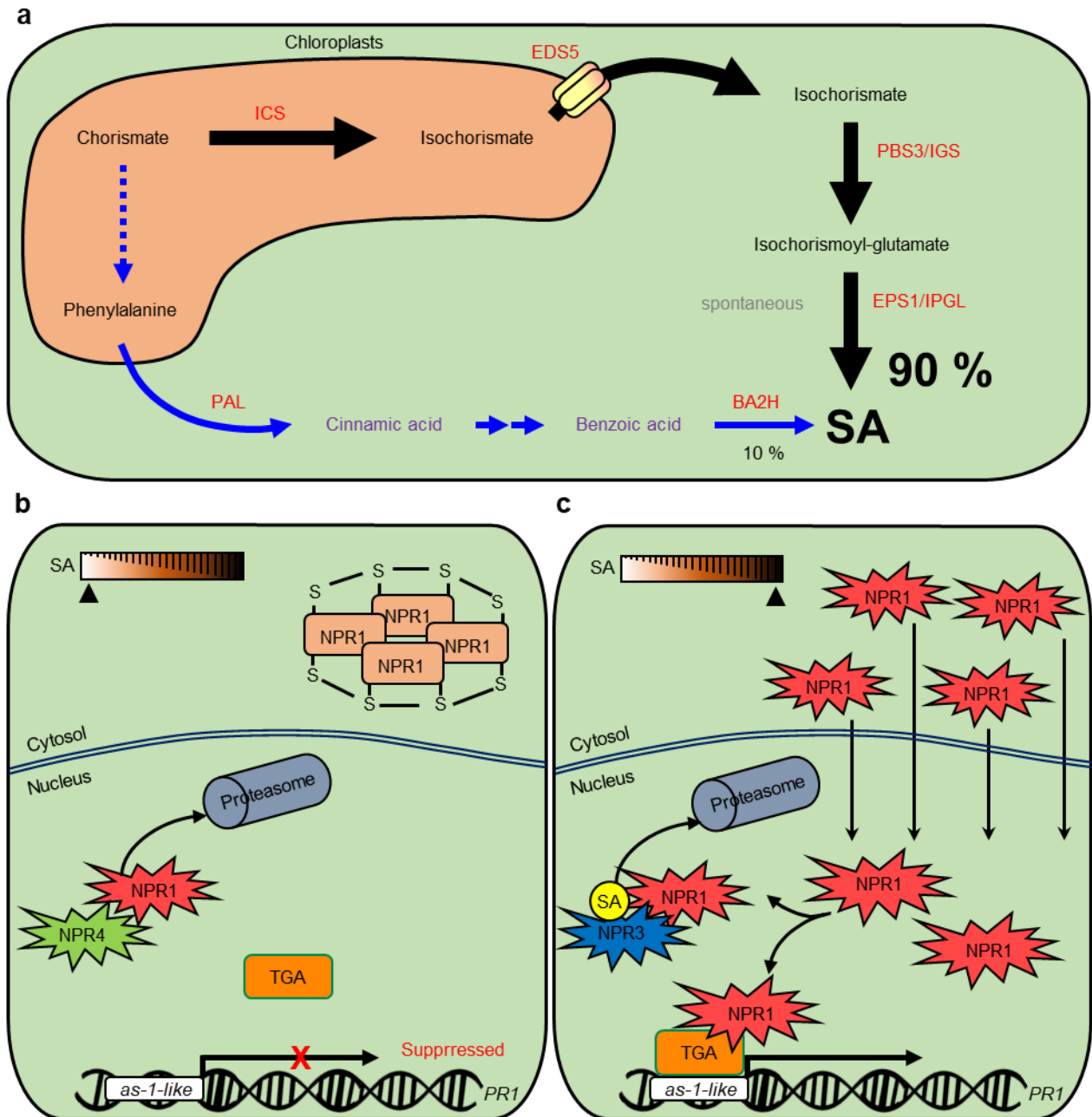


Figure 3: Salicylic acid biosynthesis and signaling cascade in Arabidopsis. (a) SA is produced in plants by two distinct pathways, the phenylalanine pathway (blue lines), and the isochorismate pathway (black lines). Both pathways are initiated in chloroplast from the precursor chorismate. Subsequently, the enzyme PHENYLALANINE AMMONIA LYASE (PAL) catalyzes the conversion of the chorismate-derived L-phenylalanine into cinnamic acid in the cytoplasm, which eventually is transformed into SA in a process catalyzed by BENZOIC ACID-2-HYDROXYLASE (BA2H) to produce about 10 % of pathogen induced SA. ICS catalyzes the conversion of chorismate to isochorismate. Next, the ENHANCED DISEASE SUSCEPTIBILITY5 (EDS5) protein exports isochorismate from the chloroplast to the cytosol to produce 90 % of the pathogen-induced SA in a process mediated by the *avrPphB* SUSCEPTIBLE3 (PBS3) and the ENHANCED PSEUDOMONAS SUSCEPTIBILITY1 (EPS1). (b,c) SA signaling cascade is regulated in an SA concentration-dependent manner. (b) At basal SA levels, the SA

1. INTRODUCTION

nucleocytoplasmic master transcriptional regulator NON-EXPRESSER OF PR1 (NPR1) is in the oligomeric form, and NPR4 physically interacts with NPR1 promoting its proteasomal degradation. (c) At higher SA levels, the NPR1 monomerization takes place. Subsequently, the monomeric NPR1 translocates into the nucleus to physically interact and recruits the TGA transcription factors, which associate with the *as-1-like* element in the promoter of the SA responsive genes such as *PATHOGENESIS-RELATED GENE1 (PR1)* promoting its expression. Moreover, NPR3 interacts with NPR1 promoting its degradation. Figure is adapted from Backer et al. (2019), Caarls et al. (2015), Rekhter et al. (2019), and Torrens-Spence et al. (2019).

1.6.2.3. Upregulation of salicylic acid accumulation and signaling promotes plant resistance during different biotrophic interactions

The upregulation of SA biosynthesis, perception, and signaling is pivotal for the adequate activation of both PTI and ETI, particularly the ETI-triggered cell death (Katagiri & Tsuda 2010; Zhang et al. 2018). In non-infected plants, SA levels are kept at low concentrations, whereas SA concentration is significantly elevated after interaction of a host plant with biotrophic invaders, pointing to a crucial role of SA in resistance to such pathogens (Broekgaarden et al. 2015). Hence, SA biosynthetic and signaling mutants, as well as transgenic *Arabidopsis* expressing the bacterial salicylate hydroxylase gene (*nahG*) exhibit compromised plant resistance, whereas exogenous application of SA restored the resistance to plant pathogens in these lines (Ding et al. 2018; Li et al. 2019b). For instance, *ics1 sid2* double mutant, which are known to have a compromised SA production, show significantly diminished plant resistance (Garcion et al. 2008; Lu et al. 2016; Wildermuth et al. 2001). In addition, the *npr1* mutant also displays a compromised resistance as well as declined transcript levels of *PR* genes (Cao et al. 1994; Glazebrook et al. 1996), the previously mentioned phenotypes are complemented in the *AtNPR1*-transformed *npr1* mutants (Cao et al. 1997). *AtNPR1* overexpressing plants display enhanced resistance to a wide range of plant pathogens (Backer et al. 2019). Furthermore, Zhang et al. (2006) investigated the negative impact of NPR1 paralogs NPR3 and NPR4 on SA-dependent PR1 gene expression as well as pathogen resistance. Hence, they mediate NPR1 proteasome degradation and they physically interact with the TGA2 transcription factor. Subsequently, they complemented the elevated *PR1* expression and disease

resistance in the *npr3 npr4* double mutant upon *Agrobacterium* mediated transformation of *NPR3* or *NPR4* into *npr3 npr4* double mutant.

1.6.3. Jasmonate biosynthesis and signaling promote resistance against necrotrophs

Six decades ago, the lipid-derived jasmonates (JAs) had been discovered and classified as essential hormones governing many developmental and defense processes *in planta* (Ruan et al. 2019). JAs play essential roles in plant resistance against necrotrophic pathogens and herbivorous insects (Han 2016). In addition, JAs have multiple other functions in plants, such as in flower and seed development, as well as in trichome formation (Campos et al. 2014; Kazan 2015). Furthermore, they play a role during plant exposure to diverse abiotic stresses (Yuan & Zhang 2015). The most abundant biologically active form of JAs is the isoleucine conjugate JA (JA-Ile) (Fonseca et al. 2009). JA production, allocation, metabolism, perception, signaling, and crosstalk with other hormones have been intensely studied in different plants (Han 2016).

1.6.3.1. Jasmonate biosynthesis occurs sequentially in multi-cellular compartments

JAs are generated by the lipoxygenase (LOX) pathway (Wasternack & Strnad 2018). In chloroplasts, the highly unstable galactolipids are transformed into α -linolenic acid (α -LeA) by the A1-type plastid lipases (PHOSPHOLIPASE A1; PLA1 and PLASTID LIPASE; PLIP) (Figure 4a). Next, *cis*-(+)-12-oxophytodienoic acid (*cis*-(+)-OPDA) is produced in a process catalyzed by a 13-LOX, ALLENE OXIDE SYNTHASE (AOS), and ALLENE OXIDE CYCLASE (AOC). Subsequently, the intermediate OPDA is translocated into peroxisomes where it undergoes reduction and oxidation processes catalyzed by OPDA REDUCTASE3 (OPR3) and acyl-coenzyme A oxidase1 (ACX1), respectively to form (+)-7-iso-JA. JA is then transported by JASMONIC ACID TRANSPORTER2 (JAT2) (Wang et al. 2019) into the cytosol to be conjugated with amino acids, a step which is catalyzed by JA-AMINO ACID SYNTHETASE (JAR1), or it is exported to the nucleus or the apoplast by JAT1 (Wang et al. 2019; Ruan et al.

2019). JAT1, which is encoded by *AtJAT1/AtABCG16*, exhibits a dual localization in the plasma membrane and the nuclear envelope, thus, it mediates both cellular efflux of JA as well as the nuclear influx of JA-Ile for JA signal transduction (Li et al. 2017; Wasternack & Song 2016; Wasternack & Strnad 2018).

1.6.3.2. Jasmonate signaling is activated via two different JA-dependent transcriptional networks

With respect to JA Signaling, the discovery of JASMONATE ZIM DOMAIN (JAZ) proteins as negative regulators of JA signaling in 2007 was a breakthrough (Wasternack 2007; Wasternack & Hause 2013). Moreover, the F-box protein CORONATINE INSENSITIVE1 (COI1) has been identified by Xie et al. (1998) as a receptor component of JA signaling (Srivastava et al. 2018). Three different groups have independently revealed that in the presence of JA-Ile, JAZ repressor protein is a target of the SCF^{COI1} complex, which functions as an E3 ubiquitin ligase (Chini et al. 2007; Thines et al. 2007; Yan et al. 2007). In the absence of JA, the repressor protein JAZ interacts with the co-repressor TOPLESS (TPL) or with RPD3-type HISTONE DEACETYLASE6 (HDA6) via an adapter protein called Novel Interactor of JAZ (NINJA), leading to the suppression of the transcription factors MYC2 or ETHYLENE-INSENSITIVE 3 (EIN3) and ETHYLENE-INSENSITIVE 3-LIKE 1 (EIL1), respectively (Song et al. 2014) (Figure 4b).

On the other hand, the accumulation of JA-Ile (Figure 4c) mediates the binding of JAZ to COI1 (Katsir et al. 2008), targeting JAZ for degradation by the 26S proteasome leading to the activation of downstream transcription factors to enhance the expression of JA responsive genes (Caarls et al. 2015). Two different branches of transcriptional networks have been identified as targets for the JA signaling pathway: the MYC branch which is known to be upregulated by JA, leading to the expression of JA marker gene *VEGETATIVE STORAGE PROTEIN 2 (VSP2)* (Figure 4c, upper panel) (Vos et al. 2013) and ET-RESPONSIVE FACTOR (ERF) branch, which is co-regulated not only by JA, but also by ET and controlled by the transcription factors EIN3/ EIL1, ERFs and *OCTADECANOID-RESPONSIVE ARABIDOPSIS 59 (ORA59)* leading finally to the expression of JA/ET marker gene *PLANT DEFENSIN1.2 (PDF1.2)* (Figure 4c,

1. INTRODUCTION

lower panel) (Caarls et al. 2015; Pieterse et al. 2012; Wasternack & Hause 2013; Zhu et al. 2011).

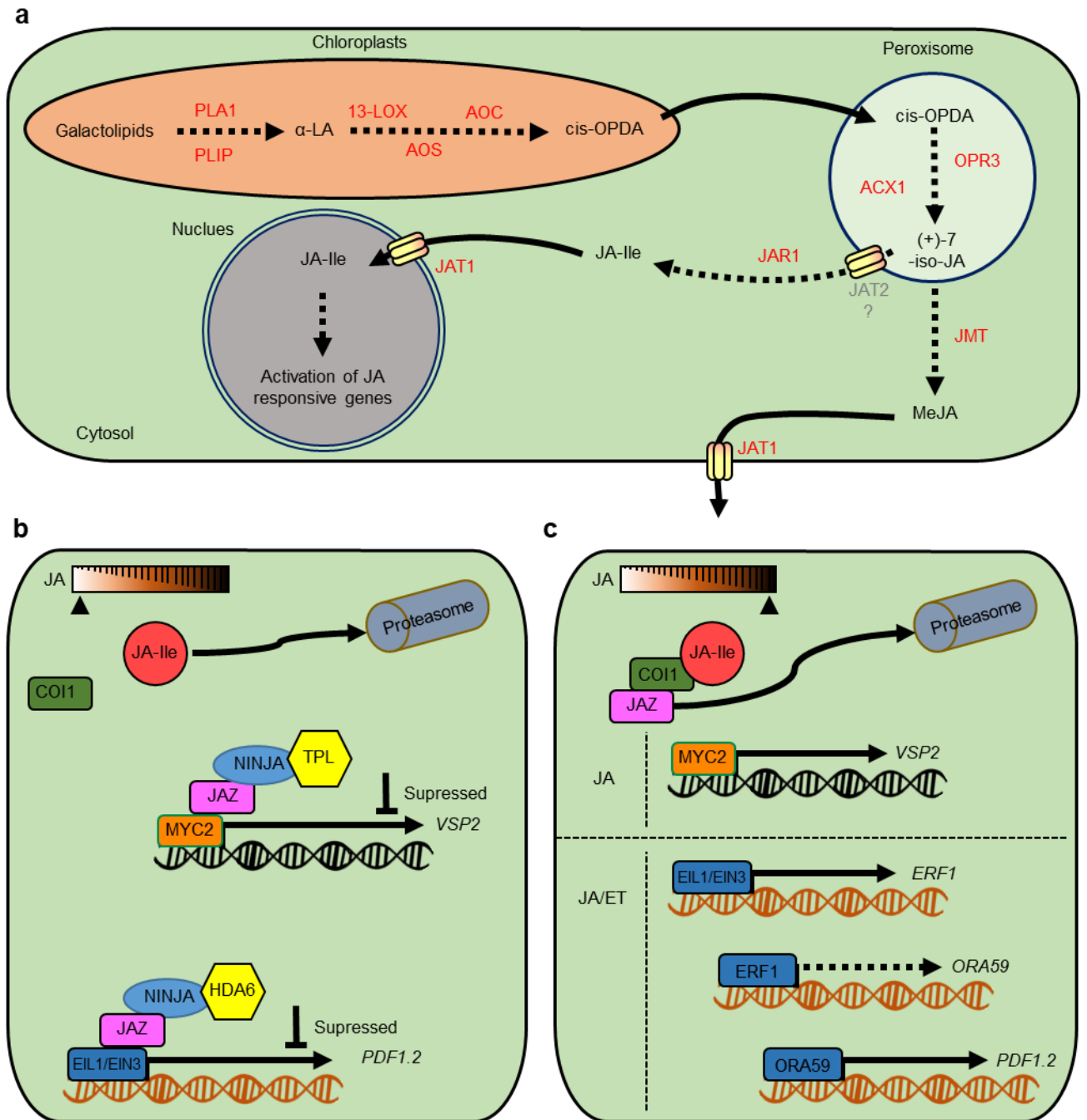


Figure 4: Jasmonic acid biosynthesis and signaling cascade in Arabidopsis. (a) Jasmonates are generated by the lipoxygenase (LOX) pathway in different cellular compartments. In chloroplasts, the A1-type plastid lipases (PHOSPHOLIPASE A1; PLA1 and PLASTID LIPASE; PLIP) catalyze the conversion of galactolipids into α-linolenic acid (α-LeA), that subsequently is transformed into cis-12-oxophytodienoic acid (cis-OPDA) by a 13- lipoxygenase (LOX), ALLENE OXIDE SYNTHASE (AOS), and ALLENE OXIDE CYCLASE (AOC). Subsequently, the cis-OPDA

1. INTRODUCTION

is translocated into the peroxisomes where it undergoes redox interactions catalyzed by OPDA REDUCTASE3 (OPR3) and acyl-coenzyme A oxidase1 (ACX1) to form (+)-7-iso-JA. Further, (+)-7-iso-JA is transported by JASMONIC ACID TRANSPORTER2 (JAT2) into the cytosol to be conjugated with amino acids by JA-AMINO ACID SYNTHETASE (JAR1), or it is exported to the nucleus or the apoplast by JAT1 that mediates both cellular efflux of JA as well as the nuclear influx of JA-Ile for the activation of the JA responsive genes expression. (b,c) JA signaling cascade is regulated dependently on the JA concentration. (b) In the absence of JA, the repressor protein JAZ interacts with the co-repressor TPL or with HDA6 via an adapter protein NINJA leading to the suppression of the transcription factors MYC2 or EIN3 and EIL1. (c) In high JA concentrations, it mediates the JAZ interaction with COI1 targeting JAZ for degradation by the 26S proteasome leading to the activation of JA transcription factors to enhance the expression of JA responsive genes in two different transcriptional networks: the MYC2 transcription factor that upregulates the expression of *VEGETATIVE STORAGE PROTEIN 2* (*VSP2*) (upper panel). The second branch of JA signal transduction is the ERF branch which is co-regulated by ET, and transcriptionally upregulated by EIN3/EIL1, ET RESPONSE FACTOR (ERFs) and OCTADECANOIC-RESPONSIVE ARABIDOPSIS 59 (ORA59) leading finally to the expression of JA/ET marker gene *PLANT DEFENSIN1.2* (*PDF1.2*) (lower panel). Figure is adapted from Zhu et al. (2011), Caarls et al. (2015), Caarls et al. (2017), Li et al. (2017), Wasternack & Strnad (2018), and Li et al. (2019a).

1.6.3.3. Jasmonic acid shows a dual contribution to defense responses against several necrotrophs

Many studies have shown a dual contribution of JA in resistance to several necrotrophs as well as to herbivorous insects and nematodes. For instance, the JA biosynthetic *FATTY ACID DESATURASE* genes (*FADs*) loss of function triple mutant *fad3 fad7 fad8*, as well as the JA signaling mutant *coi1* showed enhanced susceptibility to the fungal necrotroph *A. brassicicola* (McConn & Browse 1996; Stintzi et al. 2001; Thatcher et al. 2009). Similarly, increased pathogenic growth was also observed with the JA biosynthetic mutants *aos*, *jar1*, and DEFENSIN1 mutant *def1* (Abuqamar et al. 2008; Kachroo & Kachroo 2009). On the contrary, other JA biosynthetic and signaling mutants such as *opr3* and *myc2/jin1* exhibited higher resistance compared to wildtype plants against *Fusarium graminearum* (Bhattarai et al. 2008) and to both *B. cinerea* and *P. cucumerina* (Kachroo & Kachroo 2009), respectively. This enhanced resistance might possibly result from the ET triggered resistance to necrotrophs because of MYC-repressed EIN3 (Song et al. 2014). It has been shown that JA biosynthesis is triggered not only locally at the sites of damage, but also systemically

to activate the expression of defense-related genes and the production of toxic secondary metabolites to defend against invaders (Yan & Xie 2015).

1.6.4. Ethylene modulates high complexity *in planta* aspects

The two-carbon gaseous molecule, ET is a potent regulator for plant growth and development, as well as for adaptation to various biotic and abiotic stresses (Wang et al. 2002). Similar to the aforementioned phytohormones, numerous studies have been conducted to elucidate ET biosynthesis, perception and signaling (Gallie 2015).

1.6.4.1. Members of multigene families regulate ethylene biosynthesis

The major breakthroughs during the analyses of ET biosynthesis were the discovery of the methyl group donor S-adenosylmethionine (S-AdoMet) and the ET precursor 1-aminocyclopropane-1-carboxylic acid (ACC) (Yang & Hoffman 1984). The first step in ET biosynthesis is the conversion of methionine to S-AdoMet in a process catalyzed by S-AdoMet synthase. Subsequently, ACC synthase (ACS) mediates the conversion of S-AdoMet to ACC, which is oxidized by ACC oxidase (ACO) to produce ET (Figure 5a). Both ACS and ACO are members of multigene families that are regulated by different stimuli (Ravanbakhsh et al. 2018).

1.6.4.2. Both ethylene and jasmonic acid up-regulate the expression of *PDF1-2*

The *Arabidopsis* genome encodes five structurally and functionally different receptors localized to the endoplasmic reticulum that are responsible for ET perception. Without binding of the ligand ET, they function as suppressors of ET signaling (Gallie 2015). Several ET receptor mutants exhibit constitutive ET responses (Hall & Bleecker 2003). The two-component histidine kinase-like ET receptors have been classified into two subfamilies: subfamily I includes ethylene receptor 1 (ETR1) and ethylene response sensor 1 (ERS1), while subfamily II includes ETR2, ERS2, and ethylene insensitive 4 (EIN4) (Urao et al. 2001; Hall et al. 2012). At low ET concentrations (Figure 5b), these receptors negatively regulate the ET signaling cascade by the activation of CONSTITUTIVE TRIPLE RESPONSE1 (CTR1). CTR1 has a negative impact on ET signal transduction via suppression of the positive regulator of ethylene signaling EIN2

1. INTRODUCTION

(Alonso et al. 1999). Suppression of EIN2 activity initiates EIN3 ubiquitination mediated by the F-box proteins EBF1/2 and allows degradation of EIN3 and its homolog ethylene-insensitive 3-like 1 (EIL1) by the 26S proteasome (Ravanbakhsh et al. 2018). Thus, ET perception by its receptors results in suppression of the kinase activity of CTR1 and activation of the ET transcriptional cascade via the stabilization of EIN3 and EIL1 by blocking EBF1/2-mediated EIN3 degradation (An et al. 2010). EIN3/EIL1 mediates the upregulation of *ERFs*, *ORA59* and eventually the expression of *PDF1.2* (Figure 5c and Figure 4c, lower panel) (Groen et al. 2013).

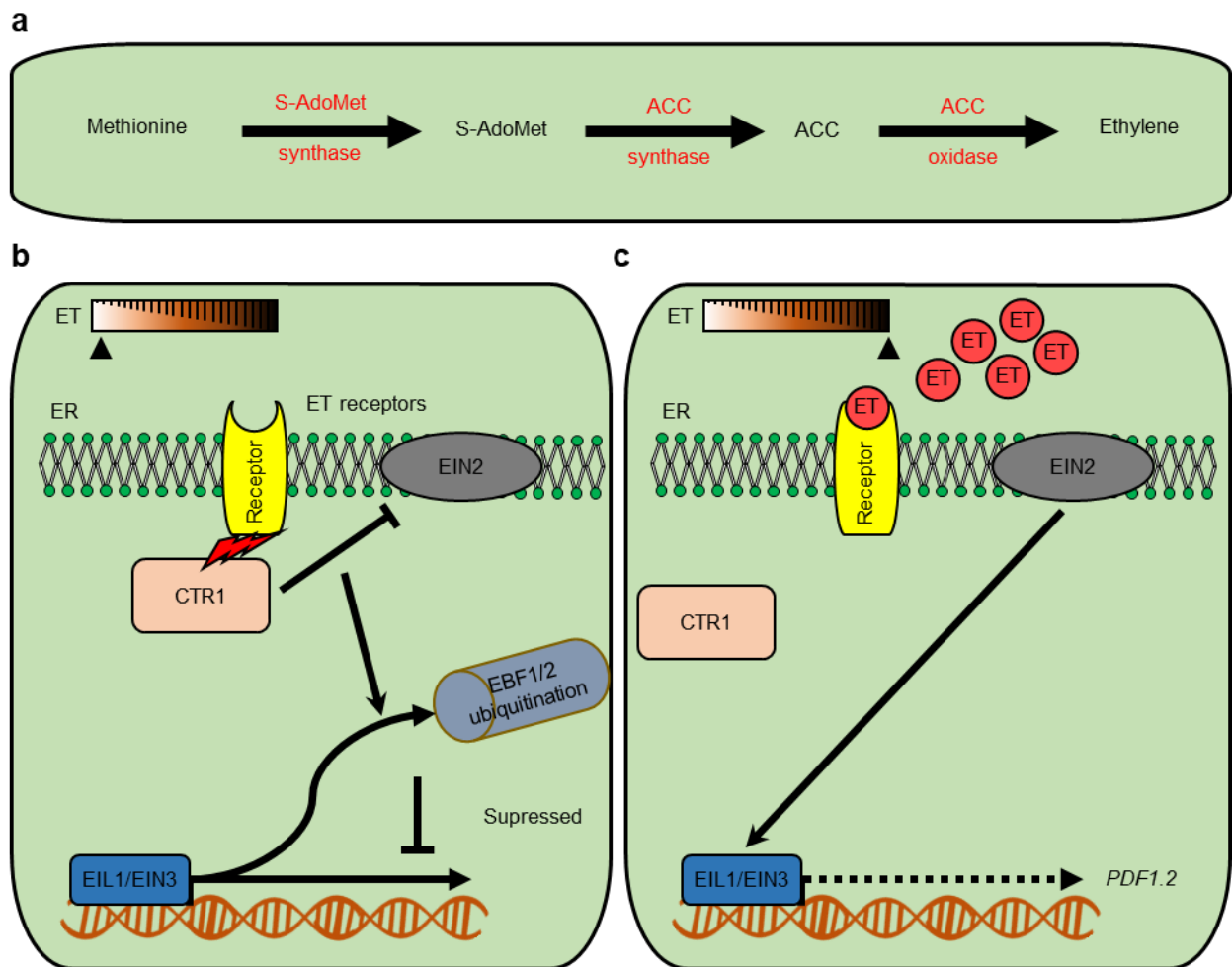


Figure 5: Ethylene biosynthesis and signaling cascade in Arabidopsis. (a) Ethylene biosynthesis, the first step in ET biosynthesis, is the conversion of the methionine to the methyl group donor S-adenosylmethionine (S-AdoMet) in a process catalyzed by S-AdoMet synthase. Subsequently, 1-aminocyclopropane-1-carboxylic acid (ACC) synthase (ACS) mediates the conversion of S-AdoMet to ACC, which is oxidized by ACC oxidase (ACO) to produce ET. (b,c) ET signaling cascade, (b) The endoplasmic reticulum - localized ET receptors are responsible for ET perception. At low ET concentrations, these receptors negatively regulate the ET signaling cascade by the activation

1. INTRODUCTION

of CONSTITUTIVE TRIPLE RESPONSE1 (CTR1). CTR1 has a negative impact on ET signal transduction via suppression of the positive regulator of ethylene signaling ET insensitive 2 (EIN2). The suppression of EIN2 activity initiates EIN3 ubiquitination mediated by the F-box proteins EBF1/2 and allows degradation of EIN3 and its homolog ethylene-insensitive 3-like 1 (EIL1) by the 26Sproteasome. (c) At high ET concentration, ET perception by its receptors results in suppression of the kinase activity of CTR1, leading to the activation of the ET transcriptional cascade via the stabilization of EIN3 and EIL1 that mediate the upregulation of PDF1.2. This figure is adapted from An et al. (2010), Gallie (2015), Groen et al. (2013), and Ravanbakhsh et al. (2018).

1.6.4.3. Ethylene promotes resistance against necrotrophs and susceptibility against biotrophs

ET plays an important role in defense responses against different necrotrophs, acting synergistically with JA. The upregulation of ET downstream transcription factors ERF1 and ORA59 contributes to the resistance against necrotrophic pathogens (Robert-Seilaniantz et al. 2011). Therefore, the overexpression of *ERF1* promotes resistance against the necrotrophic pathogen *B. cinerea* and susceptibility to the hemibiotrophic pathogen *P. syringae* (Berrocal-Lobo & Molina 2004). Additionally, treatment of Arabidopsis with flg22 enhances ET biosynthesis as well as the EIN3 accumulation (Asai et al. 2002; Nühse et al. 2000), thus the flg22-induced MPK3/MPK6 might have a major contribution to ACC synthase activation and EIN3 stabilization (Chen et al. 2009). Although *ein2* displayed impaired FLS2-mediated responses (Boutrot et al. 2010), *ein3-1 ein1-1* double mutant and *ein2-1* showed enhanced resistance to *P. syringae* (Chen et al. 2009), revealing a prospective role for ET in mediating susceptibility to biotrophic and hemibiotrophic pathogens.

1.7. Hormone crosstalk in plant immunity equips plants with a powerful adaptive capacity.

While deciphering the underlying hormone perception and signal transduction mechanisms in the past decades, various molecular, biochemical, and genomic analyses have provided pieces of evidence that plant hormones interact antagonistically or synergistically to regulate phytohormone biosynthesis, transport, perception, gene expression and post-transcriptional modifications (Pieterse et al. 2009). These interactions between plant hormones have been displaced by the concept of hormonal crosstalk. During plant-pathogen interactions, hormone crosstalk equips plants with a powerful adaptive capacity to utilize their resources in a cost-efficient manner in order to finely regulate various energy-consuming processes (De Bruyne et al. 2014; De Vleeschauwer et al. 2014).

1.7.1. JA-ET synergistic crosstalk

Various investigations showed contributory roles for JA and ET in resistance against necrotrophic pathogens (Broekaert et al. 2006; Solano & Gimenez-Ibanez 2013), indicated by the upregulation of biosynthetic and signaling cascades of both hormones during infection with necrotrophic pathogens (Pieterse et al. 2012). JA and ET cooperatively stimulate *PDF1.2* expression in *A. thaliana* after inoculation with the necrotrophic pathogen *A. brassicicola* and *B. cinerea*, as well as with the hemibiotrophic bacterium *Erwinia carotovora* (Penninckx et al. 1996; Norman-Setterblad et al. 2000; Berrocal-Lobo & Molina 2004; Van der Does et al. 2013). Furthermore, both hormones induce ethylene-inducible GCC-box containing genes, such as *PR1b* and the stress-responsive antifungal protein OSMOTIN in tobacco, when exogenously applied to plant tissue (Kunkel & Brooks 2002; Xu et al. 1994). Hence, the GCC box in the promoter of *PDF1.2* is targeted by ERF proteins, such as ERF1 and ORA59, which confers JA responsiveness and synergy between JA and ET (Figure 5c) (Brown et al. 2003; Pré et al. 2008).

1.7.2. JA-JA/ET antagonistic crosstalk

Although ET and JA synergistically regulate the ERF branch (Figure 5c), there is growing evidence that JA and JA/ET signaling pathways antagonize each other in the regulation of the MYC branch of the JA signaling cascade (Lorenzo et al. 2004; Lorenzo & Solano 2005). Hence, the JA-master regulator MYC2 negatively regulates *PDF1-2* expression via the repression of the JA/ET transcription factors ERF1 and ORA59 (Dombrecht et al. 2007; Zander et al. 2010; Verhage et al. 2011). In addition, Zhu et al. (2011) showed that at intermediate JA concentrations, JAZ proteins interact and partially suppresses the transcriptional activity of ET transcription factors EIN3 and EIL1 by induction of the transcriptional co-repressor HDA6. However, elevated ET stabilizes EIN3 and EIL1, providing a second level of transcriptional regulation through JA.

1.7.3. SA-JA/ET antagonistic crosstalk

The enhanced SA-mediated resistance to biotrophs, indicated by the compromised resistance in SA deficient and signaling mutants (Adam et al. 2018) is often associated with a reduced JA/ET-mediated resistance to necrotrophs. This is reflected by the upregulation of biosynthetic and signaling cascades of JA and ET during infection with necrotrophic pathogens (Li et al. 2019b; Robert-Seilanianantz et al. 2011; Van der Does et al. 2013). For instance, Spoel et al. (2007) demonstrated an antagonistic effect of SA on JA/ET signaling pathway in Arabidopsis, as plants challenged with the hemibiotrophic pathogen *P. syringae* exhibited hypersusceptibility to the necrotroph *A. brassicicola* due to the repressive effect of elevated SA on JA/ET signaling cascades. Additionally, the expression of the JA biosynthetic genes *LOX2*, *AOS*, *AOC2*, and *OPR3* is downregulated by SA treatment (Leon-Reyes et al. 2010; Thaler et al. 2012). Leon-Reyes et al. (2009) and Broekgaarden et al. (2015) concluded that the SA transcriptional co-activator NPR1 acts as a substantial modulator for SA and JA/ET signaling crosstalk. Additionally, Chen et al. (2009), Lorenzo & Solano (2005), and Thaler et al. (2012) documented a direct interaction of the JA/ET transcription factor EIN3 and EIL1 with the promoter of *ICS2* to suppress SA biosynthesis, reflecting a reciprocal SA-JA/ET antagonism.

1. INTRODUCTION

Mur et al. (2006) demonstrated that expression of both SA- and JA/ET- responsive defense genes *PR1* and *PDF1.2* was synergistically and antagonistically affected during SA and JA cotreatment in a concentration-dependent manner. Treatment of Arabidopsis plants with 10 μ M JA resulted in upregulated *PDF1.2* expression, which is elevated after cotreatment with 10 μ M JA and SA up to 250 μ M, while higher SA concentrations showed declined *PDF1.2* transcript levels. Similarly, the 10 μ M SA induced expression of *PR1* showed further elevation after cotreatment with 10 μ M SA and increasing concentrations of JA up to 125 μ M, while treatment above 125 μ M up to 500 μ M JA showed a declined *PR1* expression. Thus, SA and JA/ET crosstalk was synergistically affected during SA/JA cotreatment at low concentrations, but antagonistically at higher hormone concentrations.

Despite the reports on SA-JA/ET antagonisms (Robert-Seilaniantz et al. 2011; Derksen et al. 2013; Caarls et al. 2015), only a few studies indicated that JA/ET might be an essential regulator of SA signaling. For example, Ramšak et al. 2018 inferred that the SA-dependent upregulation of *NPR1* and *PR1* expression is blocked in *ein3-1*, reflecting the positive impact of JA/ET on the SA network (Frye et al. 2001; Mikkelsen et al. 2003).

1.7.4. ABA-SA crosstalk

Several studies outlined antagonistic crosstalk between ABA and SA during different biotic and abiotic stress responses (De Torres-Zabala et al. 2009; Denancé et al. 2013; Fan et al. 2009; Manohar et al. 2017; Nahar et al. 2012; Tan et al. 2019; Yasuda et al. 2008). In the latter study, an elevated expression level of *PR1* was observed in the ABA biosynthetic mutant *aba2-1* after *p. syringae* infections, while the transcript level is compromised in the *35S-ABA2* overexpression line and ABA-treated wildtype Arabidopsis plants. This displays comparable effects for the intrinsic ABA production and extrinsic ABA on antagonizing SA signaling. Subsequently, they revealed that the endogenous and exogenous ABA-dependent antagonistic effect on SA signaling and callose deposition are the main reasons for the susceptibility of the *35S-ABA2* and ABA-treated wildtype and ABA-treated *aba2-1* to *p. syringae*. Furthermore, Nahar et al. (2012) demonstrated that the rice SA-mediated defense against nematodes collapsed after exogenous application of ABA and showed that

1. INTRODUCTION

these defense responses are modulated by ABA-mediated down-regulation of SA signaling pathways.

Manohar et al. (2017) used different high throughput assays to highlight the molecular mechanisms underlying SA-ABA antagonism. The authors demonstrated that most of the PP2Cs, being negative regulators of the ABA signaling pathway, are salicylic acid binding proteins (SABPs). Furthermore, they showed that the exogenous application of SA negatively regulates the ABA-enhanced degradation of PP2Cs by competing for its binding with the ABA receptors PYR/PYL/RCAR. Consequently, this also inhibits the expression of ABA-responsive genes. Moreover, using the SA-biosynthesis mutant *sid2-1*, they provided further evidence for this antagonism as they observed a stronger negative ABA impact on the germination of SA-deficient mutant seeds in comparison to the wildtype. Furthermore, Meguro & Sato (2014) tested the impact of ABA treatment alone and in combination with SA on the growth and development of rice. The authors observed that ABA inhibits shoot growth as well as the expression of cell cycle-related genes. On the other hand, SA in SA-ABA cotreated seedlings antagonizes the ABA-inhibitory effect on the shoot apical meristem, as well as leading to elevated expression levels of *OsKRP* genes, which provides additional proof for the reciprocal SA-ABA antagonistic crosstalk.

However, not all data support the hypothesis on antagonistic crosstalk between ABA and SA. Some studies reported on the synergistic interactions between SA and ABA signaling cascades (Alazem et al. 2019). For instance, SA and ABA signaling pathways positively interact through Ca^{2+} -dependent protein kinases in modulating stomatal closure (Prodhan et al. 2018). Moreover, both SA and ABA pathways synergistically recruit RNA silencing pathways to promote viral resistance (Alazem & Lin 2015; Alazem & Lin 2017; Alazem et al. 2018; Alamillo et al. 2006).

1.7.5. ABA-JA/ET crosstalk

Many studies addressed the antagonistic interaction between ABA and JA/ET signaling pathways (Anderson et al. 2004; Kazan & Manners 2013; Nahar et al. 2012). For example, exogenous ABA application down-regulates the expression of the JA transcription factors ERF1, ORA59, within approximately 30 minutes after treatment

(Winter et al. 2007). ERF1 and ORA59 activate the expression of the JA/ET responsive gene *PDF1-2*, and this provides an explanation for the declined expression levels of the pathogen-induced *PDF1.2* upon exogenous application of ABA. However, the transcript level was highly upregulated in the ABA-biosynthetic mutants; *aba1-1*, *aba1-2*, *aba1-5* and *aba2-1* (Anderson et al. 2004). Moreover, Nahar et al. (2012) observed a down-regulatory effect of ABA on the expression of the positive regulator of ET signaling *OsEIN2a* as well as the JA biosynthetic gene *OsAOS2*.

1.8. Hormone sensing

1.8.1. Limitations of classical hormone detection and quantification assays

Although significant advances have been made in understanding the biosynthesis, signaling, and perception of phytohormones, the understanding of their cell- and tissue-specific production, transport, and crosstalk are still lagging behind. In this regard, diverse assays have been used to qualitatively and quantitatively address the changes in plant hormones. Classical biochemical quantification, marker gene expression measurements, immunochemical assays such as enzyme-linked immunosorbent assays (ELISA) as well as mutant analysis have been used for hormone detection and quantification (Davis et al. 1985; Murmu et al. 2014; Wang et al. 2011; Wirthmueller et al. 2018). Although such methods have a high sensitivity for detecting hormones, their ability to resolve spatial activities and cell-type-specificity are still relatively low (Müller et al. 2002; Weiler et al. 1982).

1.8.2. Assays using biologically active fluorescently labeled hormones

To gain novel insights into hormone abundance and activity in intact living cells or intact tissues, new techniques have been developed. Irani et al. (2012), Hong Gao et al. (2013), Shani et al. (2013), Sokołowska et al. (2014) and Hayashi et al. (2014) developed biologically active, fluorescently labeled BRs, JA, GA, and auxin, respectively. These newly developed tools promoted the understanding of the cellular perception and transportation of the hormones as mentioned above, however, they can only be used in the exogenous hormone application experiments (Waadt et al. 2015).

1.8.3. FRET based reporters

So far, for plant hormones, only the ABACUS and ABAleon Förster resonance energy transfer (FRET)-based reporters have been engineered in Arabidopsis plants to investigate the spatial dynamics of ABA accumulation rather than ABA signaling (Jones et al. 2014; Waadt et al. 2014). In these studies, the authors generated a fluorescent protein FRET-pair utilizing improved versions of cyan fluorescent protein (CFP) as an excited donor and the yellow fluorescent protein (YFP) as an acceptor connected to a hormone sensory module harboring a PYR1/PYL1 receptor of ABA fused via a linker to ABI1 (Jones et al. 2014; Waadt et al. 2014; Waadt et al. 2015). The direct binding of ABA to the sensory module thereby alters the distance and orientation of the FRET-pair leading to an energy transfer from the donor to the acceptor (Heim & Tsien 1996; Pollok & Heim 1999). Subsequent measurements of YFP/CFP emission ratios enable the quantification of the bound hormone amount (Waadt et al. 2015). The two orientally flipped ABACUS, and ABAleon reporters exhibited different affinities to ABA perception and inconsistent energy transfer. ABACUS versions displayed a low ABA affinity and high energy transfer to the YFP acceptor, whereas ABAleon showed a high ABA affinity with a low energy transfer (Jones et al. 2014; Waadt et al. 2014; Waadt et al. 2015). Although the development of these reporters presented obvious advances, they still need to be further improved because they displayed an insensitive and limited utility to map the basal levels of endogenous ABA (Waadt et al. 2015; Hayes 2018; Wu et al. 2018).

1.8.4. Degrons based reporters

A degron is a portion of a protein which regulates its degradation (Trauth et al. 2019). Degrons have been used for the development of two reporters allowing the tracking of auxins and JA. Brunoud et al. (2012) developed the auxin reporter DII-VENUS to quantify auxins in plant cells. This reporter is based on the DII interaction domain of AUX/IAA proteins, which are degraded upon auxin binding. Therefore, the output fluorescence negatively correlates with auxin concentrations. Larrieu et al. (2015) developed a JA reporter system using the advantage of the JAZ-degradation dependency upon the activation of JA signaling on a specific Jas motif in JAZ proteins responsible for their interaction with COI1. They fused the Jas motif of AtJAZ9 with the

VENUS fluorescent protein to express it under the control of the constitutive promoter Cauliflower Mosaic Virus 35S RNA (*CaMV35S*). In comparison to a mutated version (*mJas9-VENUS*), they could correlate the magnitude of JA signaling activity to the reduction in VENUS intensity in *Jas9-VENUS*.

1.8.5. Hormone-inducible promoter-based reporters

Next, hormone-responsive gene reporters within the field of hormone sensing have been developed to visualize the hormone-dependent expression of marker genes. The most prominent examples for such systems have been generated to map the plant hormones auxin, CK, ABA, JA, SA, and ET. The newly developed hormone sensors for the six hormones mentioned above were grouped into the following:

1.8.5.1. Native promoter-based reporters

The native promoters of hormone responsive genes have been fused to different reporter genes such as luciferase-coding sequence (LUC), b-glucuronidase (GUS) , Green fluorescent protein (GFP) and YFP to address the changes in biosynthesis, signaling and allocation activities of the plant hormones CKs (D'Agostino et al. 2000), ABA (Christmann et al. 2005; Himmelbach et al. 2002; Ishitani et al. 1997; Söderman et al. 1999;), SA (Betsuyaku et al. 2018), JA (Mousavi et al. 2013; Betsuyaku et al. 2018) and JA/ET (Manners et al. 1998). For instance, D'Agostino et al. (2000) addressed the positive correlation of the *Arabidopsis response regulators (ARRs)* expression with CK. Next, they used the promotor of *ARR5*, which showed the maximal expression in comparison to other *ARRs* in response to CK to develop the *pARR5-GUS* reporter system.

Christmann et al. (2005), Himmelbach et al. (2002), Ishitani et al. (1997), and Söderman et al. (1999) fused the promoters of the ABA responsive genes; *HOMEODOMAIN PROTEIN 6 (AtHB6)*, *RESPONSIVE TO DESICCATION 29A/B (AtRD29A/B)*, and *ARABIDOPSIS RAB GTPASE HOMOLOG B18 (AtRAB18)* to drive the expression of LUC, GUS and GFP reporters in order to monitor the changes in ABA signaling during different abiotic stresses, and the ABA signaling during crosstalks between abiotic and biotic stresses. Ishitani et al. (1997) assessed *pAtRD29A-LUC*

1. INTRODUCTION

reporter activity in various mutants using luminescence imaging, and consequently, they identified a large number of osmotic and cold stress-responsive gene mutants after treatment with different abiotic stresses, and ABA. Moreover, Himmelbach et al. (2002) and Söderman et al. (1999) fused the promoter of *AtHB6* gene with the LUC and GUS reporters. The *pAtHB6*-GUS reporter exhibited a cell division and/or differentiation area confined signal in different developing plant organs, therefore, Söderman et al. (1999) concluded that *AtHB6* has a cell division and/or differentiation function. In addition, the *pAtHB6*-LUC reporter showed a PP2C (ABI1)-dependent activity, thus Himmelbach et al. (2002) revealed that *AtHB6* functions as an ABI1 downstream negative regulator of ABA signaling. Finally, Christmann et al. (2005) observed low ABA reporter activities in the columella cells and quiescent center of the root as well as in the vascular tissues and stomata of cotyledons in untreated plants, while exogenous ABA treatment enhanced a uniform pattern of reporter expression in different Arabidopsis tissues.

Concerning SA, JA and JA/ET, Murray et al. (2002) developed SA reporter using the promoter of *PR1* fused to LUC to address the epistasis analyses of the recessive mutant *cir1*, which display constitutively expressed SA, JA, ET, and ROS intermediate-dependent genes, utilizing *npr1*, *nahG*, *jar1*, and *ein2* mutants. Consequently, they concluded that *NPR1*-dependent and -independent SA signaling plays a central role in defense responses against *P. syringae* and Noco2, while the *cir1*-mediated resistance against the necrotrophic pathogen, but not the biotrophic pathogen, necessitates the activation of JA and ET signaling. Manners et al. (1998) and Mousavi et al. (2013) assessed the expression of the GUS reporter under the promoters of JA and JA/ET marker genes *VSP2*, and *PDF1.2*, respectively in order to investigate the correlation of JA and JA/ET signaling with wounding, biochemical and biotic stresses after challenging with *A. brassicicola* and *B. cinerea*. In addition, Poncini et al. (2017) used the biosynthesis and signaling marker gene promoters of *ICS1*, *AOS*, *ACS6*, *HEL/PR4* to develop reporter lines for SA (*pICS1*-YFP-NLS), JA (*pAOS*-YFP-NLS), ET (*pACS6*-YFP-NLS), and JA/ET (*pHEL/PR4*-YFP-NLS). Next, they investigated the tissue specific contribution of SA, JA, and JA/ET production in Arabidopsis roots in response to the MAMP molecules chitin and flg22, the DAMP molecule *AtPep1* and the infection with *F. oxysporum*. Subsequent microscopic analysis exhibited a strong DAMP-

1. INTRODUCTION

mediated activation of SA and JA production in comparison to the tested MAMPs, underpinning the strong perception of *AtPep1*. In addition, the pathogen invasion showed local activations of JA, ET and JA/ET marker genes expression.

Recently, Betsuyaku et al. (2018) created a sensor system using the promotor of the SA marker gene *PR1* driving the expression of the YFP fused to a nuclear localization signal (NLS). Furthermore, they established another reporter for JA using the same cassette replacing the native promoter of *PR1* with the native promoter of the JA downstream component *VSP1*. Subsequent analyses using the *pPR1*-YFP-NLS and *pVSP2*-YFP-NLS reporters exhibited a distinct spatial activation of SA-JA signaling in *P. syringae* challenged Arabidopsis plants. Hence, the SA signaling is enhanced in the adjacent cells surrounding infection sites, while JA signaling is induced in the domain surrounding the SA-active domain. Furthermore, in a recent study, Marhavý et al. (2019) employed a set of aforementioned reporter lines developed by Mousavi et al. (2013) and Poncini et al. (2017) to investigate the transcriptional activation pattern of SA, JA, ET, and JA/ET in response to single-cell wounding by laser ablation in comparison to nematode attack. Authors of the later studies observed a similar pattern of elevated ET but not SA or JA marker genes associated with Ca^{2+} channel and NAPH oxidase activation.

1.8.5.2. Synthetic promoter-based reporters

Synthetic promoters are fused DNA repeats of a hormone responsive element used to gain a regulatory capacity to respond to changes in corresponding hormone accumulation. Ulmasov et al. (1997) have established an auxin reporter system using the synthetic promoter *DR5*, which carries several repeats of the auxin-responsive element (AuxRE: TGTCTC). Subsequently, Liao et al. (2015) developed a new version with higher sensitivity using the *DR5v2* synthetic promoter, which is a *DR5* promoter fused to a novel perception site for Auxin response factors (ARFs). Müller & Sheen (2008) developed a CK reporter based on the *TWO COMPONENT SIGNALING SENSOR (TCS)* synthetic promoter fused to *GFP*. However, this construct exhibited a weak and rapid silencing of *GFP* expression in some developmental contexts. Therefore, Zürcher et al. (2013) established a new *TCS (TCSn)*, which showed higher sensitivity to CK. Transgenic Arabidopsis *TCSn-GFP* plants manifested strong and

robust GFP expression patterns compatible to known cytokinin roles, and high stability of GFP expression over generations. This allowed crossing of reporter plants with different CK signaling and biosynthesis mutants.

Additionally, the expression of ABA downstream components is known to be mediated by cis-regulatory elements known as ABA-responsive elements (ABREs) with the sequence motif ACGTGTC in the promoter of ABA-inducible genes (Choi et al. 2000; Mundy et al. 1990). Based on this knowledge, Wu et al. (2018) created a synthetic promoter of six ABRE repeats driving the expression of endoplasmic reticulum localized GFP to create an ABA-reporter to map the cellular distribution of ABA. However, they observed that this reporter is not suitable to monitor ABA in all cell types as they observed an ABA-independent activation of the reporter in distinct cell types even under nonstress conditions.

1.9. Tools for normalization of reporter activity

The visualization of hormonal response and hormonal crosstalk allows real-time monitoring of plant defense mechanisms and developmental processes. In this respect, Federici et al. (2012) reported that there are two essential elements; a fluorescent protein constitutively expressed which serves as a reference for additional fluorescent markers, and plasma membrane markers to help to identify the cell boundaries. These additional modules have been predicted to improve the performance of emerging biosensor technology. Ghareeb et al. (2016), generated a set of binary vectors, so-called COLORFUL-Circuits allowing for a straightforward multigene assembly. Using these constructs, the simultaneous expression of different fluorescent proteins (FP) under inducible and constitutive promoters is facilitated providing the scientific community with an unlimited number of robust utilities for different aspects of plant cell biology.

1.10. Objectives

The ultimate outcome of plant-pathogen interactions is predetermined at the initial site of attack, where the pathogen invades a single or few cell(s) of the host. Accordingly, monitoring hormone signaling cascades at early time points—directly after pathogen

1. INTRODUCTION

infestation in these cells—is crucial. However, the spatio-temporal cellular activities of ABA, SA, JA, and JA/ET in plant defense at a single-cell resolution have so far not been adequately addressed. Therefore, we aimed in the current study to map the spatio-temporal dynamics of plant hormones ABA, SA, JA, and JA/ET during compatible and incompatible biotrophic interactions with *Arabidopsis thaliana* using a set of hormone reporter lines for ABA, SA, JA and, JA/ET recently developed at our lab by Hassan Ghareeb (personal communication), termed COLORFUL-biosensors. These reporter lines were established based on a multigene assembly vector platform termed "COLORFUL-Circuit" (Ghareeb et al. 2016). For the aforementioned purpose, we planned to:

- Validate the functionality of these newly developed COLORFUL-biosensors via investigating:
 - The responsiveness of COLORFUL-reporter activity to the exogenous application of the corresponding hormone in a dose- and incubation time-dependent manner.
 - The cell- and tissue-specific differential distribution of the tested hormones.
- Develop high-throughput imaging automated software to expedite comparative large-scale data analyses in order to verify the cell-specific contribution of the hormones mentioned above in plant innate immunity.
- Address the hormone crosstalk after the exogenous application of ABA, SA, MeJA, and ET precursor ACC individually and in combinations.
- Quantify and visualize the invasion dynamics of virulent and avirulent pathogens used in this project.
- Address the hormone signaling signature and crosstalk during compatible and incompatible interactions.
- Unravel the role of ABA as well as the ABA signalosome components involved in mediating the ABA signaling pattern.

2. MATERIALS AND METHODS

2.1. Materials

2.1.1. Arabidopsis plant materials

In this study, we used the COLORFUL-reporter lines; COLORFUL-ABA, -SA, -JA, and -JA/ET that were developed using *Agrobacterium*-mediated transformation of *A. thaliana* (Col-0) (Table 1).

Table 1: COLORFUL-biosensors employed in this study.

Biosensor	Transformed in	Reporter activity is	Selection marker
COLORFUL-ABA	Col-0	<i>PP2CA</i> expression dependent	BASTA
COLORFUL-SA	Col-0	<i>PR1</i> expression dependent	BASTA
COLORFUL-JA	Col-0	<i>VSP2</i> expression dependent	BASTA
COLORFUL-JA/ET	Col-0	<i>PDF1-2a</i> expression dependent	BASTA

In addition, different mutants in *Arabidopsis* Col-0 ecotype used in this investigation are listed below in table (2).

2. MATERIALS AND METHODS

Table 2: Arabidopsis transgenic lines and suppliers.

Mutant	Gene	Accession no.	Ecotype	Reference
<i>aba1-101/ser3</i>	<i>ABA1</i>	AT5G67030	Col-0	Barrero et al. 2005
<i>aba2-1</i>	<i>ABA2</i>	AT1G52340	Col-0	González-Guzmán et al. 2002
<i>ahg3-1</i>	<i>AHG3</i>	AT3G11410	Col-0	Yoshida et al. 2006
<i>pp2ca-1</i> (SALK_028132)	<i>PP2CA</i>	AT3G11410	Col-0	Kuhn et al. 2006
<i>snrk2d/srk2.2</i> GABI-Kat 807G04	<i>SNRK2D/SK2.2</i>	AT3G50500	Col-0	Nakashima et al. 2009
<i>snrk2e/srk2.6</i> SALK_008068	<i>SNRK2E/SRK2.6</i>	AT4G33950	Col-0	Nakashima et al. 2009
<i>snrk2i/srk2.3</i> SALK_096546	<i>SNRK2I/SRK2.3</i>	AT5G66880	Col-0	Nakashima et al. 2009
<i>snrk2d snrk2e</i>	<i>SNRK2D SNRK2E</i>	AT3G50500 AT4G33950	Col-0	Nakashima et al. 2009
<i>snrk2d snrk2i</i>	<i>SNRK2D SNRK2I</i>	AT3G50500 AT5G66880	Col-0	Nakashima et al. 2009
<i>snrk2e snrk2i</i>	<i>SNRK2E SNRK2I</i>	AT4G33950 AT5G66880	Col-0	Nakashima et al. 2009
<i>snrk2d snrk2e snrk2i</i>	<i>SNRK2D SNRK2E SNRK2I</i>	AT3G50500 AT4G33950 AT5G66880	Col-0	Nakashima et al. 2009
<i>edr1</i>	<i>EDR1</i>	AT1G08720	Col-0	Frye & Innes 1998
<i>eds1</i>	<i>EDS1</i>	AT3G48090.2	Col-0	Parker et al. 1996
<i>nahG</i>	<i>NahG</i>	AT5G33340	Col-0	Van Wees & Glazebrook 2003
<i>snc1</i>	<i>SNC1</i>	AT4G16890	Col-0	Li et al. 2001

2.1.2. Crosses of COLORFUL-biosensor lines with different mutants

The seeds of COLORFUL-ABA line #1 and COLORFUL-SA line #1 in Col-0 background (T3 generations) and *aba1-101*, *snrk2d*, *snrk2i*, *snrk2d snrk2i*, *ahg3-1*, and *pp2ca-1* were sown onto 8.0 cm² pots and vernalized in the dark at 4.0 °C for three days. Grown seedlings were moved to a long-day condition climate chamber for six weeks or until the beginning of the inflorescence. The COLORFUL-ABA line #1 was crossed with *aba1-101*, *snrk2d*, *snrk2i*, *snrk2d snrk2i* double mutant, *ahg3-1*, and *pp2ca-1*, while COLORFUL-SA line #1 was crossed with *ahg3-1* and *pp2ca-1*. After crossing, the plants were cultivated for a subsequent four weeks until the siliques were developed and matured. Consequent analyses were carried out until the selection of homozygous lines in at least F3 generations. Genomic DNA analyses were performed to confirm the homozygosity of the mutant background. For the COLORFUL-system, BASTA-resistance selection was performed first, followed by CLSM (Leica, Germany) screening for the reference and membrane marker signals in comparison to the wildtype signals.

2.1.3. Chemicals

Chemicals used in this study are listed below in table (3).

Table 3: List of chemicals and suppliers.

Chemical	Manufacturer
Murashige & Skoog Medium	Duchefa Biochemie, Netherlands
MES	Roth, Germany
Plant Agar	Duchefa Biochemie, Netherlands
Potassium chloride (KCl)	Merck, Germany
2-cis, 4-trans-Abscisic acid 98%	Aldrich, Germany
Sodium salicylate	Sigma-Aldrich, Germany
1-Aminocyclopropane-1-carboxylic acid (ACC)	Sigma-Aldrich, Germany
Methyl Jasmonate 95%	Aldrich, Germany
Calcium Chloride (CaCl ₂)	Merck, Germany

2. MATERIALS AND METHODS

Chemical	Manufacturer
Fluorescent Brightener 28	Sigma-Aldrich, Germany
QIAzol Lysis Reagent	Qiagen, Germany
UltraPure™ Agarose	Biozym, Germany
RiboLock RNase Inhibitor	Thermo Fisher Scientific, Germany
HDGreen Plus DNA Stain	Intas, Germany
Ethanol	Merck, Germany
Methanol	Roth, Germany
Chloroform	Sigma-Aldrich, Germany
Phenol	Merck, Germany
Isoamyl alcohol	Roth, Germany
Isopropanol	Roth, Germany

2.1.4. Buffers and solutions

General solutions and buffers in our lab are listed in table (4) and were used for Agarose gel electrophoresis.

Table 4: List of general solutions and buffers

Buffer	Contents
Agarose gel	Agarose 0.4 - 2 % (w/v)
	TAE buffer 1 x
TAE buffer [50x]	Tris 2.0 M
	Glacial acetic acid 57.1 ml/l
	EDTA (pH 8.0) 50 mM
Loading Dye [6x]	Orange G 0.25 % (w/v)
	Xylencyanol FF 0.25 % (w/v)
	Glycerol 30 % (v/v)

2.1.5. Oligonucleotides

The forward (F) and reverse (R) oligonucleotides (Table 5) were designed using Geneious® v. 8.1.8 (<https://www.geneious.com>; Kearse et al. 2012) and ordered from Thermo Fisher Scientific, Germany. The oligonucleotides stock solution concentration was adjusted to 100 µM with ddH₂O and stored at -20 °C.

Table 5: List of oligonucleotides and their use.

Name	Sequence (5'→ 3')	Used for
oHG239	TTCTTCCCTCGAAAGCTCAA	qRT-PCR for <i>PR1</i> (F)
oHG240	AAGGCCCAACCAGAGTGTATG	qRT-PCR for <i>PR1</i> (R)
oHG146	CTTGTTCTCTTTGCTGCTTTC	qRT-PCR for <i>PDF1-2</i> (F)
oHG147	CATGTTTGGCTCCTTCAAG	qRT-PCR for <i>PDF1-2</i> (R)
oHG148	CGCAAAATATGGATACGGAAC	qRT-PCR for <i>VSP2</i> (F)
oHG149	GACATTCTTCCACAACCTCC	qRT-PCR for <i>VSP2</i> (R)
oHG170	ATTTTGCCGATTTCGGAAC	Confirmation of SALK T-DNA insertions
oMS001	TGAATGATGATGAATGAGACAGC	Confirmation of GABI-Kat 807G04 T-DNA insertion in <i>SNRK2D</i> (F)
oMS002	TGGTTTAGGTGATTTTGACGC	Confirmation of GABI-Kat 807G04 T-DNA insertion in <i>SNRK2D</i> (R)
oMS003	CATATCTTTAGACGAGGGGCC	Confirmation of SALK_008068 T-DNA insertion in <i>SNRK2E</i> (F)
oMS004	GTGAGTGGTCCAATGGATTTG	Confirmation of SALK_008068 T-DNA insertion in <i>SNRK2E</i> (R)
oMS005	GGTTTTGAGTGTTCTGCTTTTG	Confirmation of SALK_096546 T-DNA insertion in <i>SNRK2I</i> (F)
oMS006	ACATCTGCAATCTGGTAACCG	Confirmation of SALK_096546 T-DNA insertion in <i>SNRK2I</i> (R)
oMS007	ATAATAACGCTGCGGACATCTACATTTT	Confirmation of GABI-Kat T-DNA insertions
oMS008	GTTTGAGTCTGAGGCATAAC	<i>aba1-101</i> genotype confirmation (R)
oMS009	TCTCGAGTACCACAGTAACC	<i>aba1-101</i> genotype confirmation (F)
oMS010	GAATTGCAGTCTCCTCAGTGT	qRT-PCR for <i>PP2CA</i> (F)

2. MATERIALS AND METHODS

Name	Sequence (5'→ 3')	Used for
oMS011	TCGATCCGGCTTGTGATCTA	qRT-PCR for <i>PP2CA</i> (R)
oMS012	ATCATGAGAATGGTGCGACT	qRT-PCR for <i>ARD29A/ LTI78</i> (F)
oMS013	TAATTCCTCCGATGCTGGA	qRT-PCR for <i>ARD29A</i> (R)
oMS014	TGCAGAGGAAGGAAAAGGTG	qRT-PCR for <i>ARD29B/ LTI65</i> (F)
oMS015	CTCCCTTACCTCCGCCACT	qRT-PCR for <i>ARD29B</i> (R)
oMS016	CCAGTACGATTCTCTCCGTCA	qRT-PCR for <i>HB6</i> (F)
oMS017	GCCGCGTTGTTCTCTTCTT	qRT-PCR for <i>HB6</i> (R)
oMS018	GGACTGAAGGCTTTGGAAC	qRT-PCR for <i>RAB18</i> (F)
oMS019	CTTCCTCCTCCCTCCTTGTC	qRT-PCR for <i>RAB18</i> (R)
oMS020	TTTTTTTTTTTTTTTTTTTTTV	oligo_dT for cDNA synthesis

2.1.6. Nucleic acid modifying enzymes

DNA polymerases and nucleic acid modifying enzymes are listed in table (6). All enzymes were used as recommended by the manufacturer.

Table 6: Nucleic acid modifying enzymes used in this study

Enzyme	Used in Method	Manufacturer
DNase I	Treatment of RNA before cDNA synthesis	Thermo Fisher Scientific, Germany
RevertAid Reverse Transcriptase	cDNA synthesis from RNA	Thermo Fisher Scientific, Germany
RNase A	Treatment of DNA	Thermo Fisher Scientific, Germany
SsoFast™ EvaGreen® supermix	qRT-PCR	Bio-Rad

2.1.7. Pathogens

The pathogens used in this study are listed in table (7).

Table 7: Biotrophic pathogens investigated in this study

Pathogen	Kingdom	Lifestyle	Virulence
<i>H. arabidopsidis_Noco2</i>	Oomycetes	biotrophic	Virulent on Col-0
<i>H. arabidopsidis_Emwa1</i>	Oomycetes	biotrophic	Avirulent on Col-0
<i>G. orontii</i>	Fungus	biotrophic	Virulent on Col-0

2.1.8. Devices

Device	Model	Manufacturer
Centrifuge	Pico 21	Thermo Fisher Scientific (Germany)
Clean bench	Hera safe	Thermo Fisher Scientific (Germany)
Climate chambers	-	Johnson Controls (USA)
Computer	Optiplex 760	Dell (Germany)
Counting chamber	Thoma	Optik Labor (UK)
Digital camera	Lumix FZ150	Panasonic (Germany)
Confocal laser scanning microscope (CLSM)-SP5	Leica DM6000B CS SP5	Leica (Germany)
CLSM-SP8	Leica DM6 CS SP8	Leica (Germany)
Freezer (-20 °C)	Mediline	Liebherr (Germany)
Freezer (-80 °C)	Hera freeze	Thermo Fisher Scientific (Germany)
Gel documentation system	GenoPlex	VWR (Germany)
Gel electrophoresis equipment	-	Bio-Rad (USA)
Gel running chamber	Sub cell® GT	Bio-Rad (USA)

2. MATERIALS AND METHODS

Device	Model	Manufacturer
Ice machine	-	Ziegra (Germany)
Magnetic stirrer	RH basic 2 IKAMAG	IKA (Germany)
Microwave	R-26ST	Sharp (Japan)
PCR Cyclor	MyCyclor	Biorad (USA)
pH meter	Inolab®	WTW (Germany)
Photometer	Infinite M200 microplate reader	Tecan (Switzerland)
Pipet	Research	Eppendorf (Germany)
Printer I	UP-D897	Sony (UK)
qRT-PCR Cyclor	C100 Touch with CFX96 system	Bio-Rad (USA)
Refrigerator	Mediline	Liebherr (Germany)
Rotator	-	Heinemann (Germany)
Steam sterilizer	Varioklav 75S / 135S	Thermo Fisher Scientific (Germany)
Stereomicroscope	M165FC	Leica (Germany)
Vortexer	VF2	IKA (Germany)
Water filter system	Arium® 611 DI	Sartorius (Germany)

2.2. Methods

If not specified otherwise, all methods were performed at room temperature.

2.2.1. Growth conditions and cultivation of *A. thaliana*

2.2.1.1. Seed production

Five seeds of each *A. thaliana* genotype were sown onto 8 cm² pots filled with 200 ml of steam sterilized clay granules (Seramis GmbH, Mogendorf, Germany) and 800 ml of a sand-soil mixture in a ratio of 1:1. Subsequently, the sand-soil mixture was watered with 250 ml H₂O supplemented with 0.1 % (v/v) Wuxal[®] liquid fertilizer (Manna, Ammerbuch-Pfäffingen, Germany). The sown seeds were vernalized in the dark at 4.0 °C for three days before pots were transferred to a climate chamber (Johnson Controls, USA) under long-day conditions (16 h light/8 h dark; with 150 µmol·m⁻²·s⁻¹ at 22 °C/18 °C, and 65 % relative humidity). With regular watering, seedlings were incubated covered with a clear plastic hood for a week. The hood was removed and the growing plants were subsequently cultivated under regular watering for six weeks or until flowering for crossing and seed production. For seed collection, the regular watering was ceased to allow the plants to dry out, next, the dry siliques, or shoots were tucked into paper bags for further manual seed harvest and sterilization.

2.2.1.2. Infection experiments

For infection experiments, the seeds of investigated *A. thaliana* genotypes were sown onto 8 cm² pots filled with the aforementioned soil mixture. Seeds were vernalized and covered with a clear plastic hood for three days at 4.0 °C before cultivation under short-day conditions (8 h light/16 h dark) with 150 µmol·m⁻²·s⁻¹ at 22 °C/18 °C for a week in a climate chamber (Johnson Controls, USA). Next, uncovered seedlings were grown for a varying duration of additional weeks depending on the tested pathogen type.

2.2.1.3. Hormone treatment experiments

The seeds of the COLORFUL-biosensors and their filial generations obtained by self-fertilization or crossing with mutant lines were sterilized in 1.5 ml Eppendorf tubes by adding 500 μ l of absolute ethanol (99%) and mixing using a rotator (20 rpm) for 20-30 seconds. Next, the absolute ethanol was discarded and 700 μ l commercial ethanol (70 %) containing 0.05 % Tween 20 was added for 5 min on a rotator (20 rpm). Afterward, the seeds were washed twice with sterilized distilled water and then suspended in sterilized 0.1 % agarose, Germany. Next, sterilized seeds were distributed onto ½ MS/MES agar plates [2.2 g/l Murashige & Skoog Medium (MS) (Duchefa Biochemie, Netherlands), 0.5 g/l MES (Roth, Germany), 7.0 g/l plant agar (Duchefa Biochemie, Netherlands), pH 5.8]. The plates were then vernalized in the dark 4.0 °C for three days before transfer to a climate chamber (Johnson Controls, USA) under long-day conditions (16 h light/8 h dark) with 150 μ mol·m⁻²·s⁻¹ at 22 °C/18 °C and 65 % relative humidity.

2.2.2. Cultivation of the oomycete *H. arabidopsidis*

For *H. arabidopsidis* culture maintenance, the two-week-old susceptible *A. thaliana* Col-0 and Wassilewskija-0 (Ws-0) seedlings were spray inoculated with the virulent isolate (Noco2) and the avirulent isolate (Emwa1), respectively. Then, the infected seedlings were kept in covered trays and maintained in a growth chamber (CLF PlantClimatics GmbH, Germany) under short-day conditions (9.0 h light/15 h dark) with 150 μ mol·m⁻²·s⁻¹ at 17 °C and 92-98% relative humidity. At five to six days post-inoculation (dpi), the asexual spores were readily collected in water and sprayed onto fresh seedlings to produce a new generation of spores for subsequent infection experiments.

2.2.3. Cultivation of the fungus *G. orontii*

For *G. orontii* culture maintenance and propagation, the powdery mildew fungus was grown on *A. thaliana* (Col-0) seedlings. Col-0 plants that were infected for two weeks were brush inoculated directly upon the five-week-old susceptible wildtype *A. thaliana* (Col-0) and the hyper-susceptible mutant (*eds1*). Then, the infected plants were

incubated uncovered in a growth chamber (CLF PlantClimatics GmbH, Germany) under short-day conditions (9.0 h light/15 h dark) with $150 \mu\text{mol}\cdot\text{m}^{-2}\cdot\text{s}^{-1}$ at 17 °C and 70-75 % relative humidity. At two weeks after inoculation, Col-0 infected plants could be used for the reinfection of fresh plants for spore production, while the *eds1* infected plants were used for the infection experiments in this study.

2.2.4. Functional characterization of COLORFUL-biosensors

After the development of the COLORFUL-reporter systems, the functionality of these reporter systems was tested. Seeds of COLORFUL-ABA, -SA, -JA, and -JA/ET (T4 generations), as well as COLORFUL-ABA line #1 in *aba1-101* mutant background (F4 generations) were sterilized and distributed onto ½ MS/MES agar plates as mentioned above. Three, eleven- and twelve-day-old seedlings were used to test the responsiveness of different reporter activities to exogenous application of different hormones in a time series. Also, the concentration dependency of hormone responses was tested. The 3rd leaf from hormone-treated seedlings was always used during microscopy.

2.2.4.1. The responsiveness of the COLORFUL-biosensors to exogenous hormone applications

Seedlings of COLORFUL-ABA, -SA, -JA and -JA/ET were grown for eleven days under long-day conditions (mentioned above) to test the response of these biosensor systems on exogenous application of different hormones. COLORFUL-SA, -JA and -JA/ET have been investigated by Ghareeb et al. (unpublished) using different hormone concentrations and incubation times. In this study, additional experiments were performed to test the impact of various treatments of 0.5 mM sodium salicylate (SA) (Sigma-Aldrich, Germany) dissolved in water, 50 μM methyl-jasmonate (MeJA) (95%, Sigma-Aldrich, Germany) dissolved in 99% ethanol and 2.0 μM of the ethylene precursor 1-aminocyclopropane-1-carboxylic acid (ACC) (Sigma-Aldrich, Germany) dissolved in water on the magnitude of activity of these reporter systems. Following the protocol of Van der Does et al. 2013, five seedlings of eleven-day-old COLORFUL-biosensor lines were incubated in a 24-well plate containing 2.0 ml KCl/MES buffer

2. MATERIALS AND METHODS

(1.0 mM KCl and 5.0 mM MES, pH 5.8) per well with the previously mentioned treatments for 24 hours (h). The mock plants were treated by the addition of 2.0 ml KCl/MES buffer containing the corresponding volume of solvents used for hormone stock preparation.

2.2.4.2. Selection of COLORFUL-biosensor lines

Thirty independent transgenic COLORFUL-ABA reporter lines were tested in response to exogenous application of 50 μ M ABA in order to select two independent transgenic lines for subsequent experiments: COLORFUL-ABA #1 and #2.

2.2.4.3. ABA treatment experiments

Eleven-day-old COLORFUL-ABA plants were incubated in 24-well plates. Five seedlings per well were incubated in different concentrations of 2-cis, 4-trans-Abscisic acid (ABA); 0.1 μ M, 0.5 μ M, 1.0 μ M, 5.0 μ M, 10.0 μ M, 50.0 μ M and 100 μ M ABA in 2.0 ml KCl/MES buffer (1.0 mM KCl and 5.0 mM MES, pH 5.8) for 24 h, whereas, the mock seedlings were treated with the addition of 2.0 ml KCl/MES buffer containing the corresponding volume of methanol used in the hormone treatments.

2.2.4.4. Time course experiments

The responsiveness of COLORFUL-ABA to exogenous ABA over time was analysed by the incubation of ABA biosensor seedlings in 50 μ M ABA for 0, 1.0, 3.0, 6.0, 12 and 24 h in comparison to the corresponding mock treatment. Two independent lines of COLORFUL-ABA—line #1 and line #2—, were tested in two independent repeats. The adaxial surface of the 3rd leaf from hormone-treated seedlings was always selected for CLSM. Ten replicates from ten different independent plants were placed on a microscopic slide (Thermo Fisher Scientific, Germany), emerged in water, and pressed well to get rid of the air pupils over the leaves.

2.2.4.5. Tissue-specific distribution of COLORFUL-ABA reporter activity and dependency of reporter activity on ABA biosynthesis

In order to investigate the tissue-specificity of the COLORFUL-ABA reporter system, the VENUS signal intensities were tested in different cells and different tissues. After three days vernalization in the dark at 4.0 °C, sterilized COLORFUL-ABA line #1 in Col-0 and *aba1-101* background seeds were grown for three days under the long-day conditions. Afterward, the cotyledons, hypocotyl, elongation zone, and root tip were screened in the Col-0 background in comparison to the ABA deficient mutant *aba1-101* with and without 50 µM ABA treatment.

2.2.5. ABA, SA, JA, and JA/ET marker gene expression analyses in response to hormone treatment

2.2.5.1. Sample collection

Samples of the wildtype *A. thaliana* (Col-0), *aba1-101*, and *snrk2d snrk2e snrk2i* triple mutants were collected in liquid nitrogen after treatment with 50 µM ABA for 24 h, in addition to untreated samples for each genotype. Moreover, samples for COLORFUL-ABA line #1, -SA line #1, -JA line #1, and -JA/ET line #1 were collected in liquid nitrogen after treatment with 50 µM ABA, 0.5 mM SA, 50 µM MeJA alone, and in combination with 2.0 µM ACC, respectively, at 0.0, 1.0, 3.0, 6.0, 12 and 24 hpt in addition to mock samples for each reporter line. Each sample (200 mg) contained ten seedlings, which were collected together, frozen in liquid nitrogen, and stored at -80 °C until use.

2.2.5.2. RNA extraction from plant materials

Total RNA was extracted according to Ghareeb et al. (2011). The collected samples were ground with liquid nitrogen, and 1.0 ml QIAzol Lysis Reagent (Qiagen, Germany) was added and the sample was mixed. The mixture was incubated for 15 min at room temperature and then 300 µl chloroform was added followed by 10 sec vortexing. The mixture was centrifuged at 13000 rpm and 4.0 °C for 15 min. The aqueous phase was transferred to a clean tube, the same volume (300-500 µl) phenol-chloroform-isoamyl

(25:24:1) was added and the mixture was centrifuged at 13000 rpm, 4.0 °C for 15 min. The upper-phase was mixed with 600 µl isopropanol by inverting the tubes six times. Subsequently, the mixture was centrifuged at 13000 rpm, 4.0 °C for 15 min to precipitate the RNA. The supernatant was removed and the pellet washed with 1.0 ml 80% ethanol, followed by centrifugation at 13000 rpm, 4.0 °C for 10 min. Finally, the supernatant was discarded and the pellet air-dried. The pellet was dissolved in 80 µl RNase free water at 50 °C and 550 rpm for 10 min.

2.2.5.3. Determination of the RNA integrity and concentration

Following extraction, RNA concentration and purity was measured with a spectrophotometer (TECAN Infinite M200 microplate reader). Subsequently, the RNA was tested via 1.0 % TBE agarose gel electrophoresis by mixing 1.0 µl of RNA sample with 9.0 µl of 1x DNA-loading buffer. The mixture then was loaded on a 1.0 % Agarose-TBE-gel (containing HDGreen Plus DNA Stain (Intas, Germany)), fast run using 150-200 V for 15 min to check the RNA integrity. The RNA samples were stored at -80 °C until use.

2.2.5.4. DNase treatment of total RNA samples

To reduce the RNA samples contamination with DNA, DNA digests were performed using Thermo Scientific RapidOut DNA Removal Kit (Thermo Fisher Scientific, Germany), in which the DNase treatment was performed for 2.0 µg RNA concentration as recommended by the manufacturer adding 0.5 µl RiboLock RNase Inhibitor (Thermo Fisher Scientific, Germany) per sample. This step was followed by addition of DNase Removal Reagent (DRR). Next, the RNA was cleaned up with RNeasy Plant Mini Kit (Qiagen, Netherlands) and eluted with 20 µl and samples were stored at -80 °C.

2.2.5.5. Reverse transcription of the total RNA

To synthesize cDNA for qRT-PCR analyses, reverse transcription of the total DNA-free RNA was performed with Thermo Scientific RevertAid H Minus Reverse Transcriptase Kit (Thermo Fisher Scientific, Germany). Reaction was initiated by the preparation of

2. MATERIALS AND METHODS

mixture 1 (as indicated below) and the tubes were incubated in a thermocycler (Biorad) at 70 °C for 5 min.

Component	Volume for 10 µl
Total RNA	2.5 µg
100 µM Poly-dT primer (oMS020)	1.0 µl
ddH ₂ O	Up to 10 µl

Next, samples were chilled on ice for 2-3 min, and mixture 2 (as indicated below) was added.

Component	Volume for 19 µl
5X reaction buffer	4.0 µl
10mM dNTPs	2.0 µl
RiboLock RNase Inhibitor	0.5 µl
ddH ₂ O	2.5 µl
The total volume was 19 µl per sample	

Tubes then were incubated at 37 °C for 5.0 min, followed by the addition of 1.0 µl M-MuLV reverse transcriptase (200 U/µl) to each tube and incubation at 42 °C for 1h. The reaction was stopped by subsequent incubation at 70 °C for 10 min. Next, 100 µl ddH₂O was added per 20 µl cDNA.

2.2.5.6. Quantitative Real Time Polymerase Chain Reaction (qRT-PCR)

In order to quantify the expression level of marker genes in response to hormone treatment, quantitative real time polymerase chain reaction (qRT-PCR) was performed according to Ghareeb et al. (2011). To do so, primers as mentioned in table (5) were used for quantification of the transcript abundance for the marker genes *PP2CA*

2. MATERIALS AND METHODS

(oMS010 and oMS011), *ARD29A* (oMS012 and oMS013), *ARD29B* (oMS014 and oMS015), *HB6* (oMS016 and oMS017), *RAB18* (oMS018 and oMS019), *PR1* (oHG239 and oHG240), *VSP2* (oHG148 and oHG149), and *PDF1.2* (oHG146 and oHG147). Reactions were set up as described below with the SsoFast EvaGreen supermix (BioRad).

Component	Volume per 10 µl reaction [µl]
cDNA	45 µl
2X SsoFast EvaGreen Supermix	75 µl
F-primer	15 µl
R-primer	15 µl
The total volume was 15 µl per sample	

The reactions were pipetted into clear 96-well plates (BioRad). From each sample three technical replicates were analyzed. The experiments were repeated once with the locations of the wells containing gene of interest (GOI) and *AtUBQ5* exchanged. The plates were sealed well and the PCR was performed using the CFX384 real-time PCR detection system (Bio-Rad). Cycling parameters were the same for all primers; initial 95 °C for 6.0 min, followed by 40 cycles of 95 °C for 30 s, 60 °C for 1.0 min, plate read step, then product melting curve 55-95 °C.

Step	Temperature	Time	
Initial denaturation	95 °C	6.0 min	
Denaturation	95 °C	30 sec	
Annealing	60 °C	1.0 min	
Extension	72 °C	15 sec	40 x
Melting curve	55 - 95 °C	10 sec	80 x + 0.5 °C each cycle

After qRT-PCR, the data were analyzed using the BioRad CFX Manager software (v 3.1; BioRad). The quality of the reported data was controlled via the melting curves. Extremes and highly different melting curves reflect sampling artifacts. Therefore, such

samples were taken out of the analyses. Next, the transcript levels were calculated relative to the expression of the housekeeping gene *AtUBQ5*. The experiments were repeated once.

2.2.6. Pathogen-associated disease phenotype of ABA biosynthetic and signaling mutants

Two different virulent pathogens were used in this investigation to evaluate the pathogen-associated disease phenotype of the tested ABA biosynthetic and signaling single and double mutants: *aba1-101*, *aba2-1*, *snrk2d*, *snrk2e*, *snrk2i*, *snrk2d snrk2e*, *snrk2d snrk2i*, and *snrk2e snrk2i*. Spores of the oomycete Noco2 were collected at five to six days after infection of *A. thaliana* Col-0 seedlings. Next, the sporulated shoots of the infected Col-0 plants were harvested in 50 ml falcon tubes soon after the transfer of the infected pots from the high humidity chamber to the relatively low humidity laboratory. Subsequently, 20 ml of sterile distilled H₂O (room temperature) was added, followed by gentle shaking to release the spores into the water. The filtered spore solution was counted using a hemocytometer chamber (Labor Optik, United Kingdom) and diluted to 5×10^4 spores per ml. Next, two-week-old mutant and the susceptible wildtype Col-0 plants (20 plants / 8.0 cm² pot), were sprayed with the spore solution. The hyper-susceptible mutant *eds1* (enhanced disease susceptibility 1) (Parker et al. 1996), and the highly disease resistant mutant *snc1* (Li et al. 2001) were used as positive and negative controls, respectively. Noco2 infected plants were kept in covered trays and maintained in a growth chamber under short-day conditions for 5-6 days. Subsequently, plants were harvested in a weighed 50 mL falcon tube. Then 5 µL H₂O /mg plant tissue was added and subsequently the samples were vortexed for 15 sec. The spore density was determined using a hemocytometer chamber. Spore counting was repeated four times for each replicate.

For inoculation with *G. orontii* spores, five-week-old plants were brush-inoculated with the fungus. The *G. orontii* spores were collected at 10 days after infection for spore counting. Five plants obtained from one pot were collected in a weighed 50 mL tube. Then 5.0 µL H₂O were added per mg plant material and subsequently the samples were vortexed for 15 sec. Using the hemocytometer chamber, the spores were counted

four times per replicate. The previously mentioned mutants were tested in addition to the hypersusceptible mutant *eds1* (*enhanced disease susceptibility 1*) (Parker et al. 1996), hyperresistant mutant *edr1* (*enhanced disease resistance 1*) (Frye & Innes 1998) and the susceptible wildtype Col-0.

2.2.7. Plant-microbe interaction experiments to map pathogen-mediated hormone signaling

2.2.7.1. *H. arabidopsidis*-Noco2 and -Emwa1 infection experiments

To address the hormone signatures during interaction with the oomycete *H. arabidopsidis*, the T4 generations of COLORFUL-ABA, -SA, -JA, -JA/ET reporter lines #1 and #2 and the F4 generations of COLORFUL-ABA line #1 in *aba1-101*, *snrk2d*, *snrk2i*, *snrk2d snrk2i*, *ahg3-1* and *pp2ca1* backgrounds, as well as COLORFUL-SA line #1 in *ahg3-1* and *pp2ca1* background were used for oomycetes inoculation. Seedlings were grown under short-day conditions covered with a clear plastic hood and transplanted into individual pots (4.5 cm in diameter), three seedlings per pot, for an additional two weeks. Subsequently, three-week-old plants, as mentioned earlier, were sprayed with the Emwa1 and Noco2 spore solutions adjusted to 5×10^4 spores per ml as mentioned above in comparison with unchallenged plants, which were sprayed with water. Challenged and mock plants then were kept in covered trays and maintained in a growth chamber under short-day conditions. The 5th leaf on the rosette was consistently selected for CLSM (Leica, Germany) at 1 and 2 dpi.

2.2.7.2. *G. orontii* infection experiments

To map the hormone signaling during interaction with *G. orontii*, five-week-old plants were used for inoculation. Seeds of T4 generations of the reporter lines COLORFUL-SA line #1, -ABA line #1 and the F4 generations of COLORFUL-ABA line #1 in *aba1-101*, *snrk2d*, *snrk2i*, *snrk2d snrk2i*, *ahg3-1* and *pp2ca1* backgrounds were sown onto 8.0 cm² pots and incubated in the dark at 4.0 °C for three days. The seedlings were grown for a week covered with a clear plastic hood and transplanted into individual 8.0 cm² pots, five seedlings per pot, for an additional four weeks under the short-day

chamber conditions. Spores of heavily infected hyper-susceptible *A. thaliana eds1* plants were brushed directly upon the five-week-old plants of the aforementioned genotypes. Uninfected plants were used as control. Infected and mock plants were randomized and incubated in uncovered trays in two separate growth chambers adjusted to the short-day conditions (mentioned above). The 5th rosette leaf of plants infected with *G. orontii*, as well as corresponding uninfected mock plants were consistently selected for CLSM (Leica, Germany) at 1 and 2 dpi.

2.2.7.3. Visualization of pathogens during microscopy

To allocate different spores of *H. arabidopsidis* and *G. orontii* used in this study, to help define the real penetration sites, and help monitor the progression of these different pathogens, a fast stain named Fluorescent Brightener 28 (FB-28) (Sigma-Aldrich, Germany) was used. A stock solution of 10 mg/ml FB-28 was diluted to 1:1000 for a final solution concentration of 10 µg/ml. The adaxial surface of the 5th leaf was immersed in a drop of FB-28 for 30 sec to stain the spores. The midrib of the leaves was excised, and the leaves were placed on microscopic slides (Thermo Fisher Scientific, Germany) and mounted in the FB 28 solution.

2.2.7.4. Evaluation of growth dynamics of Emwa1 and Noco2

To address the invasion dynamics of Noco2 and Emwa1 during the compatible and incompatible interactions, respectively, the number of penetrating spores relative to the total numbers of spores per leaf was investigated for both isolates. In these experiments, data were collected from three independent experiments. Each experiment included ten leaves from ten discrete plants. Furthermore, to understand the growth dynamic difference between both Emwa1 and Noco2, the number of haustoria in the epidermal, as well as the mesophyll cell layers, at ten different penetration sites for Emwa1 and Noco2 in the epidermis and the mesophyll at 1 and 2 dpi was scored. The data from three different experiments using COLORFUL-SA, -JA and -JA/ET were pooled. Finally, images and movies were made to show the cell death symptoms induced by Emwa1 infection but not Noco2 at 3 dpi.

2.2.8. Confocal Laser Scanning Microscopy

Imaging in this project was done with the laser scanning confocal microscopes (LSCM), TSC-SP5, and TSC-SP8 (Leica, Germany) in 8-bit formats. For fluorescence quantification purposes, the HCX PL APO CS 20.0x0.70 dry objective with 1.5 zoom factor was used, sequential and bidirectional scan with a speed of 400 Hz, a single line averaging, and a resolution of 512 × 512 pixels. Whereas, for high-resolution images, HC PL APO CS2 20.0x0.75 oil-immersion objective was used with 2.0 zoom factor, and investigated sites were sequentially scanned with a speed of 200 Hz and a resolution of 1024 × 1024 pixels. The Z-stacks were variable depending on the thickness of the captured layer. For the hormone inoculation experiments, one image was made only to monitor the hormone signaling in the pavement cells. Because of the endophytic growth of *H. arabidopsidis*, two different images for the epidermis and palisade mesophyll cell layers were taken separately to analyze the tissue-specific hormone response in both cell types. As *G. orontii* grows epiphytically and only invades epidermis cells, only one image was captured to visualize the epidermal cell layer in *G. orontii* infection experiments. An argon laser with the excitation wavelength at 488 nm and detection spectrum 492-510 nm, was used for analyses of membrane-targeted GFP. Moreover, VENUS and mKATE2 were excited with 514 nm and 594 nm HeNe lines of an argon-ion laser, and then detected at the emission spectra of 528-555 nm and 610-640 nm, respectively. FB-28 applied for pathogen staining was excited with a 405 nm UV diode laser and detected at the emission spectrum 420-460 nm (Table 8). Moreover, the two fluorophores, VENUS and GFP have overlapping emission spectra. Accordingly, to avoid the bleed-through effect between them, they were sequentially scanned. The pinhole aperture was set to 1 airy unit and emitted light was detected with HyD when using VENUS, mKATE2, GFP and FB-28 as fluorescent markers and PMT (Bright field) detectors. Images were acquired with a 2x line average for the VENUS, GFP and mKATE2 channels.

Table 8: Parameters used for the detection of the different fluorophores

Fluorophore	Excitation	Emission
Calcofluor White (FB)	405 nm	420-460 nm
GFP	488 nm	492-510 nm
VENUS	514 nm	528-555 nm
mKate2	594 nm	610-640 nm
Chlorophyll autofluorescence		740-770 nm

During CLSM, the membrane-localized GFP and FB 28 channels were used to define single sites of *H. arabidopsidis* penetrations that do not overlap with other sites of penetration. Penetrations at neighboring trichome cells or directly at the edges or beside the cut midrib of the leaf were excluded. The reference (mKATE2) channel was used to assign the first and the last focal planes of the z-stack for optimal coverage of the nucleus-localized fluorescence signals. The VENUS signal in the treated samples was used to set the threshold of fluorescence detection in comparison to mock. The same imaging configurations were applied for both mock and treatment in each independent experiment and for different time points. The maximum intensity projections, contrast and image merging were performed using Fiji (ImageJ v1.51g). The fluorescent signal values were measured by the software as gray values in a range between zero and 255. Saturated signals (higher than 255) will not be quantified correctly by the software. Therefore, saturation of the fluorescent signals was avoided for all experiments.

2.2.9. Cellular fluorescence quantification

For each independent experiment, the z-stack images were converted into maximum-projected images, which were further used for quantification of the fluorescence signal intensities using COLORFUL SPOTTER which was written in Java as a plugin for ImageJ (Schindelin et al. 2012), and was designed to calculate the intensity levels of nuclear markers throughout multiple images. This plugin is open-source and freely available at <https://github.com/mikepound/colorful>.

2. MATERIALS AND METHODS

The processing of images was done automatically over a directory of input images, with an additional graphical interface to define the reference and hormone reporter channels. Hence, the signal intensities of the VENUS (reporter) and mKATE2 (reference) were separately measured in individual nuclei, and then the ratios reporter/reference were calculated. The mock ratio was normalized to one, and the treatment ratios were calculated relative to the mock. In the configuration of the ratiometric quantification, and before the detection of the nuclei within each image, a median filter was used, and the fluorescence signal of less than three pixels was filtered out to exclude any small noise artifacts from the background without significantly affecting the boundary positions of the nuclei. Once filtered, the plugin extracts the nuclei locations from the reference image by default through Otsu thresholding algorithm (Otsu 1979), which calculates an optimal threshold by maximizing the intra-class variance of the background and foreground. Optionally, additional input channels, if required, were added to the reference channel by performing a pixel-wise sum operation. All foreground pixels were then determined by automatic thresholding over this summed image.

Additionally, the ratiometric quantification generates output images of the quantified nuclei (Figure 6), which were used for quality control. Nuclei were detected within the threshold image using a 4-way connected component algorithm adopted from the single-pass approach taken in (Blob Labeller, ImageJ plugin). Each nucleus was assigned a unique index, and its area was measured. Then, the mean intensity of the reference and hormone reporter and their ratio within the nucleus was quantified. The results were automatically exported as an Excel-compatible file as well as images depicting all detected nuclei and their indexes, usable for quality control analysis, and manual sorting of single-cell readouts.

2.2.10. Image analysis

Following the automated quantification of signal intensities performed by the COLORFUL SPOTTER, the manual stage of quantification started for image analysis. Thus, images of the epidermal pavement and palisade mesophyll cell layers were processed individually to remove unrelated cell types. The nuclei of the unrelated cell types were sorted out manually using the reference and membrane marker modules.

For example, the nuclei from trichomes were removed, these could be identified by their relatively larger size and by looking for the trichomes on the bright-field channels. Furthermore, the guard cell nuclei were also removed during the epidermal image quantification to detect the hormone signatures in pavement cells.

2.2.11. Statistical analysis

All presented data were obtained from independent biological replicates (plants). For each plant a single confocal microscopy image was captured. Cell type-specific single cell readouts from individual images were averaged and represent a single replicate. For results presentation, relative values to the mean of the corresponding mock of the same cell type were calculated. Next, the data was log transformed. Normality was tested using boxplots, whenever n was more than 6. The assumption of variance homogeneity was tested using the Levene's test and boxplot of the residuals. For testing statistical significance of differences, Student's t-test, and one-way and two-way ANOVA followed with Tukey test for multiple comparison analysis were independently performed for the log-transformed data using the R software. Student's t-test was used to test the significance difference of a treated sample to the corresponding mock, and the ANOVA and Tukey tests were used to analyze the significance difference within all groups.

3. RESULTS

3.1. COLORFUL-biosensors reveal hormone signaling outputs at single-cell resolution

The main objective of this project was to outline the spatio-temporal dynamics of the phytohormones ABA, SA, JA, and JA/ET during plant-microbe interaction. In an ongoing unpublished study in the plant cell biology department, Hassan Ghareeb established a set of hormone-responsive expression-based reporter systems for ABA, SA, JA, and JA/ET, so-called COLORFUL-biosensors. The functionality of COLORFUL-SA, -JA, and -JA/ET was investigated. Here, we aimed to validate the responsiveness of the COLORFUL-ABA reporter. Subsequently, the four reporter systems were used to map the alteration in hormone homeostases upon different biotrophic pathogen attacks. In order to select a highly ABA-responsive marker, *in silico* gene expression analysis was performed by Hassan Ghareeb and validated in the current study by qRT-PCR analyses.

3.1.1. *PP2CA* expression shows the highest correlation with the exogenous ABA treatment and incubation time in comparison to other ABA tested marker genes

As a means to select an ABA responsive marker gene, the expression of *ABA-HYPERSENSITIVE GERMINATION1 (AHG3)/PROTEIN PHOSPHATASE 2CA (PP2CA)*, which is known to exhibit a strong induction upon accumulation of ABA (Kuhn et al. 2006; Nishimura et al. 2007; Yoshida et al. 2006) was investigated in comparison to other ABA-responsive genes *AtRD29A*, *AtRD29B*, *AtHB6*, and *AtRAB18*. Promoters of *AtRD29A/B*, *AtHB6*, and *AtRAB18* genes were utilized previously to develop ABA-responsive expression-based reporters (Christmann et al. 2005; Himmelbach et al. 2002; Ishitani et al. 1997; Söderman et al. 1999). In this

3. RESULTS

investigation, the transcript levels of the previously mentioned ABA marker genes were tested in an ABA biosynthetic mutant (*aba1-101*) and a triple mutant of ABA signaling (*snrk2d snrk2e snrk2i*) in comparison to the wildtype after exogenous application of 50 μ M ABA and mock treatments for 24 h using qRT-PCR analyses. The transcript abundance was normalized to the transcript level of the housekeeping gene *UBQ5*, and subsequently to the transcript level in untreated mock.

The comparative transcriptional analysis in the wildtype, relative to gene expression levels in the mock samples, showed overall high variability in expression induction of *PP2CA* (675-fold \pm 218 s.e.m.), *RD29A* (328-fold \pm 244 s.e.m.), *RD29B* (267-fold \pm 136 s.e.m.), *HB6* (212-fold \pm 199 s.e.m.), and *ARD18* (154-fold \pm 115 s.e.m.) genes. Statistical analysis showed that ABA-induced *PP2CA* transcript level was significantly higher than the other tested genes (Figure 6a). Moreover, the gene expression levels of the tested genes in *aba1-101* upon ABA treatment showed almost a similar pattern but with lower magnitudes. In the triple mutant of the ABA positive regulators SnRK2D, SnRK2E, and SnRK2I, the expression levels of the ABA-marker genes were relatively low. Thus, *HB6*, *RAB18*, and *PP2CA* did not show any change, *RD29A* and *RD29B*, though, showed a slight but significant increase in transcript levels of a 15.7-fold (\pm 24.45 s.e.m.) and a 21.58-fold (\pm 31.89 s.e.m.) relative to mocks.

These results reflected that the expression of ABA downstream components *PP2CA*, *HB6*, and *RAB18* is completely dependent on ABA positive regulators SnRK2s, whereas, *RD29A* and *RD29B* showed a partial SnRK2s-independent activation. Next, qRT-PCR analyses were performed to test the expression kinetics of *HB6*, *RAB18*, and *PP2CA*. Data analysis revealed a significant upregulation of *HB6* (Figure 6b) and *RAB18* (Figure 6c) genes after treatment with 50 μ M ABA for 24 h.; however, *PP2CA* expression level increased gradually and was significantly induced after 6 h (Figure 6d). These transcriptional results confirmed the efficiency of *in silico* analyses for the selection of the *PP2CA* promoter to develop the COLORFUL-ABA.

3. RESULTS

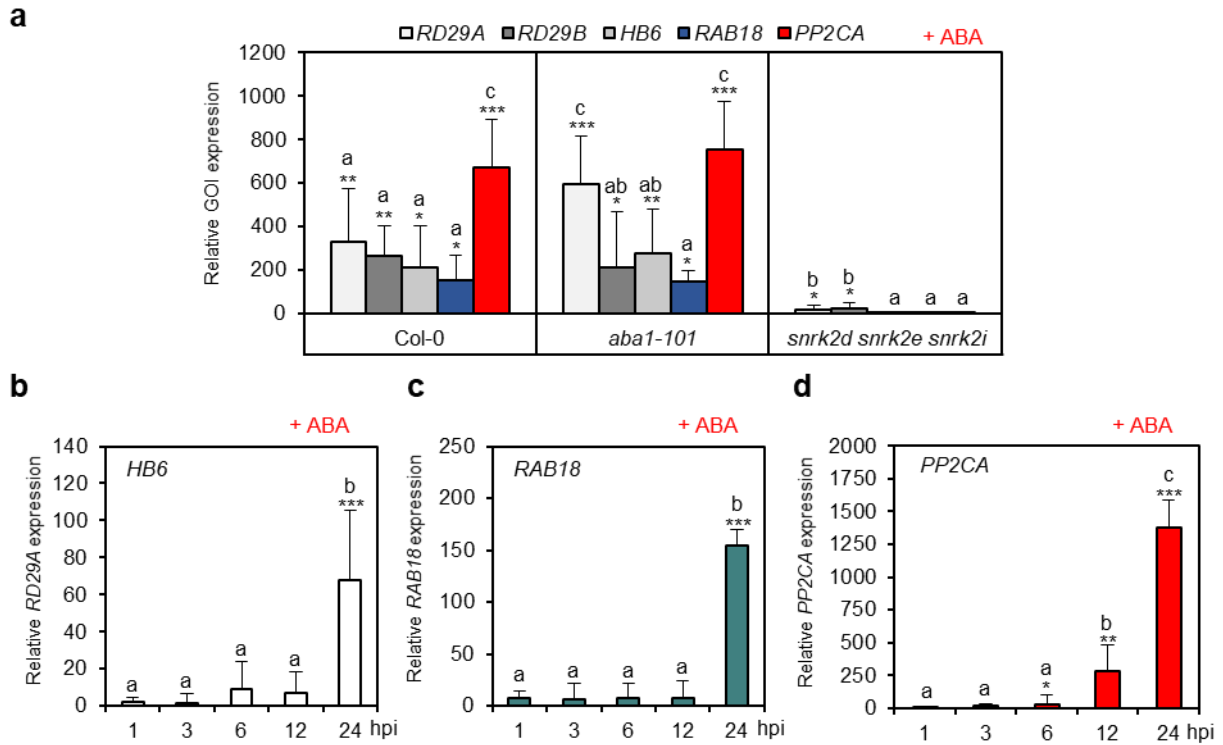


Figure 6: qRT-PCR analyses reflect a strong PP2CA responsiveness upon exogenous ABA treatment in an incubation time-dependent progression. (a) Quantitative real-time PCR (qRT-PCR) analysis of *RD29A*, *RD29B*, *HB6*, *RAB18*, and *PP2CA* transcript levels in 12-day-old wildtype Col-0, ABA biosynthetic mutant *aba1-101* and ABA signaling triple mutant *snrk2d snrk2e snrk2i* after treatment with 50 μ M ABA for 24 h. GOI: Gene of interest. (b-d) qRT-PCR analysis of *HB6* (b), *RAB18* (c), and *PP2CA* (d) transcript levels in 12-day-old wildtype Col-0 after treatment with 50 μ M ABA for 01, 03, 06, 12, and 24 h. The transcript abundance was normalized to the transcript level of the housekeeping gene *UBQ5*, and subsequently to the transcript level in mock. Data show means \pm s.e.m. of three independent biological replicates, each represents a pool of 10 plants. The experiments were repeated once showing a similar pattern. Asterisks indicate statistical differences between the transcript levels in ABA-treated and mock (* $p < 0.05$, ** $p < 0.01$, *** $p < 0.001$, Student's t-test). Different letters indicate the significant differences between groups within the same genotype (One-way ANOVA followed by Tukey's multiple comparison test, $p < 0.05$).

3.1.2. COLORFUL-ABA harbours three distinct fluorescent protein-based reporter cassettes and a BASTA-resistance selection marker

Taking advantage of the recently published multigene assembly vector platform “COLORFUL-Circuit” (Ghareeb et al. 2016), a multimodular system was established. This system uses by the combination of a hormone reporter module, a reference module, and a plasma membrane marker module, in addition to a BASTA-resistance selection marker—on a single binary vector—for simultaneous transgene expression (Figure 7a). The three modules employ the spectrally separable fluorescent proteins VENUS, mKATE2, and GFP (Nagai et al. 2002; Shcherbo et al. 2009; Zhang et al. 1996). The hormone inducible promotor of *PP2CA* was fused with VENUS to construct the ABA reporter module. Moreover, a nuclear localization signal N7 (Cutler et al. 2000) was combined with VENUS to enrich the nuclear targeting of the PP2CA-dependently expressed VENUS. Nuclear localization of ABA-controlled VENUS facilitates the quantification of ABA signaling at single-cell resolution (Figure 7b, green).

To facilitate acquisition and quantification of the nuclear-localized VENUS signal, a constitutively expressed nucleus-localized mKATE2 fluorescent marker was incorporated as a reference module. The strong and constitutively active *POLYUBIQUITIN 10* (*UBQ10*) promoter and the nuclear localization signal N7 (Cutler et al. 2000) were fused to *mKATE2*, providing the nuclear-targeted reference module *UBQ10-mKATE2-N7* which defines the nuclei in different cell types (Figure 7a-b, magenta). In addition, the constitutive promoter Cauliflower Mosaic Virus 35S RNA (*CaMV35S*) was employed to generate a membrane marker module. Thus, *CaMV35S* promoter was used to drive the expression of *GFP* tagged with the plasma membrane (PM) localized, low temperature-induced protein 6b (*LTI6b*) to generate the PM marker module *CaMV35S-GFP-LTI6b* (Cutler et al. 2000), which labels the cell boundaries (Figure 7a-b, gray). Therefore, Confocal-laser-scanning-microscopy (CLSM) of transgenic Arabidopsis plants harboring the trimodular COLORFUL-ABA construct should enable detection of contours, sizes, identities, and viability of particular cells, their relative position in a tissue context, and the simultaneous quantification of the reporter and reference signal outputs in their corresponding nuclei.

3. RESULTS

Thirty independent BASTA-resistant transgenic COLORFUL-ABA lines were generated in the Col-0 background and analyzed by CLSM before and after hormone treatments. All tested transgenic lines showed ABA-inducible VENUS fluorescence signals. For instance, at a microscopic level, the treatment of eleven-day-old plants of the COLORFUL-ABA line #1 with 50 μ M ABA for 24 h induced detectable activities of the ABA reporter channel (Figure 7b, upper panel, green), whereas the mock leaves did not show any eye-detectable signal in the reporter channel (Figure 7b, lower panel, black).

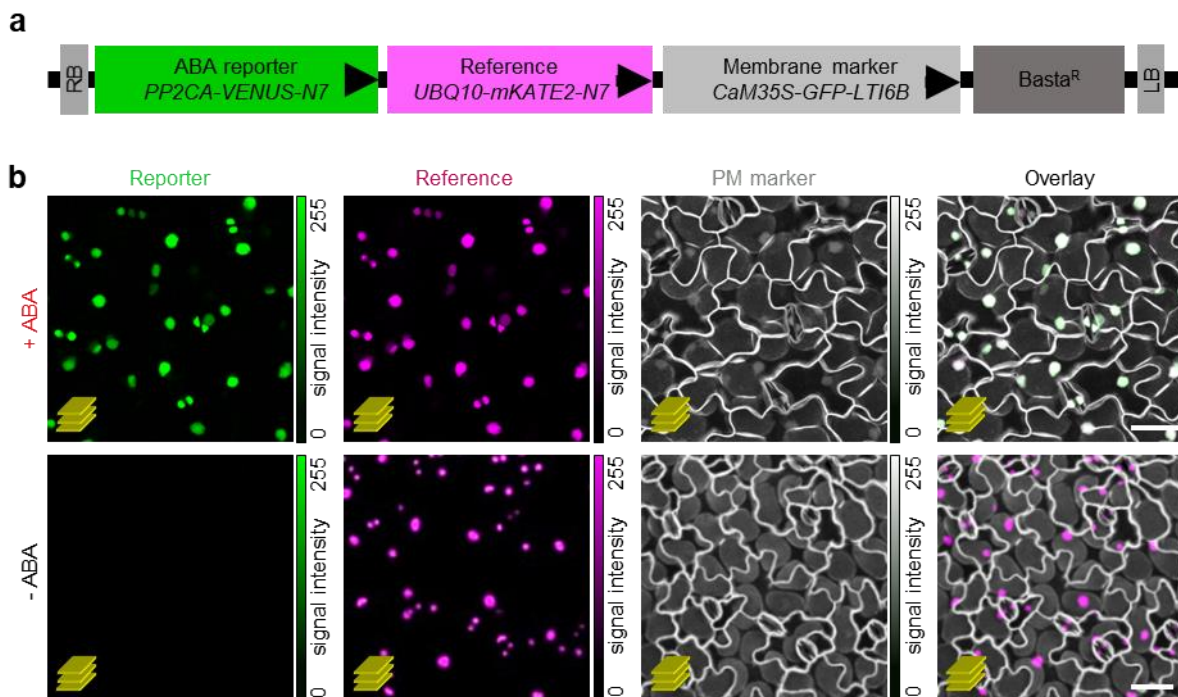


Figure 7: COLORFUL-ABA allows simultaneous transgene expression of three distinct fluorescent protein-based reporter cassettes. (a) Schematic representations of the COLORFUL-ABA T-DNA construct harboring the fluorescent marker module *pPP2CA-VENUS-N7* (nuclear-localized reporter), *pUBQ10-mKATE2-N7* (nuclear-localized reference), and *pCaMV35S-GFP-LTI6b* (plasma membrane marker). *Basta^R*, selectable marker; LB/RB, left/right borders of T-DNA (b) Maximum projections of CLSM z-stack images showing the expression of the reporter (green), the reference (magenta), the plasma membrane marker modules (gray), and the overlay of the reporter, reference, and membrane marker modules in leaves of 12-day-old transgenic COLORFUL-ABA line #1 after treatment with 50 μ M ABA treatment for 24 h (Upper panel), and mock (Lower panel). Scale bar: 50 μ m.

3.1.3. COLORFUL-SPOTTER allows comparative large-scale quantitative data analyses on single-cell level

To facilitate quantitative, comparative large-scale data analyses on single-cell resolution, an ImageJ plugin called COLORFUL-SPOTTER was developed to enable automated nuclear fluorescence detection and quantification in z-stack images (Figure 8a-b). Subsequently, CLSM z-stack images are processed by the software. After the removal of small noise artefacts (components of 3 pixels or fewer), the COLORFUL-SPOTTER-mediated processing identifies nuclear fluorescence signals in both channels of CLSM z-stack images, generates a corresponding fluorescence detection mask, assigns cell-specific index numbers (yellow overlay), and quantifies individual fluorescence intensities in reference and reporter channels separately, as well as their ratio within the nucleus.

A combined membrane marker and reference-supported visual inspection then allows dissection of epidermal from mesophyll cell layers during microscopy and subsequent quantification. Additionally, it facilitates the classification of epidermis cells into pavement/stomatal subpopulations and manual data curation. Curation is required when mesophyll-specific signals are erroneously detected in the epidermis layer (or vice versa) due to leaf curvature (signals #12, #14, #15, #24, and #28 marked in blue in Figure 8b) and when close nuclear signals are merged into a single spot (signal #18 marked in red in Figure 8b), or when merged and misassigned signals occur in combination (signals #25 and #27 marked in green in Figure 8b).

3. RESULTS

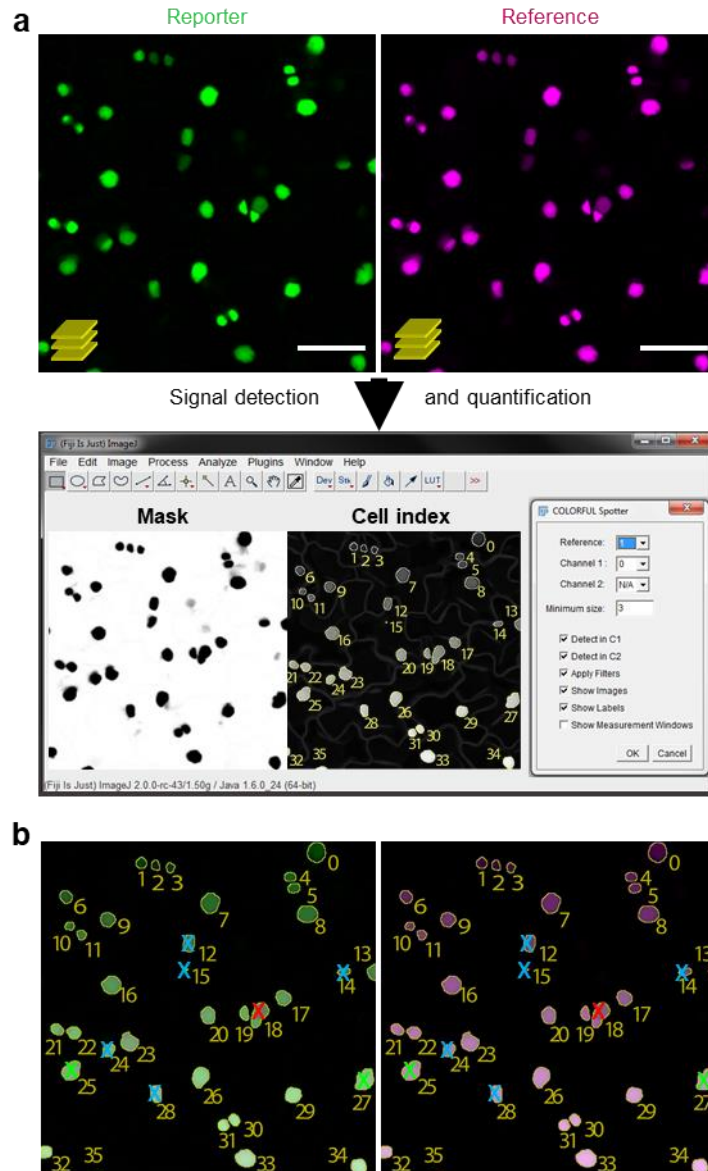


Figure 8: Quantifications using COLORFUL-SPOTTER reveal a distinct spatial activation of hormone signaling. (a-b) Automated nuclear fluorescence detection and signal quantification processing strategy of the COLORFUL-SPOTTER plugin. CLSM z-stack images corresponding to reporter channel (0), and reference channel (1) in a leaf of 12-day-old transgenic COLORFUL-ABA line #1 after treatment with 50 μ M ABA treatment for 24 h after the removal of small noise artefacts (components of 3 pixels or fewer) for the generation of tissue-specific maximum projections of ABA reporter or reference fluorescence. Subsequent COLORFUL SPOTTER-mediated processing identifies nuclear fluorescence signals in the reporter (green) and reference (magenta) channels, generates a corresponding detection mask, assigns cell-specific index numbers (yellow overlay), and automatically quantifies individual fluorescence intensities, as well as their ratio within the nucleus. Curation is represented by blue, red, and green marks. Blue X shows mesophyll-specific signals that are erroneously detected in the epidermis layer (or vice versa) due to leaf curvature (signals #12, #14, #15,

3. RESULTS

#24, and #28), red X shows close nuclear signals that are merged into a single spot (signal #18), and green X shows the combination of merged and misassigned signals (signals #25 and #27). Scale bar: 50 μm .

3.1.4. COLORFUL-reporters show consistent quantitative readouts for the reporter activity in different transgenic lines

In order to test the consistency of the reporter activities between four independent transgenic COLORFUL-ABA lines #1, #2, #3 and #4, the signal intensities in twelve-day-old seedlings were quantified with and without exogenous application of 50 μM ABA for 24 h. Remarkably, the quantitative measurements using COLORFUL SPOTTER resulted in quantitative readouts which showed no statistical difference ($p < 0.05$) between the four independent transgenic lines (Figure 9a). Therefore, ABA reporter line #1 and its filial generations obtained by self-fertilization or crossing with hormone biosynthesis or signaling mutants were used in all subsequent experiments. Stable expression of all reporter cassettes was observed at least until generation T4 (data not shown).

3.1.5. Nuclear targeted COLORFUL-modules exhibit cell-type specific activities

Exogenous treatment with ABA triggered *VENUS* expression in different leaf cell types of twelve-day-old COLORFUL-ABA line #1 seedlings. However, qualitatively different signal intensities were observed in the reporter channel (Figure 8a, green). Consequently, only standardized replicate experiments can provide statistically robust data sets for the guard, pavement, and mesophyll cell-specific response investigations. Indeed, our quantitative analyses confirmed distinct cell-specific ABA reporter activities (Figure 9b). In untreated leaves, epidermal guard cells displayed maximum relative basal ABA reporter signal intensities, while the epidermal pavement and the palisade mesophyll cells showed lower signal intensities relative to mock guard cell signals with 80 % and 90% decrease, respectively. Moreover, at 1-day post-treatment with 50 μM ABA, a significant increase of the ABA-reporter signal was observed. Epidermal guard cells displayed maximum ABA signal intensities with a 2.3-fold (± 0.6 s.e.m.) induction compared with controls, while the epidermal pavement and the palisade mesophyll cells exhibited a 1.4-fold (± 0.5 s.e.m.) and 1.1-fold (± 0.3 s.e.m.) induction,

3. RESULTS

respectively (Figure 9b). Thus, the ratio of intensities between guard cells and pavement/mesophyll cells is similar under non-induced and induced conditions.

The COLORFUL-reporter system was designed to allow ratiometric reference-reporter analyses. However, ABA treatment exhibited a slight but significant induction effect on *UBQ10* promoter-driven mKATE2 reference expression in guard cells (1.28-fold \pm [0.4 s.e.m.]), pavement cells (1.16-fold [\pm 0.34 s.e.m.]), and mesophyll cells (1.25-fold [\pm 0.6 s.e.m.]) relative to the untreated guard cell signals (Figure 9c). As a consequence, ratiometric fluorescence measurements using the *UBQ10* promoter-driven mKATE2 expression is not feasible. Thus, in this study the mKATE2 reference fluorescence was utilized only for general nuclear detection, sorting, and as a cellular viability marker.

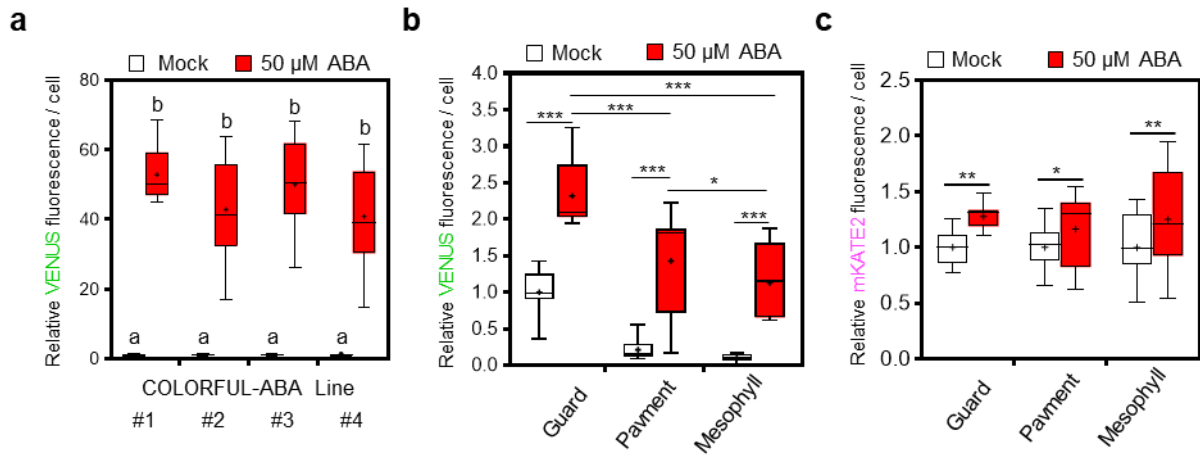


Figure 9: Quantifications using COLORFUL-SPOTTER reveal a distinct spatial activation of hormone signaling. (a) ABA reporter activities in the leaf pavement cells of four independent 12-day-old COLORFUL-ABA transgenic line #1 with 50 μ M ABA treatment for 24 h or mock. (b) VENUS signal intensities measurements in guard, pavement, and palisade mesophyll cells of 12-day-old transgenic COLORFUL-ABA line #1 at 24 h post treatment with 50 μ M ABA (red) or mock (white). (c) Effect of ABA treatment on mKATE2 signal activities in epidermal guard, epidermal pavement, and palisade mesophyll cells of transgenic COLORFUL-ABA line #1. Box plots show first quartile (lower line); median (centre line); mean (+); third quartile (upper line); whiskers extend 1.5 times the -interquartile range, and outliers are depicted as dots, $n = 7-10$ leaves. The experiments in b and c were repeated once with COLORFUL-ABA reporter line #1 and another repeat was performed using the independent transgenic COLORFUL-ABA line #2. Different repeats showed similar pattern of response. Data are relative to the mock of the wildtype. Asterisks indicate statistical differences between signal intensities in hormone treated and corresponding mock (* $p < 0.05$, ** $p < 0.01$, *** $p < 0.001$, Student's t-test). Different letters indicate the

3. RESULTS

significant differences between groups (One-way ANOVA followed by Tukey's multiple comparison test, $p < 0.05$).

3.1.6. The COLORFUL-reporter activity correlates with hormone dose and treatment incubation time

3.1.6.1. COLORFUL-ABA reporter reveals a rapid responsiveness, high specificity and accuracy to minor changes in ABA levels

In response to increasing ABA concentrations, COLORFUL-ABA showed a significant increase in ABA reporter activity in the pavement epidermal cells upon hormone treatment with a minimum of 0.1 μM ABA, reflecting a high sensitivity for sensing minor changes in ABA accumulation. Moreover, a remarkable gradient of the reporter signals increase was observed correlating with ABA concentration (Figure 10a). Data analyses showed that ABA reporter activity is less precise at low ABA concentrations (statistical groups a, ab, bc, c). Therefore, 50 μM ABA was used as a standard concentration in all subsequent ABA treatment experiments to analyze the kinetics of the ABA stimulus-dependent hormone reporter in epidermal pavement cells. Data analyses exhibited a statistically significant induction of ABA reporter activity at 3.0 h post treatment, hinting a rapid sensing capacity, and a gradual increase of ABA-induced VENUS fluorescence which positively correlates with the incubation time up to 24 h post treatment (Figure 10b). The gradually increasing VENUS signal intensities correlate with induction kinetics of *PP2CA* expression after ABA treatment (Figure 6d).

To investigate the COLORFUL-ABA specificity to ABA, the homozygous ABA biosynthetic mutant *aba1-101*, which shows a drastic reduction in ABA biosynthesis (Barrero et al. 2005), was used for crossing with the COLORFUL-ABA line #1. COLORFUL-ABA in the *aba1-101* background displayed drastically diminished levels of basic VENUS fluorescence in comparison to untreated wildtype (Figure 10c). The treatment of *aba1-101* plants with 50 μM ABA for 24 h resulted in a reporter signal similar in magnitude to the VENUS intensity in ABA treated wildtype (Figure 10c). In order to verify the complementation of ABA reporter activity in *aba1-101* by ABA, the expression of *PP2CA* was investigated after ABA and mock treatments for 24 h.

3. RESULTS

Relative to the mock of wildtype, untreated *aba1-101* showed a reduced transcript level 0.25-fold (± 0.80 s.e.m.) which is complemented by the treatment with ABA (Figure 10d).

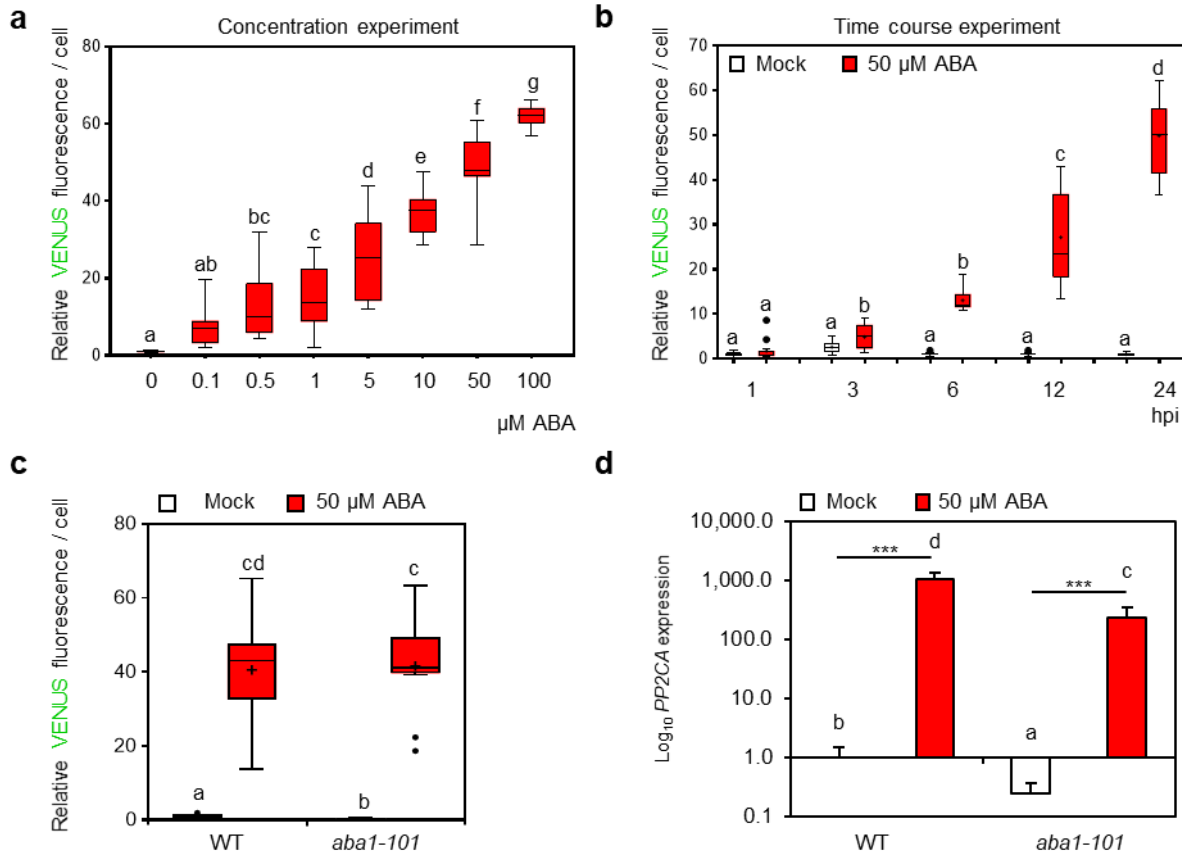


Figure 10: ABA-reporter activity positively correlates with extrinsic and intrinsic ABA in a concentration and incubation time-dependent manner. (a) ABA reporter activities in the leaf pavement cells of transgenic line COLORFUL-ABA #1 in response to ABA concentrations. 11-day-old seedlings were incubated in 0.0, 0.1, 0.5, 01, 05, 10, 50, and 100 μM ABA for 24 hpi. (b) ABA reporter activities in the leaf pavement cells of 12-day-old transgenic line COLORFUL-ABA #1 in response to incubation in 50 μM ABA for 01, 03, 06, 12, and 24 h. The experiments in a and b were repeated twice using COLORFUL-ABA reporter line #1 and once using COLORFUL-ABA line #2. Different repeats showed similar pattern of response. (c) ABA reporter activities in leaf pavement cells of 12-day-old COLORFUL-ABA line #1 in the wildtype background, in comparison to reporter activities in leaf pavement cells of 12-day-old COLORFUL-ABA line #1 in *aba1-101* background before and after ABA treatment for 24 h. (a,b,c) the experiments were repeated twice with similar pattern of response. Box plots show first quartile (lower line); median (centre line); mean (+); third quartile (upper line); whiskers extend 1.5 times the interquartile range, and outliers are shown as dots, n = 10 leaves. (d) qRT-PCR analysis of *PP2CA* transcript levels in the wildtype and *aba1-101* after treatment with 50 μM ABA for 24 h. The transcript abundance was normalized to the transcript level of the housekeeping gene *UBQ5*,

3. RESULTS

and subsequently to the transcript level in untreated mock. Data show means \pm s.e.m. of three independent repeats, each represents a pool of 10 plants. Different letters indicate significant difference between groups (One-way ANOVA followed by Tukey's multiple comparison test, $p < 0.05$). Asterisks indicate statistical differences between the transcript levels in ABA-treated and mock (* $p < 0.05$, ** $p < 0.01$, *** $p < 0.001$, Student's t-test).

3.1.6.2. Transcriptional analyses reflect positive correlations of SA, JA and JA/ET reporter activities with exogenous hormone applications

For the establishment of COLORFUL-SA, -JA and -JA/ET, the promoters of the SA-responsive *PR1* gene (Cao et al. 1994; Mou et al. 2003), the JA-inducible *VSP2* gene (Anderson et al. 2004; Lorenzo et al. 2004), and the JA/ET-responsive *PDF1.2a* gene (Penninckx et al. 1998), respectively were utilized to drive *VENUS* expression. The dosage- and incubation time-dependency of the *VENUS* reporter activity in COLORFUL-SA line #1, -JA line #1, and -JA/ET line #1 was confirmed in response to salicylic acid (SA), methyl jasmonate (MeJA) alone and in combination with the ethylene precursor 1-aminocyclopropane-1-carboxylic acid (ACC), respectively. SA-, JA-, and JA/ET-reporter activities were investigated in the F3 and F4 generations of the SA signaling mutant *npr1-1* (Cao et al. 1994), the JA-insensitive *coi1-t* mutant (Mosblech et al. 2011), and in ethylene-insensitive *ein2-1* mutants (Guzman & Ecker 1990) crossed with COLORFUL-SA line #1, -JA line #1, and -JA/ET line #1, respectively. Compared with wildtype responses, drastically reduced levels of *VENUS* fluorescence were observed before and after treatments with SA, MeJA, or MeJA + ACC, respectively, demonstrating the functionality and specificity of the reporters for monitoring the accumulation and signaling of the corresponding hormone.

In order to ascertain the correlation of the gradual increase in the SA-, JA-, and JA/ET-reporter activities with transcriptional activation of marker genes, the expression levels of *PR1*, *VSP2*, and *PDF1-2a* were quantified in twelve-day-old wildtype Col-0 plants after treatments with 0.5 mM SA, 50 μ M MeJA or the combination of 50 μ M MeJA and 2.0 μ M ACC at 1.0, 3.0, 6.0, 12 and 24 hpt. The transcript abundances were normalized to the transcript level of the housekeeping gene *UBQ5*. Expression levels were calculated relative to transcript abundances in the corresponding mock plants.

3. RESULTS

qRT-PCR analysis displayed pronounced upregulations of the aforementioned genes after hormone treatment (Figure 11a-c). The expression of *PR1* was slightly but significantly increased after SA treatment for 6 h (28-fold \pm 9 s.e.m.). At 12 h of SA treatment, Arabidopsis plants showed a stronger upregulation of *PR1* gene expression (134-fold \pm 58 s.e.m.), and at 24 h a pronounced increase in the *PR1* transcript level was observed (338-fold \pm 88 s.e.m.) (Figure 11a). The gradually increasing kinetics of *PR1* expression correlates with the time of Arabidopsis incubation in SA.

Moreover, *VSP2* and *PDF1-2a* expression levels showed similar trends of induction. MeJA treatment for 24 h induced a 198-fold (\pm 51 s.e.m.) increase in the expression of *VSP2* relative to the untreated Col-0 (Figure 11b). In addition, incubation of Col-0 plants with MeJA + ACC for 24 h enhanced the relative transcript level of *PDF1-2a* by 70-fold (\pm 18 s.e.m.) (Figure 11c). The strong hormone-dependent induction of these marker genes indicates that the corresponding promoters are useful to address changes in hormone concentrations.

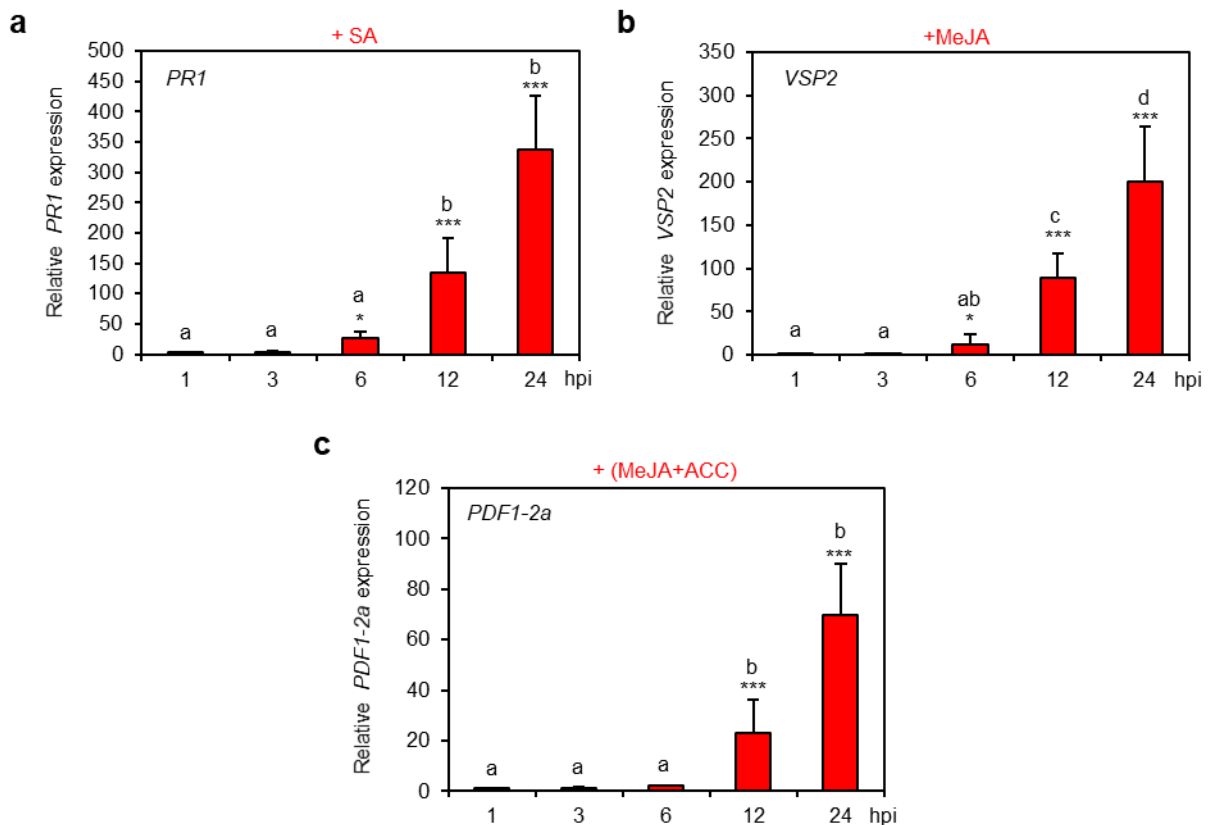


Figure 11: Expression levels of *PR1*, *VSP2*, and *PDF1-2a* positively correlate with the hormone treatment times. (a-c) qRT-PCR analysis of *PR1* (a), *VSP2* (b) and *PDF1-2a* (c) transcript levels in 12-

3. RESULTS

day-old wildtype Col-0 after treatment for 1.0, 3.0, 6.0, 12, and 24 h with 0.5 mM SA, 50 μ M MeJA and combination of MeJA with 2.0 μ M ACC. The transcript abundance was normalized to the transcript level of the housekeeping gene *UBQ5*, and subsequently to the transcript level in mock. Data show means \pm s.e.m. of three independent biological replicates, each represents a pool of 10 plants. The experiments were repeated once showing a similar pattern. Asterisks indicate statistical differences between the transcript levels in hormone-treated and the corresponding mock (* $p < 0.05$, ** $p < 0.01$, *** $p < 0.001$, Student's t-test). Different letters indicate the significant differences between groups (One-way ANOVA followed by Tukey's multiple comparison test, $p < 0.05$).

3.1.7. COLORFUL-biosensors explore distinct tissue-specific signaling outputs

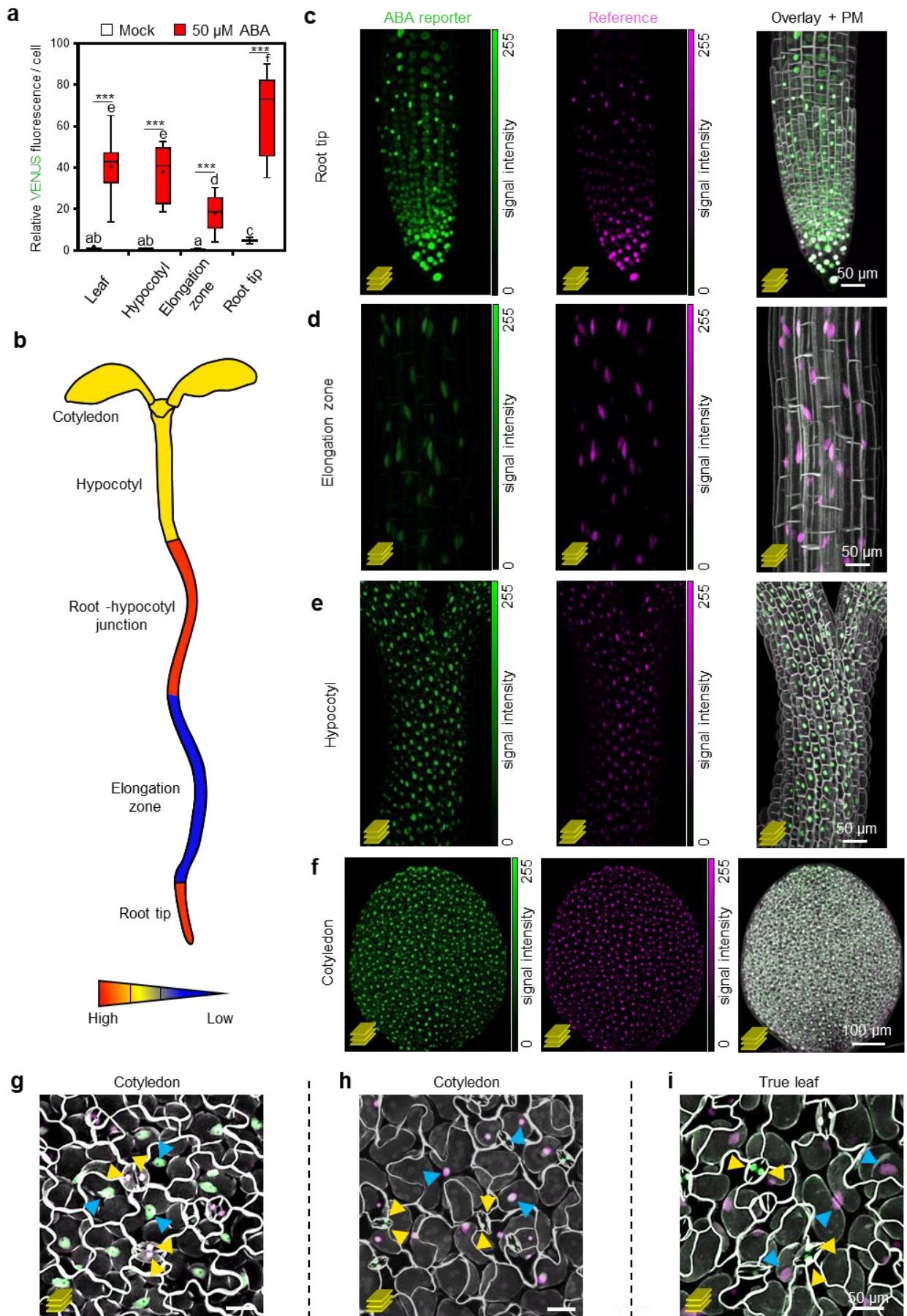
3.1.7.1. ABA reporter activity correlates with the well-known ABA differential pattern in all investigated Arabidopsis tissues

Data analyses confirmed the efficiency of COLORFUL-systems to address the cell type-specific hormone responses in Arabidopsis leaves (as mentioned above). The capacities of the generated promoter-reporter lines to monitor long-distance hormone signaling in different tissues of Arabidopsis were evaluated. In this concern, quantitative data analysis of reporter activity in twelve-day-old COLORFUL-ABA line #1, as well as qualitative CLSM imaging of three- and twelve-day-old plants, showed a maximum ABA signaling activity in the root tip (Figure 12a, c), which is a well-established experimental system for analysis of ABA effects (Dong et al. 2020; Rosales et al. 2019; Waadt et al. 2014). In contrast to the root tip, a minimal ABA signal intensity was noticed in the root elongation zone (Figure 12a-b, d). Moreover, an intermediate ABA signal was detected in the hypocotyl (Figure 12a, e) and the leaf/cotyledon (Figure 12a, f) before and after ABA treatment. A similar ABA signaling pattern was observed with (Figure 12a-b) and without ABA treatments (Figure 12b-i). Using the FRET-based sensor ABAleon, Waadt et al. (2014) and Waadt et al. (2015) demonstrated a similar pattern of tissue specific distribution of ABA in response to ABA treatment. Furthermore, ABAleon reporter exhibited a lower sensitivity to detect the basal distribution of ABA (Waadt et al. 2015).

3. RESULTS

Intriguingly, higher ABA signal intensities were observed in the pavement cells (blue arrows) in comparison to the guard cells (yellow arrows) in three-days old cotyledon (Figure 12g), although the guard cells are known to contain high levels of ABA (Boursiac et al. 2013; Cotellet & Leonhardt 2019; Kanno et al. 2012; Waadt et al. 2014; Waadt et al. 2015). In contrast, the guard cells in the twelve-day-old cotyledons (Figure 12h) and true leaves (Figure 12i) showed a higher ABA signal intensity than the pavement reporter signals indicating potential developmental stage-dependent changes in ABA levels in different cell types.

3. RESULTS



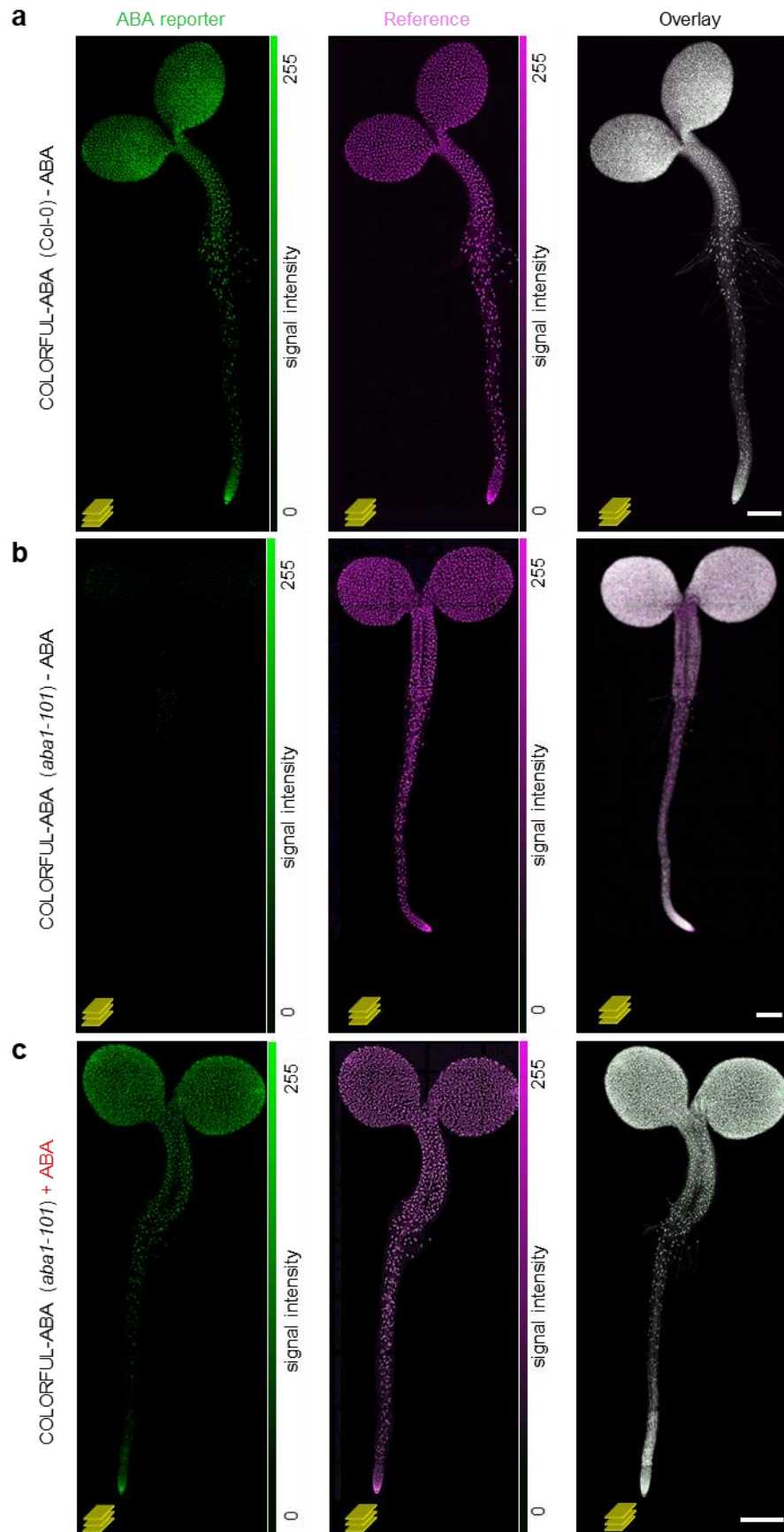
3. RESULTS

Figure 12: COLORFUL-ABA reporter activity displays a distinct tissue type and developmental stage-specific pattern of ABA signaling in different Arabidopsis tissues. (a) Quantitative analysis of ABA signaling activities in leaves, hypocotyl, elongation zone, and root tip of 12-day-old COLORFUL-ABA line #1 without and with 50 μ M ABA treatments for 24 hours. This experiment is repeated once showing the same pattern of ABA response. Box plots show the first quartile (lower line); median (centre line); mean (+); third quartile (upper line); whiskers extend 1.5 times the interquartile range and outliers are shown as dots, $n = 6-10$ samples. Data are relative to the mock. Asterisks indicate statistical differences between signal intensities in ABA-treated and mock (* $p < 0.05$, ** $p < 0.01$, *** $p < 0.001$, Student's t-test). Different letters indicate significant differences between groups (One-way ANOVA followed by Tukey's multiple comparison test, $p < 0.05$). (b) Graphical overview of the differential distribution of VENUS signals in different Arabidopsis tissues adapted from (a) before and after ABA treatment. The maximum ABA signal intensities exist in the root tip, the junction between hypocotyl-root, and in the stomata cells, while the root elongation zones reflect the minimal ABA signal intensities. ABA-intermediate signal intensities are detected in the cotyledons and hypocotyls. (c-f) Maximum projections of CLSM z-stack images of ABA-reporter (green), reference (magenta) and the overlay of the reporter, reference channels and PM-marker (gray) in 3-day-old COLORFUL-ABA#1 seedling in the root tip (c), root elongation zone (d), hypocotyl (e) and cotyledon (f). (g-i) Maximum projections of CLSM z-stack overlay for reporter module, reference module, and the overlay of the reporter, reference, and PM-marker in the 3-day-old cotyledon (g), the cotyledon (h), and a true leaf of 12-day-old Arabidopsis COLORFUL-ABA#1 (i). Different arrows mark different cell types of epidermal pavement cells (blue arrows) and guard cells (yellow arrows). Scale bar: 50 μ m. (b) is consistent with the ABA measurements using ABAleon sensor after ABA treatment (Waadt et al. 2014; Waadt et al. 2015).

3.1.7.2. *aba1-101* mutant analyses display a global reduction in ABA signaling activities in Arabidopsis

In order to examine the reliance of the basal ABA reporter activity on ABA biosynthesis, the VENUS signal was mapped in the wildtype COLORFUL-ABA line #1 (Col-0) in comparison to the ABA biosynthetic mutant *aba1-101* with and without exogenous ABA treatment (Figure 13a and Figure 14a-d, left panel). Notably, a pronounced reduction in ABA signal was observed in *aba1-101* (Figure 13b and Figure 14a-d middle panel), showing dependency of the ABA-reporter activity on the ABA biosynthesis. Also, the comparison of the reporter activity before and after 50 μ M ABA application, for at least 6 hours revealed prominent complementation of the wildtype-like signals in the entire *aba1-101* seedlings (Figure 13c and Figure 14a-d, right panel).

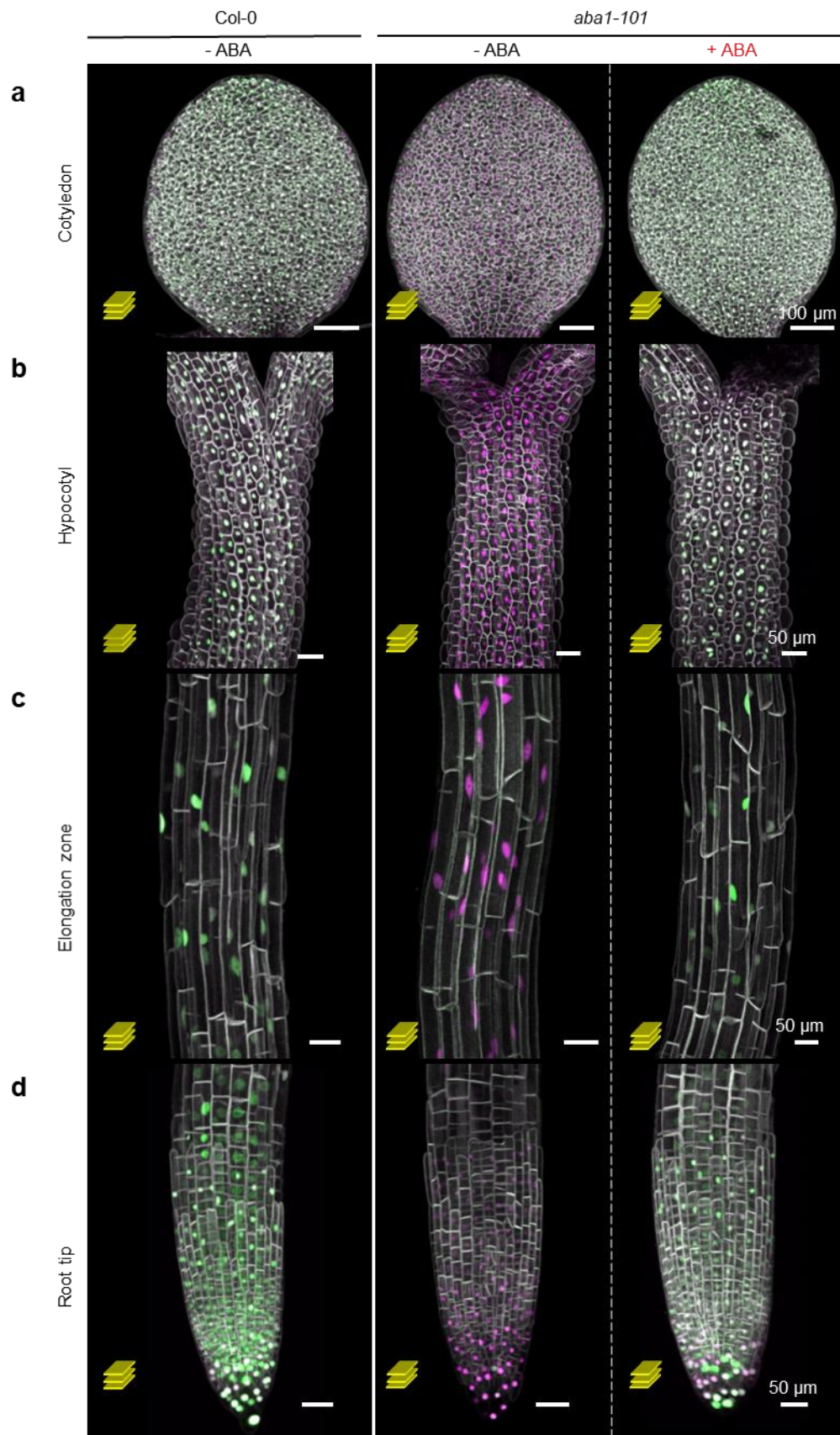
3. RESULTS



3. RESULTS

Figure 13: The differential COLORFUL-ABA reporter activity is dependent on ABA biosynthesis.
(a-c) Maximum projection of CLSM z-stack images of ABA-reporter (green), reference (magenta), and the overlay of ABA-reporter (green), reference (magenta), PM marker (gray) channels in 3-day-old seedlings of (a) Untreated COLORFUL-ABA line #1 seedling in Col-0 background. (b) Untreated COLORFUL-ABA line #1 in ABA biosynthetic mutant *aba1-101* background. (c) COLORFUL-ABA line #1 in *aba1-101* background after treatment with 50 μ M ABA for 6 h. Scale bar: 200 μ m.

3. RESULTS



3. RESULTS

Figure 14: The basal ABA signals correlate with ABA content in Arabidopsis. (a-d) The overlay of maximally projected CLSM z-stack images of ABA-reporter (green), reference (magenta), and PM marker (gray) channels in the cotyledon (a), hypocotyl (b), elongation zone (c), and the root tip (d) of 3-day-old untreated COLORFUL-ABA line #1 in Col-0 background (left panel), untreated COLORFUL-ABA line #1 in *aba1-101* background before (middle panel) and after incubation for 6 hours in 50 μ M ABA (right panel). Scale bar in a: 100 μ m, scale bar in b-d: 50 μ m.

3.1.7.3. SA, JA, and JA/ET reporters disclose reporter activities in different Arabidopsis tissues

In order to map the SA-, JA-, and JA/ET-controlled VENUS fluorescence in different Arabidopsis tissues, twelve-day-old seedlings of COLORFUL-SA line #1, -JA line #1, and -JA/ET line #1 were incubated for 24 hours in 0.5 mM SA, 50 μ M MeJA, and 50 μ M MeJA + 0.2 μ M ACC, respectively. CLSM analyses of leaves, cotyledons, and roots of the three reporter lines were performed. In comparison to mock treatments, the quantitative analyses showed a significant increase in the reporter activity in the hormone-treated tissues with different induction levels. There were almost no significant differences between the SA, JA, and JA/ET reporter activities in leaf and cotyledon, while root tips in the three reporters showed relatively lower signal intensities (Figure 15a-c), reflecting the possibility of using the COLORFUL-sensors to map the tissue-specific hormone signal distribution.

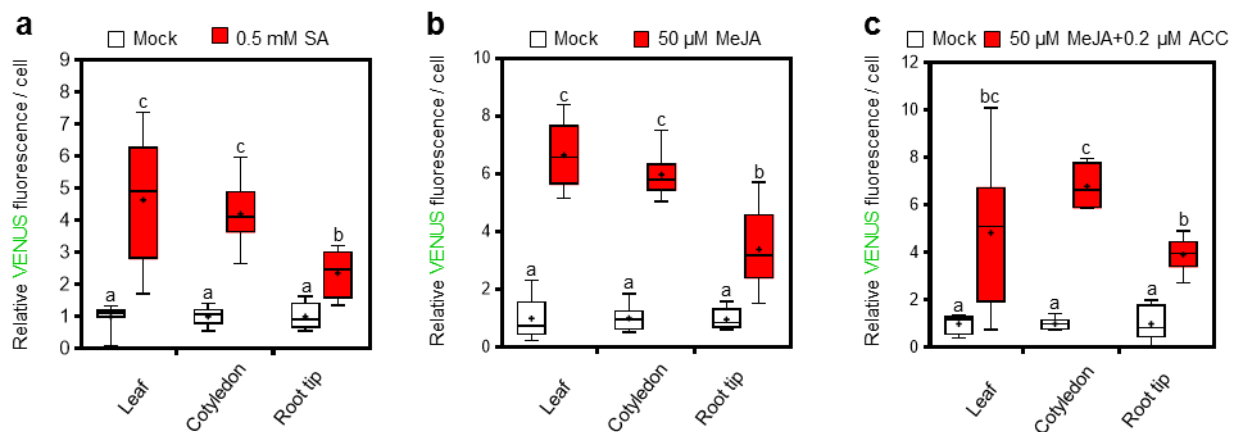


Figure 15: COLORFUL-SA, -JA, -JA/ET allow the spatial mapping of SA, JA and JA/ET signaling in different Arabidopsis organs. (a-c) Reporter activities in the epidermal pavement cells in leaves, cotyledons and root caps of 12-day-old transgenic lines COLORFUL-SA #1 (a), COLORFUL-JA #1 (b), and COLORFUL-JA/ET #1 (c), after treatment with 0.5 mM SA, 50 μ M MeJA and 50 μ M MeJA + 0.2 μ M ACC

3. RESULTS

ACC (red), respectively, for 24 hours in comparison to mocks (white). The experiments were repeated once showing consistent results. Box plots show first quartile (lower line); median (centre line); mean (+); third quartile (upper line); whiskers extend 1.5 times the interquartile range, and outliers are depicted as dots, $n = 7-10$ samples. Data are relative to the mock of the wildtype. Different letters indicate the significant differences between groups (One-way ANOVA followed by Tukey's multiple comparison test, $p < 0.05$).

3.2. COLORFUL-reporters enable the investigation of different hormone signaling cascades crosstalk

Next, individual and combinations of ABA, SA, MeJA, and ACC treatments were used to investigate the suitability of all four reporter systems to address the *in planta* ABA-SA-JA-JA/ET crosstalk (Figure 16a-d), and to test the responsiveness of COLORFUL-reporters to other hormones to ensure the corresponding hormone specific activation of these reporter systems. In this regard, CLSM was performed using leaves of twelve-day-old Arabidopsis seedlings with and without hormone treatment for 24 h. Data analyses underpinned high ABA, SA, MeJA, and MeJA + ACC specific activation capacity for *PP2CA* (Figure 16a), *PR1* (Figure 16b), *VSP2* (Figure 16c), and *PDF1-2a* (Figure 16d), respectively. The results in these experiments highlighted a reciprocal antagonistic interaction between ABA-JA/ET (Figure 16a, d). Hence, MeJA and ACC synergistically antagonize the ABA reporter activity showing a ~ half fold decrease in the basal ABA signal intensity (Figure 16a) in comparison to mock. Additionally, the JA/ET reporter exhibited a significantly reduced reporter signal upon ABA treatment (Figure 16d). Furthermore, SA and ABA combinations affected neither ABA nor SA reporter activities in COLORFUL-ABA and COLORFUL-SA, respectively (Figure 16a-b). Additionally, these data highlight the antagonistic effects of ACC on *VSP2* promoter activity (Figure 16c).

3. RESULTS

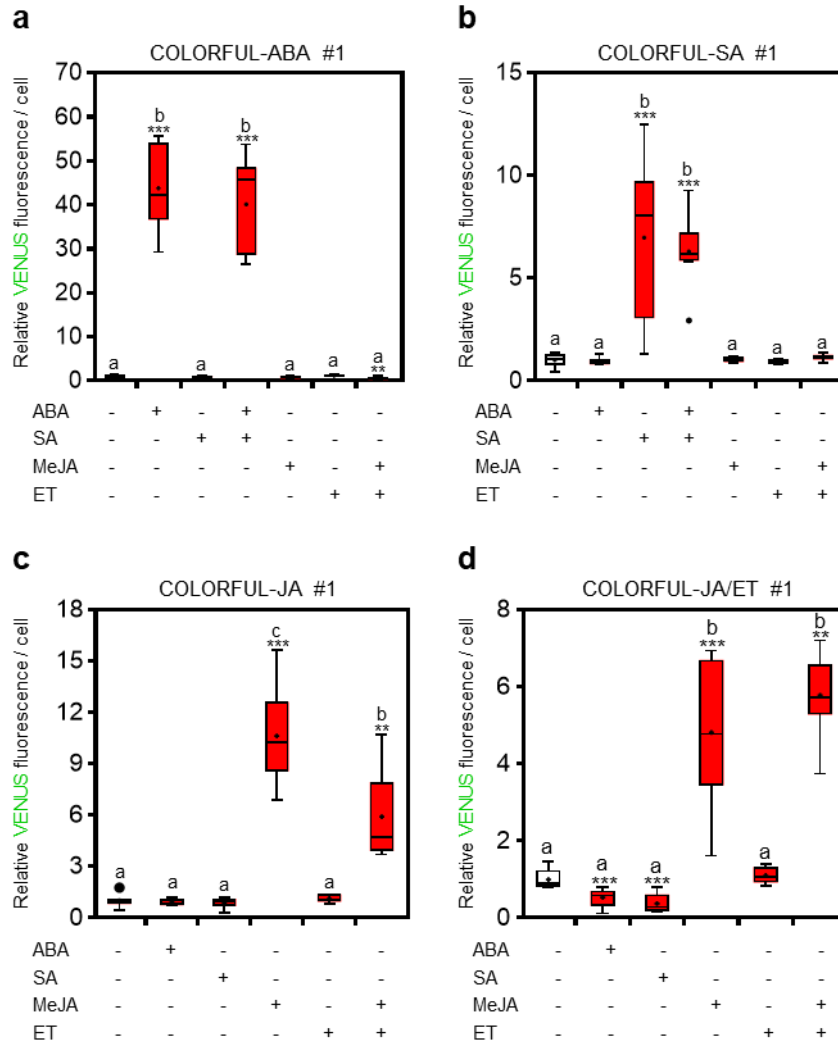


Figure 16: COLORFUL-reporters exhibit ABA-SA-JA-JA/ET crosstalk. (a-d) reporter activities of COLORFUL-ABA (a), -SA (b), -JA (c) and -JA/ET (d) in the leaf pavement cells of 12-day-old seedlings after exogenous application of 50 μ M ABA, 0.5 mM SA, 50 μ M MeJA, 2.0 μ M ACC individual or combined solutions for 24 h relative to the mock treatments. The experiments were repeated once, showing similar responses. Box plots show first quartile (lower line); median (centre line); mean (+); third quartile (upper line); whiskers extend 1.5 times the interquartile range, and outliers are shown as dots, $n = 6-10$ leaves. Data are normalized to the untreated corresponding mock. Different letters indicate significant differences between groups (Two-way ANOVA followed by Tukey's multiple comparison test, $p < 0.05$). Asterisks indicate statistical differences between signal intensities in hormone-treated and mock (* $p < 0.05$, ** $p < 0.01$, *** $p < 0.001$, Student's t-test).

3.3. The virulent and the avirulent isolates of the oomycete *H. arabidopsidis* exhibit distinct invasion dynamics

Pathogens transiently interact with plants at the original site of invasion in a cell to cell interaction, a spore of the invader attacks a single or few cell(s) of the host. Both have the ability to send and receive signals, which is an essential criterion for their survival. Understanding the spatio-temporal changes in phytohormone signaling at a single cell level directly after pathogen attack, during compatible and incompatible interactions, could provide novel insights into the immune responses positively or negatively mediated by plant hormones. Two different isolates of the downy mildew oomycete *H. arabidopsidis*, Noco2, and Emwa1 were utilized in the current study to achieve this objective.

Spores of both Noco2 and Emwa1 fall over the surface of Arabidopsis (Col-0) leaf or stem, then germinate, invaginate between two epidermal cells, and establish haustoria in epidermal and mesophyll cells (Coates & Beynon 2010). Notably, the constitutively expressed PM marker *CaMV35S-GFP-LTI6b* turned out to be ideally suited to monitor individual plant-microbe interaction sites, penetration of outer periclinal epidermal cell walls, intercellular growth into anticlinal epidermal cell walls, and invasive establishment of haustoria in epidermal (Figure 17a; Supplementary video 1) and mesophyll cells (Figure 17b; Supplementary video 2). Quantitative data analysis reported distinct isolate-specific infection kinetics and invasion success. The avirulent Emwa1 exhibited higher penetration rate in comparison to Noco2 at 1 and 2 dpi (Figure 17c), while higher frequencies of haustoriated epidermal, and mesophyll cells were reported with Noco2 at 1 dpi, and, even more pronounced, at 2 dpi (Figure 17d-e).

Immune responses are activated against both pathogens, which could be suppressed by Noco2 but not Emwa1. During both interactions, the first layer of the plant immune system, PTI is activated (Fabro et al. 2011). In the compatible interaction, effector-mediated suppression of PTI allows further proliferation, colonization of the entire leaf, and completion of the pathogen life cycle (Caillaud et al. 2013; Deb et al. 2018). Whereas, in incompatible interactions with avirulent *H. arabidopsidis* isolates, recognition of effectors secreted by Emwa1 activates a second defense mode, ETI,

3. RESULTS

which is typically associated with HR-like cell death and restriction of pathogen growth to the initially invaded plant cells (Van der Biezen et al. 2002; Wang et al. 2011). Thus, at 3 dpi, RPP4-triggered HR-like cell death responses—indicated by loss of PM and nuclear reference marker fluorescence—characterized individual sites of interaction between Emwa1 and Col-0 epidermis and mesophyll cells (Figure 17f, upper panel; Supplementary video 3). To identify dead cells, the application of the hypertonic solution NaCl (1.0 M) over the investigated leaf was performed to induce plasmolysis. Intact plant cells at that position were shrunken (yellow and blue lines), whereas the dead cells do not change in size (red dashed line) in the epidermis and mesophyll cell layers (Figure 17f, lower panel). As expected, in Noco2 compatible interactions, the presence of haustorial complexes correlated with cell integrity reflected by unaltered PM and nuclear reference marker fluorescence (Figure 17g, upper panel; Supplementary video 4). Treatment with 1.0 M NaCl caused the shrinking of all cells at the same position, underpinning the membrane integrity of Noco2 invaded cell (Figure 17g, lower panel).

3. RESULTS

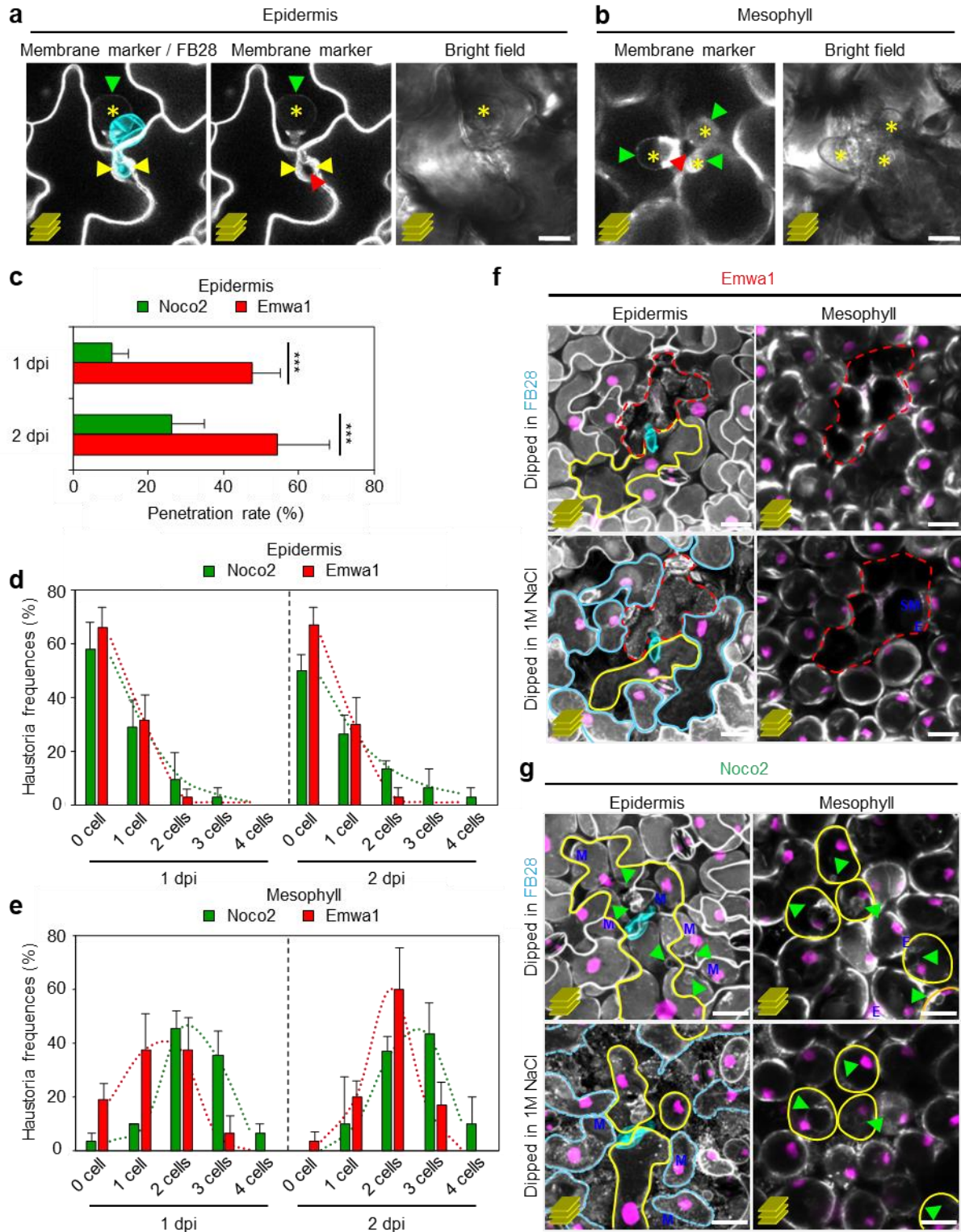


Figure 17: Noco2 and Emwa1 isolates of *H. arabidopsidis* exhibit distinct invasion dynamics on *Arabidopsis Col-0* leaves. (a,b) Maximum projections of CLSM z-stack images showing PM marker (gray; a, left and middle panels; b, left panel) in a leaf of a 3-week-old transgenic *Arabidopsis* COLORFUL-SA line #1 at 1 dpi with Emwa1 spore (cyan overlay; a, left) and after staining with Fluorescent Brightener 28 (FB28). The PM marker allows visualization of penetration between outer

3. RESULTS

periclinal epidermal cell walls (yellow arrowhead) by Emwa1, intercellular growth into anticlinal cell walls (red arrowheads; a, middle; b, left), and extrahaustorial membrane (green arrowheads), and haustoria formation (asterisks) in pavement cells (a), and palisade mesophyll cells (b). Bright-field images (right) show single plane sections. Scale bar: 10 μ m. (c) Noco2 and Emwa1 penetration rates in leaves of 3-week-old COLORFUL lines. Penetration was determined as growth into anticlinal cell walls between epidermal cells (red arrowhead; a) at 1- and 2-days post inoculation (dpi). Asterisks indicate statistical differences between penetration rates of Noco2 and Emwa1 (* $p < 0.05$, ** $p < 0.01$, *** $p < 0.001$, Student's t-test). (d,e) Frequencies of haustoria formation (%) by Noco2 and Emwa1 determined as the formation of extrahaustorial membrane (green arrowheads; a,b) in epidermal (d) and mesophyll cells (e) at 1 and 2 dpi. Measurements were obtained from three independent experiments, each containing 10 biological replicates. Data represent means \pm s.e.m. (f-g) Maximum projection of CLSM z-stack images showing overlays of reference (magenta) and PM (gray) markers in leaves of 3-week-old Arabidopsis COLORFUL-SA line #1 at 3 dpi after staining Emwa1 (f) and Noco2 (g) with FB28. (f) Emwa1 induced cell death (discontinuous lines) associated with the disappearance of PM and reference fluorescence in the epidermal (upper left panel) and in the mesophyll (upper right panel) cell layers. Dipping the same leaf in 1.0 M NaCl exhibited a shrinking only in the intact cells invaded (yellow lines) and adjacent cells (blue lines) in the epidermal cell layer (lower left panel), while the dead cells (dashed red lines) showed no change in the cell size in the epidermal (lower left panel) and mesophyll (lower right panel) cell layers. (g) Noco2 proliferation indicated by haustoria formation (green arrowheads) was extended in the epidermis (upper left panel) and mesophyll (upper right panel) beyond the initial site of invasion. Noco2 biotrophy was detected via the intact membranes and the nuclear marker at the site of invasion after dipping the same leaf in 1.0 M NaCl which showed shrinking of the membrane of the invaded cells (yellow lines) and adjacent cells (blue lines) in the epidermis (lower left panel) and in the mesophyll cell layer (lower right panel). Blue E, M, and SM indicate reference signals originating from epidermal, palisade mesophyll, and spongy mesophyll cells, respectively. Scale bar: 25 μ m.

3.4. Arabidopsis-*H. arabidopsidis* interaction sites show spatio-temporally distinct ABA, SA, JA, and JA/ET signaling outputs

The COLORFUL reporter lines were used for comparative analyses of spatiotemporal hormone homeostasis during compatible and incompatible interactions of Arabidopsis with Noco2 and Emwa1, respectively. To do a systematic COLORFUL reporter line analyses using microscopic fields of view containing a single oomycete-plant interaction site, the hormone responses associated with these sites were dissected on a cellular resolution in epidermis and mesophyll cells depending on the presence of and distance to oomycete infection structures. Thus, epidermal and mesophyll cells were categorized into “invaded” (orange), immediately “adjacent” (yellow) and “distant” domains (white) (Figure 18a-b), and conducted quantitative ABA, SA, JA, and JA/ET reporter analyses at 1 and 2 dpi with both *H. arabidopsidis* isolates.

3. RESULTS

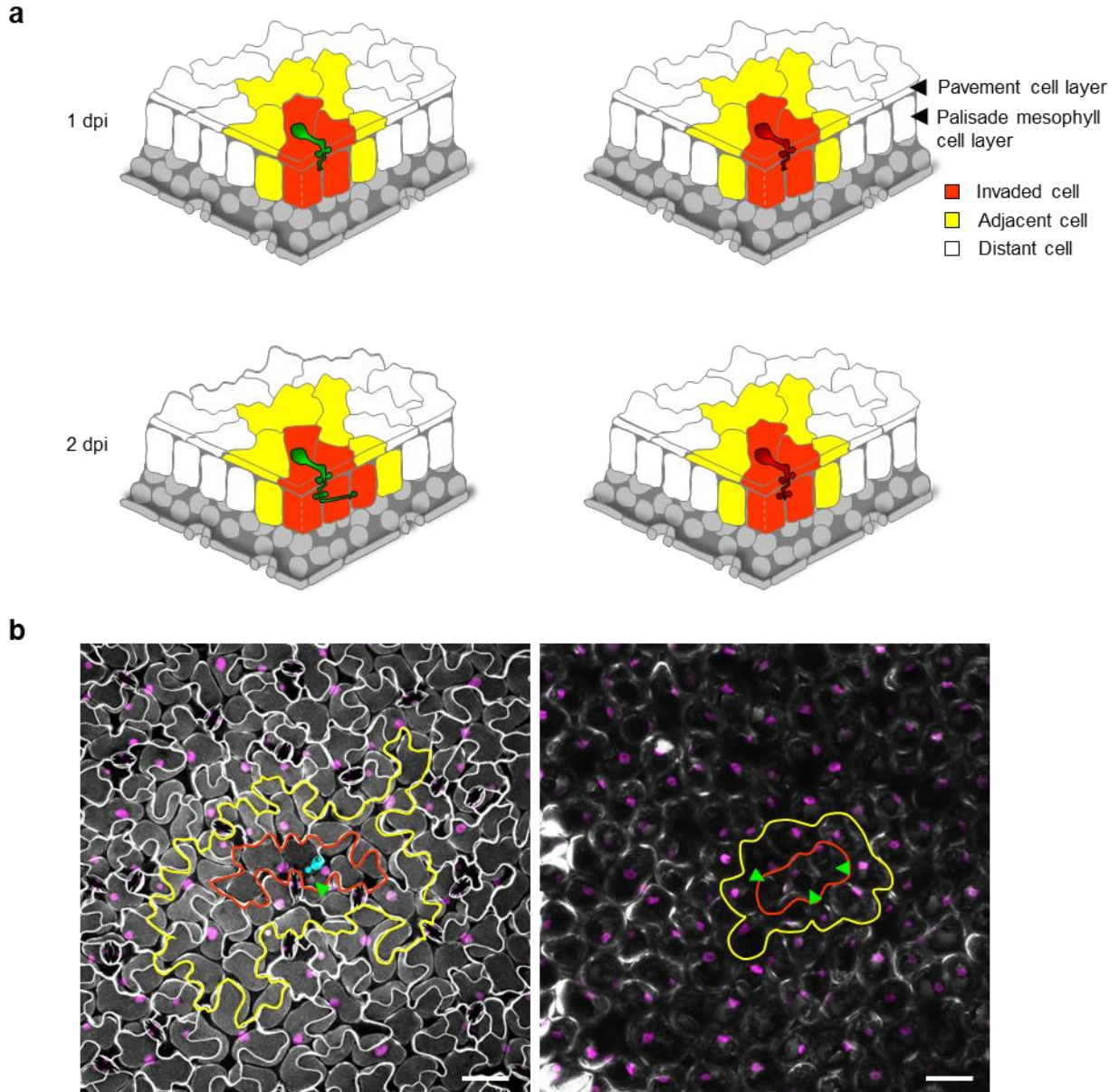


Figure 18: Dissection of cells associated with *H. arabidopsidis* invasion site. (a) Schematic representations depict the invasion dynamics of virulent (Noco2) and avirulent (Emwa1) isolates of *H. arabidopsidis* at 1 and 2 dpi, and the dissected cell zones at sites of invasion. (b) Representative Maximum projections of CLSM z-stack images used for quantification of SA responses at the site of Noco2 invasion. The Images show overlays of SA reporter (green), reference (magenta), and plasma membrane (gray) markers in leaf epidermis (left) and palisade mesophyll (right) of 3-week-old Arabidopsis line COLORFUL-SA#1 at 1 dpi after staining Noco2 spore with FB28 (cyan). Arrowheads indicate Noco2 invading structures. Invaded cells (orange continuous lines), adjacent cells (yellow continuous lines), and distant cells (not highlighted). Scale bar: 50 μm .

3.4.1. Both virulent and avirulent oomycete isolates trigger local ABA responses in the haustoriated cells

Notably, during CLSM an activated ABA signaling response was reported at the *Arabidopsis*-*H. arabidopsidis* compatible and incompatible interaction sites with the virulent isolate Noco2 (Figure 19a, middle panel), and avirulent isolate Emwa1 (Figure 19a, right panel) in comparison to the wildtype (Figure 19a, left panel). These triggered responses were confined to the haustoriated epidermal (Figure 19a, upper panel) and mesophyll cells (Figure 19a, lower panel). Parallel COLORFUL-ABA reporter analyses showed that Emwa1 significantly enhanced ABA activities in invaded pavement and mesophyll cells (4.35-fold and 13.7-fold, respectively) and in the immediately adjacent pavement and mesophyll cells (2.14-fold and 3.42-fold, respectively) at 1 dpi. In contrast, Noco2 displayed slight but significant activation of ABA signaling in invaded mesophyll cells (3.21-fold) (Figure 19b; Figure 23a-b). At 2 dpi, both *H. arabidopsidis* isolates significantly triggered ABA signaling only in the invaded pavement and mesophyll cells (Figure 19c; Figure 23a-b). These analyses provide a spatially confined cell type-specific pattern of pathogen-activated ABA signaling and suggest a potential role for ABA in modulating the basal defense responses during both compatible and incompatible *H. arabidopsidis* interactions.

3. RESULTS

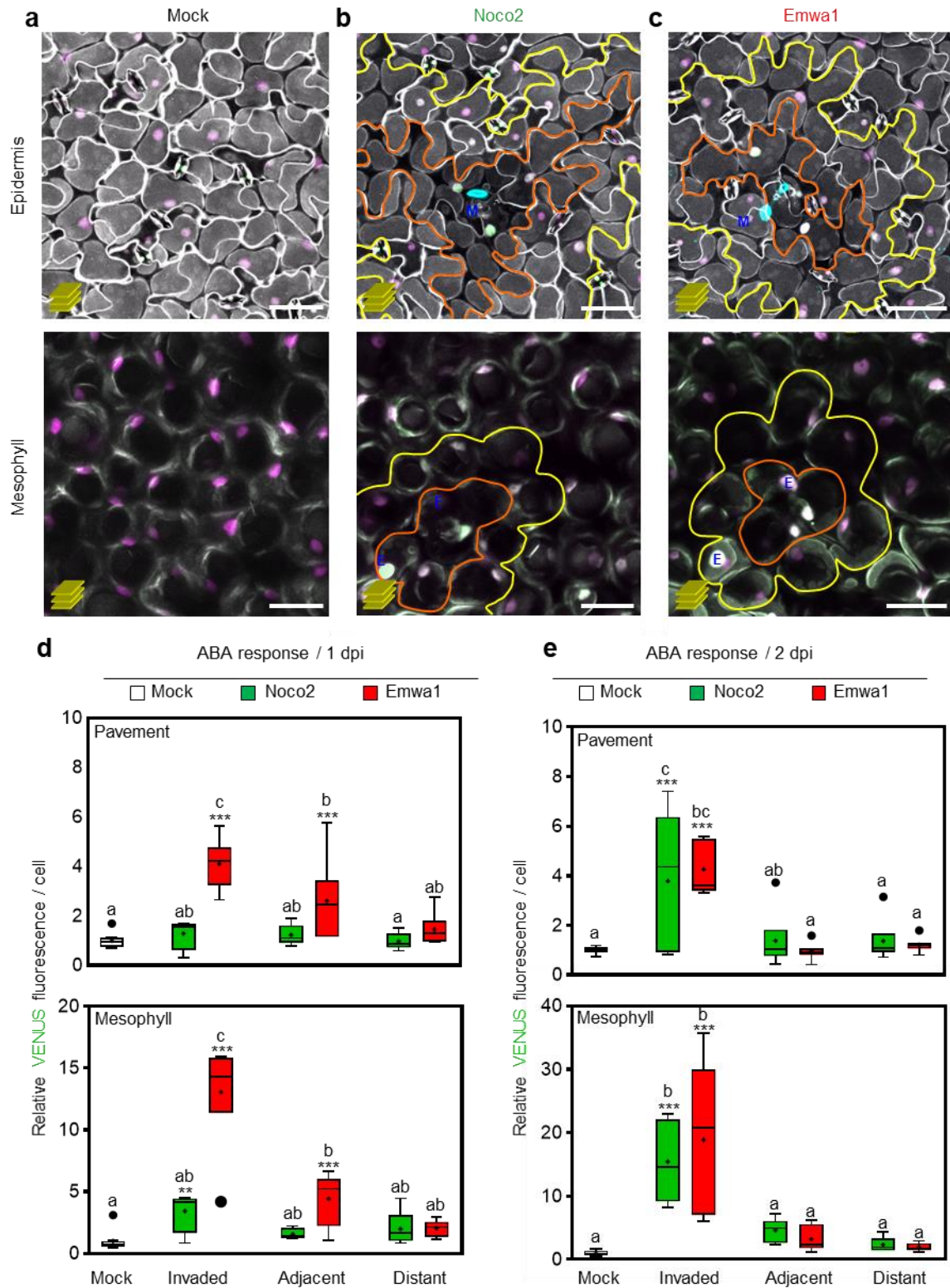


Figure 19: Arabidopsis COLORFUL-ABA reporter lines enable qualitative and quantitative monitoring for ABA signaling at *Arabidopsis-H. arabisididis* interaction sites. (a) Maximum projections of CLSM z-stack images showing the overlay of the three COLORFUL-ABA modules expression in leaves of 3-week-old transgenic Arabidopsis COLORFUL-ABA line #1 at 2 dpi with water

3. RESULTS

as a mock (left panel: top; Epidermis and bottom; Mesophyll), virulent isolate of Noco2 (middle panel: top; Epidermis and bottom; Mesophyll) and Emwa1 (right panel: top; Epidermis and bottom; Mesophyll). Scale bar: 50 μ m. Borders for invaded cells (orange lines), borders for the adjacent cells (yellow lines). Blue E and M letters indicate reference signals originating from epidermal and palisade mesophyll cells, respectively. (b, c) ABA reporter activities in pavement cells (top) and palisade mesophyll cells (bottom) at the sites of invasion by virulent (Noco2) and avirulent (Emwa1) isolates of *H. arabidopsidis* at 1 (b) and 2 (c) dpi. Box plots show first quartile (lower line); median (centre line); mean (+); third quartile (upper line); whiskers extend 1.5 times the interquartile range, and outliers are designated as dots, n = 6-9 infection sites from independent plants. Data are relative to the uninfected mock. Asterisks indicate statistical differences between spatial domains (invaded, adjacent and distant) and uninfected mock (*p < 0.05, **p < 0.01, ***p < 0.001, Student's t-test) and different letters (Two-way ANOVA followed by Tukey's multiple comparison test, p-adjusted < 0.05) indicate significant differences between groups. The experiment was repeated once using the same Arabidopsis transgenic COLORFUL-ABA line #1 and twice using independent transgenic Arabidopsis COLORFUL-ABA line #2. The quantitative analyses exhibited the same pattern of ABA response, indicating a high reproducibility within the two lines.

3.4.2. Emwa1 and Noco2 differentially regulate SA signaling in two distinct domains

In contrast to haustoriated mesophyll cells, in which both *H. arabidopsidis* isolates induced high levels of SA reporter fluorescence at 1 dpi, the invaded pavement cells did not show altered SA reporter activity in response to invasion by either the virulent isolate Noco2 or the avirulent isolate Emwa1 (Figure 20b-c; Figure 23c-d). Interestingly, with Emwa1, the highest SA reporter induction was observed in the immediately adjacent mesophyll cells at 1 dpi (13.0-fold), and at 2 dpi (13.8-fold). A similar activation signature was detectable in pavement cells adjacent to Emwa1-invaded epidermal cells at 1 and 2 dpi, but with lower magnitude (4.7-fold and 7.0-fold, respectively). Together, these data suggest a major role of mesophyll and pavement cells immediately adjacent to sites of direct plant-microbe interaction in SA-dependent defense during the incompatible interactions with Emwa1 as compared to mock signals (Figure 20a). Comparatively subtle induction of the SA reporter was also detectable in pavement and mesophyll cells neighboring Noco2-invaded cells at 2 dpi (3.5-fold and 3.1-fold, respectively), indicative of a conserved and potentially suppressed SA-controlled basal defense signature, which is observed in RPP4-dependent immunity triggered by Emwa1.

3. RESULTS

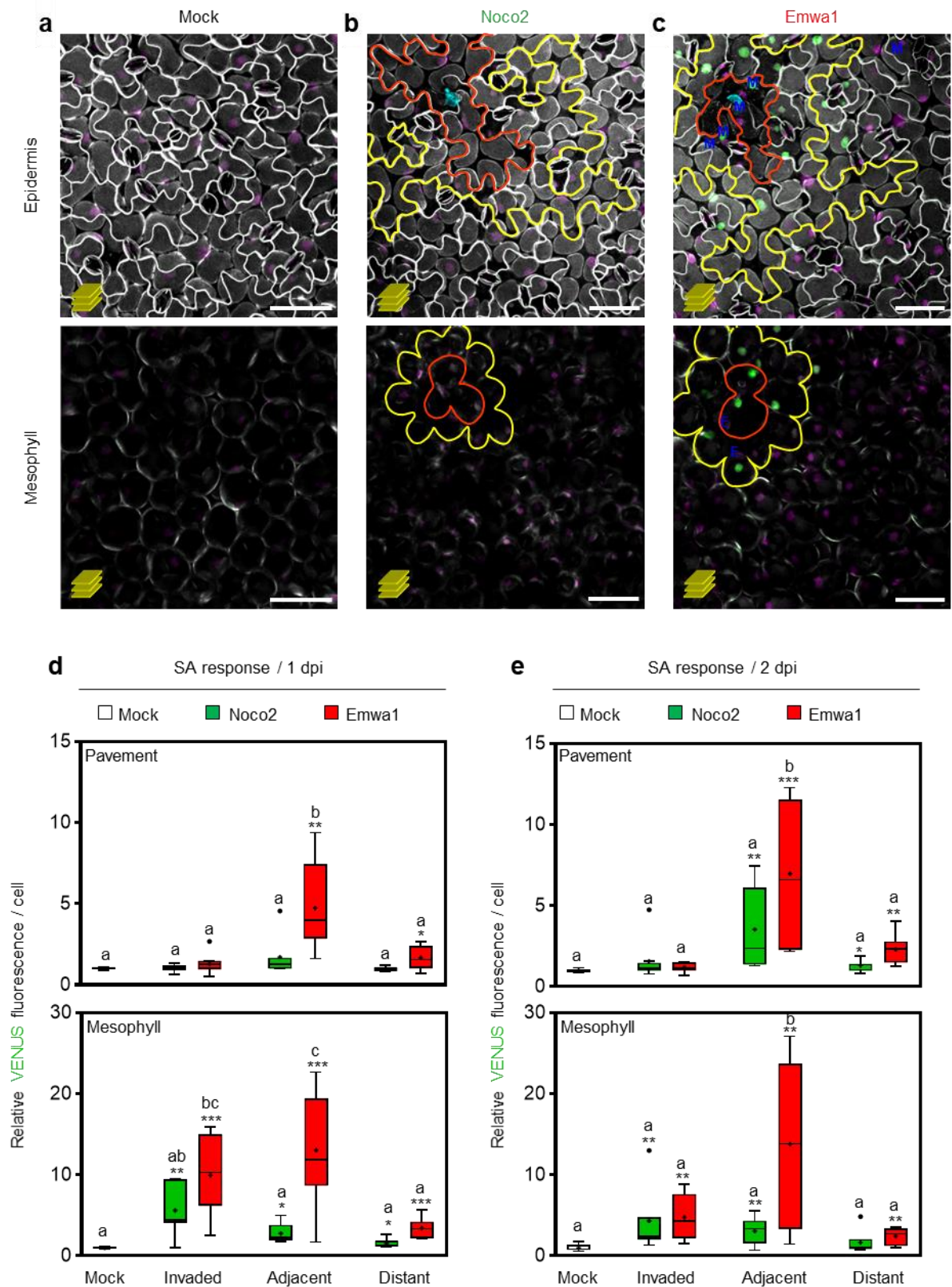


Figure 20: Arabidopsis COLORFUL-SA reporter lines enable qualitative and quantitative monitoring for SA signaling at *Arabidopsis-H. arabidopsidis* interaction sites. (a) Maximum

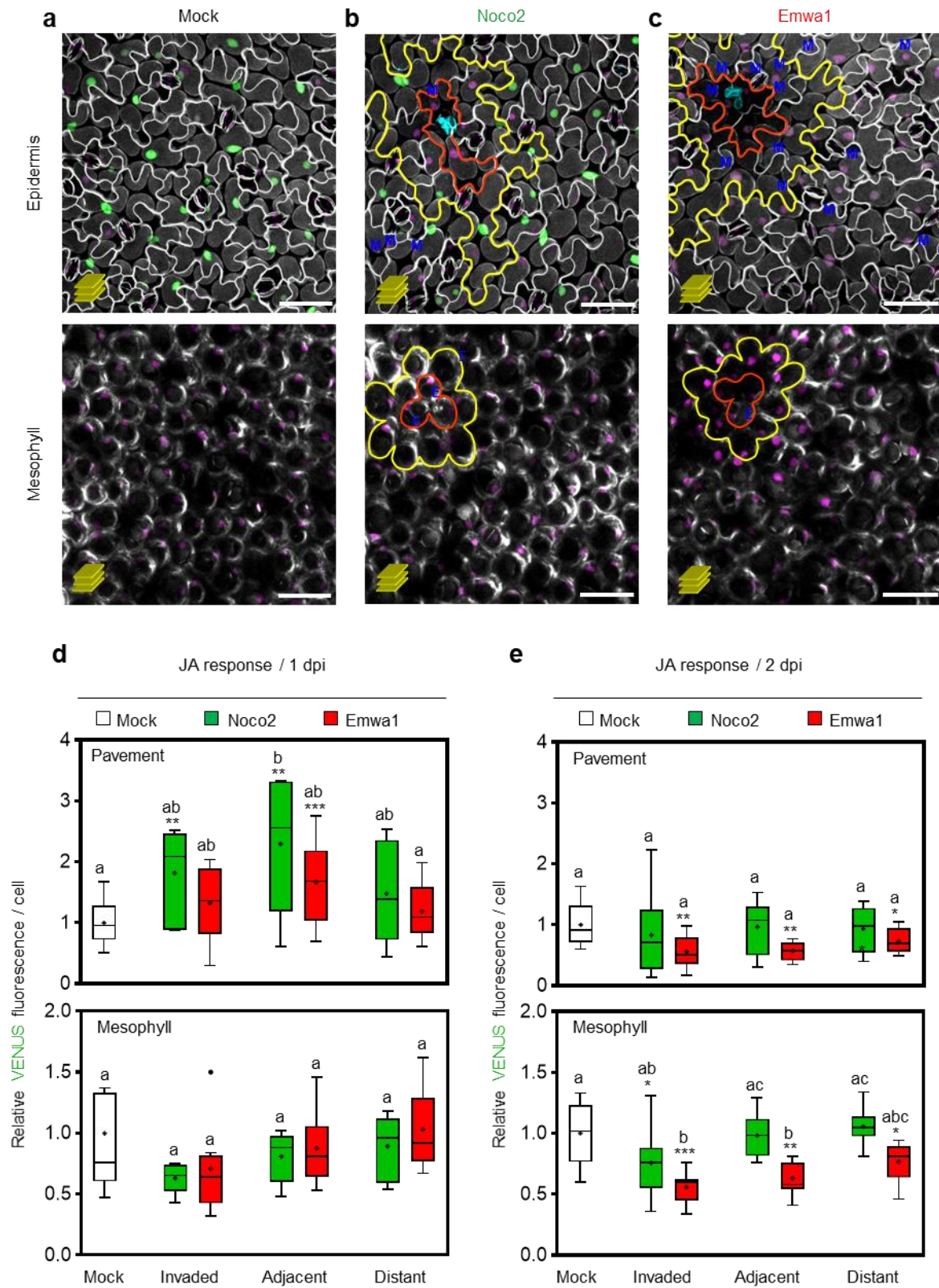
3. RESULTS

projections of CLSM z-stack images showing the overlay of the three COLORFUL-SA modules expression in leaves of 3-week-old transgenic Arabidopsis COLORFUL-SA line #1 at 2 dpi with water as a mock (left panel: top; Epidermis and bottom; Mesophyll), virulent isolate of Noco2 (middle panel: top; Epidermis and bottom; Mesophyll) and Emwa1 (right panel: top; Epidermis and bottom; Mesophyll). Scale bar: 50 μ m. Borders for invaded cells (orange lines), borders for the adjacent cells (yellow lines). Blue E and M letters indicate reference signals originating from epidermal and palisade mesophyll cells, respectively. (b, c) SA reporter activities in pavement cells (top) and palisade mesophyll cells (bottom) at the sites of invasion by virulent (Noco2) and avirulent (Emwa1) isolates of *H. arabidopsidis* at 1 (b) and 2 (c) dpi. Box plots show first quartile (lower line); median (centre line); mean (+); third quartile (upper line); whiskers extend 1.5 times the interquartile range, and outliers are designated as dots, n = 6-9 infection sites from independent plants. Data are relative to the uninfected mock. Asterisks indicate statistical differences between spatial domains (invaded, adjacent and distant) and uninfected mock (*p < 0.05, **p < 0.01, ***p < 0.001, Student's t-test) and different letters (Two-way ANOVA followed by Tukey's multiple comparison test, p-adjusted < 0.05) indicate significant differences between groups. The experiment was repeated once using the same Arabidopsis transgenic COLORFUL-SA line #1 and once using independent transgenic Arabidopsis COLORFUL-SA line #2. The quantitative analyses exhibited the same pattern of SA response, indicating a high reproducibility of the SA-reporter system.

3.4.3. Compatible and incompatible *H. arabidopsidis* interactions with Col-0 exhibit distinct cell type-specific JA responses

COLORFUL-JA reporter analyses showed temporary and slightly enhanced activities in invaded and adjacent pavement cells at 1 dpi with Noco2 (1.8-fold and 2.2-fold, respectively), whereas Emwa1 triggered a subtle response only in adjacent pavement cells (1.6-fold) (Figure 21b-c; Figure 23e-f). Later, at 2 dpi, Emwa1 interaction sites were characterized by suppressed overall JA signaling activity in pavement and mesophyll cells, which is particularly prominent in adjacent mesophyll cells (0.6-fold) (Figure 21a-c; Figure 23e-f). Together, these data provide distinct cell type-specific JA response signatures for compatible and incompatible *H. arabidopsidis* interactions.

3. RESULTS



3. RESULTS

Figure 21: Arabidopsis COLORFUL-JA reporter lines enable qualitative and quantitative monitoring for JA signaling at Arabidopsis-*H. arabidopsidis* interaction sites. (a) Maximum projections of CLSM z-stack images showing the overlay of the three COLORFUL-JA modules expression in leaves of 3-week-old transgenic Arabidopsis COLORFUL-JA line #1 at 2 dpi with water as a mock (left panel: top; Epidermis and bottom; Mesophyll), virulent isolate of Noco2 (middle panel: top; Epidermis and bottom; Mesophyll), and Emwa1 (right panel: top; Epidermis and bottom; Mesophyll). Scale bar: 50 μ m. Borders for invaded cells (orange lines), borders for the adjacent cells (yellow lines). Blue E and M letters indicate reference signals originating from epidermal and palisade mesophyll cells, respectively. (b, c) JA reporter activities in pavement cells (top) and palisade mesophyll cells (bottom) at the sites of invasion by virulent (Noco2) and avirulent (Emwa1) isolates of *H. arabidopsidis* at 1 (b) and 2 (c) dpi. Box plots show first quartile (lower line); median (centre line); mean (+); third quartile (upper line); whiskers extend 1.5 times the interquartile range, and outliers are designated as dots, n = 6-9 infection sites from independent plants. Data are relative to the uninfected mock. Asterisks indicate statistical differences between spatial domains (invaded, adjacent and distant) and uninfected mock (*p < 0.05, **p < 0.01, ***p < 0.001, Student's t-test) and different letters (Two-way ANOVA followed by Tukey's multiple comparison test, p-adjusted < 0.05) indicate significant differences between groups. The experiment was repeated once using the same Arabidopsis transgenic COLORFUL-JA line #1 and once using independent transgenic Arabidopsis COLORFUL-JA line #2. The quantitative analyses exhibited the same pattern of JA response, indicating a high reproducibility of the COLORFUL-JA reporter system.

3.4.4. In contrast to virulent isolate, Emwa1 does not trigger JA/ET signaling in the adjacent cell zone

COLORFUL-JA/ET reporter studies revealed 2.3-fold induced activities in Noco2-invaded pavement cells and remarkably high signals in immediately adjacent and distant epidermal pavement cells at 1 dpi (6.1-fold and 6.7-fold, respectively) (Figure 22b; Figure 23g-h), suggesting JA/ET-dependent rapid and gradual long-distance intercellular basal defense signaling in the epidermal tissue. At 2 dpi, Noco2-invaded pavement cells showed slight but not significantly repressed JA/ET reporter activity (0.7-fold), whilst adjacent and distant pavement cells still had elevated, but lower VENUS fluorescence than at 1 dpi (4.7-fold and 4.9-fold, respectively) (Figure 22c; Figure 23g-h). Similarly, long-distance signaling was also detectable in the mesophyll tissue (3.1-fold at 1 dpi and 2.7-fold at 2 dpi, respectively), whereas highest activities of the JA/ET reporter occurred in immediately adjacent cells (3.9-fold at 1 dpi and 3.3-fold at 2 dpi, respectively). Emwa1-inoculated plants showed similar responses in distant tissues. However, in contrast to Noco2, Emwa1 did not trigger JA/ET signaling in the adjacent cell zone (Figure 22a). At 2 dpi, Emwa1-invaded epidermal pavement and mesophyll cells, which are destined to undergo HR-like cell death within the next 24 hours (Figure 17f), displayed attenuated JA/ET reporter activity. Notably, immediately adjacent cells exhibited the highest relative fold changes observed for the SA reporter in this study, possibly representing a demarcation signature controlling initiation and local containment of the cell death response in ETI.

3. RESULTS

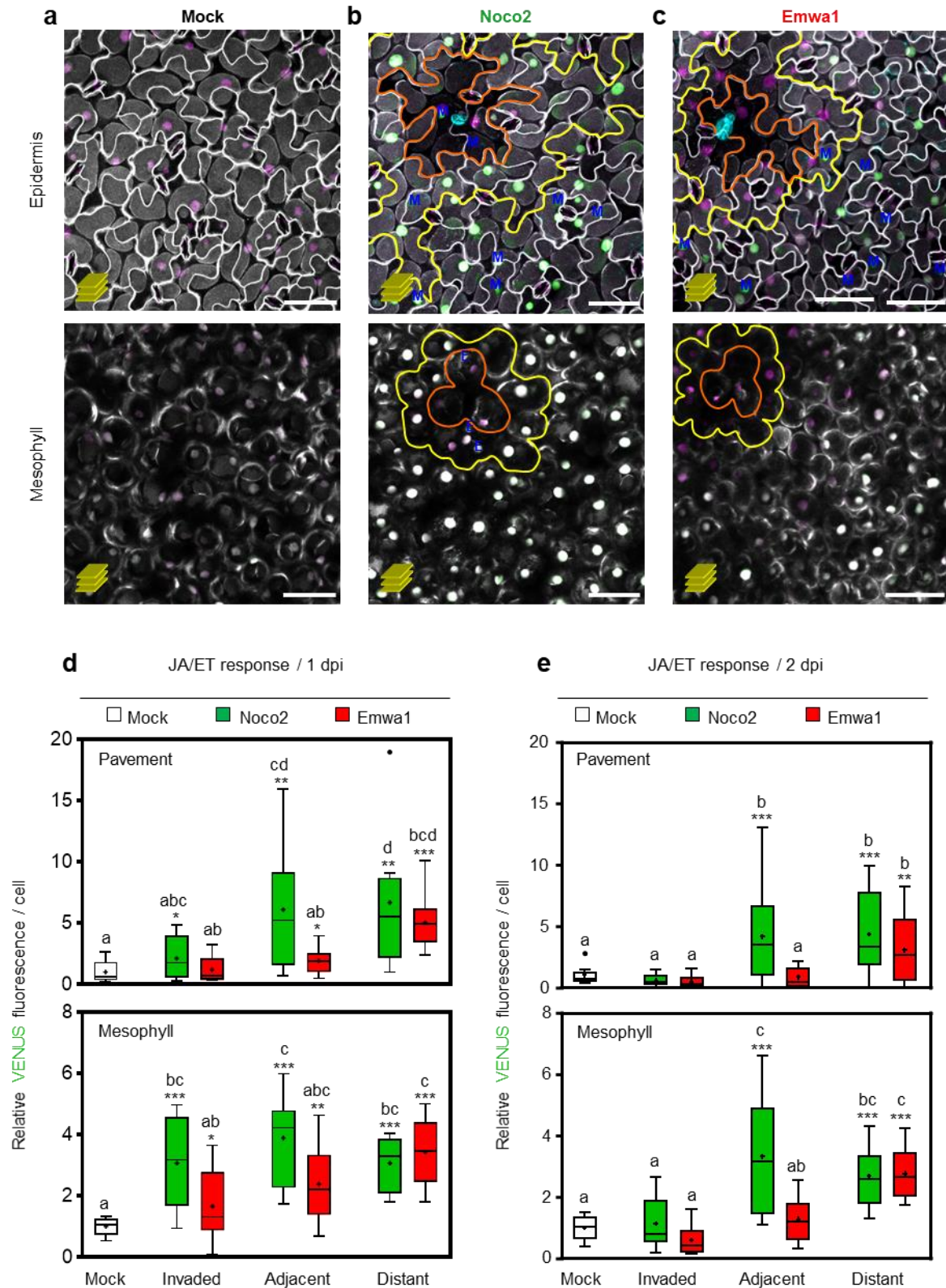


Figure 22: Arabidopsis COLORFUL-JA/ET reporter lines enable qualitative and quantitative monitoring for JA/ET signaling at Arabidopsis-*H. arabidopsidis* interaction sites. (a) Maximum projections of CLSM z-stack images showing the overlay of the three COLORFUL-JA/ET modules

3. RESULTS

expression in leaves of 3-week-old transgenic Arabidopsis COLORFUL-JA/ET line #1 at 2 dpi with water as a mock (left panel: top; Epidermis and bottom; Mesophyll), virulent isolate of Noco2 (middle panel: top; Epidermis and bottom; Mesophyll) and Emwa1 (right panel: top; Epidermis and bottom; Mesophyll). Scale bar: 50 μ m. Borders for invaded cells (orange lines), borders for the adjacent cells (yellow lines). Blue E and M letters indicate reference signals originating from epidermal and palisade mesophyll cells, respectively. (b, c) JA/ET reporter activities in pavement cells (top) and palisade mesophyll cells (bottom) at the sites of invasion by virulent (Noco2) and avirulent (Emwa1) isolates of *H. arabidopsidis* at 1 (b) and 2 (c) dpi. Box plots show first quartile (lower line); median (centre line); mean (+); third quartile (upper line); whiskers extend 1.5 times the interquartile range, and outliers are designated as dots, n = 6-9 infection sites from independent plants. Data are relative to the uninfected mock. Asterisks indicate statistical differences between spatial domains (invaded, adjacent and distant) and uninfected mock (*p < 0.05, **p < 0.01, ***p < 0.001, Student's t-test) and different letters (Two-way ANOVA followed by Tukey's multiple comparison test, p-adjusted < 0.05) indicate significant differences between groups. The experiment was repeated once using the same Arabidopsis transgenic COLORFUL-JA/ET line #1 and once using independent transgenic Arabidopsis COLORFUL-JA/ET line #2. The quantitative analyses exhibited the same pattern of JA/ET response, indicating a robust reproducible data of different COLORFUL-JA/ET reporter lines.

To show a summary of the quantitative measurements in the previous figures (19-22), quantitative heat map representations were designed for ABA (Figure 23a-b), SA (Figure 23c-d), JA (Figure 23e-f), and JA/ET (Figure 23g-h) signaling activities at sites of *A. thaliana* interactions with the virulent (Figure 23a,c,e,g) and the avirulent isolates (Figure 23b,d,f,h) of *H. arabidopsidis* at 1 (upper panels) and 2 dpi (lower panels).

3. RESULTS

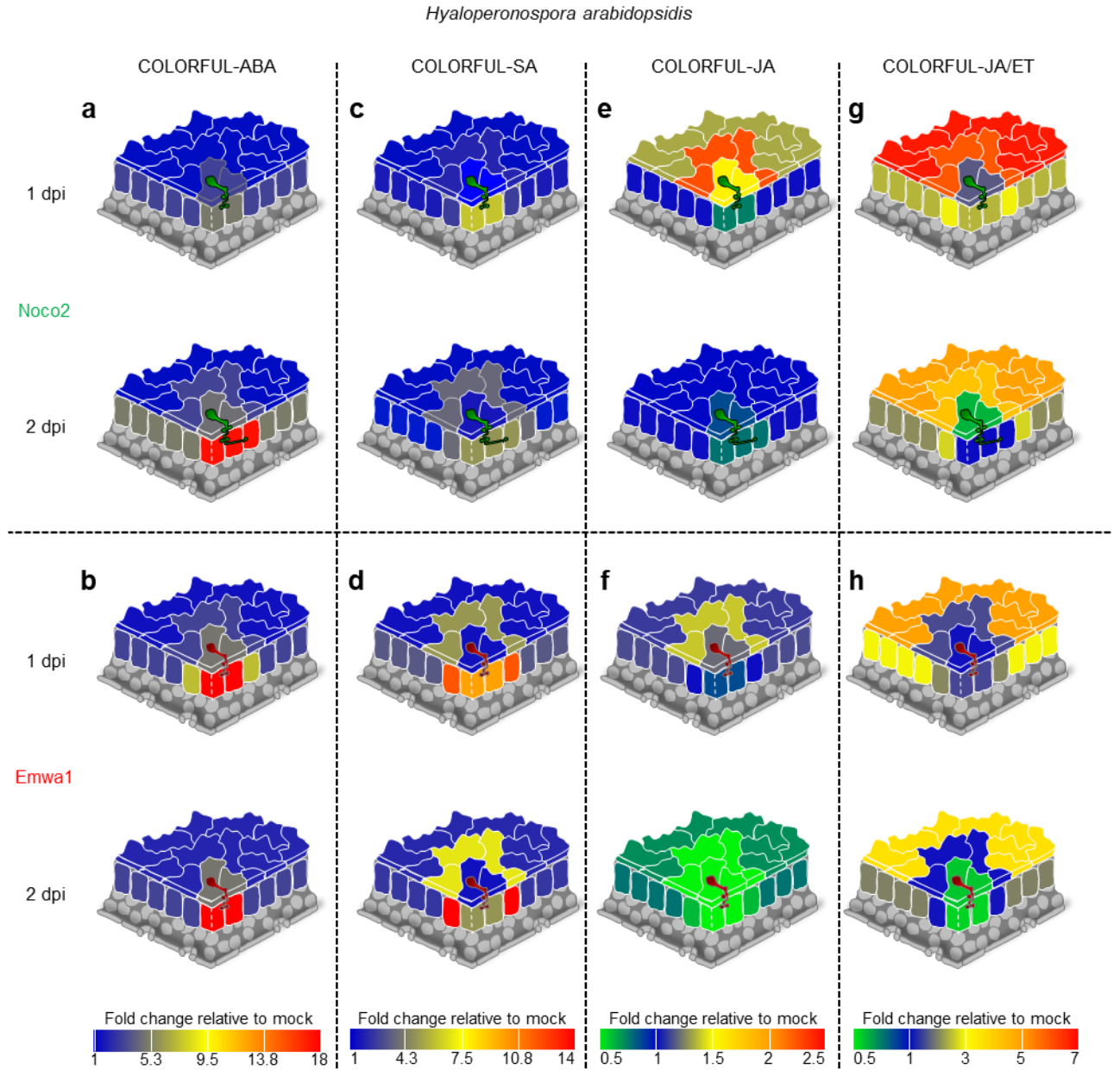


Figure 23: Spatio-temporal signatures of SA, JA, JA/ET and ABA signaling activities at sites of *Arabidopsis*-*H. arabidopsidis* interactions. (a-h) Quantitative heat map representations of ABA reporter activities at 1 (a) and 2 day(s) post inoculation (dpi) (b), SA reporter activities at 1 (c) and 2 dpi (d), JA reporter activities at 1 (e) and 2 dpi (f), and JA/ET reporter activities at 1 (g) and 2 dpi (h) in leaves of 3-week-old *Arabidopsis* lines COLORFUL-ABA#1, -SA #1, -JA #1, and -JA/ET #1) with virulent (Noco2; a,c,e,g) and avirulent (Emwa1; b,d,f,h) isolates of *H. arabidopsidis*. Data are relative to the uninfected mock.

3.5. *G. orontii* shows a conserved spatial pattern of pathogen-activated ABA but not SA signaling at their interaction sites with *A. thaliana*

In the previous analyses, local activation of ABA and SA signaling pathways were reported at Arabidopsis-*H. arabidopsidis* interaction sites, particularly in the invaded cells. In order to test for the conservation of the upregulated pattern of these two hormones during different biotrophic interactions, the fungal ascomycete pathogen *G. orontii* was employed in the current study. The powdery mildew *G. orontii* is quite distant from the oomycetes as it belongs to another kingdom and it has a different lifestyle in comparison to *H. arabidopsidis*. Hence the fungus grows epiphytically and colonizes only the epidermal cell layer. Once situated on a plant surface, the spore forms a germ tube and a primary appressorium at the tip of the germ tube to facilitate the cell wall penetration and haustoria formation without disrupting the host cell membrane at the primary penetration site. Next, secondary hyphae are formed and extend to penetrate nearby cells to form secondary invasion sites onwards until the formation of the conidiophores, which becomes macroscopically visible at 7-10 dpi (Kuhn et al. 2016).

For systematic COLORFUL reporter line analyses using microscopic fields of view containing a single *G. orontii*-Arabidopsis interaction site, the hormone responses at these sites were dissected on a cellular resolution in the epidermal cells depending on the presence of and distance to the invading spore. Epidermal cells at 1 dpi were categorized into “invaded” (orange), immediately “adjacent” (yellow), and “distant” cells (white) (Figure 24a). While at 2 dpi, cells were categorized into “1st invaded” (orange), “2nd invaded” (red), immediately “adjacent” (yellow), and “distant” cells (white) (Figure 24b), and quantitative ABA and SA reporter analyses at 1 and 2 dpi with *G. orontii* were conducted.

3. RESULTS

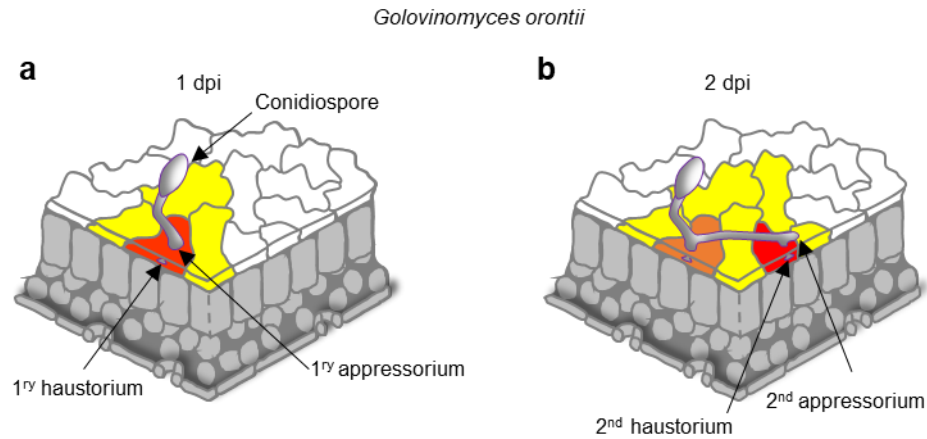


Figure 24: Dissection of cells associated with *G. orontii* invasion site. (a-b) Schematic representations depict the invasion dynamics of the epiphytically growing fungus *G. orontii* (a) at 1 dpi, epidermal cells were categorized into “invaded” (orange), immediately “adjacent” (yellow), and “distant” cells (white). (b) at 2 dpi, epidermal cells were categorized into “1st invaded” (orange), “2nd invaded” (red), immediately “adjacent” (yellow), and “distant” cells (white).

Intriguingly, the COLORFUL-ABA reporter quantifications displayed significantly enhanced ABA activities at 1 (Figure 25a-b) and 2 dpi (Figure 25c), which is mainly confined to the invaded cells. COLORFUL-SA reporter analyses, though, showed that *G. orontii* did not affect the SA signaling activities in different domains at 1 (Figure 25d) or 2 dpi (Figure 25e) in comparison to uninfected plants. These results demonstrated a conserved spatial pattern of pathogen-activated ABA but not SA signaling and suggested a potential role of ABA in modulating innate immunity.

3. RESULTS

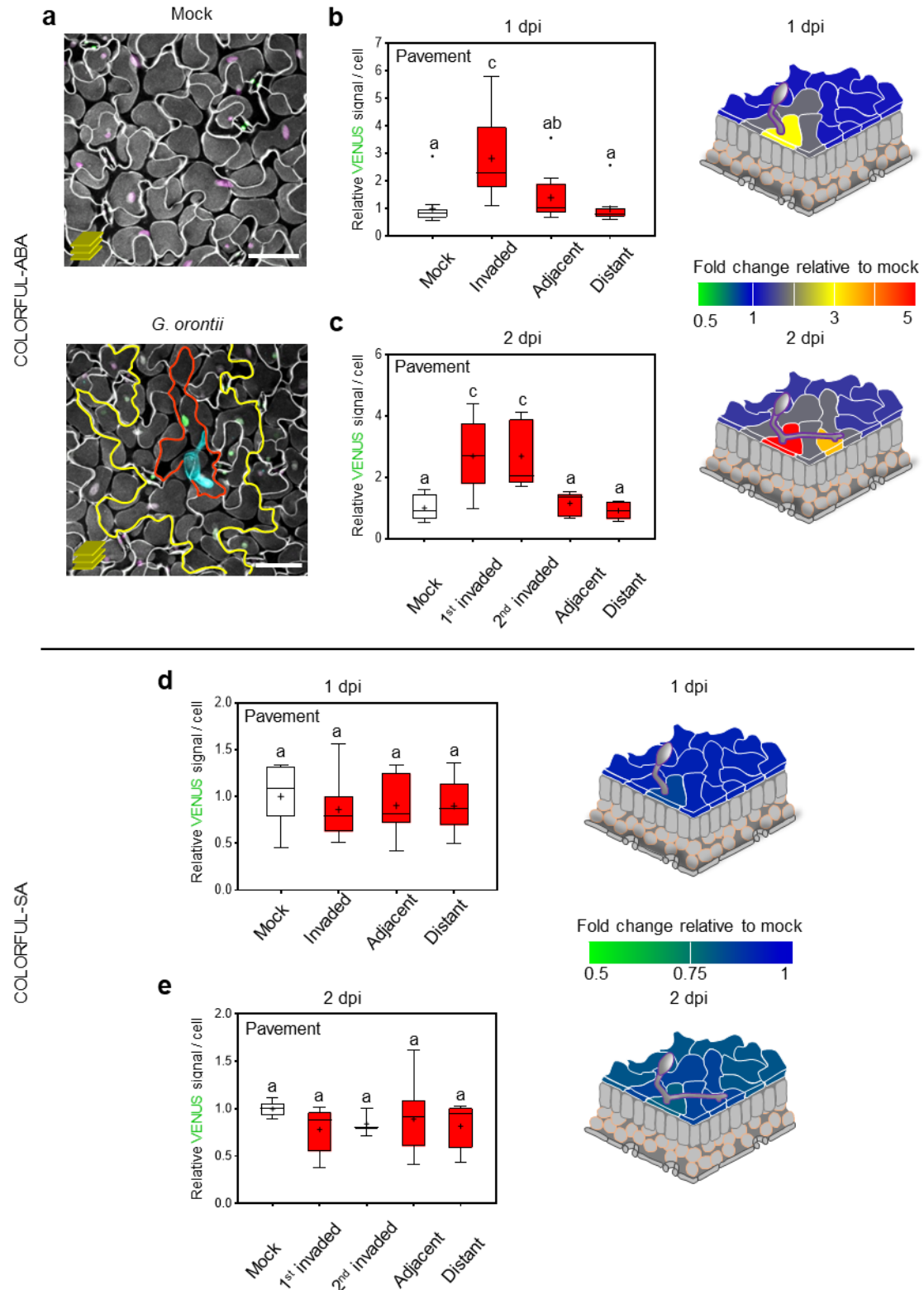


Figure 25: Cross kingdom-conserved induction of a cellularly confined ABA signaling signature at *Arabidopsis* biotrophic interaction sites. (a) Maximum projections of CLSM z-stack images showing the overlay of the expression of the three COLORFUL-ABA modules in leaves of 5-week-old

3. RESULTS

transgenic Arabidopsis COLORFUL-ABA line #1 at 1 dpi after brush-inoculation with the epiphytically growing *G. orontii* fungus (lower panel) in comparison to mock (upper panel). Scale bar: 50 μ m. Borders for the invaded cells are indicated as orange lines, borders for the adjacent cells are indicated as yellow lines. (b-c) VENUS fluorescence intensities in pavement cells at Arabidopsis-*G. orontii* interaction sites at 1 (b) and 2 dpi (c). (b-c, right panels) Quantitative heat map representations of ABA reporter activities at 1 (b, right panel) and 2 dpi (c, right panel) in leaves of 5-week-old transgenic Arabidopsis COLORFUL-ABA line #1. (d-e) COLORFUL-SA reporter activities in pavement cells at the sites of invasion by the *G. orontii* at 1 (d) and 2 dpi (e). (d-e, right panels) Quantitative heat map representations of SA reporter activities at 1 (d, right panel) and 2 dpi (e, right panel) in leaves of 5-week-old COLORFUL-SA line #1. Box plots show first quartile (lower line); median (centre line); mean (+); third quartile (upper line); whiskers extend 1.5 times the interquartile range, and outliers are shown as dots, n =6-10 infection sites from independent plants. Data are relative to the uninfected mock. Different letters indicate significant differences between groups (Two-way ANOVA followed by Tukey's multiple comparison test, $p < 0.05$). The experiments were repeated once using the same Arabidopsis transgenic COLORFUL-ABA #1 and COLORFUL-SA #1. The same pattern of ABA and SA response was observed.

3.6. ABA mediates susceptibility to Noco2 and *G. orontii*

In order to investigate the cross-kingdom role of the enhanced ABA signaling in modulating innate immunity during Arabidopsis interactions with the virulent isolate of *H. arabidopsidis*-Noco2 and the fungus *G. orontii*, the pathogen-associated disease phenotype was tested for the ABA biosynthetic mutants *aba1-101* and *aba2-1* in comparison to the wildtype. These mutant lines display stunted growth relative to the wildtype, but the normalization of spore counts to fresh weight allowed comparing sporulation on wildtype and mutant plants. Both mutants were challenged independently with Noco2 and *G. orontii*. Quantitative analyses of Noco2 sporulation at 6 dpi revealed significantly lower spore counts on *aba1-101* but not on *aba2-1* in comparison to the *A. thaliana* wildtype Col-0 (Figure 26a), which could be explained by the lower ABA content in the *aba1-101* than *aba2-1* (Rock & Zeevaart 1991; Barrero et al. 2005; Marin et al. 1996). Next, the constitutively expressed PM marker GFP-LTI6b was employed to measure the invasion dynamics of Noco2 on both Col-0 and *aba1-101* genotypes. Thus, the invasive establishment of haustoria was scored in epidermal and mesophyll cells at 1, 2, and 3 dpi. Notably, CLSM of the COLORFUL-ABA line #1 in *aba1-101* background in comparison to the wildtype revealed similar haustoria frequencies in both genotypes at 1 and 2 dpi. In contrast, at 3 dpi, a significantly higher haustoria formation was observed at individual Col-0-Noco2

3. RESULTS

interaction sites in comparison to *aba1-101* (Figure 26b). These findings strongly correlate with the aforementioned altered disease phenotype. Furthermore, both ABA biosynthetic mutants showed enhanced resistance to *G. orontii* (Figure 26c-d). The quantitative analyses of *G. orontii* infected plants at 10 dpi displayed significantly lower spore counts on both mutants in comparison to the wildtype (Figure 26c). These results indicate that ABA promotes virulence to different biotrophic pathogens.

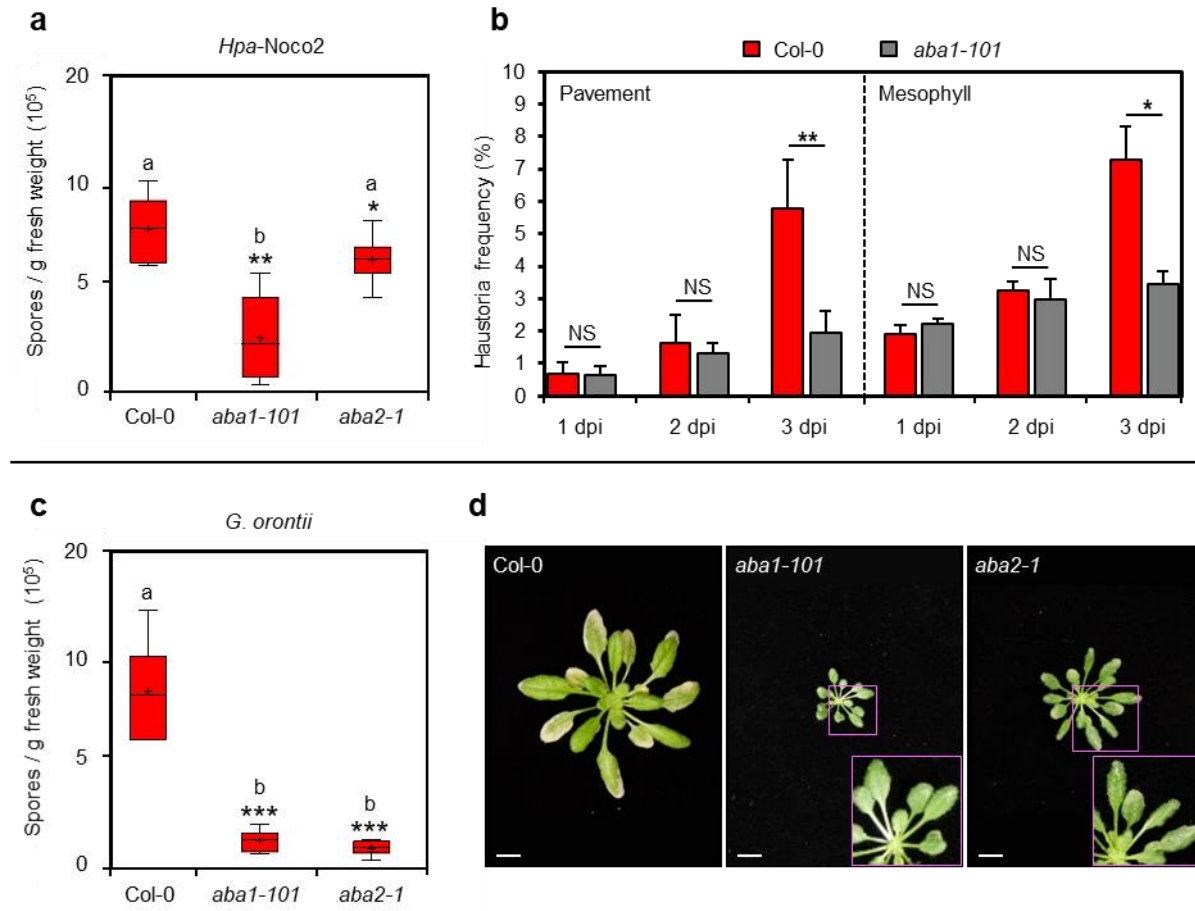


Figure 26: ABA promotes susceptibility to different biotrophic pathogens. (a) Sporulation of the spray-inoculated oomycete *H. arabidopsidis* virulent isolate-Noco2 on 2-week-old ABA deficient mutants (*aba1-101* and *aba2-1*) in comparison to the wildtype Col-0 at 6 dpi. Measurements were repeated twice, each containing five biological replicates, exhibiting the same disease phenotype. (b) Frequencies of haustoria formation by Noco2 determined as the formation of extrahaustorial membranes in pavement and palisade mesophyll cell layers. Measurements were obtained from three independent experiments, each containing ten biological replicates. Data represent means \pm s.e.m. (c) Sporulation of the fungus *G. orontii* on 2-week-old brush-inoculated *aba1-101*, *aba2-1* and Col-0. (d) Macroscopic *G. orontii* disease phenotypes at 10 dpi for Col-0, *aba1-101*, and *aba2-1*. Scale bar: 1 cm.

3. RESULTS

Measurements were obtained from three independent repeats, each containing seven biological replicates. Measurements were repeated twice, each containing seven biological replicates, showing the same disease phenotype. Box plots show first quartile (lower line); median (centre line); mean (+); third quartile (upper line); whiskers extend 1.5 times the interquartile range, and outliers are designated as dots, n: 5-7 biological replicates. Asterisks indicate significant differences to the wildtype (* $p < 0.05$, ** $p < 0.01$, *** $p < 0.001$, Student's t-test) and different letters (One-way ANOVA followed by Tukey's multiple comparison test, p -adjusted < 0.05) indicate significant differences between groups.

3.7. Pathogen-induced ABA signaling is dependent on ABA biosynthesis

To test the dependency of the locally-confined triggered ABA signaling after pathogen invasion at early time points, further quantitative analyses were performed after infection of the COLORFUL-ABA line #1 in *aba1-101* background and the wildtype Col-0 with the virulent biotrophic pathogens *Noco2* and *G. orontii* at 1 and 2 dpi. In the wildtype, the COLORFUL SPOTTER quantifications showed significant increase in the ABA signaling activity in invaded pavement and mesophyll cells with the endophytic oomycete *Noco2* as well as with the epiphytic fungus *G. orontii* (Figure 27a-d). At 1 dpi, *Noco2* induces ABA signaling activity with 3.47-fold and 5.23-fold of changes in the invaded pavement (Figure 27a, upper panel) and mesophyll cells (Figure 27a, lower panel) relative to the uninfected wildtype signaling activities, respectively. Furthermore, at 2 dpi, the magnitude changed to 4.21-fold and 13.78-fold in pavement (Figure 27b, upper panel) and mesophyll cells (Figure 27b, lower panel), respectively. Interestingly, VENUS signal intensities in *aba1-101* mutant were significantly reduced to 0.78-fold and 0.56-fold at 1 dpi and, 0.89-fold and 1.21-fold at 2 dpi in pavement (Figure 27a, upper panel) and mesophyll cells (Figure 27a, lower panel), respectively.

Similarly, *G. orontii* at 1 dpi induces 2.7-fold VENUS intensity increases in the invaded cells, which was lower in the *aba1-101* line relative to the mock of wildtype (by a factor of 0.59-fold) (Figure 27c). At 2 dpi, *G. orontii* triggered 3.1-fold and 2.9-fold increases in ABA reporter activities in the primary and the secondary invaded cells of the wildtype plants, respectively. A predominant drastic reduction was shown in different domains around the invasion sites in the ABA biosynthetic mutant, with a factor of 0.42-fold and 0.47-fold in the invaded cells relative to the wildtype (Figure 27d).

3. RESULTS

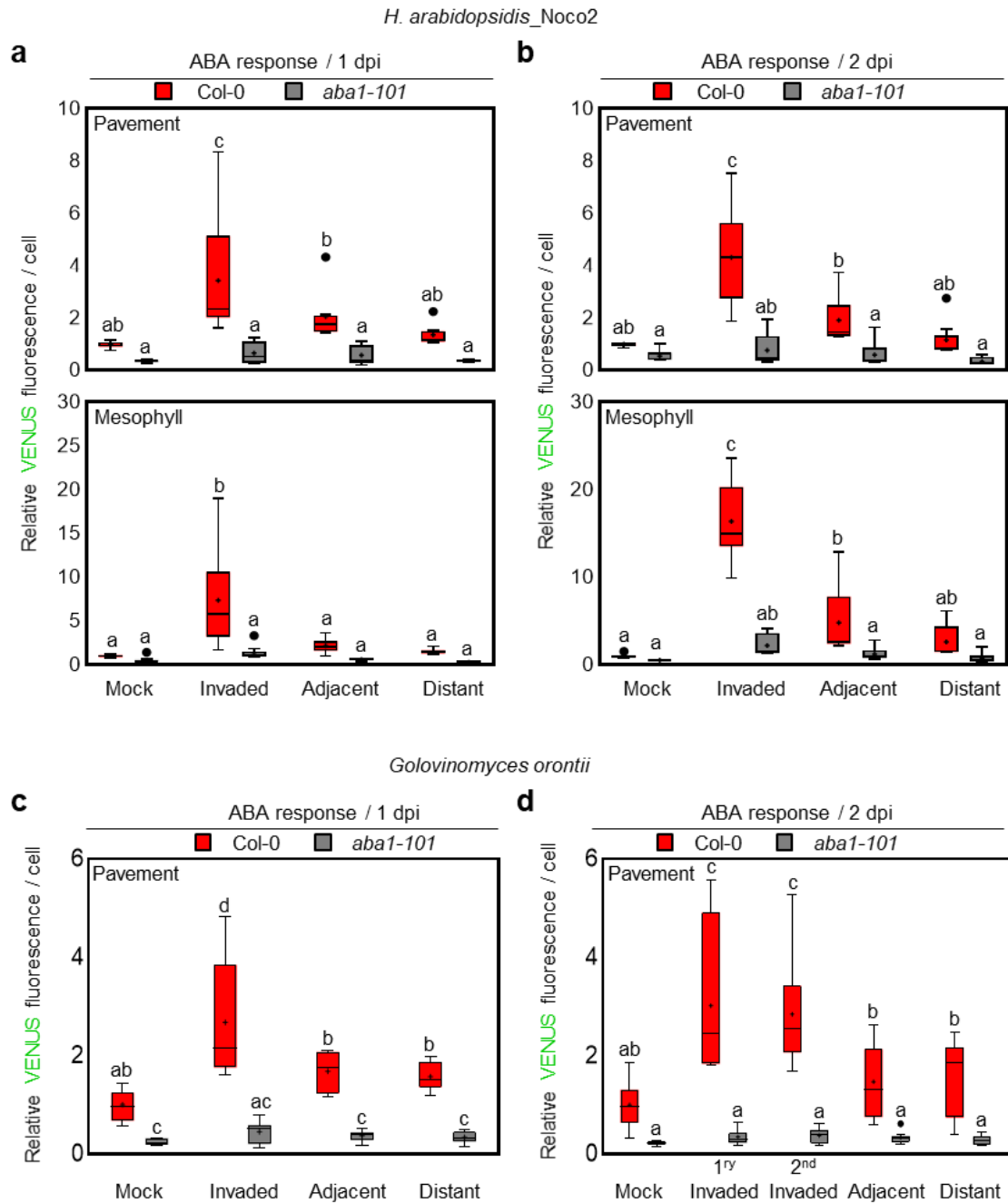


Figure 27: *H. arabidopsidis*-Noco2 and *G. orontii* induced COLORFUL-ABA reporter activity is dependent on the ABA biosynthesis. (a-b) The COLORFUL-ABA reporter activities at the sites of invasion by the Noco2 at 1 (a) and 2 (b) dpi in pavement cells (a, upper panel, b, upper panel) and mesophyll cells (a, lower panel, b, lower panel) of the wildtype Col-0 (red) and *aba1-101* (gray) backgrounds. Data are normalized to the uninfected wildtype. (c, d) The COLORFUL-ABA reporter activities in pavement cells at the sites of invasion by the fungus *G. orontii* at 1 (c) and 2 (d) dpi in pavement cells of the wildtype Col-0 (red) and *aba1-101* (gray) backgrounds. Data are normalized to the uninfected wildtype. Box plots show first quartile (lower line); median (centre line); mean (+); third quartile (upper line); whiskers extend 1.5 times the interquartile range, and outliers (dots), n = 7-10

3. RESULTS

infection sites. Different letters (Two-way ANOVA followed by Tukey's multiple comparison test, p -adjusted < 0.05) indicate significant differences. The two experiments were repeated once, showing the same pattern of response.

To show a summary of the quantitative measurements in the previous figures, quantitative heat map representations were designed for ABA signaling activities at sites of Arabidopsis interactions with *Noco2* and *G. orontii* (Figure 28). The schemes reflect the drastic reduction in ABA signaling activities (in green) in the ABA biosynthetic mutant *aba1-101* (Figure 28a-d, lower panels), in comparison to the wildtype (Figure 28a-d, upper panels).

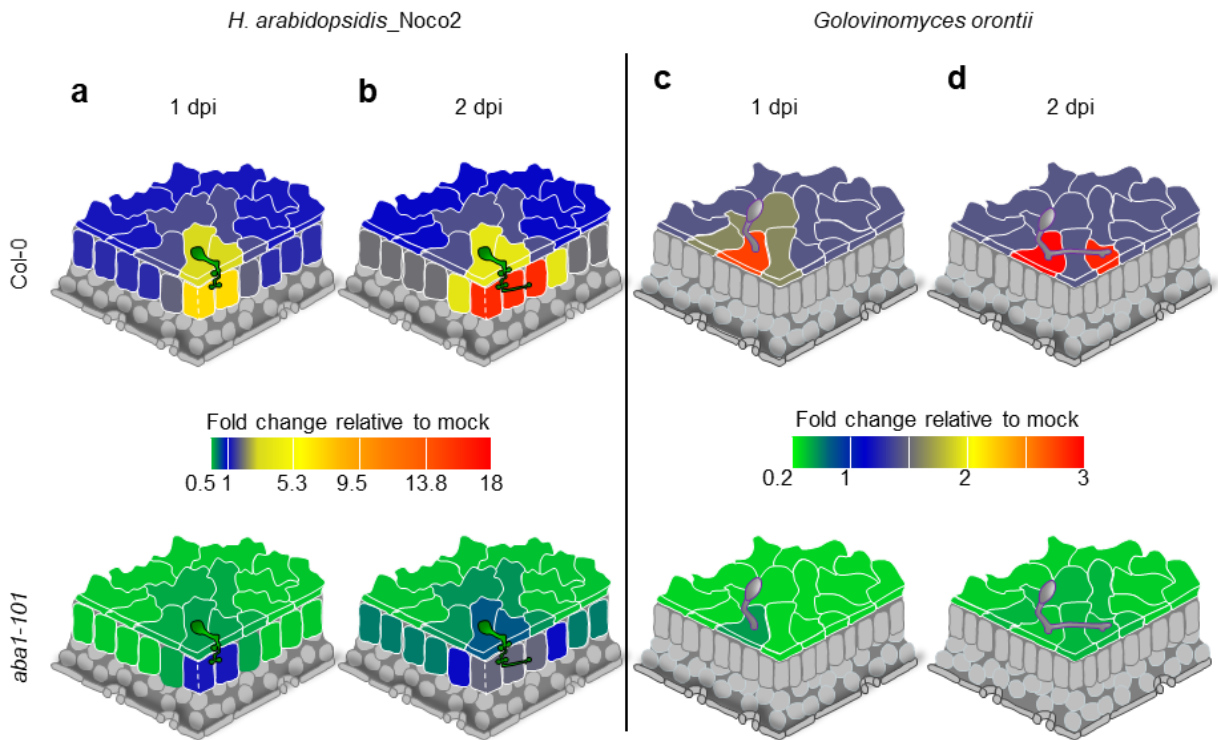


Figure 28: Quantitative heat map representations of ABA signaling activities at sites of Arabidopsis interactions with *H. arabidopsidis-Noco2* and *G. orontii*. (a-b) ABA reporter activities at 1 (a) and 2 dpi (b) in leaves of 3-week-old Arabidopsis COLORFUL-ABA line #1 in the wildtype Col-0 background (a and b, upper panel) and in the ABA biosynthetic mutant *aba1-101* (a and b, lower panel). (c-d) ABA reporter activities at 1 (c) and 2 dpi (d) in leaves of 5-week-old Arabidopsis COLORFUL-ABA line #1 in the wildtype Col-0 background (c and d, upper panel) and in the ABA biosynthetic mutant *aba1-101* (c and d, lower panel).

3.8. The ABA core regulatory components SnRK2D, SnRK2I, and PP2CA mediate the pathogen-induced ABA and SA responses

One of the main objectives of the current study was to uncover the core regulatory network in ABA that mediates pathogen-induced ABA signaling. Therefore, positive and negative regulators of ABA signaling cascade, SNF1-related protein kinases 2 (SnRK2s), and type 2C protein phosphatase (PP2Cs), respectively, were investigated in the following part to characterize their contributions in plant immune responses.

3.8.1. SnRK2D and SnRK2I display negative impacts on the plant immune responses

Among the ten members of the SnRK2 family, subclass III (which includes three members: SnRK2D/SnRK2.2, SRK2E/OPEN STOMATA1 (OST1)/SnRK2.6, and SnRK2I/SnRK2.3) showed high phosphorylation activity upon accumulation of ABA as well as during pathogen infections within 30 min (Umezawa et al. 2010; Yoshida et al. 2006). Therefore, mutant analyses were performed on the individual T-DNA insertion mutants *snrk2d*, *snrk2e*, *snrk2i*, and the double mutants *snrk2d snrk2e*, *snrk2d snrk2i*, *snrk2e snrk2i* (Nakashima et al. 2009) to identify the SnRK2s that mediate the previously described pathogen-associated ABA signaling pattern promoting susceptibility to different biotrophic pathogens. Fujii & Zhu (2009) and Nakashima et al. (2009) demonstrated that the triple mutant *snrk2d snrk2e snrk2i* showed severely impaired germination, growth, and reproduction. Moreover, the mutant did not grow under normal short- or long-day chambers conditions due to severe dryness associated with impaired ABA-signaling. Therefore, this mutant was excluded from these analyses.

To examine the regulatory role of SnRK2s in the pathogen mediated ABA upregulation, the sporulation of *Noco2* and *G. orontii* was tested on the mutants as mentioned earlier in Col-0 background, as well as on the hypersusceptible mutant *eds1* (Parker et al. 1996) and the highly resistant mutant *snc1* (Li et al. 2001) (data are not shown). After infection with *Noco2*, *snrk2d snrk2i* seedlings displayed a disease resistance

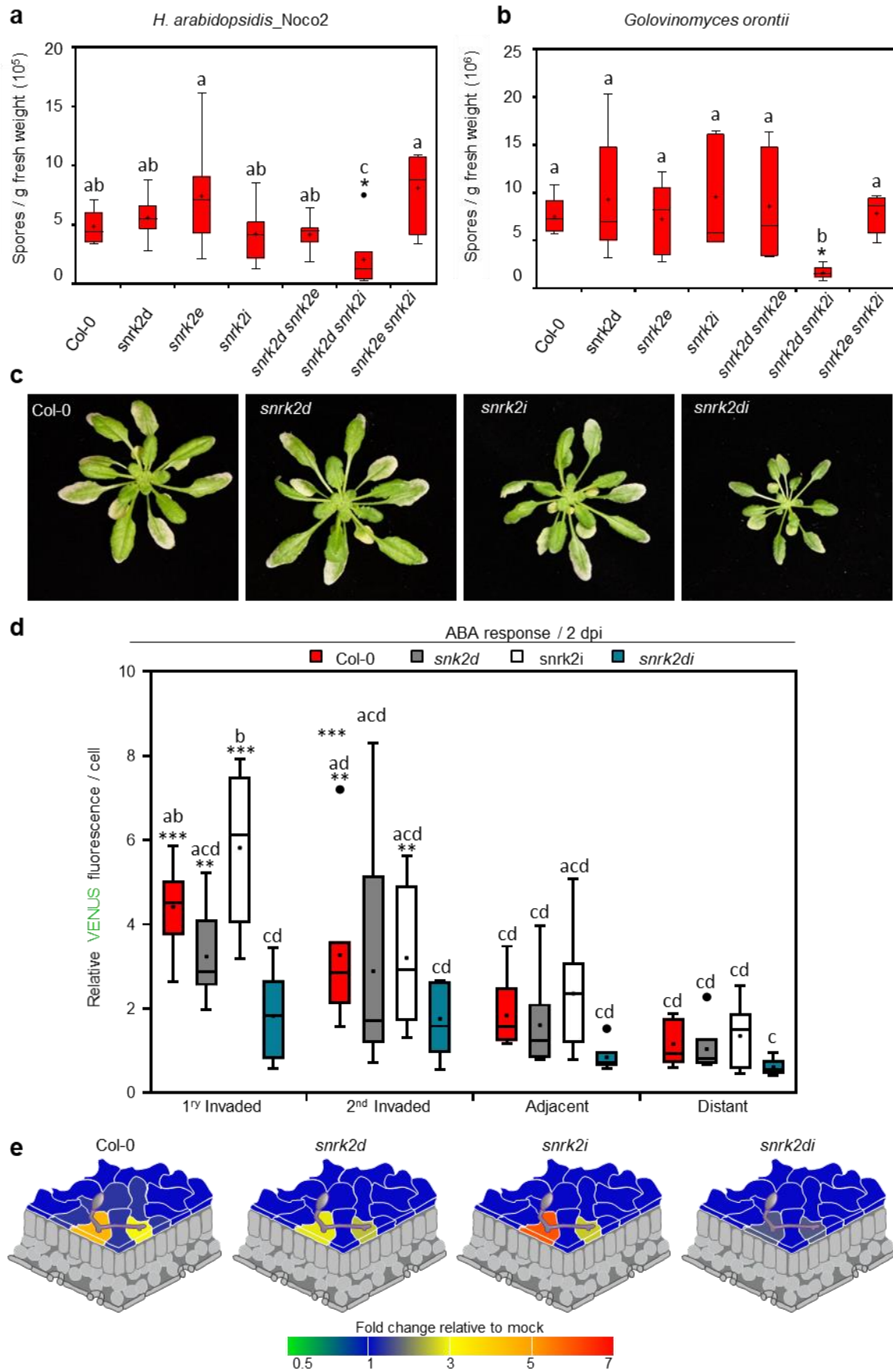
3. RESULTS

phenotype at 6 dpi in comparison to the other tested mutants and the susceptible wildtype Col-0 (Figure 29a). Moreover, a similar result was obtained with *G. orontii* infection experiments at 10 dpi on the same mutants (Figure 29b-c). The interaction of *snrk2d* and *snrk2i* individual mutants with Noco2 and *G. orontii* showed a wildtype-like phenotype (Figure 29c), underpinning the redundancy of the role of SnRK2D and SnRK2I kinases in the pathogen-induced phosphorylation of ABA downstream components.

Next, *snrk2d*, *snrk2i*, *snrk2d snrk2i* mutants were crossed with the COLORFUL-ABA line #1 to investigate the dependency of pathogen mediated ABA signaling activity on these kinases. Surprisingly, after the selection of the homozygous lines for F3 generation, a partial silencing of the reference and membrane marker modules was observed in F3 and F4 generations of only *snrk2d snrk2i* double mutant. Therefore, the reporter signal intensities in each genotype were normalized to the corresponding uninfected mock not to the uninfected Col-0. Quantitative data analyses at 2 dpi showed significantly enhanced VENUS signals in the primary (4.72-fold), and secondary (2.68-fold) *G. orontii* invaded domains of the wildtype. Moreover, the double mutant *snrk2d snrk2i* remarkably exhibited a significant reduction in ABA signal intensities upon *G. orontii* infections in comparison to the wildtype. VENUS fluorescence intensities in primary and secondary invaded domains were 1.64-fold and 1.32-fold, respectively. Pathogen induced ABA signaling in individual mutant genotypes *snrk2d* and *snrk2i* showed a wildtype-like pattern (Figure 29d), providing additional proof that SnRK2D and SnRK2I are redundantly involved in pathogen mediated upregulation of the ABA signaling cascade to promote susceptibility.

In order to outline the quantitative measurements of ABA signaling activities at sites of Arabidopsis interactions with *G. orontii* (Figure 29d), quantitative heat map representations were designed (Figure 28e). The schemes show the drastic reduction in ABA signaling activities (in gray) in the ABA signaling double mutant *snrk2d snrk2i* (Figure 29e, 4th panel), in comparison to the wildtype Col-0 background (Figure 29e, 1st panel), the individual ABA signaling mutants *snrk2d* (2nd panel), and *snrk2i* (3rd panel).

3. RESULTS



3. RESULTS

Figure 29: *SnRK2D* and *SnRK2I* redundantly suppress the immune responses during different biotrophic interactions. (a) Sporulation of the virulent isolate of the oomycete *H. arabidopsidis*-Noco2 spray-inoculated on 2-week-old ABA signaling mutants (*snrk2d*, *snrk2e*, *snrk2i*, *snrk2d snrk2e*, *snrk2d snrk2i*, and *snrk2e snrk2i*) in comparison to the susceptible wildtype Col-0 plants at 6 dpi. n = 5 biological replicates (b) Sporulation of the fungus *G. orontii* on 5-week-old brush-inoculated ABA signaling mutants (*snrk2d*, *snrk2e*, *snrk2i*, *snrk2d snrk2e*, *snrk2d snrk2i*, and *snrk2e snrk2i*) in comparison to the susceptible wildtype Col-0 at 10 dpi. n = 7. Measurements in (a) and (b) were repeated twice, and the same disease phenotype pattern was observed in all repeats. (c) Macroscopic *G. orontii* infection phenotypes at 10 dpi for the wildtype col-0, *snrk2d*, *snrk2i* and *snrk2i*. (d) The COLORFUL-ABA reporter activities at the sites of invasion by the *G. orontii* at 2 dpi in the epidermal cell layer in Col-0, *snrk2d*, *snrk2i*, *snrk2d snrk2i*. (e) Quantitative heat map representations of ABA signaling activities at sites of Arabidopsis interactions with *G. orontii* at 2 dpi at the epidermal cell layer in leaves of 5-week-old Arabidopsis COLORFUL-ABA line #1 in the wildtype Col-0 background (1st panel), in the ABA signaling mutants *snrk2d* (2nd panel), *snrk2i* (3rd panel), and *snrk2d snrk2i* (4th panel). Box plots show first quartile (lower line); median (centre line); mean (+); third quartile (upper line); whiskers extend 1.5 times the interquartile range, outliers are designated as dots, n = 7-10. Data were normalized to corresponding mock. (a-b) Different letters (One-way ANOVA followed by Tukey's multiple comparison test, p-adjusted < 0.05) indicate significant differences between groups. Asterisks indicate the significant difference to the infected wildtype Col-0 (*p < 0.05, **p < 0.01, ***p < 0.001, Student's t-test) (d) Asterisks indicate the significant difference to the uninfected corresponding mock (*p < 0.05, **p < 0.01, ***p < 0.001, Student's t-test) and different letters (Two-way ANOVA followed by Tukey's multiple comparison test, p-adjusted < 0.05) indicate significant differences between groups.(d) was repeated once showing the same pattern of ABA responses.

3.8.2. *PP2CA* negatively regulates immune responses

Of the ten PP2C subclades, the members of the PP2C group A phosphatases have been investigated intensively in Arabidopsis as negative regulators of ABA signaling, such as ABA-INSENSITIVE1 (ABI1), ABI2 (Saez et al. 2006), the HYPERSENSITIVE TO ABA1 (HAB1) (Saez et al. 2004), ABA-HYPERSENSITIVE GERMINATION 1 (AHG1), and 3 (AHG3)/PP2CA (Kuhn et al. 2006). T-DNA insertion lines *abi1-2* and *hab1-2* (Nishimura et al. 2007; Yoshida et al. 2006), *pp2ca-1* (Kuhn et al. 2006), as well as the single nucleotide mutation loss-of-function mutants, *ahg1-1* and *ahg3-1* (Nishimura et al. 2007; Yoshida et al. 2006) showed an increase in the expression of ABA inducible genes and ABA hypersensitivity phenotype in germination and growth.

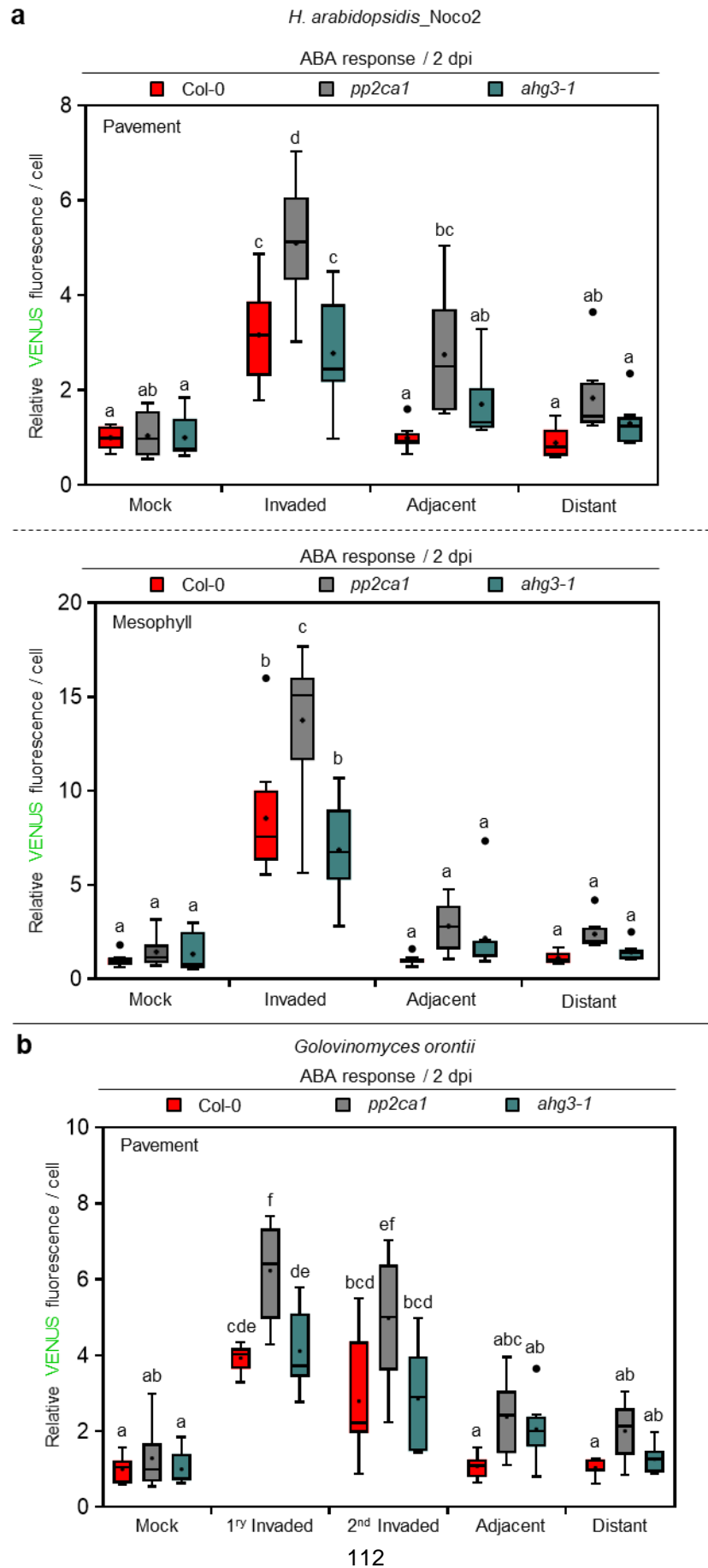
3. RESULTS

In two recent studies in our lab, Schliekmann (2017) and Lübbers (2018) characterized the disease phenotype and sporulation of *Noco2* and *G. orontii* on different *Arabidopsis* PP2C loss-of-function mutants. These analyses showed that *ahg1-1*, *hab1-1*, *abi1-2*, *ahg3-1* do not exhibit any altered disease phenotype in comparison to the wildtype Col-0 after *Noco2* and *G. orontii* infections. On the contrary, *pp2ca-1* knockout mutant showed enhanced disease resistance to both pathogens (Lübbers 2018). Additionally, Manohar et al. (2017) investigated the SA-binding molecules and demonstrated that the ABA negative regulators PP2Cs bind SA. Therefore, the two mutants of AHG3/PP2CA, *ahg3-1*, and *pp2ca-1* were crossed with COLORFUL-ABA line #1 and COLORFUL-SA line #1 to map the changes in ABA and SA signaling following pathogen attack.

3.8.2.1. *pp2ca-1* exhibits significantly induced ABA signaling activities in comparison to the wildtype

In order to investigate the changes in ABA signaling in the PP2CA deficient mutants, which showed enhanced resistance, the F3 homozygous lines COLORFUL-ABA line #1 in *pp2ca-1* and *ahg3-1* backgrounds were used to map ABA signaling after infection with *Noco2* and *G. orontii* comparative to the wildtype, followed by quantitative analyses of ABA signaling activities at 2 dpi. In Col-0 and *ahg3-1* backgrounds, ABA signaling activities were significantly enhanced with a 3.21-fold and 2.43-fold increase, respectively, in *Noco2* invaded epidermal domains. A similar pattern with a higher magnitude (7.46-fold and 6.51-fold increase) was observed in the mesophyll. The statistical analysis did not show any differences in the responses of *ahg3-1* mutant and the wildtype with respect to invaded, adjacent, and distant domains also with *G. orontii* (Figure 30a-b). On the contrary, the knockout mutant *pp2ca-1* revealed a significant enhancement in ABA signal intensities not only in the invaded cells but also in the immediately adjacent domain to *Noco2* or *G. orontii* haustoriated domains. These results reflect the negative regulatory role of PP2Cs in mediating ABA signaling following pathogen invasion.

3. RESULTS



3. RESULTS

Figure 30: Noco2 and *G. orontii* trigger the enhanced ABA signaling at their interaction sites in *pp2ca-1* in comparison to the wildtype. (a) The COLORFUL-ABA reporter activities at the sites of Noco2 invasion at 2 dpi in the epidermal cell layer (upper panel) and mesophyll cell layer (lower panel) of 3-week-old COLORFUL-ABA line #1 in Col-0, *pp2ca-1*, and *ahg3-1* backgrounds. (b) The COLORFUL-ABA line #1 reporter activity at the sites of *G. orontii* invasion at 2 dpi in the epidermal cell layer of 5-week-old COLORFUL-ABA line #1 in Col-0, *pp2ca-1*, and *ahg3-1* backgrounds. Box plots show first quartile (lower line); median (centre line); mean (+); third quartile (upper line); whiskers extend 1.5 times the interquartile range, and outliers are indicated as dots, n = 7-10 infection sites. Different letters (Two-way ANOVA followed by Tukey's multiple comparison test, p-adjusted < 0.05) indicate significant differences. These experiments were repeated once showing the same pattern of ABA response.

Concisely, the quantitative heat map schemes (Figure 31a-b) reflect the strongly triggered ABA signaling in Noco2 and *G. orontii* haustoriated, as well as the adjacent cells at Noco2 interaction sites in *pp2ca-1* mutant in comparison to the wildtype, and the *ahg3-1* mutant.

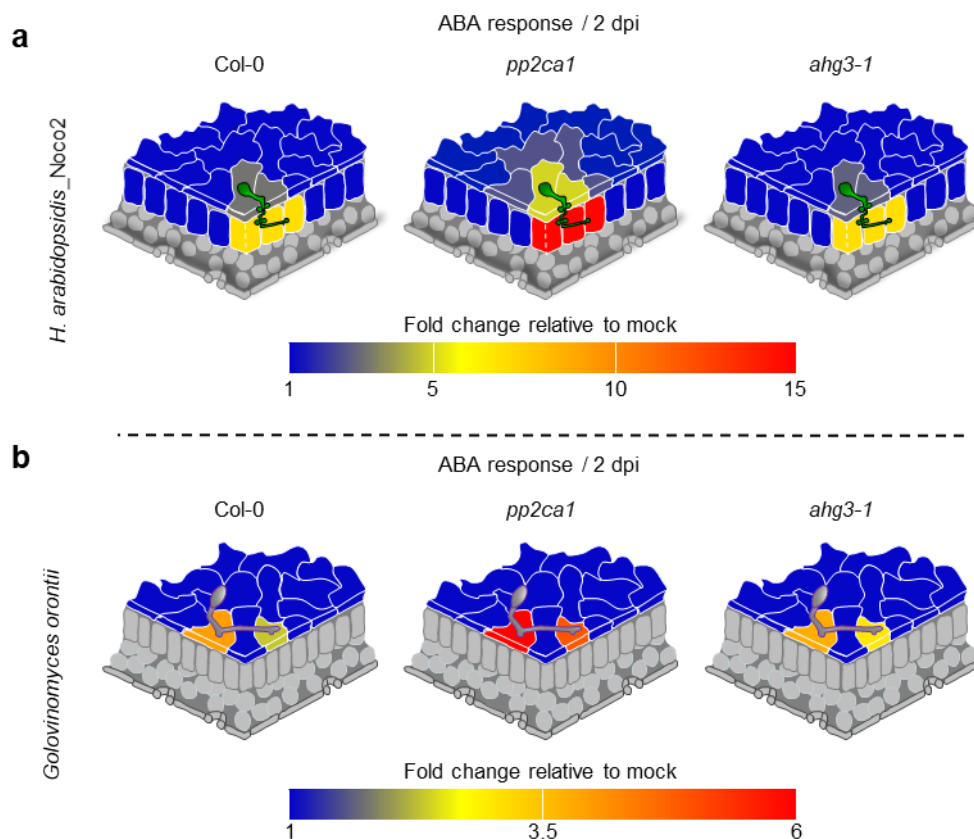


Figure 31: Quantitative heat map representations of ABA signaling activities at sites of Arabidopsis interactions with *H. arabidopsidis*-Noco2 and *G. orontii*. (a) The ABA reporter activities

3. RESULTS

at Noco2 interaction sites at 2 dpi in leaves of 3-week-old Arabidopsis COLORFUL-ABA line #1 in the wildtype Col-0 background (left panel), the ABA signaling mutant *pp2ca-1* (middle panel), and in the ABA signaling mutant *ahg3-1* (right panel). (b) The ABA reporter activities at *G. orontii* interaction sites at 2 dpi in leaves of 5-week-old Arabidopsis COLORFUL-ABA line #1 in the wildtype Col-0 background (left panel), the ABA signaling mutant *pp2ca-1* (middle panel), and in the ABA signaling mutant *ahg3-1* (right panel).

3.8.2.2. SA signaling is highly activated at *pp2ca1-H. arabidopsidis* interactions sites relative to the wildtype and the missense mutant *ahg3-1*

PP2CA knockout mutant *pp2ca-1* showed enhanced resistance to different biotrophic pathogens, though it showed enhanced ABA signaling, while the PP2CA single amino acid exchange mutant *ahg3-1* did not show any differences in the disease phenotype and the ABA-signaling pattern in comparison to the wildtype. Manohar et al. (2017) investigated the SA binding capacity of different PP2Cs rather than AHG3/PP2CA, and they reported that PP2Cs act as SA-binding proteins (SABP). Accordingly, *pp2ca1* and *ahg3-1* were crossed with COLORFUL-SA #1 to map the changes in SA signaling following pathogen assays.

Notably, quantitative analyses at 2 dpi with the virulent isolate of *H. arabidopsidis* Noco2 exhibited a significant activation of SA signaling in *pp2ca1* mutant in comparison to the wildtype and *ahg3-1* mutant in the haustoriated and directly adjacent domains in the pavement (Figure 32a,c) and mesophyll cell layer (Figure 32b,c). Moreover, the pathogen induced-SA pattern in both Col-0 and *ahg3-1* backgrounds did not show any significant differences. These findings might explain the resistance phenotype associated with this mutant to biotrophic pathogens by the loss-of binding activity of PP2CA with SA, which is unchanged in the single amino acid exchange mutant *ahg3-1*.

3. RESULTS

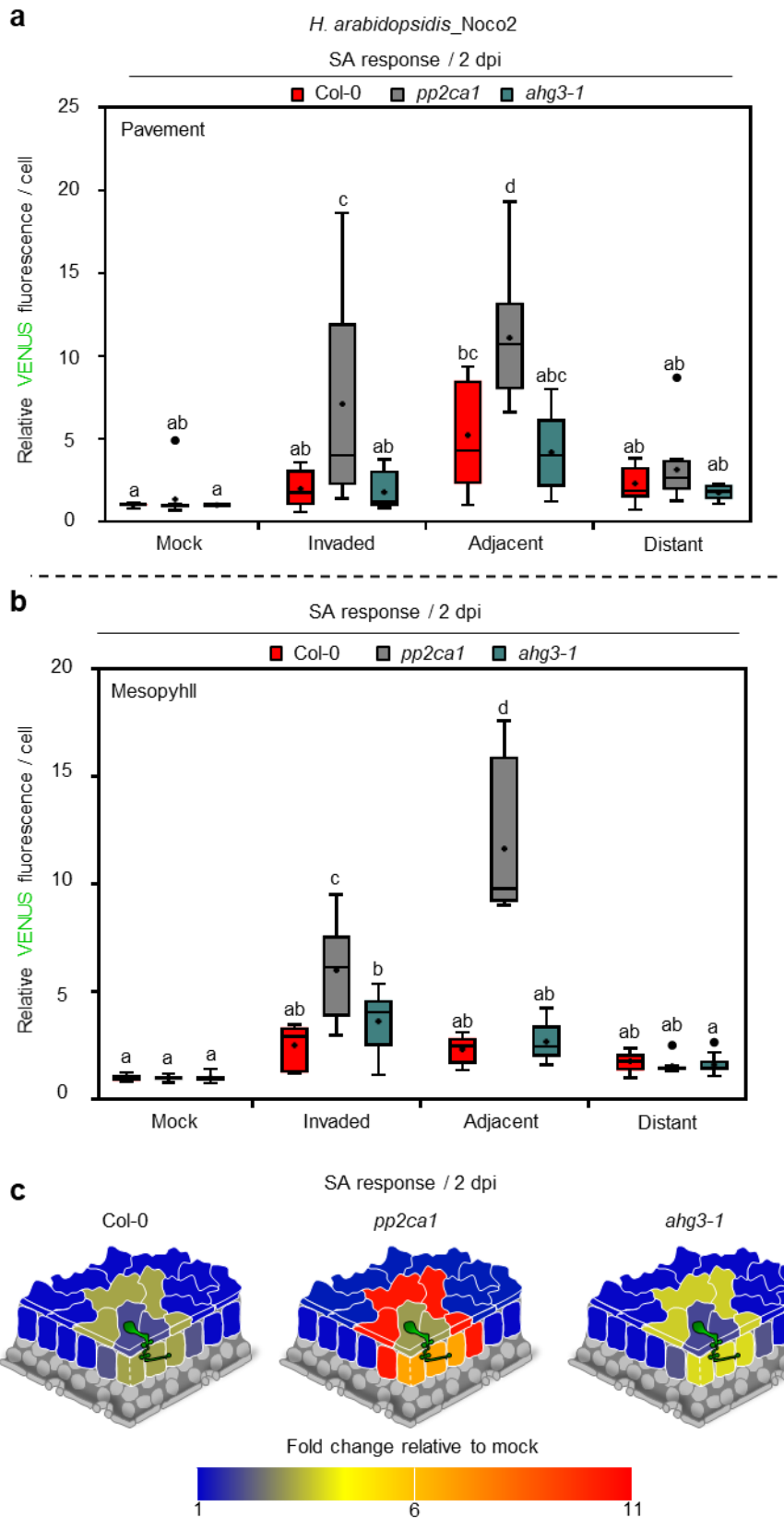


Figure 32: SA signaling is significantly triggered at the Noco2 invaded and adjacent domains of *pp2ca-1* in comparison to the *Col-0* and *ahg3-1*. (a-b) The COLORFUL-SA reporter activities at

3. RESULTS

the sites of Noco2 invasion at 2 dpi in the epidermal cell layer (a) and mesophyll cell layer (b) of 3-week-old seedlings of COLORFUL-SA line #1 in Col-0, *pp2ca-1*, and *ahg3-1* backgrounds. (e) Quantitative heat map representations of SA signaling activities at sites of Arabidopsis interactions with Noco2 at 2 dpi in leaves of 3-week-old Arabidopsis COLORFUL-SA line #1 in the wildtype Col-0 background (left panel), and in the ABA signaling mutants *pp2ca1* (middle panel), and *ahg3-1* (right panel). Box plots show first quartile (lower line); median (centre line); mean (+); third quartile (upper line); whiskers extend 1.5 times the interquartile range, and outliers are designated as dots, n = 7-10 infection sites. Different letters (Two-way ANOVA followed by Tukey's multiple comparison test, p-adjusted < 0.05) indicate significant differences. This experiment was repeated once showing the same pattern of SA response.

4. DISCUSSION

The main objective of the current study was to explore hormone-signaling cascades on a cellular scale shortly after pathogen invasion. Understanding the spatio-temporal signaling of ABA, SA, JA and JA/ET during compatible and incompatible biotrophic interactions with *A. thaliana* could provide an insight into the mechanisms by which the pathogen can overcome the plant immune system. To this end, recently generated transgenic Arabidopsis transcriptional output reporter lines for the hormones ABA, SA, JA and JA/ET were used in this study and complemented by the in-depth characterization of the ABA reporter-reference line. The resulting COLORFUL hormone signaling reporter line collection was subsequently employed in comparative plant-microbe interaction analyses.

4.1. COLORFUL reporters facilitate robust live-cell readouts of hormone signaling output

4.1.1. The reference and the membrane marker modules allowed live-cell imaging and monitoring of tissue integrity

In this project, the transgenic Arabidopsis COLORFUL-ABA reporter that enabled the mapping of ABA signaling outputs at single-cell resolution was established and subsequent functional characterization analyses were performed. In contrast to previously described marker gene promoter-based reporters for ABA (Christmann et al. 2005; Himmelbach et al. 2002; Ishitani et al. 1997; Söderman et al. 1999), SA (Betsuyaku et al. 2018), JA (Betsuyaku et al. 2018; Mousavi et al. 2013) and JA/ET (Manners et al. 1998), the COLORFUL biosensors feature an N7 nuclear-targeted (Cutler et al. 2000) reference (Figure 7a-b, magenta) readout that serves as a cellular viability marker, and allows live-cell imaging as well as robust and precise quantification of single-cell reporter activities in distinct cell types. Another key feature

4. DISCUSSION

of the COLORFUL system is an LTI6b-PM localized (Cutler et al. 2000) cell membrane marker module (Figure 6i, gray), which was used in this study to allocate the single-cell signals and to monitor tissue integrity, pathogen invasion sites, invading structures, and induced cell death responses. Moreover, *CaMV35S* driven GFP enabled the detection of topology, size, identity, and viability of individual cells and their relative position in a tissue context.

Although the reference module was designed and inserted into the COLORFUL biosensors to allow ratiometric reference-reporter analyses, *UBQ10* driven mKATE2 signal intensities were shown to be slightly induced upon ABA treatment (Figure 9c). Therefore, the *UBQ10*-mKATE2 marker was not used as a reference in this study, but rather employed for general nuclear detection, for sorting, and as a cellular viability reporter. Moreover, the COLORFUL SPOTTER plugin tool provided a high-throughput capacity for confocal image processing and robust cellular hormone response analyses.

4.1.2. The reporter module activities are controlled by promoters of highly responsive and well-known marker genes

4.1.2.1. ABA treatment induced a higher *PP2CA* transcript level in comparison to other investigated ABA responsive genes

In contrast to previously developed ABA reporters (Christmann et al. 2005; Himmelbach et al. 2002; Ishitani et al. 1997; Söderman et al. 1999), the promoter of the ABA marker gene *PP2CA* (Kuhn et al. 2006) was utilized in the current study to develop an ABA reporter line. A comparative expression analysis was carried out to test the ABA-responsive expression of *PP2CA*, *RD29A/B*, *HB6*, and *RAB18*. In the wildtype and in an ABA deficient mutant, ABA treatment enhanced a higher *PP2CA* transcript level in comparison to the other tested genes (Figure 6a). Zhao et al. (2018) and Harb et al. (2010) reported that in response to exogenous application of ABA or mannitol to *Arabidopsis* plants, *RAB18* exhibited a higher transcript level in comparison to *RD29A/RD29B* in Col-0. Conversely, our data analyses exhibited a higher *RD29A/B*

4. DISCUSSION

expression level in comparison to *RAB18*. What is more, *HB6*, *RAB18*, and *PP2CA* did not show any significant differences in expression after ABA treatment in an ABA signaling mutant as compared with untreated seedlings. This is in line with the findings of Zhao et al. (2018), who observed that exogenous ABA treatment did not alter the expression level of *RAB18* in the ABA signaling mutant *snrk2d snrk2e snrk2i*.

Additionally, the expression of *RD29A* and *RD29B* was slightly yet significantly enhanced in the wildtype as reported by Cruz et al. (2014) and Cui et al. (2014). However, *RD29A* and *RD29B* expression was induced by exogenous ABA treatment in the ABA signaling mutant as well. Fujii et al. (2011) investigated the contribution of different SnRK2 to the expression of osmotic stress-controlled genes in the triple *snrk2d snrk2e snrk2i* and septuple *srk2g srk2a srk2h srk2f srk2c srk2j srk2b* mutants in comparison to the wildtype Col-0. The authors of the later study showed that osmotic stress significantly induced the expression of all tested genes including *RD29A* and *RD26* in the aforementioned genotypes, supporting the idea that *RD29A* could not be used as a robust ABA-controlled signaling marker, since it reflected a partial SnRK2-independent upregulation. On the contrary, Zhao et al. (2018) demonstrated that neither ABA nor mannitol treatments activated the expression of *RD29B* in ABA receptor mutants. Moreover, Christmann et al. (2005) reported low sensitivity of a *RD29B* driven LUC reporter in comparison to an *HB6* driven LUC reporter for mapping the changes in ABA signaling following exogenous ABA treatment as well as water stress. These findings demonstrated that *PP2CA* exhibited a higher responsiveness only to ABA, and was thus selected here to drive the expression of VENUS in the COLORFUL-ABA reporter.

4.1.2.2. COLORFUL-biosensors displayed hormone dosage- and incubation time-dependent activities on a transcriptional level

Promoters of the ABA-responsive *PP2CA* gene (Kuhn et al. 2006), SA-responsive *PR1* marker gene (Cao et al. 1994; Mou et al. 2003), the JA-inducible *VSP2* marker gene (Anderson et al. 2004; Lorenzo et al. 2004), and the JA/ET-responsive *PDF1.2a* marker gene (Penninckx et al. 1998) were selected to drive the expression of VENUS fused with the nuclear localization signal N7 (Cutler et

4. DISCUSSION

al. 2000) in COLORFUL-ABA, -SA, -JA, and -JA/ET, respectively. Targeting the hormone-controlled VENUS to the nucleus allows the quantification of hormone signaling at single-cell level. The nuclear localization of a stimulus-controlled fluorescent protein is known to improve the signal to noise ratio in quantitative analyses (Kinkema et al. 2000; Rhee et al. 2006; Seibel et al. 2007).

4.1.2.2.1. VENUS reporter signal activation displays high sensitivity of the employed promoters to minor changes in hormone signaling

Hormone treatment experiments exhibited that *PP2CA-VENUS-N7* (ABA-reporter, Figure 7a) showed ABA dosage- and incubation time-dependent activities. Following the incubation of COLORFUL-ABA seedlings in different ABA concentrations, a remarkable concentration-dependent increase in the reporter activity was observed, which proportionally correlated with the increasing ABA dose (Figure 8a). The ABA reporter showed a significant increase in VENUS signal intensities upon treatment with 0.5 μ M ABA, reflecting the high sensitivity of the COLORFUL-ABA reporter to map the minimal changes in ABA levels. The content of ABA in the wildtype Col-0 is mainly dependent on the tissue type, as the ABA level was 0.003 μ g/g fresh weight (FW) in leaf tissues (Li et al. 2012) and 0.01 μ g/g FW in root tissues (Geng et al. 2013), while Forcat et al. (2008) reported that ABA is generally undetectable in unstressed Arabidopsis leaves.

The aforementioned studies revealed up to 30-fold increases in ABA content under biotic and abiotic stress conditions. Sauter et al. (2001) reported that unknown amounts of the exogenously applied ABA are absorbed via Arabidopsis roots. To address this, Wang et al. (2018) measured the leaf content of active ABA and inactive glucose-conjugated ABA (ABA-GE) in response to the exogenous applications of ABA. Data analyses showed a 0.058, 0.409, and 1.17 μ g/g FW cellular ABA content and 2.22, 13.90, and 33.98 μ g/g FW cellular ABA-GE content after 24 h treatments with 10, 50, and 100 μ M ABA, respectively. A gradual increase of ABA content was observed with all treatments. Wang et al. (2018) concluded that ABA is absorbed by the roots and transformed into other inactive forms through the conjugation or hydroxylation prior to accumulation in different plant tissues. These combined findings indicate that the

4. DISCUSSION

absorbed amount of ABA after treatment with 0.1 μ M ABA might not be detectable using the classical ABA detection and quantification assays. However, COLORFUL-ABA showed a strongly enhanced reporter activity in response to such precise changes in hormone concentration.

4.1.2.2.2. COLORFUL-ABA exhibits a high dependency of the reporter signal on endogenous hormone levels

Analyses of ABA biosynthetic mutants before and after hormone treatments showed the specificity of the selected promoters. The significantly lower signal intensities in ABA-untreated seedlings of the *aba1-101* mutant in comparison to the wildtype revealed the specificity of this reporter system to ABA as a stimulus (Figure 10c). The impaired ABA biosynthesis in *aba1-101* is the main reason for reporter signal downregulation, as *aba1* showed a lower ABA biosynthetic capacity in comparison to the wildtype (Rock & Zeevaart 1991; Barrero et al. 2005). Moreover, the complementation of the low reporter activity in *aba1-101* by exogenous ABA treatment is an additional proof for this specificity. Notably, the reduction in VENUS signals in the ABA deficient line (Figure 10c) relative to the wildtype was reflected on the transcriptional level, hence the *PP2CA* expression was lower in *aba1-101* relative to wildtype (Figure 10d).

4.1.2.2.3. Hormone treatment progressively induces *PP2CA*, *PR1*, *VSP2* and *PDF1-2a* transcript levels

For an additional level of functional characterization, the transcriptional activations of the aforementioned marker genes in response to hormone treatments were investigated over a specific time period. qRT-PCR analyses showed upregulation of *PP2CA* (Figure 6d), *PR1* (Figure 11a), *VSP2* (Figure 11b), and *PDF1-2* (Figure 11c) after ABA, SA, MeJA, and MeJA+ACC treatments, respectively. Similarly, Chen et al. (2017), Gruner et al. (2018), Vos et al. (2015) and Zander et al. (2014) observed enhanced expression levels of *PR1*, *VSP2* and *PDF1-2* relative to mock plants in five-week-old *Arabidopsis* plants after treatment with SA, MeJA, and ACC, respectively for at least 24 h. Similar to our findings at early points in time after SA treatment, Gruner

et al. (2018) observed a significantly enhanced *PR1* expression. Moreover, kinetics of *PP2CA* expression correlated with the timing of increasing ABA reporter activity, but increases of promoter-reporter activity could be detected earlier (3.0 h) (**Figure 10b**) than changes in *PP2CA* transcript levels (12 h) (**Figure 6h**). These findings reflect the higher suitability and sensitivity of the COLORFUL reporter system in comparison to previously published transcriptional reporters, thus enabling hormone response measurements.

4.2. COLORFUL-ABA explore distinct cell-type specific hormone sensitivities and signaling outputs

During this project, the main focus was to map changes in hormone signaling in Arabidopsis leaf tissues. A remarkable cell-type-specific activation of hormone-controlled VENUS fluorescence was observed in hormone-treated leaves. In case of the ABA-reporter, the epidermal guard cells displayed the maximum ABA signal intensity in comparison to the epidermal pavement and the palisade mesophyll cells (Figure 9b). In Arabidopsis guard cells, vascular tissues of leaves and roots are known to synthesize ABA (Bauer et al. 2013; Boursiac et al. 2013; Seo & Koshiba 2011; Waadt et al. 2014). Subsequently, ABA is exported to the guard cells via ABA transporters (Kang et al. 2010; Kuromori et al. 2011; Kanno et al. 2012; Boursiac et al. 2013). Therefore, guard cells act as reservoirs for ABA (Waadt et al. 2014; Waadt et al. 2015). The variation of the ABA signal intensities in discrete leaf cell types before and after ABA treatment demonstrates that each cell type has a different ABA sensitivity. Given that mature guard cells are not connected to epidermal pavement and palisade mesophyll cells via plasmodesmata (Wille & Lucas, 1984) are, this may reflect low hormone uptake from the apoplastic space. Conceivably, other ABA signaling components may also show cell-type-specific activity patterns. In the future, COLORFUL reporters may facilitate identification of novel cell-specific master regulators in mutant screens using automated, high-throughput, confocal imaging, and may uncover tissue-specific activities of already established signaling hubs that have so far been overlooked, thereby clarifying seemingly contradictory or inconsistent findings.

4.3. COLORFUL-biosensors map long-distance ABA signaling in different *Arabidopsis* tissues

ABA transport and distribution has been intensively studied (Boursiac et al. 2013; Jones et al. 2014; Seo & Koshiba 2011; Waadt et al. 2014; Wilkinson & Davies 2002). ABACUS and ABAleon FRET based sensors enabled direct measurements of ABA concentration, as well as the ABA transport in different tissues only after exogenous ABA treatment (Jones et al. 2014; Waadt et al. 2014). However, Waadt et al. (2015), Hayes (2018) and Wu et al. (2018) concluded that both ABACUS and ABAleon reporters possess a limited capacity to map the extremely low basal levels of endogenous ABA in *Arabidopsis*. In the current study, the measurements of VENUS signal intensities in different *Arabidopsis* tissues with and without ABA treatment reflected the high sensitivity of the COLORFUL-ABA reporter system to map basal and ABA-induced long-distance hormone signaling (Figure 12a-b). Quantitative and qualitative data showed the maximum ABA signal in the root tip (Figure 12-c), while the lowest signal intensities were found in the root elongation zone (Figure 12-b, d). Moreover, the leaves, cotyledon, and hypocotyl showed intermediate signal intensities (Figure 12-b, e, f). A similar ABA mapping pattern was provided by Waadt et al. (2014), which indirectly correlated ABA concentrations to the developmental and stress-induced spatiotemporal expression pattern of ABA biosynthetic enzymes encoded by *NCED* genes (Jones 2016; Tan et al. 2003; Waadt et al. 2015). Moreover, differential ABA signaling showed a high dependency on ABA biosynthesis—hence an ABA deficient mutant showed an undetectable reporter signal in all tested *Arabidopsis* tissues—that could be complemented by exogenous ABA treatment (Figure 13 and 14).

Furthermore, a contrasting distribution of ABA signal strength was seen in different cell types of young cotyledons in comparison to the old cotyledons and true leaves. More specifically, pavement cells of three-day-old cotyledons displayed higher ABA signal intensities in comparison to the signal in the guard cell (Figure 12g), while twelve-day-old cotyledons or true leaves showed the opposite (Figure 12h-i). Several previous studies addressed the role of ABA in early and late developmental stages of

4. DISCUSSION

Arabidopsis plants and showed that ABA is involved in stomatal movement in several plant species (Cai et al. 2017; Chen et al. 2016; Wang et al. 2013; Wolf et al. 2006). Moreover, several studies emphasized the role of ABA in newly developing tissues not only in stomatal development and distribution (Chater et al. 2014; Lake et al. 2002; Tanaka et al. 2013; Xie et al. 2006), but also with regard to the expansion of pavement and mesophyll cells, where higher ABA levels are required (Pantin et al. 2012; Parent et al. 2009; Tardieu et al. 2011). Consequently, ABA deficient mutants exhibited enhanced stomatal density and a stunted growth phenotype in comparison to the wildtype Col-0 (Cai et al. 2017). Mature Arabidopsis tissues are known to export ABA to the developing ones (Jordan et al. 1975; Zeevaart, 1977; Cornish & Zeevaart 1984). These findings indicate the correlation of cell sensitivity to ABA accumulation, perception, and signaling with cell development. Aliniaieifard & Van Meeteren (2013), Pantin et al. (2013a) and Pantin et al. (2013b) revealed that guard cells in young leaf tissues are unresponsive to ABA, whereas, Tanaka et al. (2013) proved the high responsiveness of epidermal cells to ABA in comparison to the guard cells in newly developing tissues. In conclusion, the difference with respect to ABA content in the guard and pavement cells is dependent on the tissue developmental stage and further analyses are needed to obtain deeper insights into this phenomenon.

COLORFUL plants did not show any difference in growth phenotype in comparison to Col-0 seedlings (data not shown), indicating that the transformation of Arabidopsis with this multimodular COLORFUL-cassette did not affect the developmental processes in the seedlings. In contrast, Jones et al. (2014) and Waadt et al. (2014) demonstrated that the FRET-based ABA reporters ABACUS and ABAleon affected ABA signaling, inasmuch as ABACUS seedlings displayed a hypersensitivity in seed germination and root growth (Jones et al. 2014). Similarly ABAleon seedlings showed a stunting phenotype relative to the wildtype, as well as hyposensitivity to ABA during seed germination (Waadt et al. 2014; Waadt et al. 2015).

4.4. Hormone treatment induces differential organ-specific SA-, JA-, and JA/ET-reporter activities

Before hormone treatments, COLORFUL-SA, -JA, and -JA/ET did not show any spatial differences in VENUS signal intensities between leaves, cotyledons, and roots, while the three reporters showed lower reporter activities in the roots following hormone treatments in comparison to cotyledons and leaves (Figure 15a-c). It is known that in response to different stimuli, changes in plant hormones result in differential hormone-responsive gene expression patterns in different tissues (Gao et al. 2017; Glauser et al. 2008; Paponov et al. 2008; Raines et al. 2016). Prerostova et al. (2018) observed a strong yet negligible SA accumulation in the leaf and root tissues respectively after exogenous application of SA. In addition, Glauser et al. (2008) demonstrated that wounding stimulated jasmonate biosynthesis and JA-responsive gene expression in a tissues-specific pattern in *Arabidopsis* plants. Furthermore, Tytgat et al. (2013) analyzed the biochemical and molecular changes in shoots and roots of *Brassica oleracea* in response to MeJA treatments. A distinct spatio-temporal activation of primary and secondary metabolites was observed, shoots showed immediate and strong JA-driven responses, while roots showed less extensive responses. Thus, quantitative analyses of hormone signaling using COLORFUL-biosensors reflected not only a tissue-specific but also an organ-specific activation of SA, JA, and JA/ET signaling pathways.

4.5. GFP-LTI6b and mKATE2-N7 modules allow visualization of the invasion process and are used as markers for cell viability

For plant-microbe interaction studies, it is essential to monitor the vegetative growth and the invasion dynamics of the attacking pathogen inside plant tissues. Trypan blue has been commonly used to visualize pathogenic structures, as well as to monitor plant cell death (Aarts et al. 1998; Asai et al. 2015; Holt et al. 2005; McDowell 2011). Moreover, aniline blue has been used to visualize cell wall remodeling or to detect

4. DISCUSSION

depositions at sites of invasion in plant cell walls such as callose and other auto-fluorescent metabolites (McDowell 2011; Cabral et al. 2011; Sohn et al. 2007). In this study, the GFP-LTI6b module combined with FB28 staining, provided an easier detection of individual plant-microbe interaction sites and allowed the monitoring of invasion dynamics of different biotrophic pathogens used in this study. Following infection with a spore, the PM-module helped in the identification of the outer periclinal epidermal cell wall penetrations, the invaginations between two cells, as well as the pathogen induced thickening of the invaded cell wall. Additionally, the PM-marker indirectly enabled the tracing of intercellular pathogenic growth into the anticlinal epidermal cell walls and the invasive establishment of pathogen feeding structures into the epidermal and mesophyll cells (Figure 17a-b).

At 1 dpi, the avirulent *H. arabidopsidis* isolate Emwa1 showed a higher penetration rate (Figure 17c) and haustoria formation capacity (Figure 17d) in comparison to the virulent isolate Noco2. While at 2 dpi, the haustoria formation capacity of Noco2 showed a drastic increase relative to Emwa1 (Figure 17d). At later time points, the membrane marker was used for the detection of cell death, which is indicated by the gradual disruption of the membrane signal that disappears at later time points (Figure 17f). In addition, the nuclear marker reference mKATE2-N7 provided another indicator for the integrity and the viability of invaded cells, since dying cells showed degradation and subsequent disappearance of the fluorescence signal (Figure 17f). Cell death using these markers was detected during the incompatible interaction of Emwa1, which involves the ETI mediated by the Col-0 RPP4 resistance gene (Massoud et al. 2012; Van der Biezen et al. 2002). During the compatible interaction of Noco2 with Col-0 (Carstens et al. 2014), membrane and nuclear markers reflected the integrity of the invaded cells (Figure 17g). Furthermore, the intact cells responded to plasmolysis treatment, thus confirming the vitality of the infected cells (Figure 17f-g).

In comparative analyses for SA levels in Arabidopsis Col-0 leaves subsequent to infection with both Noco2 and Emwa1, Mauch-Mani & Slusarenko (1996) reported that R gene-mediated resistance against Emwa1 is accompanied by significant accumulation of free SA, while no changes were observed with Noco2. Though often neglected, distinct pathogen invasion kinetics as evidenced here for Noco2 and

Emwa1 are similarly important for comparative analyses, since they have considerable effects on timing and amplitude of plant defense responses. Therefore, comparative analysis of spatio-temporal hormone signaling dynamics at single cell resolution during both compatible and incompatible interactions could provide valuable insights into the role of these hormones in mediating plant immune responses.

4.6. Arabidopsis-*H. arabidopsidis* interactions display spatio-temporally distinct ABA, SA, JA and JA/ET signaling outputs

COLORFUL Arabidopsis reporter lines were used to trace the spatio-temporal dynamics ABA, SA, JA, and JA/ET signaling outputs at nascent interaction sites with virulent and avirulent *H. arabidopsidis* isolates Noco2 and Emwa1. These lines were used in the current study for systematic COLORFUL reporter line analyses of single oomycete plant interaction sites, which revealed distinct reporter activity signatures in epidermis and mesophyll cells depending on the presence of and distance to the oomycete infection structures. Consequently, in order to describe spatial changes in hormone signaling during cell-to-cell interactions in the epidermal and mesophyll cell layers, cells were separately categorized into “invaded”, immediately “adjacent”, and “distant” domains (Figure 18a-b). Quantitative ABA, SA, JA, and JA/ET reporter analyses after infection with Noco2 or Emwa1 were conducted (Figure 18a). The initiation of HR-like cell death was observed on the third day after infection with the avirulent pathogen. Similarly, recent studies addressed the HR dynamics and recorded the HR-like cell death onset at the same time point with different biotrophs (Lukan et al. 2018; Pitino et al. 2016). Therefore, the quantitative analyses of hormone signaling in this study were performed at 1 and 2 dpi.

4.6.1. Emwa1 and Noco2 trigger unsynchronized predominant ABA signaling outputs locally confined to the invaded cells

Changes in endogenous ABA levels were investigated in previous studies in response to biotic and abiotic stresses in several plant species using classical methods, e.g., marker gene expression measurements, immunochemical assays, and biochemical assays for hormone quantification (Audenaert et al. 2002; García-Andrade et al. 2011; Kettner & Dörffling, 1995; Oide et al. 2013; Rezzonico et al. 1998; Steadman & Sequeira, 1970; Van Gijsegem et al. 2017; Whenham et al. 1986). For instance, ABA concentration has been quantified by LC-ESI-MS-MS-based hormone measurements over one day after infection of *A. thaliana* with the bacterium *Dickeya dadantii*, and Van Gijsegem et al. (2017) have observed increased ABA levels depending on the secretion of bacterial cell wall degrading enzymes. The authors of the later study reported that the magnitude of ABA increase correlated to the concentration of the infiltrated bacterial solution. However, these studies reported the changes in ABA content on a global level. Other research groups have developed a set of ABA reporters utilizing the promoter of ABA responsive genes to drive the expression of LUC, GUS, and GFP in order to monitor the changes in ABA signaling during different biotic and abiotic stresses (Ishitani et al. 1997; Söderman et al. 1999; Himmelbach et al. 2002; Christmann et al. 2005). However, data analyses from these studies provided only a fragmentary picture of pathogen-induced ABA signaling along with a general, non-specific overview about the spatiotemporal signaling of ABA during plant immunity.

In this project, which focused on individual plant-microbe interaction sites, it has been shown that both virulent and avirulent isolates induce ABA-dependent signaling outputs in haustoriated epidermal and mesophyll cells (Figure 19a-e). The Emwa1-induced ABA response was immediate and strong at 1 dpi, while the Noco2-induced ABA response was less extensive at 1 dpi. The spatially confined cell type-specific pattern of pathogen-activated ABA signaling suggests a potential role for ABA in modulating plant innate immunity during both compatible and incompatible *Arabidopsis-H. arabidopsidis* interactions. In previous studies, the hemibiotrophic bacterium *P. syringae* secretes effector molecules into *Arabidopsis* to induce the

4. DISCUSSION

expression of ABA biosynthetic and responsive genes, which subsequently inactivate MPK3/MPK6 in order to suppress the defense responses in Arabidopsis (De Torres-Zabala et al. 2007; De Torres-Zabala et al. 2009; Mine et al. 2017). COLORFUL-ABA reported high VENUS signal intensities in Noco2 haustoriated cells at a later point in time after infection, most likely for the purpose of suppressing ETI responses in order to promote the biotrophy.

4.6.2. The virulent and avirulent isolates of *H. arabidopsidis* differentially induce SA signaling in two distinct domains

Sensing the alteration in SA signaling at individual plant-microbe interaction sites using the COLORFUL-SA reporter showed that both virulent and avirulent isolates induced SA-dependent signaling outputs in haustoriated mesophyll and immediately adjacent cells (Figure 20a-e). These modifications in SA signaling at the nascent site of attack are in line with the well-documented role of SA in basal defense against virulent *H. arabidopsidis* isolates as well as RPP4-mediated resistance (Delaney et al. 1994; Mauch-Mani & Slusarenko 1996; McDowell et al. 2000; Van der Biezen et al. 2002). However, though invaded pavement cells did not exhibit elevated SA reporter activities during the compatible interaction, neighboring cells showed a high SA response (Figure 20a-e). Comparable to the results of this study, Caillaud et al. (2013) showed that virulent *H. arabidopsidis* Waco9 at a late stage of tissue colonization (6 dpi) actively suppresses *PR1* promoter-driven GUS expression in attacked mesophyll cells. Suppression of *PR1*-dependent SA signaling was suggested to be mediated by the effector molecule HaRxL62, which was found to be conserved in several *H. arabidopsidis* isolates (Asai et al. 2014).

Together, these results indicate that virulent and avirulent isolates efficiently suppress *PR1*-dependent SA signaling in invaded epidermal cells, but that mesophyll cells, particularly in the adjacent domain, mount a strong SA output response during ETI. This prominent boost of SA reporter activity provides an ETI-specific spatial signature, which correlates with the cellular boundaries of the ensuing HR-like cell death response. In support of a mechanistic context, SA is known to induce the expression of *PDLP5*, a plasmodesmatal protein that is important for SA triggered plasmodesmal

4. DISCUSSION

closure (Lee et al. 2011). A complex signaling circuit and well-coordinated intercellular communication might conceivably be required for activation and local containment of cell death, which would likely involve antagonistic hormone activities.

4.6.3. JA/ET signaling is activated to neutralize the activity of the SA pathway and to enhance biotrophy

In both compatible and incompatible interactions, JA signaling outputs were only marginally altered (**Figure 21a-e**). Possibly, this reflects a minor role of JA-dependent signaling in *Arabidopsis*-*H. arabidopsidis* interactions, which is supported by Thomma et al. (1998) who found no detectable changes of susceptibility to *H. arabidopsidis* in JA treatment experiments and in the JA receptor mutant *coi1*.

In marked contrast, inverted output signatures of the *PDF1.2*- and the *PR1*-controlled VENUS fluorescence intensities were observed during incompatible *Arabidopsis*-*Emwa1* interaction sites, particularly in adjacent and distant cells. This may suggest that antagonistic JA/ET signaling processes restrict the boost of the SA signal and cell death execution to the site of pathogen attack, thereby minimizing plant tissue damage and mitigating the growth-defense tradeoff in ETI (Karasov et al. 2017). JA/ET signaling was also triggered in cells immediately adjacent and distant to sites of Noco2 invasion (Figure 22a-e), but at considerably higher levels. This finding is consistent with the upregulation of *PDF1.2* expression in *Arabidopsis* infected with the virulent *H. arabidopsidis* isolate Waco9 (Caillaud et al. 2013), which is mediated by the *H. arabidopsidis* effector HaRxL44 in order to neutralize the activity of the SA pathway and to enhance biotrophy.

4.7. COLORFUL-biosensors are effective and suitable systems to address hormone crosstalk

In response to exogenous hormone treatment, COLORFUL-biosensors displayed a high specificity to the corresponding hormone. Combinations of different hormones were exogenously applied to verify the specificity of the hormone-controlled reporter,

4. DISCUSSION

as well as the appropriateness of all four COLORFUL reporters to investigate hormone crosstalk at cellular resolution. COLORFUL-ABA, -SA, -JA, and -JA/ET showed a corresponding hormone specific induction of the *PP2CA*, *PR1*, *VSP2*, and *PDF1-2a* promoters, respectively (Figure 16a-d). In addition, the COLORFUL-reporter system revealed an antagonistic effect of MeJA and ACC co-treatment on basal ABA reporter activity (Figure 16a). This finding is directly in line with a previous conclusion of Han et al. (2018) who demonstrated that the activation of the JA/ET signaling pathway antagonizes ABA signaling.

Contrary to the findings of De Torres-Zabala et al. (2009), Denancé et al. (2013), Fan et al. (2009), Manohar et al. (2017), Nahar et al. (2012), Tan et al. (2019) and Yasuda et al. (2008), who reported the antagonistic crosstalk between ABA and SA signaling pathways, COLORFUL-ABA and -SA reporter readouts did not show any interaction between both hormones (Figure 16a-b). These findings suggest that other ABA and SA signaling components might mediate such antagonistic interaction between ABA and SA signaling pathways.

Moreover, MeJA and ACC combination treatment showed slight but significant antagonistic effects on COLORFUL-SA reporter activity (Figure 16b). Overall this finding is in accordance with those reported by Lorenzo & Solano (2005), Chen et al. (2009), and Thaler et al. (2012). The authors in previous studies outlined that the JA/ET transcription factors EIN3 and EIL1 directly interact with the promoter of *ICS2* to suppress SA biosynthesis. Moreover, the cotreatment of COLORFUL-JA reporter seedlings with MeJA and ACC showed lower VENUS signal intensities relative to MeJA induced VENUS, suggesting that the activation of JA/ET signaling suppressed the JA reporter signal (Figure 16c). This is consistent with Lorenzo et al. (2004) and Lorenzo & Solano (2005) who revealed that JA and JA/ET antagonize each other via the MYC transcription factor of the JA pathway.

Finally, *PDF1.2a* controlled VENUS expression was induced after MeJA alone and in combination with ACC treatments, while ABA and SA treatments suppressed the basal VENUS signal intensity in the COLORFUL-JA/ET reporter (Figure 16d). Several studies reported the suppression of the JA/ET signaling cascade by ABA (Anderson et al. 2004; Kazan & Manners 2013; Nahar et al. 2012; Winter et al. 2007) as well as by

the SA signaling activation (Koornneef et al. 2008; Robert-Seilaniantz et al. 2011; Van der Does et al. 2013; Li et al. 2019b; Spoel et al. 2007; Leon-Reyes et al. 2010; Thaler et al. 2012).

4.8. COLORFUL-reporters show a pathogen type dependent hormone crosstalk

Several studies outlined the hormone crosstalk during biotic stress responses using hormone measurements or hormone responsive gene expression analyses on a global level (Li et al. 2019b; Robert-Seilaniantz et al. 2011; Vos et al. 2015). In this study, the biotrophic virulent Noco2 and the avirulent Emwa1 of the oomycete *H. arabidopsidis* showed a distinct spatial regulation of hormone signaling pathways. Hence, ABA, SA, and JA/ET signaling cascades were activated by both pathogens in distinct domains, while the JA signaling cascade was downregulated near to the site of invasion (Figure 33a-b).

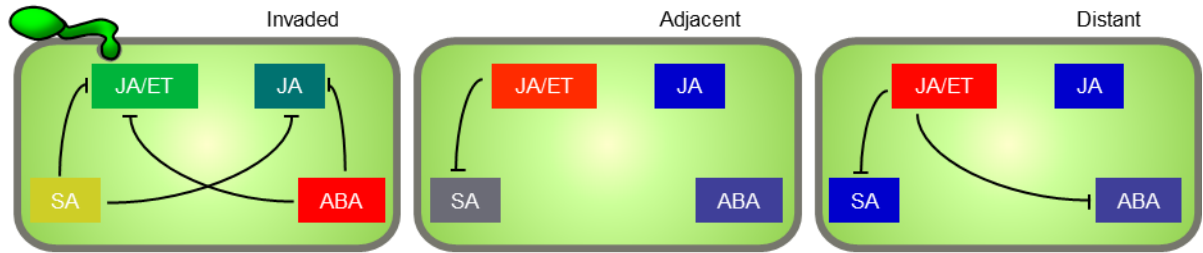
During the compatible interaction, SA and ABA responses were upregulated in Noco2-haustoriated cells, whereas JA and JA/ET signaling was downregulated in the very same cells. In the immediately adjacent and distant cells JA/ET signaling was strongly activated without any change in ABA and SA signaling (Figure 33a). In the incompatible interaction, *PR1*- and *PP2CA*-controlled VENUS expression was strongly induced in Emwa1 invaded domains, while *VSP2*- and *PDF1-2a*-controlled VENUS expression was suppressed in the same domains. The SA signaling that was strongly activated in the immediately adjacent cells was accompanied with a strong downregulation of JA/ET signaling (Figure 33b), possibly representing a demarcation signature to control initiation and local containment of the cell death response in ETI against Emwa1.

In short, these findings likely suggest inter- and intracellular as well as pathogen type-specific antagonistic hormone crosstalk. The Noco2- and Emwa1-triggered ABA and SA signaling in the invaded cells suppressed JA and JA/ET at the same domain. Moreover, Emwa1-induced SA signals in the adjacent cells suppressed JA/ET and JA signaling. On the other hand, the Noco2-activated JA/ET responses in the adjacent cells likely antagonized both ABA and SA.

4. DISCUSSION

Recently, the *PR1*-YFP-NLS and *VSP2*-YFP-NLS reporters were developed by Betsuyaku et al. (2018) who outlined distinct spatial activities of SA and JA signaling at *Arabidopsis*-*P. syringae* interaction sites. However, the set-up of these reporters lacks nuclear targeted reference and cell membrane markers. Therefore, the authors were not able to analyze the changes in hormone signaling at individual invasion sites.

a Virulent Isolate Noco2



b Avirulent Isolate Emwa1

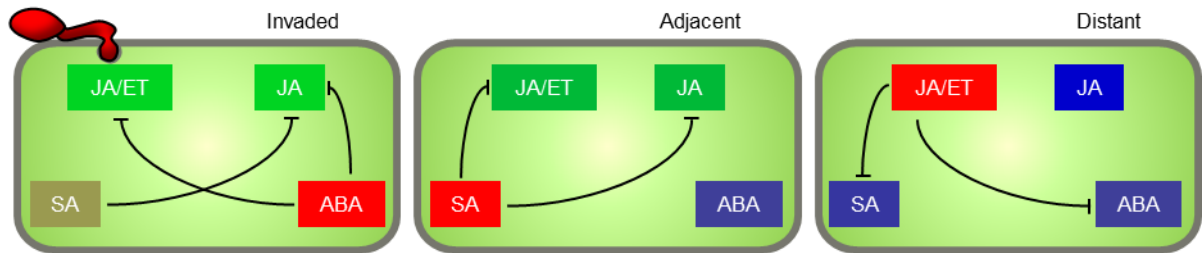


Figure 33: ABA, SA, JA and JA/ET spatio-temporal signatures and crosstalk control the pathogen performance at sites of *Arabidopsis*-*H. arabidopsidis* interactions. Quantitative heat map representations of ABA-, SA-, JA-, and JA/ET-reporter activities and crosstalk in leaves of 3-week-old *Arabidopsis* COLORFUL-ABA line #1, -SA line #1, -JA line #1, and -JA/ET line #1, respectively at 2 dpi with virulent (Noco2; **a**) and avirulent (Emwa1; **b**) isolates of the oomycete *H. arabidopsidis*. Data are adapted from figures 17e-20e. Data are relative to the uninfected mock. The black lines represent the antagonistic crosstalk between different hormones.

4.9. ABA functions as an essential common susceptibility factor at Arabidopsis biotrophic interaction sites

Notably, *G. orontii* induced an ABA signaling pattern (Figure 25a-c), which is similar to the pattern triggered by *H. arabidopsidis* Noco2 (Figure 19d-e). *G. orontii* and Noco2 are quite divergent, as both belong to two different kingdoms (Dean et al. 2014). Thus, activation of a cellularly confined ABA signaling is likely conserved across kingdoms during Arabidopsis interactions with biotrophic pathogens, while SA signaling did not change during Arabidopsis-*G. orontii* interactions (Figure 25d-e). Together, these findings imply a potential role of ABA in modulating innate immunity.

Subsequent infection analyses of ABA biosynthetic mutants with both biotrophic pathogens revealed that ABA promotes susceptibility of Arabidopsis to different biotrophs. Hence, ABA deficient mutants *aba1-101* and *aba2-1* showed lower frequencies of haustorial formation and enhanced disease resistance in comparison to the wildtype (Figures 26). This is consistent with what has been found in previous studies investigating the effect of ABA on plant immune responses using ABA treatments prior to pathogen assays or ABA deficient and signaling mutants (Cao et al. 2011).

ABA pretreatment conferred a suppressive effect on plant immune outputs during compatible and incompatible biotrophic interactions (Fan et al. 2009; Jiang et al. 2010; Koga et al. 2004; Mohr & Cahill 2003). Moreover, mutant analyses revealed that ABA deficient mutants showed enhanced resistance against different pathogens. For instance, tomato mutant *sitiens* against *B. cinerea* and *Oidium neolycopersici*, (Achuo et al. 2006; Audenaert et al. 2002). ABA biosynthetic mutants such as *aba2-12*, *aao3-2*, *aba2-1*, and *aba3-1* displayed an enhanced resistance to *B. cinerea* and *G. cichoracearum*. Additionally, ABA signaling mutants *abi2-1* and *abi1-1* were more resistant to *P. syringae*, while the ABA hypersensitive mutant *enhanced response to abscisic acid 1* (*era1*) as well as the overexpression of ABA biosynthetic genes *NCED* was hyper-susceptible relative to the wildtype (Cao et al. 2011; de Torres-Zabala et al. 2007; Fan et al. 2009; Goritschnig et al. 2008). These results suggest the activation of ABA biosynthesis and signaling in Arabidopsis plants by different adapted pathogens

to trigger ABA responsive genes in order to dampen the immune responses and promote virulence.

Comparing the COLORFUL-ABA reporter activities in the wildtype (Col-0) and *aba1-101* backgrounds after Noco2 and *G. orontii* infections confirmed the dependency of the pathogen-induced ABA signaling on ABA biosynthesis. Hence, the ABA deficient mutant exhibited significantly lower reporter signal intensities overall with both biotrophs (Figures 27-28). Based on previous studies, four possible scenarios have been suggested for ABA accumulation in pathogen-challenged plants: (1) host-controlled ABA biosynthesis upregulation (Cao et al. 2011), (2) inside-invader-controlled ABA biosynthesis and export to the host (Assante et al. 1977; Jiang et al. 2010), (3) invader-hijacked hormone biosynthesis in the host (de Torres-Zabala et al. 2007; de Torres-Zabala et al. 2009; Kettner & Dörffling 1995; Mine et al. 2017), and (4) invader-controlled inhibition of ABA catabolism via crosstalk with other hormones induced by combined abiotic and biotic stresses on Arabidopsis plants (Gupta et al. 2017). The drastic reduction of COLORFUL-ABA reporter activity in the ABA deficient mutant *aba1-101* supports the first scenario that the invading pathogen hijacks and activates the ABA biosynthetic pathways in the host to promote the susceptibility.

4.10. SnRK2D, SnRK2I, and AHG-3 are key regulatory components for pathogen-mediated ABA and SA signaling outputs

In this part of study, the objective was to unveil the core regulatory components of ABA signaling cascade that mediate ABA-dependent susceptibility in Arabidopsis after pathogen attack. Therefore, mutant analyses were performed for the individual and double knockout mutants of the ABA-positive regulators SnRK2s (Nakashima et al. 2009) after infection with the oomycete *H. arabidopsidis*_Noco2 and the fungus *G. orontii*. In addition, two studies were performed in our lab by Schliekmann (2017) and Lübbers (2018) who tested the disease phenotype of several mutants of the ABA-negative regulators of ABA signaling cascade PP2Cs (Kuhn et al. 2006; Nishimura et al. 2004).

4.10.1. The *SnRK2D* and *SnRK2I* loss-of-function double mutant exhibits reduced susceptibility and ABA signaling activities

The ABA positive regulators SnRk2D, SnRK2E and SnRK2I are highly activated upon ABA accumulation to phosphorylate the ABA downstream components (Manohar et al. 2017). Pathogen assays were performed to investigate the contribution of these kinases to the immune responses in Arabidopsis using single and double mutants. The double mutants *snrk2d snrk2i* showed a conserved role in mediating susceptibility in Arabidopsis to Noco2- and *G. orontii* comparable to the wildtype and the individual mutants *snrk2d* and *snrk2i* (Figure 29a-c). Next, comparative analyses of the pathogen associated-ABA signaling patterns were performed in *snrk2d*, *snrk2i*, *snrk2d snrk2i*, and the Col-0 genotypes. Significantly reduced ABA reporter activities were observed overall in the invaded, immediately adjacent, and distant domains of the double mutant in comparison to the wildtype and individual mutants which showed a similar pattern of ABA signaling upregulation in the invaded domain of the fungus *G. orontii* (Figure 29d-e). These findings demonstrate that both SnRK2D and SnRK2I function redundantly in mediating suppressive effects on post-penetration immune responses in Arabidopsis, as *snrk2d snrk2i* exhibited enhanced resistance, most likely because the ABA signaling cascade did not show any upregulation following pathogen attack.

The role of SnRK2 proteins in plant immune responses has not been adequately addressed (Mao et al. 2019). However, from SnRK2 subgroup III which are strongly activated by ABA (Umezawa et al. 2010), only SnRK2E/OST1 has been reported by Melotto et al. (2006) to mediate stomatal closure, leading to a preinvasive penetration resistance in response to *P. syringae* infections. Moreover, Lee et al. (2015) and Ton et al. (2009) demonstrated that several ABA-controlled and -uncontrolled SnRK2 genes were differentially and spatially regulated in response to biotic stress. For instance, Lee et al. (2015) reported the interaction between the partially ABA-dependent subgroup II member SnRK2C and NPR1. Therefore, the role of ABA responsive SnRK2 proteins need more focus in the future to uncover their interacting partners during plant-microbe interactions.

4.10.2. The *AHG-3/PP2CA* knockout mutant shows enhanced resistance as well as ABA and SA signaling responses

ABA hypersensitivity and induction of ABA-responsive genes were observed in different PP2C mutants: *abi1-2*, *hab1-2*, *pp2ca-1*, *ahg1-1*, and *ahg3-1* (Kuhn et al. 2006; Nishimura et al. 2007; Yoshida et al. 2006). It was unexpected, however, that only the *pp2ca-1* knockout mutant showed enhanced disease resistance to *H. arabidopsidis* and *G. orontii* (Schliekmann 2017; Lübbers 2018), while a point mutation in the same gene *ahg3-1* did not show any altered disease phenotype in comparison to the wildtype Col-0. Subsequent analyses of COLORFUL-ABA reporter activity in *pp2ca-1* and *ahg3-1* revealed significantly enhanced ABA signals only in the knockout mutant *pp2ca-1* (Figure 30, Figure31). Manohar et al. (2017) demonstrated that several PP2C members PP2C-D4/PP2C6, ABI1, and ABI2 displayed a high SA-binding affinity. Therefore, SA reporter activity was detected in *pp2ca1*, in contrast to the wildtype, and the missense mutation *ahg3-1* background after crossing of the COLORFUL-SA with these mutants. Interestingly, quantitative data analyses exhibited a strongly enhanced SA signaling in the Noco2 haustoriated cells as well as in the immediately adjacent cells in the *pp2ca1* mutant relative to the wildtype and the single amino acid exchange mutant *ahg3-1* (Figure 32). These data indicated a probable interaction or binding activity of PP2CA/AHG3 with SA, which seems to be lost in the knockout mutant *pp2ca1*, but not in the missense mutant *ahg3-1*. Therefore, the activated SA signaling at the site of attack may promote resistance to the tested biotrophic pathogens.

5. REFERENCES

- Aarts, N.; Metz, M.; Holub, E.; Staskawicz, B. J.; Daniels, M. J.; Parker, J. E. (1998). Different requirements for *EDS1* and *NDR1* by disease resistance genes define at least two R gene-mediated signaling pathways in Arabidopsis. *Proceedings of the National Academy of Sciences*, 95 (17), 10306-10311.
- Abuqamar, S.; Chai, M. F.; Luo, H.; Song, F.; Mengiste, T. (2008). Tomato protein kinase 1b mediates signaling of plant responses to necrotrophic fungi and insect herbivory. *The Plant Cell*, 20 (7), 1964-1983.
- Achuo, E.; Prinsen, E.; Höfte, M. (2006). Influence of drought, salt stress and abscisic acid on the resistance of tomato to *Botrytis cinerea* and *Oidium neolycopersici*. *Plant Pathology*, 55 (2), 178-186.
- Ádám, A.; Nagy, Z.; Kátay, G.; Mergenthaler, E.; Viczián, O. (2018). Signals of systemic immunity in plants: Progress and open questions. *International journal of molecular sciences*, 19 (4), 1146.
- Adie, B. A.; Pérez-Pérez, J.; Pérez-Pérez, M. M.; Godoy, M.; Sánchez-Serrano, J. J.; Schmelz, E. A.; Solano, R. (2007). ABA is an essential signal for plant resistance to pathogens affecting JA biosynthesis and the activation of defenses in Arabidopsis. *The Plant Cell*, 19 (5), 1665-1681.
- Alamillo, J. M.; Saénz, P.; García, J. A. (2006). Salicylic acid-mediated and RNA-silencing defense mechanisms cooperate in the restriction of systemic spread of plum pox virus in tobacco. *Plant Journal*, 48 (2), 217-227.
- Alazem, M.; Lin, N. S. (2015). Roles of plant hormones in the regulation of host-virus interactions. *Molecular plant pathology*, 16 (5), 529-540.
- Alazem, M.; Lin, N. S. (2017). Antiviral roles of abscisic acid in plants. *Frontiers in plant science*, 8, 1760.
- Alazem, M.; Kim, K. H.; Lin, N. S. (2019). Effects of abscisic acid and salicylic acid on gene expression in the antiviral RNA silencing pathway in Arabidopsis. *International journal of molecular sciences*, 20 (10), 2538.
- Alazem, M.; Tseng, K. C.; Chang, W. C.; Seo, J. K.; Kim, K. H. (2018). Elements involved in the Rsv3-mediated extreme resistance against an avirulent strain of soybean mosaic virus. *Viruses*, 10 (11), 581.
- Aliniaiefard, S.; Van Meeteren, U. (2013). Can prolonged exposure to low VPD disturb the ABA signalling in stomatal guard cells? *Journal of experimental botany*, 64 (12), 3551-3566.
- Alonso, J. M.; Hirayama, T.; Roman, G.; Nourizadeh, S.; Ecker, J. R. (1999). EIN2, a bifunctional transducer of ethylene and stress responses in Arabidopsis. *Science*, 284 (5423), 2148-2152.
- An, F.; Zhao, Q.; Ji, Y.; Li, W.; Jiang, Z.; Yu, X.; Zhang, C.; Han, Y.; He, W.; Liu, Y. (2010). Ethylene-induced stabilization of ETHYLENE INSENSITIVE3 and EIN3-LIKE1 is mediated by proteasomal degradation of EIN3 binding F-box 1 and 2 that requires EIN2 in Arabidopsis. *The Plant Cell*, 22 (7), 2384-2401.

5. REFERENCES

- Anderson, J. P.; Badruzsaufari, E.; Schenk, P. M.; Manners, J. M.; Desmond, O. J.; Ehlert, C.; Maclean, D. J.; Ebert, P. R.; Kazan, K. (2004). Antagonistic interaction between abscisic acid and jasmonate-ethylene signaling pathways modulates defense gene expression and disease resistance in Arabidopsis. *The Plant Cell*, 16 (12), 3460-3479.
- Asai, S.; Rallapalli, G.; Piquerez, S. J.; Caillaud, M. C.; Furzer, O. J.; Ishaque, N.; Wirthmueller, L.; Fabro, G.; Shirasu, K.; Jones, J. D. (2014). Expression profiling during Arabidopsis/downy mildew interaction reveals a highly-expressed effector that attenuates responses to salicylic acid. *PLoS pathogens*, 10 (10).
- Asai, S.; Shirasu, K.; Jones, J. (2015). *Hyaloperonospora arabidopsidis* (downy mildew) infection assay in Arabidopsis. *Bio-Protocol*, 5, e1627.
- Asai, T.; Tena, G.; Plotnikova, J.; Willmann, M. R.; Chiu, W. L.; Gomez-Gomez, L.; Boller, T.; Ausubel, F. M.; Sheen, J. (2002). MAP kinase signalling cascade in Arabidopsis innate immunity. *Nature*, 415 (6875), 977.
- Asami, T.; Nakagawa, Y. (2018). Preface to the Special Issue: Brief review of plant hormones and their utilization in agriculture. *Journal of Pesticide Science*, 43 (3), 154-158.
- Assante, G.; Merlini, L.; Nasini, G. (1977). (+)-Absciscic acid, a metabolite of the fungus *Cercospora rosicola*. *Experientia*, 33 (12), 1556-1557.
- Audenaert, K.; De Meyer, G. B.; Höfte, M. M. (2002). Absciscic acid determines basal susceptibility of tomato to *Botrytis cinerea* and suppresses salicylic acid-dependent signaling mechanisms. *Plant Physiology*, 128 (2), 491-501.
- Backer, R.; Naidoo, S.; Van den Berg, N. (2019). The NONEXPRESSOR OF PATHOGENESIS-RELATED GENES 1 (NPR1) and related family: mechanistic insights in plant disease resistance. *Frontiers in plant science*, 10 (102).
- Barrero, J. M.; Piqueras, P.; González-Guzmán, M.; Serrano, R.; Rodríguez, P. L.; Ponce, M. R.; Micol, J. L. (2005). A mutational analysis of the ABA1 gene of *Arabidopsis thaliana* highlights the involvement of ABA in vegetative development. *Journal of experimental botany*, 56 (418), 2071-2083.
- Bauer, H.; Ache, P.; Lautner, S.; Fromm, J.; Hartung, W.; Al-Rasheid, K. A.; Sonnewald, S.; Sonnewald, U.; Kneitz, S.; Lachmann, N. (2013). The stomatal response to reduced relative humidity requires guard cell-autonomous ABA synthesis. *Current Biology*, 23 (1), 53-57.
- Berrocal-Lobo, M.; Molina, A. (2004). Ethylene response factor 1 mediates Arabidopsis resistance to the soilborne fungus *Fusarium oxysporum*. *Molecular plant-microbe interactions*, 17 (7), 763-770.
- Betsuyaku, S.; Katou, S.; Takebayashi, Y.; Sakakibara, H.; Nomura, N.; Fukuda, H. (2018). Salicylic acid and jasmonic acid pathways are activated in spatially different domains around the infection site during effector-triggered immunity in *Arabidopsis thaliana*. *Plant and cell physiology*, 59 (1), 8-16.
- Bhattarai, K. K.; Xie, Q.-G.; Mantelin, S.; Bishnoi, U.; Girke, T.; Navarre, D. A.; Kaloshian, I. (2008). Tomato susceptibility to root-knot nematodes requires an intact jasmonic acid signaling pathway. *Molecular plant-microbe interactions*, 21 (9), 1205-1214.

5. REFERENCES

- Boller, T.; He, S. Y. (2009).** Innate immunity in plants: an arms race between pattern recognition receptors in plants and effectors in microbial pathogens. *Science*, 324 (5928), 742-744.
- Bonardi, V.; Cherkis, K.; Nishimura, M. T.; Dangl, J. L. (2012).** A new eye on NLR proteins: focused on clarity or diffused by complexity? *Current opinion in immunology*, 24 (1), 41-50.
- Boursiac, Y.; L  ran, S.; Corrat  -Faillie, C.; Gojon, A.; Krouk, G.; Lacombe, B. (2013).** ABA transport and transporters. *Trends in plant science*, 18 (6), 325-333.
- Boutrot, F.; Segonzac, C.; Chang, K. N.; Qiao, H.; Ecker, J. R.; Zipfel, C.; Rathjen, J. P. (2010).** Direct transcriptional control of the Arabidopsis immune receptor FLS2 by the ethylene-dependent transcription factors EIN3 and EIL1. *Proceedings of the National Academy of Sciences*, 107 (32), 14502-14507.
- Braun, U.; Shin, H. D.; Takamatsu, S.; Meeboon, J.; Kiss, L.; Lebeda, A.; Kitner, M.; G  tz, M. (2019).** Phylogeny and taxonomy of *Golovinomyces orontii* revisited. *Mycological progress*, 18 (3), 335-357.
- Broekaert, W. F.; Delaur  , S. L.; De Bolle, M. F.; Cammue, B. P. (2006).** The role of ethylene in host-pathogen interactions. *Annu. Rev. Phytopathol.*; 44, 393-416.
- Broekgaarden, C.; Caarls, L.; Vos, I. A.; Pieterse, C. M.; Van Wees, S. C. (2015).** Ethylene: traffic controller on hormonal crossroads to defense. *Plant physiology*, 169 (4), 2371-2379.
- Brown, R. L.; Kazan, K.; McGrath, K. C.; Maclean, D. J.; Manners, J. M. (2003).** A role for the GCC-box in jasmonate-mediated activation of the *PDF1. 2* gene of Arabidopsis. *Plant physiology*, 132 (2), 1020-1032.
- Brunoud, G.; Wells, D. M.; Oliva, M.; Larrieu, A.; Mirabet, V.; Burrow, A. H.; Beeckman, T.; Kepinski, S.; Traas, J.; Bennett, M. J. (2012).** A novel sensor to map auxin response and distribution at high spatio-temporal resolution. *Nature*, 482 (7383), 103-106.
- Caarls, L.; Pieterse, C. M.; Van Wees, S. (2015).** How salicylic acid takes transcriptional control over jasmonic acid signaling. *Frontiers in plant science*, 6 (170).
- Caarls, L.; Van der Does, D.; Hickman, R.; Jansen, W.; Verk, M. C. V.; Proietti, S.; Lorenzo, O.; Solano, R.; Pieterse, C. M.J.; Van Wees, S. (2017).** Assessing the role of ETHYLENE RESPONSE FACTOR transcriptional repressors in salicylic acid-mediated suppression of jasmonic acid-responsive genes. *Plant and cell physiology*, 58 (2), 266-278.
- Cabral, A.; Stassen, J. H.; Seidl, M. F.; Bautor, J.; Parker, J. E.; Van den Ackerveken, G. (2011).** Identification of *Hyaloperonospora arabidopsidis* transcript sequences expressed during infection reveals isolate-specific effectors. *PLoS One*, 6 (5): e19328.
- Cai, S.; Chen, G.; Wang, Y.; Huang, Y.; Marchant, D. B.; Wang, Y.; Yang, Q.; Dai, F.; Hills, A.; Franks, P. J. (2017).** Evolutionary conservation of ABA signaling for stomatal closure. *Plant physiology*, 174 (2), 732-747.
- Caillaud, M. C.; Asai, S.; Rallapalli, G.; Piquerez, S.; Fabro, G.; Jones, J. D. (2013).** A downy mildew effector attenuates salicylic acid-triggered immunity in Arabidopsis by interacting with the host mediator complex. *PLoS biology*, 11 (12): e1001732.
- Campos, M. L.; Kang, J. H.; Howe, G. A. (2014).** Jasmonate-triggered plant immunity. *Journal of chemical ecology*, 40 (7), 657-675.

5. REFERENCES

- Cao, F. Y.; Yoshioka, K.; Desveaux, D. (2011).** The roles of ABA in plant-pathogen interactions. *Journal of plant research*, 124 (4), 489-499.
- Cao, H.; Bowling, S. A.; Gordon, A. S.; Dong, X. (1994).** Characterization of an Arabidopsis mutant that is nonresponsive to inducers of systemic acquired resistance. *The Plant cell*, 6 (11), 1583-1592.
- Cao, H.; Glazebrook, J.; Clarke, J. D.; Volko, S.; Dong, X. (1997).** The Arabidopsis NPR1 gene that controls systemic acquired resistance encodes a novel protein containing ankyrin repeats. *Cell*, 88 (1), 57-63.
- Cao, Y.; Liang, Y.; Tanaka, K.; Nguyen, C. T.; Jedrzejczak, R. P.; Joachimiak, A.; Stacey, G. (2014).** The kinase LYK5 is a major chitin receptor in Arabidopsis and forms a chitin-induced complex with related kinase CERK1. *elife*, 3, e03766.
- Carstens, M.; McCrindle, T. K.; Adams, N.; Diener, A.; Guzha, D. T.; Murray, S. L.; Parker, J. E.; Denby, K. J.; Ingle, R. A. (2014).** Increased resistance to biotrophic pathogens in the Arabidopsis *Constitutive Induced Resistance 1* mutant is EDS1 and PAD4-dependent and modulated by environmental temperature. *PLoS One*, 9 (10): e109853.
- Cesari, S. (2018).** Multiple strategies for pathogen perception by plant immune receptors. *New Phytologist*, 219 (1), 17-24.
- Chater, C. C.; Oliver, J.; Casson, S.; Gray, J. E. (2014).** Putting the brakes on: abscisic acid as a central environmental regulator of stomatal development. *New Phytologist*, 202 (2), 376-391.
- Chen, H.; Xue, L.; Chintamanani, S.; Germain, H.; Lin, H.; Cui, H.; Cai, R.; Zuo, J.; Tang, X.; Li, X. (2009).** ETHYLENE INSENSITIVE3 and ETHYLENE INSENSITIVE3-LIKE1 repress *SALICYLIC ACID INDUCTION DEFICIENT2* expression to negatively regulate plant innate immunity in Arabidopsis. *The Plant cell*, 21 (8), 2527-2540.
- Chen, Y.; Wang, Y.; Huang, J.; Zheng, C.; Cai, C.; Wang, Q.; Wu, C. A. (2017).** Salt and methyl jasmonate aggravate growth inhibition and senescence in Arabidopsis seedlings via the JA signaling pathway. *Plant Science*, 261, 1-9.
- Chen, Z. H.; Wang, Y.; Wang, J. W.; Babla, M.; Zhao, C.; García-Mata, C.; Sani, E.; Differ, C.; Mak, M.; Hills, A. (2016).** Nitrate reductase mutation alters potassium nutrition as well as nitric oxide-mediated control of guard cell ion channels in Arabidopsis. *New Phytologist*, 209 (4), 1456-1469.
- Chini, A.; Fonseca, S.; Fernandez, G.; Adie, B.; Chico, J.; Lorenzo, O.; Garcia-Casado, G.; López-Vidriero, I.; Lozano, F. M.; Ponce, M. (2007).** The JAZ family of repressors is the missing link in jasmonate signalling. *Nature*, 448 (7154), 666-671.
- Choi, H. I.; Hong, J. H.; Ha, J. O.; Kang, J. Y.; Kim, S. Y. (2000).** ABFs, a family of ABA-responsive element binding factors. *Journal of Biological Chemistry*, 275 (3), 1723-1730.
- Christmann, A.; Hoffmann, T.; Teplova, I.; Grill, E.; Müller, A. (2005).** Generation of active pools of abscisic acid revealed by *in vivo* imaging of water-stressed Arabidopsis. *Plant physiology*, 137 (1), 209-219.
- Coates, M. E.; Beynon, J. L. (2010).** *Hyaloperonospora arabidopsidis* as a pathogen model. *Annual review of phytopathology*, 48, 329-345.

5. REFERENCES

- Cornish, K.; Zeevaart, J. A. (1984).** Absciscic acid metabolism in relation to water stress and leaf age in *Xanthium strumarium*. *Plant physiology*, 76 (4), 1029-1035.
- Cotelle, V.; Leonhardt, N. (2019).** ABA signaling in guard cells. *Advances in Botanical Research*, 92, 115-170.
- Cruz, T.; Carvalho, R. F.; Richardson, D. N.; Duque, P. (2014).** Absciscic acid (ABA) regulation of Arabidopsis SR protein gene expression. *International journal of molecular sciences*, 15 (10), 17541-17564.
- Cui, H.; Tsuda, K.; Parker, J. E. (2015).** Effector-triggered immunity: from pathogen perception to robust defense. *Annual review of plant biology*, 66, 487-511.
- Cui, Y.; Ye, J.; Guo, X.; Chang, H.; Yuan, C.; Wang, Y.; Shuai, H.; Xuanming L.; Li, X. (2014).** Arabidopsis casein kinase 1-like 2 involved in absciscic acid signal transduction pathways. *Journal of plant interactions*, 9 (1), 19-25.
- Cutler, S. R.; Ehrhardt, D. W.; Griffitts, J. S.; Somerville, C. R. (2000).** Random GFP::cDNA fusions enable visualization of subcellular structures in cells of Arabidopsis at a high frequency. *Proceedings of the National Academy of Sciences*, 97 (7), 3718-3723.
- D'Agostino, I. B.; Deruere, J.; Kieber, J. J. (2000).** Characterization of the response of the Arabidopsis response regulator gene family to cytokinin. *Plant physiology*, 124 (4), 1706-1717.
- Davis, G. C.; Hein, M. B.; Neely, B. C.; Sharp, C. R.; Carnes, M. G. (1985).** Strategies for the determination of plant hormones. *Analytical Chemistry*, 57 (6), 638A-648A.
- De Bruyne, L.; Höfte, M.; De Vleeschauwer, D. (2014).** Connecting growth and defense: the emerging roles of brassinosteroids and gibberellins in plant innate immunity. *Molecular Plant*, 7 (6), 943-959.
- De Torres Zabala, M.; Bennett, M. H.; Truman, W. H.; Grant, M. R. (2009).** Antagonism between salicylic and absciscic acid reflects early host-pathogen conflict and moulds plant defence responses. *The Plant Journal*, 59 (3), 375-386.
- De Torres-Zabala, M.; Truman, W.; Bennett, M. H.; Lafforgue, G.; Mansfield, J. W.; Egea, P. R.; Bögre, L.; Grant, M. (2007).** *Pseudomonas syringae* pv. tomato hijacks the Arabidopsis absciscic acid signalling pathway to cause disease. *The EMBO journal*, 26 (5), 1434-1443.
- De Vleeschauwer, D.; Xu, J.; Höfte, M. (2014).** Making sense of hormone-mediated defense networking: from rice to Arabidopsis. *Frontiers in plant science*, 5 (611), 1-15.
- De Vleeschauwer, D.; Yang, Y.; Cruz, C. V.; Höfte, M. (2010).** Absciscic acid-induced resistance against the brown spot pathogen *Cochliobolus miyabeanus* in rice involves MAP kinase-mediated repression of ethylene signaling. *Plant physiology*, 152 (4), 2036-2052.
- Dean, R. A.; Lichens-Park, A.; Kole, C. (2014).** Genomics of plant-associated fungi and oomycetes: dicot pathogens. *Springer*. Doi: 10.1007/978-3-662-44056-8.
- Deb, D.; Anderson, R. G.; How-Yew-Kin, T.; Tyler, B. M.; McDowell, J. M. (2018).** Conserved RxLR effectors from oomycetes *Hyaloperonospora arabidopsidis* and *Phytophthora sojae* suppress PAMP-and effector-triggered immunity in diverse plants. *Molecular plant-microbe interactions*, 31 (3), 374-385.

5. REFERENCES

- Delaney, T. P.; Uknes, S.; Vernooij, B.; Friedrich, L.; Weymann, K.; Negrotto, D.; Gaffney, T.; Gut-Rella, M.; Kessmann, H.; Ward, E. (1994).** A central role of salicylic acid in plant disease resistance. *Science*, 266 (5188), 1247-1250.
- Denancé, N.; Sánchez-Vallet, A.; Goffner, D.; Molina, A. (2013).** Disease resistance or growth: the role of plant hormones in balancing immune responses and fitness costs. *Frontiers in plant science*, 4 (155), 1-15.
- Derksen, H.; Rampitsch, C.; Daayf, F. (2013).** Signaling cross-talk in plant disease resistance. *Plant Science*, 207, 79-87.
- Dickman, M. B.; Fluhr, R. (2013).** Centrality of host cell death in plant-microbe interactions. *Annual review of phytopathology*, 51, 543-570.
- Ding, Y.; Sun, T.; Ao, K.; Peng, Y.; Zhang, Y.; Li, X.; Zhang, Y. (2018).** Opposite roles of salicylic acid receptors NPR1 and NPR3/NPR4 in transcriptional regulation of plant immunity. *Cell*, 173 (6), 1454-1467.
- Dombrecht, B.; Xue, G. P.; Sprague, S. J.; Kirkegaard, J. A.; Ross, J. J.; Reid, J. B.; Fitt, Gary P.; Sewelam, N.; Schenk, P. M.; Manners, J. M. (2007).** MYC2 differentially modulates diverse jasmonate-dependent functions in Arabidopsis. *The Plant cell*, 19 (7), 2225-2245.
- Dong, H.; Ma, X.; Zhang, P.; Wang, H.; Li, X.; Liu, J.; Bai, L.; Song, C.P. (2020).** Characterization of *Arabidopsis thaliana* root-related mutants reveals ABA regulation of plant development and drought resistance. *Journal of Plant Growth Regulation*. Doi:10.1007/s00344-020-10076-6
- Dong, T.; Park, Y.; Hwang, I. (2015).** Absciscic acid: biosynthesis, inactivation, homeostasis and signalling. *Essays in biochemistry*, 58, 29-48.
- Dou, D.; Zhou, J. M. (2012).** Phytopathogen effectors subverting host immunity: different foes, similar battleground. *Cell host microbe*, 12 (4), 484-495.
- Erwig, J.; Ghareeb, H.; Kopischke, M.; Hacke, R.; Matei, A.; Petutschnig, E.; Lipka, V. (2017).** Chitin-induced and CHITIN ELICITOR RECEPTOR KINASE1 (CERK1) phosphorylation-dependent endocytosis of *Arabidopsis thaliana* LYSIN MOTIF-CONTAINING RECEPTOR-LIKE KINASE5 (LYK5). *New Phytologist*, 215 (1), 382-396.
- Fabro, G.; Steinbrenner, J.; Coates, M.; Ishaque, N.; Baxter, L.; Studholme, D. J.; Körner, E.; Allen, R. L.; Piquerez, S. J. M.; Rougon-Cardoso, A. (2011).** Multiple candidate effectors from the oomycete pathogen *Hyaloperonospora arabidopsidis* suppress host plant immunity. *PLoS pathogens*, 7 (11), 1-18, e1002348.
- Fan, J.; Hill, L.; Crooks, C.; Doerner, P.; Lamb, C. (2009).** Absciscic acid has a key role in modulating diverse plant-pathogen interactions. *Plant physiology*, 150 (4), 1750-1761.
- Fawke, S.; Doumane, M.; Schornack, S. (2015).** Oomycete interactions with plants: infection strategies and resistance principles. *Microbiology and Molecular Biology Reviews*, 79 (3), 263-280.
- Federici, F.; Dupuy, L.; Laplace, L.; Heisler, M.; Haseloff, J. (2012).** Integrated genetic and computation methods for in planta cytometry. *Nature Methods*, 9 (5), 483.
- Feechan, A.; Turnbull, D.; Stevens, L. J.; Engelhardt, S.; Birch, P. R.; Hein, I.; Gilroy, E. M. (2015).** The hypersensitive response in PAMP- and effector-triggered immune responses. In *Plant Programmed Cell Death* (pp. 235-268): Springer.

5. REFERENCES

- Finkelstein, R. (2013).** Absciscic acid synthesis and response. *American Society of Plant Biologists, Arabidopsis Book*, 11: e0166.
- Finkelstein, R. R.; Rock, C. D. (2002).** Absciscic acid biosynthesis and response. *American Society of Plant Biologists, Arabidopsis Book*, 1: e0058.
- Fonseca, S.; Chini, A.; Hamberg, M.; Adie, B.; Porzel, A.; Kramell, R.; Miersch, O.; Wasternack, C.; Solano, R. (2009).** (+)-7-iso-Jasmonoyl-L-isoleucine is the endogenous bioactive Jasmonate. *Nature Chemical Biology*, 5 (5), 344-350.
- Forcat, S.; Bennett, M. H.; Mansfield, J. W.; Grant, M. R. (2008).** A rapid and robust method for simultaneously measuring changes in the phytohormones ABA, JA and SA in plants following biotic and abiotic stress. *Plant Methods*, 4 (16). Doi:10.1186/1746-4811-4-16.
- Fournier, E.; Giraud, T. (2008).** Sympatric genetic differentiation of a generalist pathogenic fungus, *Botrytis cinerea*, on two different host plants, grapevine and bramble. *Journal of evolutionary biology*, 21 (1), 122-132.
- Frye, C. A.; Innes, R. W. (1998).** An Arabidopsis mutant with enhanced resistance to powdery mildew. *The Plant cell*, 10 (6), 947-956.
- Frye, C. A.; Tang, D.; Innes, R. W. (2001).** Negative regulation of defense responses in plants by a conserved MAPKK kinase. *Proceedings of the National Academy of Sciences*, 98 (1), 373-378.
- Fu, Z. Q.; Yan, S.; Saleh, A.; Wang, W.; Ruble, J.; Oka, N.; Mohan, R.; Spoel, S. H.; Tada, Y.; Zheng, N. (2012).** NPR3 and NPR4 are receptors for the immune signal salicylic acid in plants. *Nature*, 486 (7402): 228-232.
- Fujii, H.; Zhu, J. K. (2009).** Arabidopsis mutant deficient in 3 absciscic acid-activated protein kinases reveals critical roles in growth, reproduction, and stress. *Proceedings of the National Academy of Sciences*, 106 (20), 8380-8385.
- Fujii, H.; Verslues, P. E.; Zhu, J. K. (2011).** Arabidopsis decuple mutant reveals the importance of SnRK2 kinases in osmotic stress responses *in vivo*. *Proceedings of the National Academy of Sciences*, 108 (4), 1717-1722.
- Fujita, Y.; Nakashima, K.; Yoshida, T.; Katagiri, T.; Kidokoro, S.; Kanamori, N.; Umezawa, T.; Fujita, M.; Maruyama, K.; Ishiyama, K. (2009).** Three SnRK2 protein kinases are the main positive regulators of absciscic acid signaling in response to water stress in Arabidopsis. *Plant and cell physiology*, 50 (12), 2123-2132.
- Gallie, D. R. (2015).** Appearance and elaboration of the ethylene receptor family during land plant evolution. *Plant molecular biology*, 87 (4-5), 521-539.
- Gao, L. W.; Lyu, S. W.; Tang, J.; Zhou, D. Y.; Bonnema, G.; Xiao, D.; Hou, X.; Zhang, C. W. (2017).** Genome-wide analysis of auxin transport genes identifies the hormone responsive patterns associated with leafy head formation in Chinese cabbage. *Scientific reports*, 7 (42229).
- García-Andrade, J.; Ramírez, V.; Flors, V.; Vera, P. (2011).** Arabidopsis *ocp3* mutant reveals a mechanism linking ABA and JA to pathogen-induced callose deposition. *The Plant Journal*, 67 (5), 783-794.
- Garcion, C.; Lohmann, A.; Lamodièrre, E.; Catinot, J.; Buchala, A.; Doermann, P.; Métraux, J. P. (2008).** Characterization and biological function of the *ISOCHORISMATE SYNTHASE2* gene of Arabidopsis. *Plant physiology*, 147 (3), 1279-1287.

5. REFERENCES

- Geng, Y.; Wu, R.; Wee, C. W.; Xie, F.; Wei, X.; Chan, P. M. Y.; Tham, C.; Duan, L.; Dinneny, J. R. (2013).** A spatio-temporal understanding of growth regulation during the salt stress response in *Arabidopsis*. *The Plant cell*, 25 (6), 2132-2154.
- Ghareeb, H.; Becker, A.; Iven, T.; Feussner, I.; Schirawski, J. (2011).** *Sporisorium reilianum* infection changes inflorescence and branching architectures of maize. *Plant physiology*, 156 (4), 2037-2052.
- Ghareeb, H.; Laukamm, S.; Lipka, V. (2016).** COLORFUL-Circuit: a platform for rapid multigene assembly, delivery, and expression in plants. *Frontiers in plant science*, 7 (246).
- Gimenez-Ibanez, S.; Hann, D. R.; Ntoukakis, V.; Petutschnig, E.; Lipka, V.; Rathjen, J. P. (2009).** AvrPtoB targets the LysM receptor kinase CERK1 to promote bacterial virulence on plants. *Current Biology*, 19 (5), 423-429.
- Gina, N.; Seabolt, S.; Zhang, C.; Salimian, S.; Watkins, T. A.; Lu, H. (2011).** Genetic dissection of salicylic acid-mediated defense signaling networks in *Arabidopsis*. *Genetics*, 189 (3), 851-859.
- Glauser, G.; Grata, E.; Dubugnon, L.; Rudaz, S.; Farmer, E. E.; Wolfender, J. L. (2008).** Spatial and temporal dynamics of jasmonate synthesis and accumulation in *Arabidopsis* in response to wounding. *Journal of Biological Chemistry*, 283 (24), 16400-16407.
- Glazebrook, J. (2005).** Contrasting mechanisms of defense against biotrophic and necrotrophic pathogens. *Annual Review Phytopathol.*; 43, 205-227.
- Glazebrook, J.; Rogers, E. E.; Ausubel, F. M. (1996).** Isolation of *Arabidopsis* mutants with enhanced disease susceptibility by direct screening. *Genetics*, 143 (2), 973-982.
- González-Guzmán, M.; Apostolova, N.; Bellés, J. M.; Barrero, J. M.; Piqueras, P.; Ponce, M. R.; Micol, J. L.; Serrano, R.; Rodríguez, P. L. (2002).** The short-chain alcohol dehydrogenase ABA2 catalyzes the conversion of xanthoxin to abscisic aldehyde. *The Plant cell*, 14 (8), 1833-1846.
- Goritschnig, S.; Weihmann, T.; Zhang, Y.; Fobert, P.; McCourt, P.; Li, X. (2008).** A novel role for protein farnesylation in plant innate immunity. *Plant physiology*, 148 (1), 348-357.
- Groen, S. C.; Whiteman, N. K.; Bahrami, A. K.; Wilczek, A. M.; Cui, J.; Russell, J. A.; Cibrian-Jaramillo, A.; Butler, I. A.; Rana, J. D.; Huang, G.-H. (2013).** Pathogen-triggered ethylene signaling mediates systemic-induced susceptibility to herbivory in *Arabidopsis*. *The Plant cell*, 25 (11), 4755-4766.
- Gruner, K.; Zeier, T.; Aretz, C.; Zeier, J. (2018).** A critical role for *Arabidopsis* MILDEW RESISTANCE LOCUS O2 in systemic acquired resistance. *The Plant Journal*, 94 (6), 1064-1082.
- Gupta, A.; Hisano, H.; Hojo, Y.; Matsuura, T.; Ikeda, Y.; Mori, I. C.; Senthil-Kumar, M. (2017).** Global profiling of phytohormone dynamics during combined drought and pathogen stress in *Arabidopsis thaliana* reveals ABA and JA as major regulators. *Scientific Reports*, 7 (1), 1-13.
- Guzman, P.; Ecker, J. R. (1990).** Exploiting the triple response of *Arabidopsis* to identify ethylene-related mutants. *The Plant cell*, 2 (6), 513-523.
- Hacquard, S.; Spaepen, S.; Garrido-Oter, R.; Schulze-Lefert, P. (2017).** Interplay between innate immunity and the plant microbiota. *Annual review of phytopathology*, 55, 565-589.

5. REFERENCES

- Hall, A. E.; Bleecker, A. B. (2003).** Analysis of combinatorial loss-of-function mutants in the Arabidopsis ethylene receptors reveals that the *ers1 etr1* double mutant has severe developmental defects that are EIN2 dependent. *The Plant cell*, 15 (9), 2032-2041.
- Hall, B. P.; Shakeel, S. N.; Amir, M.; Haq, N. U.; Qu, X.; Schaller, G. E. (2012).** Histidine kinase activity of the ethylene receptor ETR1 facilitates the ethylene response in Arabidopsis. *Plant physiology*, 159 (2), 682-695.
- Han, G. Z. (2016).** Evolution of jasmonate biosynthesis and signaling mechanisms. *Journal of experimental botany*, 68 (6), 1323-1331.
- Han, W. Y.; Li, X.; Ahammed, G. J. (2018).** Stress physiology of tea in the face of climate change. *Springer*. Doi: 10.1007/978-981-13-2140-5.
- Harb, A.; Krishnan, A.; Ambavaram, M. M.; Pereira, A. (2010).** Molecular and physiological analysis of drought stress in Arabidopsis reveals early responses leading to acclimation in plant growth. *Plant physiology*, 154 (3), 1254-1271.
- Hatsugai, N.; Igarashi, D.; Mase, K.; Lu, Y.; Tsuda, Y.; Chakravarthy, S.; Wei, H.L.; Foley, J. W.; Collmer, A.; Glazebrook, J. (2017).** A plant effector-triggered immunity signaling sector is inhibited by pattern-triggered immunity. *The EMBO journal*, 36 (18), 2758-2769.
- Hauser, F.; Waadt, R.; Schroeder, J. I. (2011).** Evolution of abscisic acid synthesis and signaling mechanisms. *Current Biology*, 21 (9), 346-355.
- Hayashi, K. I.; Nakamura, S.; Fukunaga, S.; Nishimura, T.; Jenness, M. K.; Murphy, A. S.; Motose, H.; Nozaki, H.; Furutani, M.; Aoyama, T. (2014).** Auxin transport sites are visualized *in planta* using fluorescent auxin analogs. *Proceedings of the National Academy of Sciences*, 111 (31), 11557-11562.
- Hayes, S. (2018).** Revealing the invisible: a synthetic reporter for ABA. *Plant physiology*, 177 (4), 1346-1347.
- Heim, R.; Tsien, R. Y. (1996).** Engineering green fluorescent protein for improved brightness, longer wavelengths and fluorescence resonance energy transfer. *Current Biology*, 6 (2), 178-182.
- Henry, E.; Yadeta, K. A.; Coaker, G. (2013).** Recognition of bacterial plant pathogens: local, systemic and transgenerational immunity. *New Phytologist*, 199 (4), 908-915.
- Himmelbach, A.; Hoffmann, T.; Leube, M.; Höhener, B.; Grill, E. (2002).** Homeodomain protein ATHB6 is a target of the protein phosphatase ABI1 and regulates hormone responses in Arabidopsis. *The EMBO journal*, 21 (12), 3029-3038.
- Hogenhout, S. A.; Bos, J. I. (2011).** Effector proteins that modulate plant-insect interactions. *Current opinion in plant biology*, 14 (4), 422-428.
- Holt, B. F.; Belkhadir, Y.; Dangl, J. L. (2005).** Antagonistic control of disease resistance protein stability in the plant immune system. *Science*, 309 (5736), 929-932.
- Holub, E. B. (2008).** Natural history of *Arabidopsis thaliana* and oomycete symbioses. *European Journal of Plant Pathology*, 122, 91-109.
- Hong Gao, Y.; Yu, Y.; gang Hu, X.; juan Cao, Y.; zhong Wu, J. (2013).** Imaging of jasmonic acid binding sites in tissue. *Analytical biochemistry*, 440 (2), 205-211.

5. REFERENCES

- Huang, J. S. (1986). Ultrastructure of bacterial penetration in plants. *Annual review of phytopathology*, 24 (1), 141-157.
- Huysmans, M.; Lema, S.; Coll, N. S.; Nowack, M. K. (2017). Dying two deaths-programmed cell death regulation in development and disease. *Current opinion in plant biology*, 35, 37-44.
- Irani, N. G.; Di Rubbo, S.; Mylle, E.; Van den Begin, J.; Schneider-Pizoń, J.; Hniliková, J.; Šiša, M.; Buyst, D.; Vilarrasa-Blasi, J.; Szatmári, A.-M. (2012). Fluorescent castasterone reveals BRI1 signaling from the plasma membrane. *Nature chemical biology*, 8 (6), 583- 589.
- Ishitani, M.; Xiong, L.; Stevenson, B.; Zhu, J. K. (1997). Genetic analysis of osmotic and cold stress signal transduction in Arabidopsis: interactions and convergence of abscisic acid-dependent and abscisic acid-independent pathways. *The Plant cell*, 9 (11), 1935-1949.
- Jagadeeswaran, G.; Raina, S.; Acharya, B. R.; Maqbool, S. B.; Mosher, S. L.; Appel, H. M.; Schultz, J. C.; Klessig, D. F.; Raina, R. (2007). Arabidopsis *GH3-LIKE DEFENSE GENE 1* is required for accumulation of salicylic acid, activation of defense responses and resistance to *Pseudomonas syringae*. *The Plant Journal*, 51 (2), 234-246.
- Jaillais, Y.; Chory, J. (2010). Unraveling the paradoxes of plant hormone signaling integration. *Nature structural molecular biology*, 17 (6), 642-645.
- Jiang, C. J.; Shimono, M.; Sugano, S.; Kojima, M.; Yazawa, K.; Yoshida, R.; Inoue, H.; Hayashi, N.; Sakakibara, H.; Takatsuji, H. (2010). Abscisic acid interacts antagonistically with salicylic acid signaling pathway in rice-*Magnaporthe grisea* interaction. *Molecular Plant-microbe interactions*, 23 (6), 791-798.
- Jones, A. M. (2016). A new look at stress: abscisic acid patterns and dynamics at high-resolution. *New Phytologist*, 210 (1), 38-44.
- Jones, A. M.; Danielson, J. Å.; ManojKumar, S. N.; Lanquar, V.; Grossmann, G.; Frommer, W. B. (2014). Abscisic acid dynamics in roots detected with genetically encoded FRET sensors. *elife*, 3, e01741.
- Jones, J. D.; Dangl, J. L. (2006). The plant immune system. *Nature*, 444 (7117), 323-329.
- Jordan, W. R.; Brown, K. W.; Thomas, J. C. (1975). Leaf age as a determinant in stomatal control of water loss from cotton during water stress. *Plant physiology*, 56 (5), 595-599.
- Kachroo, A.; Kachroo, P. (2009). Fatty acid-derived signals in plant defense. *Annual review of phytopathology*, 47, 153-176.
- Kang, J.; Hwang, J. U.; Lee, M.; Kim, Y. Y.; Assmann, S. M.; Martinoia, E.; Lee, Y. (2010). PDR-type ABC transporter mediates cellular uptake of the phytohormone abscisic acid. *Proceedings of the National Academy of Sciences*, 107 (5), 2355-2360.
- Kanno, Y.; Hanada, A.; Chiba, Y.; Ichikawa, T.; Nakazawa, M.; Matsui, M.; Koshiba, T.; Kamiya, Y.; Seo, M. (2012). Identification of an abscisic acid transporter by functional screening using the receptor complex as a sensor. *Proceedings of the National Academy of Sciences*, 109 (24), 9653-9658.
- Karasov, T. L.; Chae, E.; Herman, J. J.; Bergelson, J. (2017). Mechanisms to mitigate the trade-off between growth and defense. *The Plant cell*, 29 (4), 666-680.

5. REFERENCES

- Katagiri, F.; Tsuda, K. (2010).** Understanding the plant immune system. *Molecular Plant-microbe interactions*, 23 (12), 1531-1536.
- Katsir, L.; Chung, H. S.; Koo, A. J.; Howe, G. A. (2008).** Jasmonate signaling: a conserved mechanism of hormone sensing. *Current opinion in plant biology*, 11 (4), 428-435.
- Kazan, K. (2015).** Diverse roles of jasmonates and ethylene in abiotic stress tolerance. *Trends in plant science*, 20 (4), 219-229.
- Kazan, K.; Manners, J. M. (2013).** MYC2: the master in action. *Molecular Plant*, 6 (3), 686-703.
- Kearse, M.; Moir, R.; Wilson, A.; Stones-Havas, S.; Cheung, M.; Sturrock, S.; Buxton, S.; Cooper, A.; Markowitz, S.; Duran, C. (2012).** Geneious basic: an integrated and extendable desktop software platform for the organization and analysis of sequence data. *Bioinformatics*, 28 (12), 1647-1649.
- Kettner, J.; Dörffling, K. (1995).** Biosynthesis and metabolism of abscisic acid in tomato leaves infected with *Botrytis cinerea*. *Planta*, 196 (4), 627-634.
- Kim, Y. J.; Lin, N. C.; Martin, G. B. (2002).** Two distinct *Pseudomonas* effector proteins interact with the *Pto* kinase and activate plant immunity. *Cell*, 109 (5), 589-598.
- Kinkema, M.; Fan, W.; Dong, X. (2000).** Nuclear localization of NPR1 is required for activation of *PR* gene expression. *The Plant Cell*, 12 (12), 2339-2350.
- Klessig, D. F.; Choi, H. W.; Dempsey, D. M. A. (2018).** Systemic acquired resistance and salicylic acid: past, present, and future. *Molecular Plant-microbe interactions*, 31 (9), 871-888.
- Klessig, D. F.; Tian, M.; Choi, H. W. (2016).** Multiple targets of salicylic acid and its derivatives in plants and animals. *Frontiers in Immunology*, 7 (206).
- Koga, H.; Dohi, K.; Mori, M. (2004).** Absciscic acid and low temperatures suppress the whole plant-specific resistance reaction of rice plants to the infection of *Magnaporthe grisea*. *Physiological and Molecular Plant Pathology*, 65 (1), 3-9.
- Koornneef, A.; Leon-Reyes, A.; Ritsema, T.; Verhage, A.; Den Otter, F. C.; Van Loon, L.; Pieterse, C. M. (2008).** Kinetics of salicylate-mediated suppression of jasmonate signaling reveal a role for redox modulation. *Plant physiology*, 147 (3), 1358-1368.
- Kuhn, H.; Kwaaitaal, M.; Kusch, S.; Acevedo-Garcia, J.; Wu, H.; Panstruga, R. (2016).** Biotrophy at its best: novel findings and unsolved mysteries of the *Arabidopsis*-powdery mildew pathosystem. *American Society of Plant Biologists, Arabidopsis Book*. 2016; 14: e0184.
- Kuhn, J. M.; Boisson-Dernier, A.; Dizon, M. B.; Maktabi, M. H.; Schroeder, J. I. (2006).** The protein phosphatase *AtPP2CA* negatively regulates abscisic acid signal transduction in *Arabidopsis*, and effects of *abh1* on *AtPP2CA* mRNA. *Plant physiology*, 140 (1), 127-139.
- Kulik, A.; Wawer, I.; Krzywińska, E.; Bucholc, M.; Dobrowolska, G. (2011).** SnRK2 protein kinases-key regulators of plant response to abiotic stresses. *Omics: a journal of integrative biology*, 15 (12), 859-872.
- Kunkel, B. N.; Brooks, D. M. (2002).** Cross talk between signaling pathways in pathogen defense. *Current opinion in plant biology*, 5 (4), 325-331.

5. REFERENCES

- Kuromori, T.; Sugimoto, E.; Shinozaki, K. (2011).** Arabidopsis mutants of *AtABCG22*, an ABC transporter gene, increase water transpiration and drought susceptibility. *The Plant Journal*, 67 (5), 885-894.
- Lake, J. A.; Woodward, F. I.; Quick, W. P. (2002).** Long-distance CO₂ signalling in plants. *Journal of experimental botany*, 53 (367), 183-193.
- Larrieu, A.; Champion, A.; Legrand, J.; Lavenus, J.; Mast, D.; Brunoud, G.; Oh, J.; Guyomarc'h, S.; Pizot, M.; Farmer, E. E. (2015).** A fluorescent hormone biosensor reveals the dynamics of jasmonate signalling in plants. *Nature communications*, 6, 6043.
- Lee, D.; Bourdais, G.; Yu, G.; Robatzek, S.; Coaker, G. (2015).** Phosphorylation of the plant immune regulator RPM1-INTERACTING PROTEIN4 enhances plant plasma membrane H⁺-ATPase activity and inhibits flagellin-triggered immune responses in Arabidopsis. *The Plant cell*, 27 (7), 2042-2056.
- Lee, J.-Y.; Wang, X.; Cui, W.; Sager, R.; Modla, S.; Czymmek, K.; Zybaliov, B.; Van Wijk, K.; Zhang, C.; Lu, H. (2011).** A plasmodesmata-localized protein mediates crosstalk between cell-to-cell communication and innate immunity in Arabidopsis. *The Plant cell*, 23 (9), 3353-3373.
- Lee, M. W.; Lu, H.; Jung, H. W.; Greenberg, J. T. (2007).** A key role for the Arabidopsis WIN3 protein in disease resistance triggered by *Pseudomonas syringae* that secrete AvrRpt2. *Molecular Plant-microbe interactions*, 20 (10), 1192-1200.
- Lee, S. C.; Luan, S. (2012).** ABA signal transduction at the crossroad of biotic and abiotic stress responses. *Plant, cell environment*, 35 (1), 53-60.
- Leon-Reyes, A.; Spoel, S. H.; De Lange, E. S.; Abe, H.; Kobayashi, M.; Tsuda, S.; Millenaar, F. F.; Welschen, R. A.; Ritsema, T.; Pieterse, C. M. (2009).** Ethylene modulates the role of NONEXPRESSOR OF PATHOGENESIS-RELATED GENES1 in cross talk between salicylate and jasmonate signaling. *Plant physiology*, 149 (4), 1797-1809.
- Leon-Reyes, A.; Van der Does, D.; De Lange, E. S.; Delker, C.; Wasternack, C.; Van Wees, S. C.; Ritsema, T.; Pieterse, C. M. (2010).** Salicylate-mediated suppression of jasmonate-responsive gene expression in Arabidopsis is targeted downstream of the jasmonate biosynthesis pathway. *Planta*, 232 (6), 1423-1432.
- Li, G.; Dong, G.; Li, B.; Li, Q.; Kronzucker, H. J.; Shi, W. (2012).** Isolation and characterization of a novel ammonium overly sensitive mutant, *amos2*, in *Arabidopsis thaliana*. *Planta*, 235 (2), 239-252.
- Li, N.; Han, X.; Feng, D.; Yuan, D.; Huang, L. J. (2019b).** Signaling crosstalk between salicylic acid and ethylene/jasmonate in plant defense: do we understand what they are whispering? *International journal of molecular sciences*, 20 (3), 671.
- Li, N.; Muthreich, M.; Huang, L. J.; Thurow, C.; Sun, T.; Zhang, Y.; Gatz, C. (2019a).** TGACG-BINDING FACTORS (TGAs) and TGA-interacting CC-type glutaredoxins modulate hyponastic growth in *Arabidopsis thaliana*. *New Phytologist*, 221 (4), 1906-1918.
- Li, Q.; Zheng, J.; Li, S.; Huang, G.; Skilling, S. J.; Wang, L.; Li, L.; Li, M.; Yuan, L.; Liu, P. (2017).** Transporter-mediated nuclear entry of jasmonoyl-isoleucine is essential for jasmonate signaling. *Molecular Plant*, 10 (5), 695-708.

5. REFERENCES

- Li, X.; Clarke, J. D.; Zhang, Y.; Dong, X. (2001).** Activation of an EDS1-mediated R-gene pathway in the *snc1* mutant leads to constitutive, NPR1-independent pathogen resistance. *Molecular Plant-microbe interactions*, 14 (10), 1131-1139.
- Liao, C.-Y.; Smet, W.; Brunoud, G.; Yoshida, S.; Vernoux, T.; Weijers, D. (2015).** Reporters for sensitive and quantitative measurement of auxin response. *Nature Methods*, 12 (3), 207.
- Lievens, L.; Pollier, J.; Goossens, A.; Beyaert, R.; Staal, J. (2017).** Absciscic acid as pathogen effector and immune regulator. *Frontiers in plant science*, 8, 587.
- Lorenzo, O.; Solano, R. (2005).** Molecular players regulating the jasmonate signalling network. *Current opinion in plant biology*, 8 (5), 532-540.
- Lorenzo, O.; Chico, J. M.; Sánchez-Serrano, J. J.; Solano, R. (2004).** *JASMONATE-INSENSITIVE1* encodes a MYC transcription factor essential to discriminate between different jasmonate-regulated defense responses in Arabidopsis. *The Plant cell*, 16 (7), 1938-1950.
- Love, A. J.; Milner, J. J.; Sadanandom, A. (2008).** Timing is everything: regulatory overlap in plant cell death. *Trends in plant science*, 13 (11), 589-595.
- Lu, H.; Greenberg, J. T.; Holuigue, L. (2016).** Salicylic acid signaling networks. *Frontiers in plant science*, 7, 238.
- Lübbbers, J. N. (2018).** Approaching spatial crosstalk between salicylic acid and abscisic acid signaling during plant-pathogen interactions. *Bachelor thesis*. Georg-August-Universität Göttingen.
- Lukan, T.; Baebler, Š.; Pompe-Novak, M.; Guček, K.; Zagorščak, M.; Coll, A.; Gruden, K. (2018).** Cell death is not sufficient for the restriction of potato virus Y spread in hypersensitive response-conferred resistance in potato. *Frontiers in plant science*, 9, 168.
- Ma, Y.; Szostkiewicz, I.; Korte, A.; Moes, D.; Yang, Y.; Christmann, A.; Grill, E. (2009).** Regulators of PP2C phosphatase activity function as abscisic acid sensors. *Science*, 324 (5930), 1064-1068.
- Manners, J. M.; Penninckx, I. A.; Vermaere, K.; Kazan, K.; Brown, R. L.; Morgan, A.; Maclean, D. J.; Curtis, M. D.; Cammue, B. P. A.; Broekaert, W. F. (1998).** The promoter of the plant defensin gene *PDF1. 2* from Arabidopsis is systemically activated by fungal pathogens and responds to methyl jasmonate but not to salicylic acid. *Plant molecular biology*, 38 (6), 1071-1080.
- Manohar, M.; Wang, D.; Manosalva, P. M.; Choi, H. W.; Kombrink, E.; Klessig, D. F. (2017).** Members of the abscisic acid co-receptor PP2C protein family mediate salicylic acid-abscisic acid crosstalk. *Plant Direct*, 1 (5), e00020.
- Mao, X.; Li, Y.; Rehman, S. U.; Miao, L.; Zhang, Y.; Chen, X.; Yu, Ch.; Wang, J.; Li, C.; Jing, R. (2019).** The *SUCROSE NON-FERMENTING 1-RELATED PROTEIN KINASE 2* (*SnRK2*) genes are multifaceted players in plant growth, development and response to environmental stimuli. *Plant and cell physiology*. Doi: 10.1093/pcp/pcz230.
- Marhavý, P.; Kurenda, A.; Siddique, S.; Tendon, V. D.; Zhou, F.; Holbein, J.; Hasan, M. S.; Grundler, F. M. W.; Farmer, E. E.; Geldner, N. (2019).** Single-cell damage elicits regional, nematode-restricting ethylene responses in roots. *The EMBO journal*, 38 (10). Doi: 15252/embj.2018100972.

5. REFERENCES

- Marin, E.; Nussaume, L.; Quesada, A.; Gonneau, M.; Sotta, B.; Hugueney, P.; Frey, A.; Marion-Poll, A. (1996).** Molecular identification of zeaxanthin epoxidase of *Nicotiana plumbaginifolia*, a gene involved in abscisic acid biosynthesis and corresponding to the ABA locus of *Arabidopsis thaliana*. *The EMBO journal*, 15 (10), 2331-2342.
- Massoud, K.; Barchietto, T.; Le Rudulier, T.; Pallandre, L.; Didierlaurent, L.; Garmier, M.; Ambard-Bretteville, F.; Seng, J.M.; Saindrenan, P. (2012).** Dissecting phosphite-induced priming in *Arabidopsis* infected with *Hyaloperonospora arabidopsidis*. *Plant physiology*, 159 (1), 286-298.
- Maszkowska, J.; Dębski, J.; Kulik, A.; Kistowski, M.; Bucholc, M.; Lichocka, M.; Klimecka, M.; Sztatelman, O.; Szymańska, K. P.; Dadlez, M. (2019).** Phosphoproteomic analysis reveals that dehydrins ERD10 and ERD14 are phosphorylated by SNF1-related protein kinase 2.10 in response to osmotic stress. *Plant, cell environment*, 42 (3), 931-946.
- Mauch-Mani, B.; Slusarenko, A. J. (1996).** Production of salicylic acid precursors is a major function of phenylalanine ammonia-lyase in the resistance of *Arabidopsis* to *Peronospora parasitica*. *The Plant cell*, 8 (2), 203-212.
- McConn, M.; Browse, J. (1996).** The critical requirement for linolenic acid is pollen development, not photosynthesis, in an *Arabidopsis* mutant. *The Plant cell*, 8 (3), 403-416.
- McDowell, J. M. (2011).** Plant immunity: methods and protocols. Doi: 10.1007/978-1-61737-998-7.
- McDowell, J. M.; Cuzick, A.; Can, C.; Beynon, J.; Dangl, J. L.; Holub, E. B. (2000).** Downy mildew (*Peronospora parasitica*) resistance genes in *Arabidopsis* vary in functional requirements for NDR1, EDS1, NPR1 and salicylic acid accumulation. *The Plant Journal*, 22 (6), 523-529.
- Meguro, A.; Sato, Y. (2014).** Salicylic acid antagonizes abscisic acid inhibition of shoot growth and cell cycle progression in rice. *Scientific reports*, 4 (1), 1-11.
- Mehrotra, R.; Bhalothia, P.; Bansal, P.; Basantani, M. K.; Bharti, V.; Mehrotra, S. (2014).** Absciscic acid and abiotic stress tolerance-Different tiers of regulation. *Journal of Plant physiology*, 171 (7), 486-496.
- Mehta, N.; Saharan, G.; Meena, P. (2018).** Expression of disease resistance in Brassica-Hyaloperonospora host-patho system-A review. *Plant Disease Research*, 33 (2), 112-141.
- Melotto, M.; Underwood, W.; Koczan, J.; Nomura, K.; He, S. Y. (2006).** Plant stomata function in innate immunity against bacterial invasion. *Cell*, 126 (5), 969-980.
- Micali, C. O.; Neumann, U.; Grunewald, D.; Panstruga, R.; O'connell, R. (2011).** Biogenesis of a specialized plant-fungal interface during host cell internalization of *Golovinomyces orontii* haustoria. *Cellular microbiology*, 13 (2), 210-226.
- Mikkelsen, M. D.; Petersen, B. L.; Glawischnig, E.; Jensen, A. B.; Andreasson, E.; Halkier, B. A. (2003).** Modulation of CYP79 genes and glucosinolate profiles in *Arabidopsis* by defense signaling pathways. *Plant physiology*, 131 (1), 298-308.
- Mine, A.; Berens, M. L.; Nobori, T.; Anver, S.; Fukumoto, K.; Winkelmüller, T. M.; Takeda, A.; Becker, D.; Tsuda, K. (2017).** Pathogen exploitation of an abscisic acid-and jasmonate-inducible MAPK phosphatase and its interception by *Arabidopsis* immunity. *Proceedings of the National Academy of Sciences*, 114 (28), 7456-7461.
- Miya, A.; Albert, P.; Shinya, T.; Desaki, Y.; Ichimura, K.; Shirasu, K.; Narusaka, Y.; Kawakami, N.; Kaku, H.; Shibuya, N. (2007).** CERK1, a LysM receptor kinase, is essential for chitin elicitor

5. REFERENCES

- signaling in Arabidopsis. *Proceedings of the National Academy of Sciences*, 104 (49), 19613-19618.
- Mohammed, A. E.; You, M. P.; Banga, S. S.; Barbetti, M. J. (2019).** Resistances to downy mildew (*Hyaloperonospora brassicae*) in diverse Brassicaceae offer new disease management opportunities for oilseed and vegetable crucifer industries. *European journal of plant pathology*, 153 (3), 915-929.
- Mohr, P. G.; Cahill, D. M. (2003).** Abscissic acid influences the susceptibility of *Arabidopsis thaliana* to *Pseudomonas syringae* pv. tomato and *Peronospora parasitica*. *Functional Plant Biology*, 30 (4), 461-469.
- Morris, C. E.; Sands, D. C.; Vinatzer, B. A.; Glaux, C.; Guilbaud, C.; Buffiere, A.; Yan, S.; Dominguez, H.; Thompson, B. M. (2008).** The life history of the plant pathogen *Pseudomonas syringae* is linked to the water cycle. *The ISME journal*, 2 (3), 321-334.
- Mosblech, A.; Thurow, C.; Gatz, C.; Feussner, I.; Heilmann, I. (2011).** Jasmonic acid perception by COI1 involves inositol polyphosphates in *Arabidopsis thaliana*. *The Plant Journal*, 65 (6), 949-957.
- Mou, Z.; Fan, W.; Dong, X. (2003).** Inducers of plant systemic acquired resistance regulate NPR1 function through redox changes. *Cell*, 113 (7), 935-944.
- Mousavi, S. A.; Chauvin, A.; Pascaud, F.; Kellenberger, S.; Farmer, E. E. (2013).** *GLUTAMATE RECEPTOR-LIKE* genes mediate leaf-to-leaf wound signalling. *Nature*, 500 (7463), 422-426.
- Müller, A.; Dückting, P.; Weiler, E. W. (2002).** A multiplex GC-MS/MS technique for the sensitive and quantitative single-run analysis of acidic phytohormones and related compounds, and its application to *Arabidopsis thaliana*. *Planta*, 216 (1), 44-56.
- Müller, B.; Sheen, J. (2008).** Cytokinin and auxin interaction in root stem-cell specification during early embryogenesis. *Nature*, 453 (7198), 1094-1097.
- Mundy, J.; Nielsen, H. B.; Brodersen, P. (2006).** Crosstalk. *Trends in plant science*, 11 (2), 63-64.
- Mundy, J.; Yamaguchi-Shinozaki, K.; Chua, N. H. (1990).** Nuclear proteins bind conserved elements in the abscisic acid-responsive promoter of a rice rab gene. *Proceedings of the National Academy of Sciences*, 87 (4), 1406-1410.
- Mur, L. A.; Kenton, P.; Atzorn, R.; Miersch, O.; Wasternack, C. (2006).** The outcomes of concentration-specific interactions between salicylate and jasmonate signaling include synergy, antagonism, and oxidative stress leading to cell death. *Plant physiology*, 140 (1), 249-262.
- Murmu, J.; Wilton, M.; Allard, G.; Pandeya, R.; Desveaux, D.; Singh, J.; Subramaniam, R. (2014).** Arabidopsis GOLDEN2-LIKE (GLK) transcription factors activate jasmonic acid (JA)-dependent disease susceptibility to the biotrophic pathogen *Hyaloperonospora arabidopsidis*, as well as JA-independent plant immunity against the necrotrophic pathogen *Botrytis cinerea*. *Molecular Plant pathology*, 15 (2), 174-184.
- Murray, S. L.; Thomson, C.; Chini, A.; Read, N. D.; Loake, G. J. (2002).** Characterization of a novel, defense-related Arabidopsis mutant, *cir1*, isolated by luciferase imaging. *Molecular Plant-microbe interactions*, 15 (6), 557-566.

5. REFERENCES

- Nagai, T.; Iyata, K.; Park, E. S.; Kubota, M.; Mikoshiba, K.; Miyawaki, A. (2002).** A variant of yellow fluorescent protein with fast and efficient maturation for cell-biological applications. *Nature biotechnology*, 20 (1), 87-90.
- Nahar, K.; Kyndt, T.; Nzogela, Y. B.; Gheysen, G. (2012).** Absciscic acid interacts antagonistically with classical defense pathways in rice-migratory nematode interaction. *New Phytologist*, 196 (3), 901-913.
- Nakashima, K.; Fujita, Y.; Kanamori, N.; Katagiri, T.; Umezawa, T.; Kidokoro, S.; Maruyama, K.; Yoshida, T.; Ishiyama, K.; Kobayashi, M. (2009).** Three Arabidopsis SnRK2 protein kinases, SRK2D/SnRK2.2, SRK2E/SnRK2.6/OST1 and SRK2I/SnRK2.3, involved in ABA signaling are essential for the control of seed development and dormancy. *Plant and cell physiology*, 50 (7), 1345-1363.
- Nambara, E.; Marion-Poll, A. (2005).** Absciscic acid biosynthesis and catabolism. *Annual Review Plant Biology*, 56, 165-185.
- Naseem, M.; Wölfling, M.; Dandekar, T. (2014).** Cytokinins for immunity beyond growth, galls and green islands. *Trends in plant science*, 19 (8), 481-484.
- Nishimura, M. T.; Dangl, J. L. (2010).** Arabidopsis and the plant immune system. *The Plant Journal*, 61 (6), 1053-1066.
- Nishimura, N.; Sarkeshik, A.; Nito, K.; Park, S. Y.; Wang, A.; Carvalho, P. C.; Lee, S.; Caddell, D. F.; Cutler, S. R.; Chory, J. (2010).** PYR/PYL/RCAR family members are major *in-vivo* ABI1 protein phosphatase 2C-interacting proteins in Arabidopsis. *The Plant Journal*, 61 (2), 290-299.
- Nishimura, N.; Yoshida, T.; Kitahata, N.; Asami, T.; Shinozaki, K.; Hirayama, T. (2007).** ABA-HYPERSENSITIVE GERMINATION1 encodes a protein phosphatase 2C, an essential component of absciscic acid signaling in Arabidopsis seed. *The Plant Journal*, 50 (6), 935-949.
- Nishimura, N.; Yoshida, T.; Murayama, M.; Asami, T.; Shinozaki, K.; Hirayama, T. (2004).** Isolation and characterization of novel mutants affecting the absciscic acid sensitivity of Arabidopsis germination and seedling growth. *Plant and cell physiology*, 45 (10), 1485-1499.
- Nobuta, K.; Okrent, R.; Stoutemyer, M.; Rodibaugh, N.; Kempema, L.; Wildermuth, M.; Innes, R. (2007).** The GH3 acyl adenylase family member PBS3 regulates salicylic acid-dependent defense responses in Arabidopsis. *Plant physiology*, 144 (2), 1144-1156.
- Norman-Setterblad, C.; Vidal, S.; Palva, E. T. (2000).** Interacting signal pathways control defense gene expression in Arabidopsis in response to cell wall-degrading enzymes from *Erwinia carotovora*. *Molecular Plant-microbe interactions*, 13 (4), 430-438.
- Nühse, T. S.; Peck, S. C.; Hirt, H.; Boller, T. (2000).** Microbial elicitors induce activation and dual phosphorylation of the *Arabidopsis thaliana* MAPK 6. *Journal of Biological Chemistry*, 275 (11), 7521-7526.
- Oide, S.; Bejai, S.; Staal, J.; Guan, N.; Kaliff, M.; Dixelius, C. (2013).** A novel role of PR2 in absciscic acid (ABA) mediated, pathogen-induced callose deposition in *Arabidopsis thaliana*. *New Phytologist*, 200 (4), 1187-1199.
- Otsu, N. (1979).** A threshold selection method from gray-level histograms. *IEEE transactions on systems, man, and cybernetics*, 9 (1), 62-66.

5. REFERENCES

- Pantin, F.; Monnet, F.; Jannaud, D.; Costa, J. M.; Renaud, J.; Muller, B.; Simonneau, T.; Genty, B. (2013a).** The dual effect of abscisic acid on stomata. *New Phytologist*, 197 (1), 65-72.
- Pantin, F.; Renaud, J.; Barbier, F.; Vavasseur, A.; Le Thiec, D.; Rose, C.; Bariac, T.; Casson, S.; McLachlan, D. H.; Hetherington, A. M. (2013b).** Developmental priming of stomatal sensitivity to abscisic acid by leaf microclimate. *Current Biology*, 23 (18), 1805-1811.
- Pantin, F.; Simonneau, T.; Muller, B. (2012).** Coming of leaf age: control of growth by hydraulics and metabolics during leaf ontogeny. *New Phytologist*, 196 (2), 349-366.
- Paponov, I. A.; Paponov, M.; Teale, W.; Menges, M.; Chakrabortee, S.; Murray, J. A.; Palme, K. (2008).** Comprehensive transcriptome analysis of auxin responses in Arabidopsis. *Molecular Plant*, 1 (2), 321-337.
- Parent, B.; Hachez, C.; Redondo, E.; Simonneau, T.; Chaumont, F.; Tardieu, F. (2009).** Drought and abscisic acid effects on aquaporin content translate into changes in hydraulic conductivity and leaf growth rate: a trans-scale approach. *Plant physiology*, 149 (4), 2000-2012.
- Park, E.; Nedo, A.; Caplan, J. L.; Dinesh-Kumar, S. (2018).** Plant-microbe interactions: organelles and the cytoskeleton in action. *New Phytologist*, 217 (3), 1012-1028.
- Park, S. Y.; Fung, P.; Nishimura, N.; Jensen, D. R.; Fujii, H.; Zhao, Y.; Lumba, S.; Santiago, J.; Rodrigues, A.; Tsz-fung, F. C. (2009).** Abscisic acid inhibits type 2C protein phosphatases via the PYR/PYL family of START proteins. *Science*, 324 (5930), 1068-1071.
- Parker, J. E.; Holub, E. B.; Frost, L. N.; Falk, A.; Gunn, N. D.; Daniels, M. J. (1996).** Characterization of *eds1*, a mutation in Arabidopsis suppressing resistance to *Peronospora parasitica* specified by several different *RPP* genes. *The Plant cell*, 8 (11), 2033-2046.
- Penninckx, I. A.; Thomma, B. P.; Buchala, A.; Métraux, J.-P.; Broekaert, W. F. (1998).** Concomitant activation of jasmonate and ethylene response pathways is required for induction of a plant defensin gene in Arabidopsis. *The Plant cell*, 10 (12), 2103-2113.
- Penninckx, I.; Eggermont, K.; Terras, F.; Thomma, B.; De Samblanx, G. W.; Buchala, A.; Métraux, J.P.; Manners, J. M.; Broekaert, W. F. (1996).** Pathogen-induced systemic activation of a plant defensin gene in Arabidopsis follows a salicylic acid-independent pathway. *The Plant cell*, 8 (12), 2309-2323.
- Pieterse, C. M.; Leon-Reyes, A.; Van der Ent, S.; Van Wees, S. C. (2009).** Networking by small-molecule hormones in plant immunity. *Nature chemical biology*, 5 (5), 308-316.
- Pieterse, C. M.; Van der Does, D.; Zamioudis, C.; Leon-Reyes, A.; Van Wees, S. C. (2012).** Hormonal modulation of plant immunity. *Annual review of cell developmental biology*, 28, 489-521.
- Pitino, M.; Armstrong, C. M.; Cano, L. M.; Duan, Y. (2016).** Transient expression of *Candidatus Liberibacter Asiaticus* effector induces cell death in *Nicotiana benthamiana*. *Frontiers in plant science*, 7 (982).
- Pollok, B. A.; Heim, R. (1999).** Using GFP in FRET-based applications. *Trends in cell biology*, 9 (2), 57-60.
- Poncini, L.; Wyrsh, I.; Tendon, V. D.; Vorley, T.; Boller, T.; Geldner, N.; Métraux, J.P.; Lehmann, S. (2017).** In roots of *Arabidopsis thaliana*, the damage-associated molecular pattern AtPep1 is

5. REFERENCES

- a stronger elicitor of immune signalling than flg22 or the chitin heptamer. *PLoS One*, 12 (10): e0185808.
- Pré, M.; Atallah, M.; Champion, A.; De Vos, M.; Pieterse, C. M.; Memelink, J. (2008).** The AP2/ERF domain transcription factor ORA59 integrates jasmonic acid and ethylene signals in plant defense. *Plant physiology*, 147 (3), 1347-1357.
- Prerostova, S.; Dobrev, P. I.; Konradyova, V.; Knirsch, V.; Gaudinova, A.; Kramna, B.; Kazda, J.; Ludwig-Müller, J.; Vankova, R. (2018).** Hormonal responses to *Plasmodiophora brassicae* infection in *Brassica napus* cultivars differing in their pathogen resistance. *International journal of molecular sciences*, 19 (12), 4024.
- Presti, L. L.; Kahmann, R. (2017).** How filamentous plant pathogen effectors are translocated to host cells. *Current opinion in plant biology*, 38, 19-24.
- Prodhan, M. Y.; Munemasa, S.; Nahar, M. N. E. N.; Nakamura, Y.; Murata, Y. (2018).** Guard cell salicylic acid signaling is integrated into abscisic acid signaling via the Ca²⁺/CPK-dependent pathway. *Plant physiology*, 178 (1), 441-450.
- Raghavendra, A. S.; Gonugunta, V. K.; Christmann, A.; Grill, E. (2010).** ABA perception and signalling. *Trends in plant science*, 15 (7), 395-401.
- Raines, T.; Blakley, I. C.; Tsai, Y. C.; Worthen, J. M.; Franco-Zorrilla, J. M.; Solano, R.; Schaller, G. E.; Loraine, A. E.; Kieber, J. J. (2016).** Characterization of the cytokinin-responsive transcriptome in rice. *BMC plant biology*, 16 (1), 260.
- Ramšak, Ž.; Coll, A.; Stare, T.; Tzfadia, O.; Baebler, Š.; Van de Peer, Y.; Gruden, K. (2018).** Network modeling unravels mechanisms of crosstalk between ethylene and salicylate signaling in potato. *Plant physiology*, 178 (1), 488-499.
- Ravanbakhsh, M.; Sasidharan, R.; Voesenek, L. A.; Kowalchuk, G. A.; Jousset, A. (2018).** Microbial modulation of plant ethylene signaling: ecological and evolutionary consequences. *Microbiome*, 6 (1), 52.
- Rekhter, D.; Lüdke, D.; Ding, Y.; Feussner, K.; Zienkiewicz, K.; Lipka, V.; Wiermer, M.; Zhang, Y.; Feussner, I. (2019).** Isochorismate-derived biosynthesis of the plant stress hormone salicylic acid. *Science*, 365 (6452), 498-502.
- Rezzonico, E.; Flury, N.; Meins, F.; Beffa, R. (1998).** Transcriptional down-regulation by abscisic acid of pathogenesis-related β -1, 3-glucanase genes in tobacco cell cultures. *Plant physiology*, 117 (2), 585-592.
- Rhee, J. M.; Purity, M. K.; Lackan, C. S.; Long, J. Z.; Kondoh, G.; Takeda, J.; Hadjantonakis, A. K. (2006).** *In vivo* imaging and differential localization of lipid-modified GFP-variant fusions in embryonic stem cells and mice. *Genesis*, 44 (4), 202-218.
- Rivas-San Vicente, M.; Plasencia, J. (2011).** Salicylic acid beyond defence: its role in plant growth and development. *Journal of experimental botany*, 62 (10), 3321-3338.
- Robert-Seilaniantz, A.; Grant, M.; Jones, J. D. (2011).** Hormone crosstalk in plant disease and defense: more than just jasmonate-salicylate antagonism. *Annual review of phytopathology*, 49, 317-343.

5. REFERENCES

- Rock, C. D.; Zeevaart, J. (1991).** The aba mutant of *Arabidopsis thaliana* is impaired in epoxy-carotenoid biosynthesis. *Proceedings of the National Academy of Sciences*, 88 (17), 7496-7499.
- Rodriguez-Moreno, L.; Ebert, M. K.; Bolton, M. D.; Thomma, B. P. (2018).** Tools of the crook-infection strategies of fungal plant pathogens. *The Plant Journal*, 93 (4), 664-674.
- Rosales, M. A.; Maurel, C.; Nacry, P. (2019).** Absciscic acid coordinates dose-dependent developmental and hydraulic responses of roots to water deficit. *Plant physiology*, 180 (4), 2198-2211.
- Ruan, J.; Zhou, Y.; Zhou, M.; Yan, J.; Khurshid, M.; Weng, W.; Cheng, J.; Zhang, K. (2019).** Jasmonic acid signaling pathway in plants. *International journal of molecular sciences*, 20 (10), 2479-2494.
- Saez, A.; Apostolova, N.; Gonzalez-Guzman, M.; Gonzalez-Garcia, M. P.; Nicolas, C.; Lorenzo, O.; Rodriguez, P. L. (2004).** Gain-of-function and loss-of-function phenotypes of the protein phosphatase 2C *HAB1* reveal its role as a negative regulator of abscisic acid signalling. *The Plant Journal*, 37 (3), 354-369.
- Saez, A.; Robert, N.; Maktabi, M. H.; Schroeder, J. I.; Serrano, R.; Rodriguez, P. L. (2006).** Enhancement of abscisic acid sensitivity and reduction of water consumption in *Arabidopsis* by combined inactivation of the protein phosphatases type 2C *ABI1* and *HAB1*. *Plant physiology*, 141 (4), 1389-1399.
- Sah, S. K.; Reddy, K. R.; Li, J. (2016).** Absciscic acid and abiotic stress tolerance in crop plants. *Frontiers in plant science*, 7, 571.
- Sánchez-Vallet, A.; López, G.; Ramos, B.; Delgado-Cerezo, M.; Riviere, M. P.; Llorente, F.; Fernández, P. V.; Miedes, E.; Estevez, J. M.; Grant, M. (2012).** Disruption of abscisic acid signaling constitutively activates *Arabidopsis* resistance to the necrotrophic fungus *Plectosphaerella cucumerina*. *Plant physiology*, 160 (4), 2109-2124.
- Santiago, J.; Rodrigues, A.; Saez, A.; Rubio, S.; Antoni, R.; Dupeux, F.; Park, S. Y.; Márquez, J. A.; Cutler, S. R.; Rodriguez, P. L. (2009).** Modulation of drought resistance by the abscisic acid receptor PYL5 through inhibition of clade A PP2Cs. *The Plant Journal*, 60 (4), 575-588.
- Sauter, A.; Davies, W. J.; Hartung, W. (2001).** The long-distance abscisic acid signal in the droughted plant: the fate of the hormone on its way from root to shoot. *Journal of experimental botany*, 52 (363), 1991-1997.
- Schindelin, J.; Arganda-Carreras, I.; Frise, E.; Kaynig, V.; Longair, M.; Pietzsch, T.; Preibisch, S.; Rueden, C.; Saalfeld, S.; Schmid, B. (2012).** Fiji: an open-source platform for biological-image analysis. *Nature methods*, 9 (7), 676-682.
- Schliekmann, E. (2017).** Uncovering the role of ABA signaling in biotrophic plant-pathogen interaction. *Bachelor thesis*. Georg-August-Universität Göttingen.
- Schoonbeek, H. J.; Wang, H. H.; Stefanato, F. L.; Craze, M.; Bowden, S.; Wallington, E.; Zipfel, C.; Ridout, C. J. (2015).** *Arabidopsis* EF-Tu receptor enhances bacterial disease resistance in transgenic wheat. *New Phytologist*, 206 (2), 606-613.
- Seibel, N. M.; Eljouni, J.; Nalaskowski, M. M.; Hampe, W. (2007).** Nuclear localization of enhanced green fluorescent protein homomultimers. *Analytical biochemistry*, 368 (1), 95-99.

5. REFERENCES

- Seo, M.; Koshiba, T. (2011).** Transport of ABA from the site of biosynthesis to the site of action. *Journal of plant research*, 124 (4), 501-507.
- Serrano, M.; Wang, B.; Aryal, B.; Garcion, C.; Abou-Mansour, E.; Heck, S.; Geisler, M.; Mauch, F.; Nawrath, C.; Métraux, J.-P. (2013).** Export of salicylic acid from the chloroplast requires the multidrug and toxin extrusion-like transporter EDS5. *Plant physiology*, 162 (4), 1815-1821.
- Shani, E.; Weinstain, R.; Zhang, Y.; Castillejo, C.; Kaiserli, E.; Chory, J.; Tsien, R. Y.; Estelle, M. (2013).** Gibberellins accumulate in the elongating endodermal cells of Arabidopsis root. *Proceedings of the National Academy of Sciences*, 110 (12), 4834-4839.
- Shcherbo, D.; Murphy, C. S.; Ermakova, G. V.; Solovieva, E. A.; Chepurnykh, T. V.; Shcheglov, A. S.; Verkhusha, V. V.; Pletnev, V. Z.; Hazelwood, K. L.; Roche, P. M. (2009).** Far-red fluorescent tags for protein imaging in living tissues. *Biochemical journal*, 418 (3), 567-574.
- Shigenaga, A. M.; Argueso, C. T. (2016).** No hormone to rule them all: Interactions of plant hormones during the responses of plants to pathogens. *Seminars in Cell Developmental Biology*, 56, 174-189.
- Sivakumaran, A.; Akinyemi, A.; Mandon, J.; Cristescu, S. M.; Hall, M. A.; Harren, F. J.; Mur, L. A. (2016).** ABA suppresses *Botrytis cinerea* elicited NO production in tomato to influence H₂O₂ generation and increase host susceptibility. *Frontiers in plant science*, 7, 709.
- Söderman, E.; Hjellström, M.; Fahleson, J.; Engström, P. (1999).** The HD-Zip gene *ATHB6* in Arabidopsis is expressed in developing leaves, roots and carpels and up-regulated by water deficit conditions. *Plant molecular biology*, 40 (6), 1073-1083.
- Sohn, K. H.; Lei, R.; Nemri, A.; Jones, J. D. (2007).** The downy mildew effector proteins ATR1 and ATR13 promote disease susceptibility in *Arabidopsis thaliana*. *The Plant cell*, 19 (12), 4077-4090.
- Sokołowska, K.; Kizińska, J.; Szewczuk, Z.; Banasiak, A. (2014).** Auxin conjugated to fluorescent dyes-a tool for the analysis of auxin transport pathways. *Plant Biology*, 16 (5), 866-877.
- Solano, R.; Gimenez-Ibanez, S. (2013).** Nuclear jasmonate and salicylate signaling and crosstalk in defense against pathogens. *Frontiers in plant science*, 4, 72.
- Song, S.; Huang, H.; Gao, H.; Wang, J.; Wu, D.; Liu, X.; Yang, S.; Zhai, Q.; Li, C.; Qi, T. (2014).** Interaction between MYC2 and ETHYLENE INSENSITIVE3 modulates antagonism between jasmonate and ethylene signaling in Arabidopsis. *The Plant Cell*, 26(1): 263-279.
- Spanu, P. D.; Panstruga, R. (2017).** Biotrophic plant-microbe interactions. *Frontiers in plant science*, 8, 192.
- Spoel, S. H.; Dong, X. (2008).** Making sense of hormone crosstalk during plant immune responses. *Cell host microbe*, 3 (6), 348-351.
- Spoel, S. H.; Johnson, J. S.; Dong, X. (2007).** Regulation of tradeoffs between plant defenses against pathogens with different lifestyles. *Proceedings of the National Academy of Sciences*, 104 (47), 18842-18847.
- Srivastava, A. K.; Orosa, B.; Singh, P.; Cummins, I.; Walsh, C.; Zhang, C.; Grant, M.; Roberts, M. R.; Anand, G. S.; Fitches, E. (2018).** SUMO suppresses the activity of the jasmonic acid receptor CORONATINE INSENSITIVE1. *The Plant cell*, 30 (9), 2099-2115.

5. REFERENCES

- Steadman, J. R.; Sequeira, L. (1970).** Absciscic Acid in tobacco plants: tentative identification and its relation to stunting induced by *Pseudomonas solanaccarum*. *Plant physiology*, 45 (6), 691-697.
- Stintzi, A.; Weber, H.; Reymond, P.; Farmer, E. E. (2001).** Plant defense in the absence of jasmonic acid: the role of cyclopentenones. *Proceedings of the National Academy of Sciences*, 98 (22), 12837-12842.
- Strawn, M. A.; Marr, S. K.; Inoue, K.; Inada, N.; Zubieta, C.; Wildermuth, M. C. (2007).** Arabidopsis isochorismate synthase functional in pathogen-induced salicylate biosynthesis exhibits properties consistent with a role in diverse stress responses. *Journal of Biological Chemistry*, 282 (8), 5919-5933.
- Tan, B. C.; Joseph, L. M.; Deng, W. T.; Liu, L.; Li, Q. B.; Cline, K.; McCarty, D. R. (2003).** Molecular characterization of the Arabidopsis 9-cis epoxycarotenoid dioxygenase gene family. *The Plant Journal*, 35 (1), 44-56.
- Tan, L.; Liu, Q.; Song, Y.; Zhou, G.; Luan, L.; Weng, Q.; He, C. (2019).** Differential function of endogenous and exogenous abscisic acid during bacterial pattern-induced production of reactive oxygen species in Arabidopsis. *International journal of molecular sciences*, 20 (10), 2544.
- Tanaka, Y.; Nose, T.; Jikumaru, Y.; Kamiya, Y. (2013).** ABA inhibits entry into stomatal-lineage development in Arabidopsis leaves. *The Plant Journal*, 74 (3), 448-457.
- Tardieu, F.; Granier, C.; Muller, B. (2011).** Water deficit and growth. Co-ordinating processes without an orchestrator? *Current opinion in plant biology*, 14 (3), 283-289.
- Thaler, J. S.; Humphrey, P. T.; Whiteman, N. K. (2012).** Evolution of jasmonate and salicylate signal crosstalk. *Trends in plant science*, 17 (5), 260-270.
- Thatcher, L. F.; Manners, J. M.; Kazan, K. (2009).** *Fusarium oxysporum* hijacks COI1-mediated jasmonate signaling to promote disease development in Arabidopsis. *The Plant Journal*, 58 (6), 927-939.
- Thines, B.; Katsir, L.; Melotto, M.; Niu, Y.; Mandaokar, A.; Liu, G.; Nomura, K.; He, S. Y.; Howe, G. A.; Browse, J. (2007).** JAZ repressor proteins are targets of the SCF COI1 complex during jasmonate signalling. *Nature*, 448 (7154), 661-665.
- Thomma, B. P.; Eggermont, K.; Penninckx, I. A.; Mauch-Mani, B.; Vogelsang, R.; Cammue, B. P.; Broekaert, W. F. (1998).** Separate jasmonate-dependent and salicylate-dependent defense-response pathways in Arabidopsis are essential for resistance to distinct microbial pathogens. *Proceedings of the National Academy of Sciences*, 95 (25), 15107-15111.
- Ton, J.; Flors, V.; Mauch-Mani, B. (2009).** The multifaceted role of ABA in disease resistance. *Trends in plant science*, 14 (6), 310-317.
- Torrens-Spence, M. P.; Bobokalonova, A.; Carballo, V.; Glinkerman, C. M.; Pluskal, T.; Shen, A.; Weng, J.-K. (2019).** PBS3 and EPS1 complete salicylic acid biosynthesis from isochorismate in Arabidopsis. *Molecular Plant*, 12 (12), 1577-1586.
- Trauth, J.; Scheffer, J.; Hasenjäger, S.; Taxis, C. (2019).** Synthetic control of protein degradation during cell proliferation and developmental processes. *ACS Omega*, 4 (2), 2766-2778.
- Tsuda, K.; Somssich, I. E. (2015).** Transcriptional networks in plant immunity. *New Phytologist*, 206 (3), 932-947.

5. REFERENCES

- Tytgat, T. O.; Verhoeven, K. J.; Jansen, J. J.; Raaijmakers, C. E.; Bakx-Schotman, T.; McIntyre, L. M.; Van der Putten, W. H.; Biere, A.; Van Dam, N. M. (2013). Plants know where it hurts: root and shoot jasmonic acid induction elicit differential responses in *Brassica oleracea*. *PLoS One*, 8 (6), e65502.
- Ulferts, S.; Delventhal, R.; Splivallo, R.; Karlovsky, P.; Schaffrath, U. (2015). Absciscic acid negatively interferes with basal defence of barley against *Magnaporthe oryzae*. *BMC plant biology*, 15 (1), 7. Doi: 10.1186/s12870-014-0409-x
- Ulmasov, T.; Murfett, J.; Hagen, G.; Guilfoyle, T. J. (1997). Aux/IAA proteins repress expression of reporter genes containing natural and highly active synthetic auxin response elements. *The Plant cell*, 9 (11), 1963-1971.
- Umezawa, T.; Nakashima, K.; Miyakawa, T.; Kuromori, T.; Tanokura, M.; Shinozaki, K.; Yamaguchi-Shinozaki, K. (2010). Molecular basis of the core regulatory network in ABA responses: sensing, signaling and transport. *Plant and cell physiology*, 51 (11), 1821-1839.
- Urao, T.; Yamaguchi-Shinozaki, K.; Shinozaki, K. (2001). Plant Histidine Kinases: An Emerging Picture of Two-Component Signal Transduction in Hormone and Environmental Responses. *Science's STKE*, 2001 (109), re18.
- Vági, P.; Kovacs, G. M.; Kiss, L. (2007). Host range expansion in a powdery mildew fungus (*Golovinomyces* sp.) infecting *Arabidopsis thaliana*: *Torenia fournieri* as a new host. *European journal of plant pathology*, 117 (1), 89-93.
- Valette-Collet, O.; Cimerman, A.; Reignault, P.; Levis, C.; Boccara, M. (2003). Disruption of Botrytis cinerea pectin methylesterase gene Bcpme1 reduces virulence on several host plants. *Molecular Plant-microbe interactions*, 16 (4), 360-367.
- Van Der Biezen, E. A.; Freddie, C. T.; Kahn, K.; Parker, J. E.; Jones, J. D. (2002). Arabidopsis RPP4 is a member of the RPP5 multigene family of TIR-NB-LRR genes and confers downy mildew resistance through multiple signalling components. *The Plant Journal*, 29 (4), 439-451.
- Van der Does, D.; Leon-Reyes, A.; Koornneef, A.; Van Verk, M. C.; Rodenburg, N.; Pauwels, L.; Goossens, A.; Körbes, A. P.; Memelink, J.; Ritsema, T. (2013). Salicylic acid suppresses jasmonic acid signaling downstream of SCF^{COI1}-JAZ by targeting GCC promoter motifs via transcription factor ORA59. *The Plant cell*, 25 (2), 744-761.
- Van Gijsegem, F.; Pédrón, J.; Patrit, O.; Simond-Côte, E.; Maia-Grondard, A.; Petriacq, P.; Gonzalez, R.; Blottière, L.; Kraepiel, Y. (2017). Manipulation of ABA content in *Arabidopsis thaliana* modifies sensitivity and oxidative stress response to *Dickeya dadantii* and influences peroxidase activity. *Frontiers in plant science*, 8, 456.
- Van Wees, S. C.; Glazebrook, J. (2003). Loss of non-host resistance of *Arabidopsis NahG* to *Pseudomonas syringae* pv. *phaseolicola* is due to degradation products of salicylic acid. *The Plant Journal*, 33 (4), 733-742.
- Verberne, M. C.; Verpoorte, R.; Bol, J. F.; Mercado-Blanco, J.; Linthorst, H. J. (2000). Overproduction of salicylic acid in plants by bacterial transgenes enhances pathogen resistance. *Nature biotechnology*, 18 (7), 779-783.
- Verhage, A.; Vlaardingerbroek, I.; Raaijmakers, C.; Van Dam, N.; Dicke, M.; Van Wees, S.; Pieterse, C. M. (2011). Rewiring of the jasmonate signaling pathway in Arabidopsis during insect herbivory. *Frontiers in plant science*, 2, 47.

5. REFERENCES

- Vlot, A. C.; Dempsey, D. M. A.; Klessig, D. F. (2009).** Salicylic acid, a multifaceted hormone to combat disease. *Annual review of phytopathology*, 47, 177-206.
- Vos, I. A.; Moritz, L.; Pieterse, C. M.; Van Wees, S. (2015).** Impact of hormonal crosstalk on plant resistance and fitness under multi-attacker conditions. *Frontiers in plant science*, 6, 639.
- Vos, I. A.; Verhage, A.; Schuurink, R. C.; Watt, L. G.; Pieterse, C. M.; Van Wees, S. (2013).** Onset of herbivore-induced resistance in systemic tissue primed for jasmonate-dependent defenses is activated by abscisic acid. *Frontiers in plant science*, 4, 539.
- Waadt, R.; Hitomi, K.; Nishimura, N.; Hitomi, C.; Adams, S. R.; Getzoff, E. D.; Schroeder, J. I. (2014).** FRET-based reporters for the direct visualization of abscisic acid concentration changes and distribution in Arabidopsis. *elife*, 3, e01739.
- Waadt, R.; Hsu, P. K.; Schroeder, J. I. (2015).** Abscisic acid and other plant hormones: methods to visualize distribution and signaling. *Bioessays*, 37 (12), 1338-1349.
- Wan, J.; Zhang, X. C.; Neece, D.; Ramonell, K. M.; Clough, S.; Kim, S. Y.; Stacey, M. G.; Stacey, G. (2008).** A LysM receptor-like kinase plays a critical role in chitin signaling and fungal resistance in Arabidopsis. *The Plant cell*, 20 (2), 471-481.
- Wang, F.; Yu, G.; Liu, P. (2019).** Transporter-Mediated Subcellular Distribution in the Metabolism and Signaling of Jasmonates. *Frontiers in plant science*, 10, 390.
- Wang, K. L. C.; Li, H.; Ecker, J. R. (2002).** Ethylene biosynthesis and signaling networks. *The Plant cell*, 14 (suppl 1), 131-151.
- Wang, M.; Lee, J.; Choi, B.; Park, Y.; Sim, H.-J.; Kim, H.; Hwang, I. (2018).** Physiological and molecular processes associated with long duration of ABA treatment. *Frontiers in plant science*, 9, 176.
- Wang, W.; Barnaby, J. Y.; Tada, Y.; Li, H.; Tör, M.; Caldelari, D.; Lee, D.; Fu, X. D.; Dong, X. (2011).** Timing of plant immune responses by a central circadian regulator. *Nature*, 470 (7332), 110-114.
- Wang, Y.; Chen, Z. H.; Zhang, B.; Hills, A.; Blatt, M. R. (2013).** PYR/PYL/RCAR abscisic acid receptors regulate K⁺ and Cl⁻ channels through reactive oxygen species-mediated activation of Ca²⁺ channels at the plasma membrane of intact Arabidopsis guard cells. *Plant physiology*, 163 (2), 566-577.
- Wasternack, C. (2007).** Jasmonates: an update on biosynthesis, signal transduction and action in plant stress response, growth and development. *Annals of botany*, 100 (4), 681-697.
- Wasternack, C.; Hause, B. (2013).** Jasmonates: biosynthesis, perception, signal transduction and action in plant stress response, growth and development. An update to the 2007 review in Annals of Botany. *Annals of botany*, 111 (6), 1021-1058.
- Wasternack, C.; Strnad, M. (2018).** Jasmonates: News on occurrence, biosynthesis, metabolism and action of an ancient group of signaling compounds. *International journal of molecular sciences*, 19 (9), 2539.
- Weiler, E. W.; Schnabl, H.; Hornberg, C. (1982).** Stress-related levels of abscisic acid in guard cell protoplasts of *Vicia faba* L. *Planta*, 154 (1), 24-28.
- Wen, L. (2013).** Cell death in plant immune response to necrotrophs. *Plant Biochem Physiol*, 1, 1-3.

5. REFERENCES

- Whenham, R.; Fraser, R.; Brown, L.; Payne, J. (1986).** Tobacco-mosaic-virus-induced increase in abscisic-acid concentration in tobacco leaves: intracellular location in light and darkgreen areas, and relationship to symptom development. *Planta*, 168 (4), 592-598.
- Wildermuth, M. C.; Dewdney, J.; Wu, G.; Ausubel, F. M. (2001).** Isochorismate synthase is required to synthesize salicylic acid for plant defence. *Nature*, 414 (6863), 562-565.
- Wilkinson, S.; Davies, W. J. (2002).** ABA-based chemical signalling: the co-ordination of responses to stress in plants. *Plant, cell environment*, 25 (2), 195-210.
- Wille, A. C.; Lucas, W. J. (1984).** Ultrastructural and histochemical studies on guard cells. *Planta*, 160 (2), 129-142.
- Williamson, B.; Tudzynski, B.; Tudzynski, P.; Van Kan, J. A. (2007).** *Botrytis cinerea*: the cause of grey mould disease. *Molecular Plant pathology*, 8 (5), 561-580.
- Winter, D.; Vinegar, B.; Nahal, H.; Ammar, R.; Wilson, G. V.; Provart, N. J. (2007).** An “Electronic Fluorescent Pictograph” browser for exploring and analyzing large-scale biological data sets. *PLoS One*, 2 (8), e718.
- Wirthmueller, L.; Asai, S.; Rallapalli, G.; Sklenar, J.; Fabro, G.; Kim, D. S.; Lintermann, R.; Jaspers, P.; Wrzaczek, M.; Kangasjärvi, J.; MacLean, D.; Menke, F. L. H.; Banfield, M. J.; Jones, J. D. G. (2018).** Arabidopsis downy mildew effector HaRxL106 suppresses plant immunity by binding to RADICAL-INDUCED CELL DEATH. *New Phytologist*, 220 (1), 232-248.
- Wolf, T.; Heidelmann, T.; Marten, I. (2006).** ABA regulation of K⁺-permeable channels in maize subsidiary cells. *Plant and cell physiology*, 47 (10), 1372-1380.
- Wu, J.; Baldwin, I. T. (2010).** New insights into plant responses to the attack from insect herbivores. *Annual review of Genetics*, 44, 1-24.
- Wu, R.; Duan, L.; Pruneda-Paz, J. L.; Oh, D. H.; Pound, M.; Kay, S.; Dinneny, J. R. (2018).** The 6xABRE synthetic promoter enables the spatiotemporal analysis of ABA-mediated transcriptional regulation. *Plant physiology*, 177 (4), 1650-1665.
- Wu, Y.; Zhang, D.; Chu, J. Y.; Boyle, P.; Wang, Y.; Brindle, I. D.; De Luca, V.; Després, C. (2012).** The Arabidopsis NPR1 protein is a receptor for the plant defense hormone salicylic acid. *Cell reports*, 1 (6), 639-647.
- Xie, D. X.; Feys, B. F.; James, S.; Nieto-Rostro, M.; Turner, J. G. (1998).** COI1: an Arabidopsis gene required for jasmonate-regulated defense and fertility. *Science*, 280 (5366), 1091-1094.
- Xie, K.; Li, L.; Zhang, H.; Wang, R.; Tan, X.; He, Y.; Hong, G.; Li, J.; Ming, F.; Yao, X. (2018).** Absciscic Acid Negatively Modulates Plant Defense against Rice Black-Streaked Dwarf Virus Infection by Suppressing the Jasmonate Pathway and Regulating ROS Levels in Rice. *Plant, cell environment*.
- Xie, X.; Wang, Y.; Williamson, L.; Holroyd, G. H.; Tagliavia, C.; Murchie, E.; Theobald, J.; Knight, M. R.; Davies, W. J.; Leyser, H. O. (2006).** The identification of genes involved in the stomatal response to reduced atmospheric relative humidity. *Current Biology*, 16 (9), 882-887.
- Xin, X. F.; Nomura, K.; Aung, K.; Velásquez, A. C.; Yao, J.; Boutrot, F.; Chang, J. H.; Zipfel, C.; He, S. Y. (2016).** Bacteria establish an aqueous living space in plants crucial for virulence. *Nature*, 539 (7630), 524-529.

5. REFERENCES

- Xiong, L.; Zhu, J.-K. (2003).** Regulation of abscisic acid biosynthesis. *Plant physiology*, 133 (1), 29-36.
- Xiong, L.; Lee, H.; Ishitani, M.; Zhu, J. K. (2002).** Regulation of Osmotic Stress-responsive Gene Expression by the *LOS6/ABA1* Locus in Arabidopsis. *Journal of Biological Chemistry*, 277 (10), 8588-8596.
- Xu, Y.; Chang, P. F. L.; Liu, D.; Narasimhan, M. L.; Raghothama, K. G.; Hasegawa, P. M.; Bressan, R. A. (1994).** Plant defense genes are synergistically induced by ethylene and methyl jasmonate. *The Plant cell*, 6 (8), 1077-1085.
- Yan, C.; Xie, D. (2015).** Jasmonate in plant defence: sentinel or double agent? *Plant biotechnology journal*, 13 (9), 1233-1240.
- Yan, Y.; Stolz, S.; Chételat, A.; Reymond, P.; Pagni, M.; Dubugnon, L.; Farmer, E. E. (2007).** A downstream mediator in the growth repression limb of the jasmonate pathway. *The Plant cell*, 19 (8), 2470-2483.
- Yang, S. F.; Hoffman, N. E. (1984).** Ethylene biosynthesis and its regulation in higher plants. *Annual review of Plant physiology*, 35 (1), 155-189.
- Yang, W.; Zhang, W.; Wang, X. (2017).** Post-translational control of ABA signalling: the roles of protein phosphorylation and ubiquitination. *Plant biotechnology journal*, 15 (1), 4-14.
- Yasuda, M.; Ishikawa, A.; Jikumaru, Y.; Seki, M.; Umezawa, T.; Asami, T.; Maruyama-Nakashita, A.; Kudo, T.; Shinozaki, K.; Yoshida, S. (2008).** Antagonistic interaction between systemic acquired resistance and the abscisic acid-mediated abiotic stress response in Arabidopsis. *The Plant cell*, 20 (6), 1678-1692.
- Yoshida, T.; Nishimura, N.; Kitahata, N.; Kuromori, T.; Ito, T.; Asami, T.; Shinozaki, K.; Hirayama, T. (2006).** *ABA-Hypersensitive Germination3* encodes a protein phosphatase 2C (AtPP2CA) that strongly regulates abscisic acid signaling during germination among Arabidopsis protein phosphatase 2Cs. *Plant physiology*, 140 (1), 115-126.
- Yuan, Z.; Zhang, D. (2015).** Roles of jasmonate signalling in plant inflorescence and flower development. *Current opinion in plant biology*, 27, 44-51.
- Zander, M.; La Camera, S.; Lamotte, O.; Métraux, J. P.; Gatz, C. (2010).** *Arabidopsis thaliana* class-II TGA transcription factors are essential activators of jasmonic acid/ethylene-induced defense responses. *The Plant Journal*, 61 (2), 200-210.
- Zander, M.; Thurow, C.; Gatz, C. (2014).** TGA transcription factors activate the salicylic acid-suppressible branch of the ethylene-induced defense program by regulating ORA59 expression. *Plant physiology*, 165 (4), 1671-1683.
- Zeevaart, J. A. (1977).** Sites of abscisic acid synthesis and metabolism in *Ricinus communis* L. *Plant physiology*, 59 (5), 788-791.
- Zembek, P.; Danilecka, A.; Hoser, R.; Eschen-Lippold, L.; Benicka, M.; Grech-Baran, M.; Rymaszewski, W.; Barymow-Filoniuk, I.; Morgiewicz, K.; Kwiatkowski, J. (2018).** Two Strategies of *Pseudomonas syringae* to Avoid Recognition of the HopQ1 Effector in *Nicotiana* Species. *Frontiers in plant science*, 9, 978.
- Zhang, G.; Gurtu, V.; Kain, S. R. (1996).** An enhanced green fluorescent protein allows sensitive detection of gene transfer in mammalian cells. *Biochemical and biophysical research communications*, 227 (3), 707-711.

5. REFERENCES

- Zhang, J.; Zhou, J. M. (2010).** Plant immunity triggered by microbial molecular signatures. *Molecular Plant*, 3 (5), 783-793.
- Zhang, W.; Zhao, F.; Jiang, L.; Chen, C.; Wu, L.; Liu, Z. (2018).** Different pathogen defense strategies in Arabidopsis: more than pathogen recognition. *Cells*, 7 (12), 252.
- Zhang, X. L.; Jiang, L.; Xin, Q.; Liu, Y.; Tan, J. X.; Chen, Z. Z. (2015).** Structural basis and functions of abscisic acid receptors PYLs. *Frontiers in plant science*, 6, 88.
- Zhang, Y.; Cheng, Y. T.; Qu, N.; Zhao, Q.; Bi, D.; Li, X. (2006).** Negative regulation of defense responses in Arabidopsis by two *NPR1* paralogs. *The Plant Journal*, 48 (5), 647-656.
- Zhao, Y.; Zhang, Z.; Gao, J.; Wang, P.; Hu, T.; Wang, Z.; Hou, Y.J.; Wan, Y.; Liu, W.; Xie, S. (2018).** Arabidopsis duodecuple mutant of PYL ABA receptors reveals PYL repression of ABA-independent SnRK2 activity. *Cell reports*, 23 (11), 3340-3351. e3345.
- Zhou, J.; Zhang, H.; Yang, Y.; Zhang, Z.; Zhang, H.; Hu, X.; Chen, J.; Wang, X.C.; Huang, R. (2008).** Abscisic acid regulates TSRF1-mediated resistance to *Ralstonia solanacearum* by modifying the expression of GCC box-containing genes in tobacco. *Journal of experimental botany*, 59 (3), 645-652.
- Zhu, Z.; An, F.; Feng, Y.; Li, P.; Xue, L.; Mu, A.; Jiang, Z.; Kim, J.M.; To, T. K.; Li, W. (2011).** Derepression of ethylene-stabilized transcription factors (EIN3/EIL1) mediates jasmonate and ethylene signaling synergy in Arabidopsis. *Proceedings of the National Academy of Sciences*, 108 (30), 12539-12544.
- Zipfel, C. (2014).** Plant pattern-recognition receptors. *Trends in immunology*, 35 (7), 345-351.
- Zipfel, C.; Kunze, G.; Chinchilla, D.; Caniard, A.; Jones, J. D.; Boller, T.; Felix, G. (2006).** Perception of the bacterial PAMP EF-Tu by the receptor EFR restricts Agrobacterium-mediated transformation. *Cell*, 125 (4), 749-760.
- Zipfel, C.; Robatzek, S.; Navarro, L.; Oakeley, E. J.; Jones, J. D.; Felix, G.; Boller, T. (2004).** Bacterial disease resistance in Arabidopsis through flagellin perception. *Nature*, 428 (6984), 764.
- Zürcher, E.; Tavor-Deslex, D.; Lituiev, D.; Enkerli, K.; Tarr, P. T.; Müller, B. (2013).** A robust and sensitive synthetic sensor to monitor the transcriptional output of the cytokinin signaling network in planta. *Plant physiology*, 161 (3), 1066-1075.

6. Supplemental material

Supplementary video 1. *H. arabidopsidis* isolate Emwa1 invading leaf epidermis of COLORFUL-SA#1 at 1 day post inoculation. Site of penetration (yellow arrowhead), extrahaustorial membrane surrounding the haustoria (green arrowhead).

Supplementary video 2. *H. arabidopsidis* isolate Emwa1 invading leaf palisade mesophyll of COLORFUL-SA#1 at 1 day post inoculation. Extrahaustorial membrane surrounding the haustoria (green arrowhead).

Supplementary video 3. *H. arabidopsidis* isolate Noco2 invading leaf of COLORFUL-SA#1 at 3 days post inoculation. Extrahaustorial membrane surrounding the haustoria (green arrowhead).

Supplementary video 4. *H. arabidopsidis* isolate Emwa1 invading leaf of COLORFUL-SA#1 at 3 days post inoculation. Extrahaustorial membrane surrounding the haustoria (green arrowhead).

ACKNOWLEDGEMENTS

Firstly, I would like to express my sincere gratitude to my advisor Prof. Dr. Volker Lipka for giving me the chance to be a member of the Plant Cell Biology Department as well as for his continuous invaluable support, for his patience, motivation, and his immense knowledge. His guidance helped me throughout my research. I also thank him for correcting this dissertation and for reviewing my work.

Beside my advisor, I also extend my gratitude towards the second member of my thesis committee PD Dr. Thomas Teichmann. He not only helped me with software and computer problems but also labored to correct my thesis and review my work.

I wish to express my sincere appreciation to my mentor of three years, Dr. Hassan Ghareeb, who has the substance of a genius: he has guided and encouraged me to be professional and to do the right thing even when the road got tough. Without his persistent help, patience, and continuous support, the goal of this project would not have been realized. His dynamism, vision, sincerity, and motivation have deeply inspired me.

I would like to thank all the members of my thesis committee, not only for their insightful comments and encouragement, constructive criticisms, brain-storming, and discussion sessions during the project meetings, but also for the hard questions which incentivized me to broaden my research from various perspectives.

I gratefully acknowledge the financial support of German Egyptian Research Long-Term Scholarship (GERLS) program through a bilateral scholarship from the Egyptian government and the Deutscher Akademischer Austauschdienst (DAAD), as well as Georg-August University School of Science (GAUSS) program for the family-oriented completion grant.

I thank and express my respect to Prof Dr. Lipka, PD Dr. Teichmann, Prof. Dr. Ivo Feußner, Prof. Dr. Andrea Polle, PD. Dr. Marcel Wiermer, and PD Dr. Till Ischebeck for their willingness to take part in my examination board.

I would like to thank Lisa Schäfer and Jan-Niclas Lübbers for the genomic DNA analyses and the selection of the homozygous lines of *snrk2d*, *snrk2i* and *snrk2d snrk2i* after crossing with COLORFUL-ABA.

I would like to pay my special regards to Mrs. Felicitas Glasenapp and Mrs. Gabriele Schauermann for their practical contribution as well as our great secretary Mrs. Anja Auspurg for her efficient management of my official staff.

My experience in the lab has been very positive and I can honestly say it was enjoyable thanks to my office and lab-mates particularly Konrad Subieta for his useful feedback and also everyone outside of the office space who made the work environment comfortable and friendly.

Sincerely,

Mohamed El-Sayed

CURRICULUM VITAE

Personal data

Name: Mohamed El-Sayed
Address: Albrecht-Thaer-Weg 22, 37075 Göttingen
Tel.: +4917673220188/+201113243996
Email: melsaye@gmx.de
Birthday: 02.12.1984 in Egypt
Nationality: Egyptian

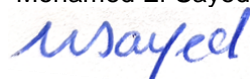
School Education

09/1998 - 06/2001 El-Sadat Secondary School
09/1995 - 06/1998 Omar Ibn El-Khatib Preparatory School
09/1990 - 06/1995 Ali Ibn Abi Talib Primary School

University Education and Academic Activities

04/2020 - 09/2020 Göttingen international team fellowship.
10/2019 - 03/2020 GAUSS Family oriented completion grant funded by GAUSS.
PhD student and DAAD-scholarship-holder at Plant Cell Biology Department, Albrecht-von-Haller-Institute for Plant Sciences, Georg-August-Universität Göttingen, Germany.
04/2016 - 09/2019 Dissertation title: "Cell-specific phytohormone responses mapped by the COLORFUL-biosensors during plant-microbe interactions" at the doctoral program the Georg-August University School of Science (GAUSS) to obtain the Doctor rerum naturalium degree in biology under supervision of Prof. Dr. Volker Lipka.
06/2015 - 03/2016 DAAD-scholarship-holder funded by the German Egyptian Research Long-Term Scholarship (GERLS) program through a bilateral scholarship from the Egyptian government and the Deutscher Akademischer Austauschdienst (DAAD).
07/2014 - Now Assistant Researcher permanent position in Plant Biotechnology Department, National Research Center, Giza, Egypt.
10/2011 - 09/2014 Master in Biochemistry, Faculty of Science, Cairo University, Giza, Egypt. Thesis topic "Micropropagation and molecular characterization of Jatropha plants".
07/2011 - 07/2014 Research Assistant permanent position in Plant Biotechnology Department, National Research Center, Giza, Egypt.
03/2006 - 07/2011 Specialist in Plant Biotechnology Department, National Research Center, Giza, Egypt.
09/2001 - 07/2005 Bachelor in Chemistry and Biochemistry, Faculty of Science, Zagazig University, Egypt.

Mohamed El-Sayed



Göttingen, 20.02.2020